A study on the role of polarity, Rho family GTPases, and cell fate in cytokinesis

Yelena Zhuravlev

Submitted in partial fulfillment of the

requirements for the degree of

Doctor of Philosophy

in the Graduate School of Arts and Sciences

Columbia University

2017

Abstract

A study on the role of polarity, Rho family GTPases, and cell fate in cytokinesis

Yelena Zhuravlev

Cytokinesis is the physical partition of one cell into two. In Chapter 1, I provide a brief introduction to cytokinesis and some of the proteins whose functions I parse out throughout my studies. In Chapter 2, I present work I've contributed to elucidate the role of polarity proteins in cytokinesis, as well as a look at the differential requirement for canonically essential cytokinetic proteins in the 4-cell embryo. In Chapter 3, I address a long-standing controversy in the field regarding the relationship between the Rac GAP protein Cyk-4 and the small GTPase Rac, and in particular the inhibitory role of Rac during cell division. My major body of work highlights the necessity not to close the books on the GAP activity of Cyk-4 and its inhibition of Rac. I show that Rac is unable to rescue cytokinesis failure in downstream Rho effectors whose loss weakens the contractile ring, suggesting it is not a promiscuous suppressor of cytokinesis. Additionally, I found that levels of non-muscle myosin-II and the actin binding domain of Utrophin were unchanged with loss of Cyk-4. From this, I infer that Cyk-4 is unlikely to be an activator of the RhoGEF Ect-2. These results emphasize the need to probe further into the cross-talk between these GTPases. In chapter 4, I show inconclusive data addressing the role of cell fate signaling in protection against cytokinesis failure. Overall, this thesis represents my contributions to the field, revealing the complexity involved in assuring successful completion of cytokinesis.

Table of Contents

List of Figures

Chapter 1:

Chapter 2:

Chapter 3:

Chapter 4:

Supplemental Figures

Chapter 2:

Chapter 3:

List of Tables

Chapter 4:

List of Supplementary Tables

Chapter 2:

Chapter 3:

Chapter 4:

Abbreviations

ts= temperature-sensitive;

lof=loss of function;

gof= gain of function;

RNAi= RNA interference;

MLC= myosin light chain;

ROCK= Rho-kinase;

GAP= GTPase Activating Protein;

GEF= Guanine-nucleotide Exchange Factor;

Utr^{ABD}= Utrophin (Actin Binding Domain);

cyk-4= cytokinesis defect [gene] 4;

cyk-1= *C. elegans* cytokinesis defect [gene] 1/diaphanous-family formin;

nmy-2= *C. elegans* non-muscle myosin-II;

zen-4= zygotic epidermal enclosure defective;

spd-1= spindle defective/ protein regulator of cytokinesis 1 (PRC1);

mom-2= more of MS;

wrm-1= worm armadillo;

ect-2= epithelial cell transforming factor 2

cdc42= cell division cycle related 42;

ced-10= cell death abnormality;

SEM= standard error of the mean;

SD= standard deviation;

Ave.= average;

AO= anaphase onset;

PAR= PARtitioning defective;

aPAR= anterior PAR protein;

pPAR= posterior PAR protein;

A-P= Anterior-Posterior

ROI= region of interest

Acknowledgements

"Let the words of my mouth and the meditation of my heart be acceptable in your sight, O Lord, my rock and my redeemer." –Psalm 19:14

"Limited minds can only recognize limitations in others" –Jack London, Martin Eden. I am thankful for my thesis advisor Dr. Julie Canman for her support and encouragement throughout my graduate studies. I was honored to have been a member of her lab and to have learned from her. During my graduate school journey, she invested so much time and effort into helping me give good presentations and produce good scientific writing. In her care, I've learned how to be a more critical thinker and if nothing else, how to color coordinate figures.

The positive atmosphere I was so fortunate in working in was largely due to Shawn Jordan, a former graduate student in the lab. Not only does he have a brilliant mind, but also a good character. He encouraged me during the graduate school doldrums and believed enough in me that I started to believe a bit more in myself.

I cannot express my appreciation enough for Tim Davies, a postdoc in the lab. Always a clever turn of phrase, a quality contribution made during lab meeting, and a mentor in the final months before my PhD completion, I know Tim will be an amazing PI and those in his lab will be so fortunate to have him as their guide and mentor.

Sriram Sundaramoorthy, for his insightful advice on experiments and patience in teaching me how to use the FLIRT system, despite his reluctance in flirting. May his love for Charles Darwin never dwindle.

I am so grateful to Vandana Chand, a former lab tech, for showing me the ropes when I first rotated in the lab. She taught me how to use the mouth pipette for sucking up embryos—a skill I've used nearly every day in the laboratory.

I thank Sophia Hirsch for listening to me vent, as no one but a fellow graduate student can relate to the tortures we go through. I know her intellect and hard work will take her far.

I am grateful to the Department of Genetics and Development for supporting budding scientists and giving them the tools they need to do research. Especially, I would like to thank Frank Costantini, who took me in as a research assistant and put me under the amazing mentorship of Cristina Cebrian. Cristina entertained my naive questions and challenged me intellectually. I'll always be her minion! The entire Costantini lab made science fun and accessible. I blame them all for my PhD pursuits!

A big thank you to my committee members Gregg Gundersen, Cathy Mendelsohn, and Mimi Shirasu-Hiza, as well as to Rebecca Haeusler for serving as the outside expert on my thesis defense committee. The feedback and support I received from them during our meetings have taught me how to formulate scientific hypotheses and to never take other people's data at face value without double checking it. "Our chief want is someone who will inspire us to be what we know we could be" –Ralph W. Emerson. I am so grateful for the many times Mimi Shirasu-Hiza counseled me, ranging from science queries to personal dilemmas. She is truly a friend and mentor to graduate students and her lab is very much my lab away from lab. Another thank you to Cathy Mendelsohn for seeing the bigger picture during my presentations and also for seeing bigger opportunities for me to stay in science.

To the Canman lab undergraduates, for doing the important work that makes the lab run efficiently but often gets little recognition. They are the bare agar pad (bones) our *C. elegans* couldn't do without it.

I am so grateful to my family. "Whoever brings ruin on their family will inherit only wind, and the fool will be servant to the wise." –Proverbs 11:29. I thank my parents for giving me so many of the opportunities and advantages they themselves did not have. Above all else, they have taught me how to be a good person. Whatever I pursue to do in the future, I can do it with a good heart. I thank my grandparents for helping to raise me with such warmth and love. I have such happy memories from my childhood thanks to them. My sister, who else is there better to fight with? She is a true warrior, even if she does not know it and has inspired me to never give up despite the struggle that may come. Inna and Sveta for telling me I was the girl from the stars. Is there anything I could do they wouldn't be proud of? To my tyootya, Melena, for always being there for me as my confidant in hard times. I am filled with gratitude to my in-laws, for making me feel like a daughter and not a daughter-in-law. I value our intellectual dialogues as they force me to confront and challenge my beliefs (in a good way). I am also grateful to our nanny, Ilda,, for giving me peace of mind knowing that I leave my most precious blessings in capable hands.

Mikhail, my partner in life, the father of our children, my bashert. "Like an apple tree among the trees of the forest is my beloved among the young men. I delight to sit in his shade, and his fruit is sweet to my taste."- Song of Solomon 2:3. I thank him so much for believing in me when I lose faith in myself. For choosing to bind his life with mine, giving me the kind of love old poetry is made of. May we always encourage each other to be better. I thank him

for the comfortable deep silence or conversation, when they're needed respectively. Above all else, I thank him for our children and the life we're building for them.

I am filled with gratitude for my darlings: Galel Meir and Rena Bella. I thank them for forcing me to put any stress from work aside when we are together and to focus on making memories in the moment. Thanks for their smiles, pudgy thighs; their unexpected intellect, curiosity, and creativity, for giving me a purpose beyond myself. They remind me that no experiment is more important than changing a dirty diaper or rubbing an aching belly. They have taught me patience, a virtue I never had before and likely have with no others but them. "And so it will be as if all the stars were laughing, when you look at the sky at night" – Antione de Saint-Exupery, The Little Prince.

I am appreciative to Anna Shostya. Her teaching fostered my love of writing and literature. It is an honor to be confused for her daughter. I hope to emulate her strength, perseverance, and passion for life.

To my friends: I thank them for understanding I couldn't go out to play because worms don't know about weekends or government holidays. That when there was finally an opportunity to reconnect, sometimes after months of absence, it was like no time had passed. "Iron sharpens iron; so one man sharpens another." –Proverbs 27:17

Dedication

To my beloved partner, Mikhail Zhuravlev, for staying up late

and getting up early.

Introduction

Basics principles of cytokinesis

Definition and basic mechanism of cytokinesis in animal cells

All multicellular organisms originate from the division of a single cell. Cytokinesis is the process by which one cell physically divides into two. To accomplish this, the mitotic apparatus must communicate with the cortex of the cell as the membrane ingresses. As the chromosomes undergo mitosis, the cell must go through cortical remodeling and cell shape changes to partition itself to ensure each daughter cell is distributed a full genomic complement. This is accomplished through the constriction of an actomyosin contractile ring, which is positioned by signals from the mitotic spindle (Balasubramanian et al., 2004; Barr and Gruneberg 2007; Green et al., 2012; Murthy, 2005; Stark et al., 2010). As the cell undergoes cytokinesis, the shape of the invaginating plasma membrane is generally referred to either as the cleavage furrow or the cytokinetic furrow. While different animal cells may vary in some cytokinetic processes, the specification of the division plane, the formation of the mitotic spindle, constriction of the contractile ring, and abscission of the intercellular bridge are all essential steps of normal cell division.

Assembly and constriction of the metazoan actomyosin ring

In animal cells, cytokinesis occurs via the constriction of an actomyosin ring (Balasubramanian et al., 2004; Barr and Gruneberg 2007; Green et al., 2012; Murthy, 2005; Stark et al., 2010). At the division plane, non-muscle myosin-II motors associate with f-actin filaments to drive contractile ring constriction (Mabuchi and Okuno, 1977; Guhas et al., 2005; Murthy and Wadsworth, 2005). How exactly myosin-II and f-actin filaments function together

to accomplish this is still a matter of debate. Many studies suggest myosin-II slides along actin filaments, thereby constricting the ring (referred to as a purse-string mechanism), but structural organization of myosin-II and actin within the contractile ring has yet to clearly demonstrate this (Henson et al. 2017; Maupin and Pollard 1986; Sanger and Sanger, 1980; Schroeder 1972).

Once the contractile ring is formed it remains a dynamic structure, the volume decreases as it ingresses and the ring is progressively disassembled, (Carvalho et al., 2009; Davies et al., 2015; Pelham and Chang, 2002; Schroeder, 1972). In mammalian cells, actin filaments are also dynamic and require constant turnover (Murthy, 2005). Cells treated with jasplakinolide, a drug that stabilizes actin, are unable to complete cytokinesis or recover fluorescence after photobleaching (Murthy, 2005). In addition, cells treated with a myosin-II inhibitor, blebbistatin, accumulate less GFP:actin at the division plane and cytokinesis is blocked, demonstrating that myosin-II also plays a role in actin turnover (Murthy, 2005; Straight et al., 2005). In contrast, FRAP experiments revealed myosin-II levels do not exhibit much turnover as recovery after bleaching was slow and the bleached region decreased with ring constriction (Carvalho et al., 2009). In animal cells, the contractile ring constricts in two phases, first at a constant rate for a majority of the constriction process, then, in the second phase the rate of constriction is progressively slowed (Carvalho et al., 2009; Mabuchi, 1994; Zumdieck et al., 2007). While actin and non-muscle myosin-II exhibit different turnover rates, both interact together to constrict the ring.

The mitotic apparatus and cytokinesis

The mitotic apparatus controls the assembly and constriction of the contractile ring at the division plane. It is composed of several organelles: spindle microtubules, associated organelles, chromosomes, and centrosomes (chromatin). Removal of the mitotic apparatus via aspiration completely blocked cytokinesis if it was done prior to anaphase but had no effect if performed later (Hiramoto, 1956; Rappaport, 1981) (Figure 1). This implies that the signal passed from the mitotic apparatus to the cortex to initiate furrow formation is time-sensitive.

The timing of contractile ring constriction is related to the distance from the mitotic apparatus to the cell cortex. Experimentalists trying to elucidate the connection between the mitotic spindle and cortex have classically looked at geometric relationships between the spindle and the cell surface. In the interest of investigating if the mitotic spindle was sufficient to induce furrowing, experimenters manipulated cells to increase the interaction of the mitotic spindle with the cortex and decrease the interaction of the surface with the poles. In these experiments, furrows still formed when the cortex was in contact with the spindle even as contact with the asters was reduced, suggesting the mitotic spindle was sufficient to induce furrowing (Kawamura, 1977; Rappaport and Rappaport, 1974; Ris, 1949).

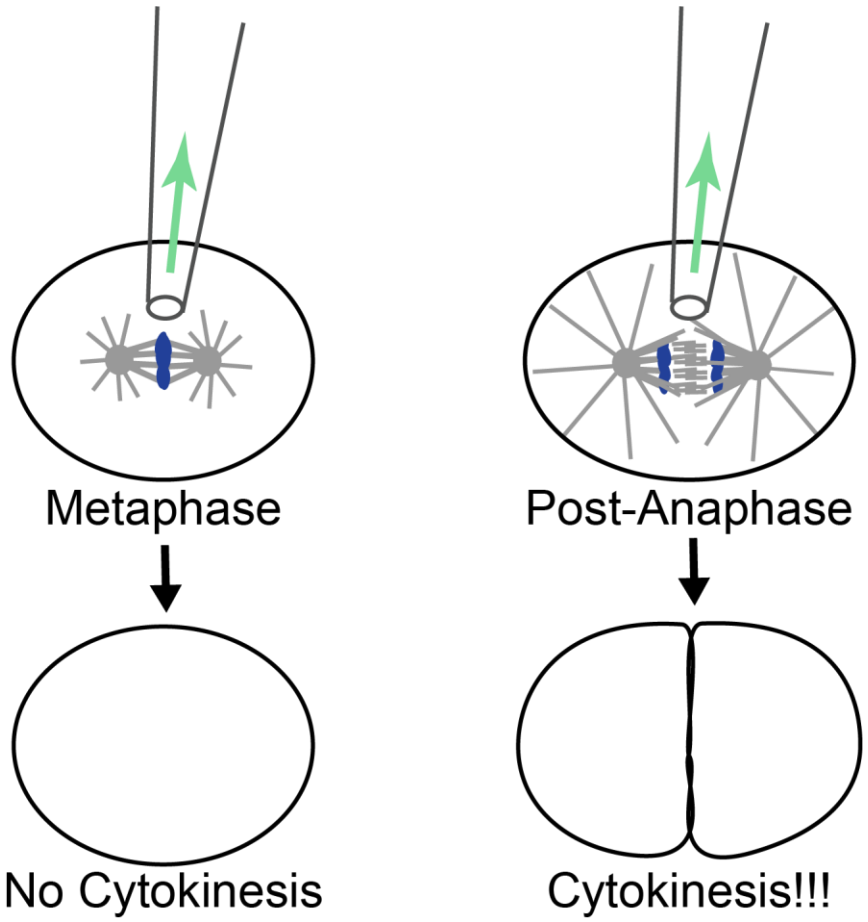

Figure 1: Prior to anaphase the cell cortex responds to signals from the mitotic apparatus

The cell cortex is responsive to signals from the mitotic apparatus at certain stages of the cell cycle. Removal prior to anaphase results in no cytokinesis or furrowing while removal after anaphase does not affect furrowing or cytokinesis completion.

However, this does not take away from the contribution of other components of the mitotic apparatus, particularly the asters, in furrow formation. Researchers found that squishing cells to shorten the distance between the mitotic apparatus such that spindle poles were ~56% closer to the cell surface compared to controls, resulted in earlier onset of furrow formation by ~four min vs controls after anaphase onset (Shuster and Burgess, 2002).

Signals from the mitotic spindle microtubules also regulate overall cortical stiffness. During mitosis, cells round up to prepare for cytokinesis. Initially, research showed that stiffness of the cortex changed with progression of cytokinesis, with stiffness increasing 10 minutes before cleavage and decreasing thereafter (Hiramoto, 1970). While initially, these stiffness fluctuations were assumed to be a potential readout of the surface responding to spindle microtubules, with high stiffness representing the time at which the surface is most responsive, little connection between the two has been found. These cycles of stiffness and relaxation are microtubule-independent, persisting even after enough treatment with colchicine to depolymerize microtubules (Bell, 1962; Swann and Mitchison, 1953). PtK1 cells treated with nocodazole to depolymerize microtubules also displayed cortical contractility after anaphase onset, suggesting microtubules are not essential for changes to the cell shape or rigidity (Canman et al., 2000). Furthermore, *Xenopus* treated with taxol or vinblastine, to inhibit microtubule dynamics, did not disturb cytoskeletal changes that occur as the cells undergo convergent extension (a coordinated cell movement by which the cell elongates via intercalation) (Kwan and Kirschner, 2005).

To study the effect of the mitotic spindle on the surface, sand dollar egg cells were bound such that the mitotic spindle was restricted to only half instead of the entire surface. This caused a differential internal pressure between the two sides and as a consequence a

change in cytoplasmic flow as the mitotic spindle moved from one part of the cell to the other. Upon removal of the mitotic spindle, but continued constriction of the cell, no flow was observed, suggesting the mitotic spindle was responsible for increased tension at the cell surface (Rappaport, 1988). These experiments indicate a signal passing from the mitotic spindle to the cortex.

Mitotic spindle microtubules are essential to induce furrow formation and cytokinesis. When spindle microtubules are depolymerized during metaphase or early anaphase, cytokinesis is blocked and no furrow forms (Hamaguchi, 1975; Swann and Mitchison, 1953). However, microtubule depolymerization after anaphase onset did not block cytokinesis, suggesting the functional period required for microtubules, like the mitotic apparatus, is prior to anaphase (Hamaguchi, 1975; Swann and Mitchison, 1953). When the spindle in echinoderm eggs was repositioned with a glass needle, the contractile ring regressed from its former position and a new contractile ring formed at the new site of the spindle, suggesting the spindle had a function in specifying the division plane (Rappaport, 1985). The same was found to be true in grasshopper spermatocytes (Kawamura, 1960). In additional experiments, researchers found furrowing could occur along the entire cortex depending on the position of the mitotic spindle, suggesting the entire cortex is receptive to furrowing (Rappaport, 1975; Rappaport, 1985). Thus, mitotic spindle microtubules are responsible for positioning the division plane.

Centrosomes, the main microtubule organizing centers in animal cells, have also been tested for their role in cell division (Oliferenko et al., 2009). In experiments where centrosomin null mutants, which are unable to assemble fully functional mitotic centrosomes, were still able to undergo the necessary divisions to develop into adulthood (Megraw TL,

2001). When centrosomes were laser ablated in mammalian cultured cells, it did not affect the assembly of spindles or the process of cell division (Khodjakov, 2000). Further, fruit flies are able to undergo most of their development without centrosomes, though spindle assembly is delayed (Basto et al., 2006). This suggests centrosomes are not essential for cytokinesis although they likely play a role in astral microtubule regulation.

Centrosome separation is, however, important for cytokinesis. When sea urchin egg cells were flattened, furrow formation rarely occurred when the inter-centrosomal distance exceeded 35 µm (Rappaport, 1969). In another experiment where the centrosomes were moved far enough apart (137 µm in sand dollar eggs) that they no longer furrowed, but then were pushed closer together (until they are 50 µm apart), they were again able to form furrows. In anucleate cells, centrosome pairs (and associated astral microtubules) were able to compensate for the loss of a spindle if they were far enough apart such that the distance between the centrosomes exceeded the distance from the surface (George von Dassow, 2009). If they were around the same distance apart, only shallow furrows were observed and no furrow developed at all if centrosomes were closer to each other than the distance to the surface (George von Dassow, 2009). Taken together, the separation of centrosomes seems to be important for normal cytokinesis, although monopolar cells are also able to divide, thus centrosome separation is not always required (see more below) (Canman et al., 2003).

Chromosomes (and associated DNA) have been long proposed to be involved in controlling the temporal and spatial regulation of cytokinesis by coordinating the timing of anaphase onset and dictating the position of the division plane. Sand dollar eggs perforated such that in some cells the chromatin and asters were on the same side developed normal furrows, while cells that had only asters with no chromatin (anucleate) formed transient

furrows that never fully developed (Rappaport, 1991). However, success of mitosis (and segregation of duplicated chromosomes) is not always coupled with cytokinesis completion (Castagnetti et al., 2010; Wheatley et al., 1997). In a series of elegant experiments using grasshopper spermatocytes, chromosomes removed after the formation of a spindle did not interrupt progression of "anaphase" or cytokinesis. This lends support to the control of cytokinesis being intrinsic to the spindle and the cell (Zhang, 1996).

Division plane specification/spindle signaling

Stimulatory roles of the mitotic apparatus and responses of the cortex in preparation for furrowing

Rappaport described the stability of the mitotic spindle as "in a sense illusory, because most of the microtubules that are the principle organizing elements of the spindle fibers and aster rays are dynamically unstable; they reversibly extend and retract" (Rappaport, 1971). Microtubules are highly dynamic structures, with ß-tubulin plus ends and alpha-tubulin minus ends, which cycle between growing (polymerization) and shrinking (depolymerization) phases (Desai et al., 1997). The switch from a growing microtubule to a rapidly shrinking one is termed catastrophe (Mitchison and Kirschner, 1984; Wollman et al., 2005). Microtubules also undergo rescue events, when they switch from a shrinking to growth phase. A mature pre-anaphase mitotic spindle is made up of 3 different sets of microtubules: interpolar microtubules, kinetochore microtubules, and astral microtubules (Canman et al., 2003; Foe and von Dassow, 2008; Mastronarde et al., 1993). Upon anaphase onset, the spindle undergoes modification with kinetochore fibers shortening, astral microtubules lengthening

and translocation of central spindle assembly proteins from the cytoplasm to the center of the cell to initiate bundling of antiparallel plus end microtubules (Glotzer, 2009) (Figure 2).

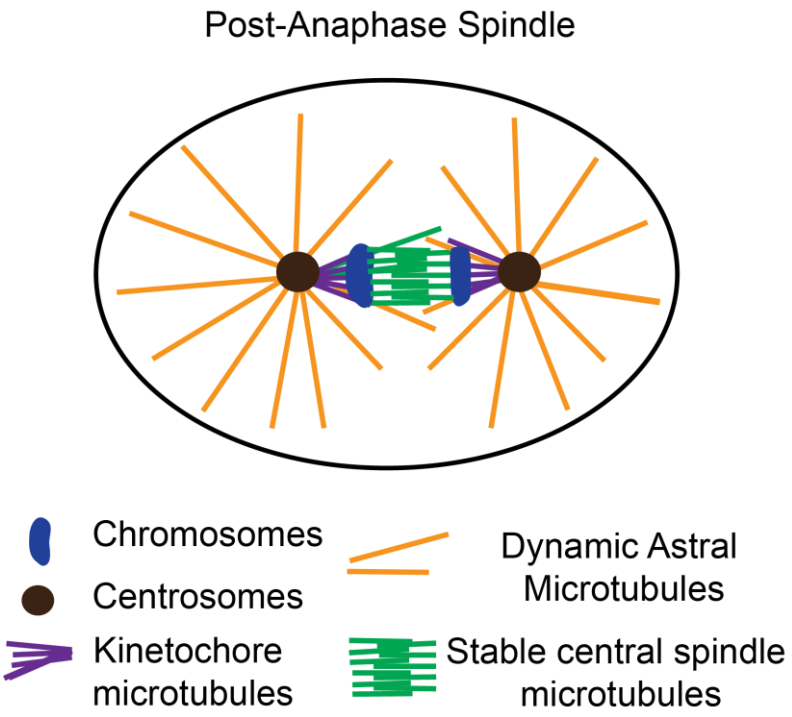

Figure 2: Components of a Post-Anaphase Spindle

Schematic of the post-anaphase spindle depicting chromosomes in blue, centrosomes in brown, astral microtubules, radiating out to the cortex, in orange, central spindle microtubules in green and kinetochore microtubules in purple.

Polar relaxation vs equatorial stimulation

There are two long-standing hypotheses that have been proposed to explain how the mitotic spindle communicates with the cortex to position the division plane. The first of these models is known as astral/polar relaxation, which asserts that as tension of the cortex is increased globally, asters signal the poles to relax. This creates a heightened tension at the equator which then allows for contraction in that region (White and Borisy, 1983; Wolpert, 1960). Modeling has shown that an elevated concentration of microtubules at the poles could produce the highest surface tension at the equator in the region of the division plane (White and Borisy, 1983; Yoshigaki, 1999). On the other hand, in the equatorial stimulation model, it is proposed that the astral centers signal to position the division plane (Devore et al., 1989; Rappaport, 1986). Experiments in support of this idea were performed by Rappaport who pressed a glass sphere into the center of sand dollar eggs to produce a donut-shaped cell. In the second division, he saw formation of a horseshoe-shaped cell between the spindles. As the cell contorted, asters moved in closer proximity to one another and an additional third furrow, which went onto completion, appeared between the two asters (Figure 3). The formation of this furrow occurred between the two asters in the absence of any chromosomes or a spindle, suggesting these are not necessary for furrow formation (Rappaport, 1961). Based on this, Rappaport stated that astral centers are able to trigger cortical contractility instead of just sending inhibitory signals as proposed in the polar relaxation model.

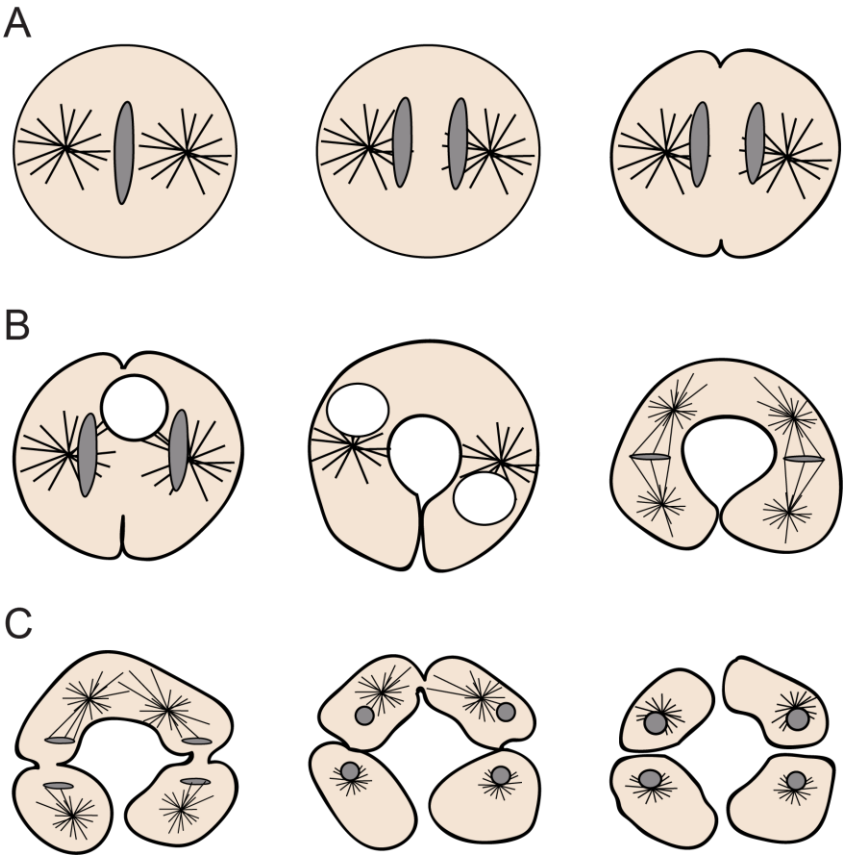

Figure 3: Torus Experiment: Formation of a non-spindle furrow

Schematic of the Torus experiment where a A) Sand dollar egg was manipulated by insertion of a B) glass bead, depicted as the white circle, to constrict the cell into a horseshoe shape. As the cell contorts with each division C) the asters move together until a furrow forms, though no spindle and chromosome is present, and the cell completes cytokinesis.

Observations made by manipulating grasshopper spermatocytes has led to the proposal of another hypothesis for division plane specification, midzone microtubule stimulation. This hypothesis posits that the signals to position the cytokinetic apparatus emanate from the subset of microtubules that form the mitotic spindle. Tissue culture cells presented with a barrier to block potential signaling between the mitotic spindle and cortex result in no furrowing prior to anaphase, further supporting that a stimulus from the mitotic spindle is an elicitor of contractility (Cao and Wang, 1996). When grasshopper spermatocytes were manipulated such that some cells contained only asters, some a mitotic spindle with no asters and chromosomes, and some with only asters and a mitotic spindle, experimenters saw a furrow form wherever mitotic spindle microtubules were present. Based on this, the investigators concluded that microtubules at the mitotic spindle were sufficient to induce furrowing (Alsop and Zhang, 2003).

Experimenters analyzing monopolar spindles in PtK1 cells somewhat bridged the above hypotheses, as results suggested that two populations of microtubules contribute to the position of the division plane and that spindle bipolarity is dispensable for cytokinesis (Canman et al., 2000). While there were many dynamic microtubules, a sub-population of stable microtubules that extended past the chromosomes prior to connecting to the cell cortex were found in both bipolar and monopolar spindles (Canman et al., 2003). Cytokinesis completed even in cells that had no microtubule overlap (Canman et al., 2003). This led the researchers to conclude that both equatorial stimulation and astral relaxation forces play a role in positioning the division plane. While a subset of microtubules are stabilized by chromosomes and are able to initiate furrowing, the more dynamic microtubules formed by asters away from chromosomes block furrowing at the polar areas of the cell (Figure 4).

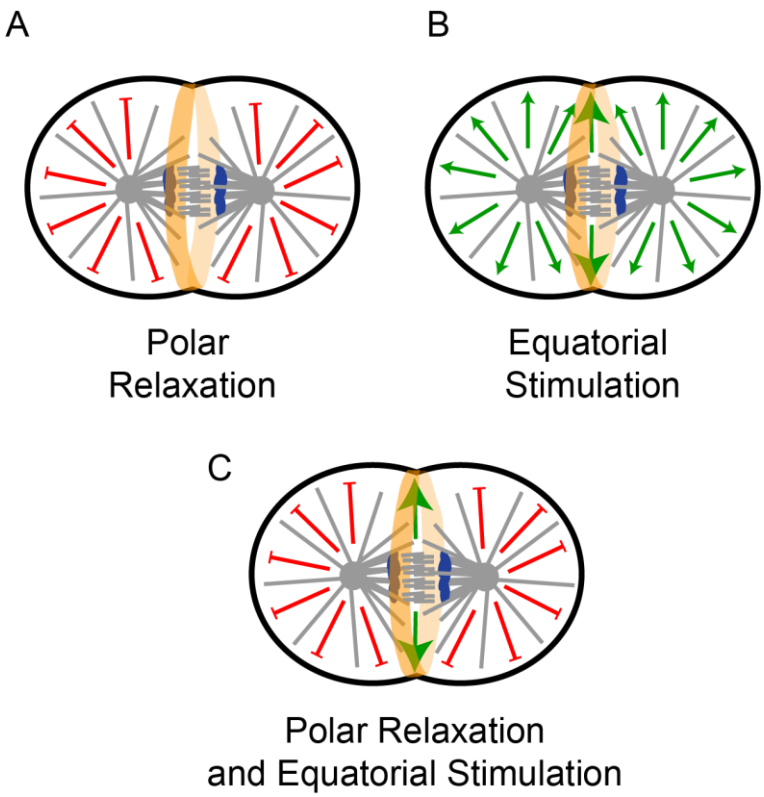

Figure 4: Relationship between the spindle and cortex

Schematics depicting A) polar relaxation model where asters relax tensions at the polar regions to heighten contractility at the equator B) equatorial stimulation model where astral centers lead to increased contractility C) polar relaxation and equatorial stimulation where two concurrent signals position the division plane. One, via a subset of sable microtubules that initiate furrowing and the other via dynamic microtubules formed by asters to inhibit furrowing away from the center.

In *C. elegans*, a combination of equatorial (midzone) stimulation and polar (astral) relaxation have been postulated to contribute to cytokinesis. Researchers used an ultraviolet laser to ablate the mitotic spindle and separated one of the asters, forcing the midzone closer to one centrosome than the other (Bringmann and Hyman, 2005). They found a cytokinetic furrow initiated between the asters but soon after, a second furrow initiated at the midzone (Bringmann and Hyman, 2005). Both furrows met to complete cytokinesis, further bolstering that the midzone and asters share redundant and consecutive functions in specifying the contractile ring (Bringmann and Hyman, 2005). However, importantly, it was not tested if ablation of the asters led to a failure to form the putative astral furrow.

De novo central spindle microtubule assembly versus pre-existing microtubules

For some time, it was unclear how the central spindle microtubules were formed--whether they were generated *de novo* or established from pre-existing microtubules derived from the pre-anaphase mitotic spindle. In microtubule depolymerization and regrowth assays, investigators observed *de novo* microtubule nucleation in the region contributing to the central spindle, suggesting that despite emerging from the mitotic spindle, the central spindle is organized by distinct factors and is largely assembled *de novo* (Uehara and Goshima, 2010). In cells where microtubules were disassembled during prophase and prometaphase via microinjection of anti-Mad2 (to bypass the spindle checkpoint) and treated with nocodazole, cortical contractility was still observed. Anti-tubulin staining revealed a central spindle complex in those cells that underwent cell division. This suggests that central spindle microtubules can form independently of a pre-anaphase mitotic spindle and/or an astral array (Canman et al., 2000).

In *C. elegans,* the kinetochore has been shown to play an important role in promoting *de novo* microtubule assembly via CLS-2 (part of the CLASP family) between separating sister chromatids (Gilliane Maton, 2015). Embryos with reduced levels of CLS-2 resulted in a loss of GFP signals from proteins that localize to the central spindle. No hemi-spindle was present and the absence of a central spindle was apparent right after anaphase onset. In HeLa cells, a kinetochore model has not yet been tested and *de novo* microtubule nucleation is partially assembled by the Augmin complex (not currently found in yeast or worms) to assemble the central spindle (Uehara and Goshima, 2010). Hence, in some organisms kinetochores contribute to microtubule assembly.

Localization of cytokinesis-essential proteins to the central spindle

The central spindle is an anti-parallel bundled microtubule array which forms at the division plane between the separating chromosomes in anaphase. Centralspindlin is a tetrameric complex made up of the kinesin-6 MKLP1 and MgcRacGAP (ZEN-4 and CYK-4 in worms) (Mishima, 2002; Pavicic-Kaltenbrunner et al., 2007). It localizes to the central spindle where it bundles antiparallel microtubules and recruits central spindle and abscission regulators (Davies et al., 2015; Green et al., 2012); White and Glotzer (2012). MKLP1 and CYK-4 are co-dependent for their localization (Jantsch-Plunger et al., 2000; Pavicic-Kaltenbrunner et al., 2007) (Figure 5).

The kinesin-6 mitotic kinesin-like protein 1 (MKLP1) has a motor domain at the N-terminal, a long linker region, a parallel coiled-coil and a C-terminal globular tail domain; mammalian cells depleted of MKLP1 fail in cytokinesis (Zhu et al., 2005). Disruption of the *Drosophila* MKLP1 ortholog, Pavarotti and *C. elegans* ortholog ZEN-4 also result in

cytokinesis failure, further supporting its conserved role in cytokinesis (Adams et al., 1998; Powers et al., 1998; Raich et al., 1998). *Pavarotti* mutants are unable to initiate contractile ring assembly while *zen-4* mutants have a mid-constriction defect, no central spindle formation, and mislocalization of actin and anillin (a scaffolding protein), and other contractile ring components in the zygote but never form a stable midbody and ultimately regress and fail to divide (Powers et al., 1998). Thus, MKLP1/ZEN-4 is an essential protein for central spindle integrity and cytokinesis completion.

The second component of centralspindlin is CYK-4. It was initially discovered in human cells as a GTPase activating protein (GAP) with high activity toward Rac (a GTPase of the Rho family discussed in more detail later) and so was named MgcRacGAP (Toure et al., 1998). Loss of CYK-4 results in an identical phenotype as loss of ZEN-4 (Jantsch-Plunger et al., 2000). It contains a short N-terminal domain, a coiled-coil C1 domain and a C-terminal GAP domain (Mishima et al., 2002). CYK-4 associates to a globular domain at the neck region of MKLP1 and causes a conformational change of two motor domains so they are more able to bundle antiparallel microtubules (Davies et al., 2015). The C1 domain of CYK-4 is also important for proper cell division as it contributes to the membrane localization of centralspindlin (Lekomtsev et al., 2012). The function of the GAP domain of CYK-4 is somewhat controversial and is the subject of Chapter 3. Thus, CYK-4 is a well conserved Rac-GAP protein that is essential for cytokinesis.

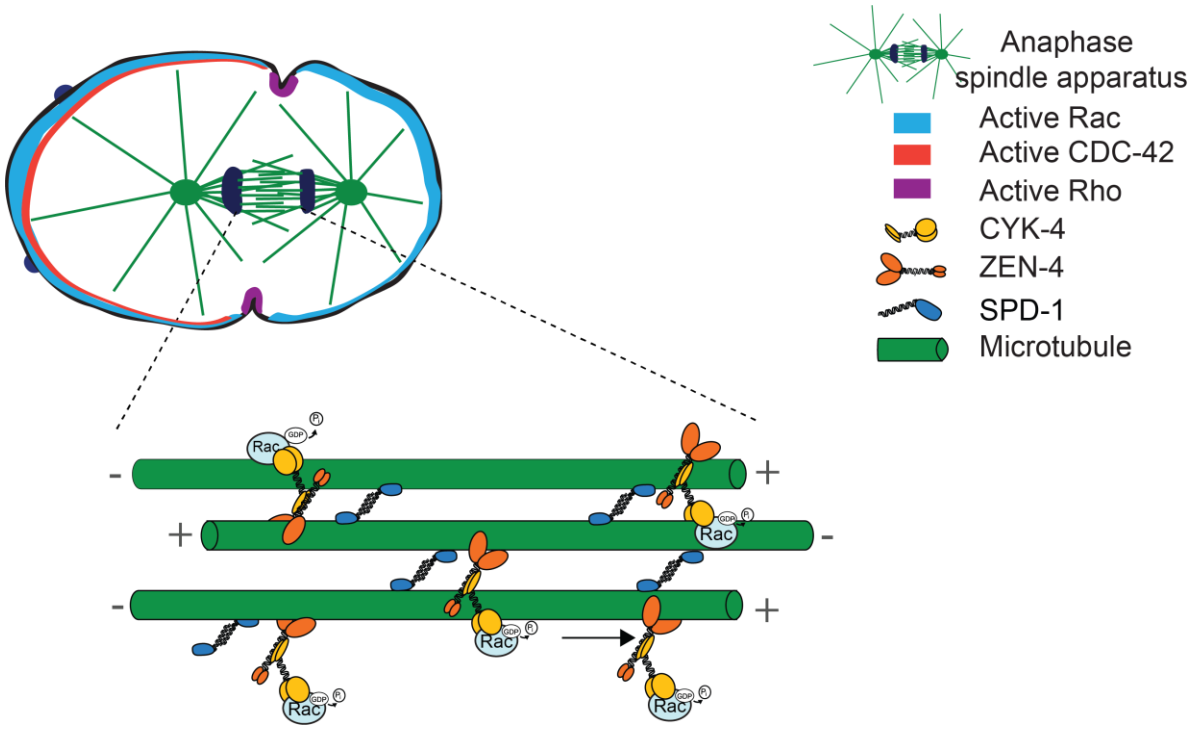

Figure 5: Key central spindle proteins

Simplified schematic of a cell undergoing anaphase depicting distinct zones of Rho GTPases. Activated Rho localizes to the division plane. Rac is shown to be enriched at the polar domains (though this has only been experimentally observed in mammalian cells). CDC-42 is shown enriched in the anterior polar region. A zoom in of the central spindle reveals binding of centralspindlin, composed of ZEN-4 and CYK-4, which go on to bundle microtubules along with SPD-1.

In addition to relying on the microtubule motor MKLP1/ZEN-4, integrity of the central spindle is also dependent on PRC1/SPD-1. PRC1, short for protein regulator of cytokinesis 1, is a mitotic-spindle-associated protein that forms homodimers to capture and bundle anti-parallel microtubules and is required to assemble the central spindle (Jiang et al., 1998; Subramanian et al., 2010). When phosphorylated, it is kept in its monomeric, inactive state by Cdk1, a cell division cycle protein (Zhu et al., 2006). Upon entry into anaphase it is dephosphorylated and able to interact with Kif4, which is responsible for transporting PRC1 to mitotic spindles (Kurasawa et al., 2004; Subramanian et al., 2010; Zhu C, 2005). Knockdown of KLP-19, which shares 41% identity with Kif-4 in *C. elegans*, did not result in cytokinesis failure, though it was important for correcting merotelic attachments (Powers et al., 2004). PRC1 was first shown to be important for cytokinesis when HeLa cells microinjected with a function-blocking antibody failed to divide, resulting in binucleation (Jiang et al., 1998). The absence of PRC1 results in no central spindle formation (Cristiana Mollinari, 2002; Kurasawa et al., 2004).

In mammalian cells, PRC1 and CYK-4 have been shown to directly interact as PRC1 binds with CYK-4, implicating a role for PRC1 in bundling microtubules (Ban et al., 2004). Although PRC1's function is essential for cytokinesis success in mammalian cells, disruption of the homolog, spindle defective 1 (*spd-1)* in *C. elegans* does not affect the 1st embryonic division and the cell completes cytokinesis. In worms, *spd-1* relocalizes from the nucleus to the central spindle at anaphase (Verbrugghe and White, 2004). In a *spd-1* temperature sensitive mutant, the spindle oscillated irregularly with the spindle poles moving independently and chromosomes appearing to "fly apart" as the spindle elongated (Baruni et al., 2008). The speed with which spindles elongate in *spd-1* and *zen-4* mutants suggests

cortical pulling forces are acting more aggressively on astral microtubules whereas normally the central spindle would resist the forces and slow segregation (Gilliane Maton, 2015). In *spd-1* mutants where the mitotic spindle was separated from one of the asters using a UV laser, only the equatorial furrow was affected (Bringmann and Hyman, 2005). Even though the central spindle was disrupted, embryos were still able to undergo cytokinesis but showed chromosomal segregation defects (Verbrugghe and White). Furrow initiation was not disturbed in *spd-1* mutants, and if anything occurred significantly earlier than in control embryos, suggesting spindle length/spindle elongation is not correlated with furrow initiation (Verbrugghe and White, 2007; Verbrugghe, 2007). Hence, although there is no central spindle in *spd-1* mutants, its requirement for cytokinesis appears context-dependent (necessary in mammalian cells but not *C. elegans* embryos).

Cytokinesis and the cell cycle- when does cytokinesis occur?

Cytokinesis completion requires coordination of important signaling networks and key protein kinases involved in the cell cycle such as cyclin dependent kinases (Cdks), Polo-like kinases (Plks), and Aurora B to activate central spindle proteins (Guse et al., 2005). Cyclin-dependent kinase 1 (Cdk1) and Cyclin B are inhibited as the cell exits from mitosis to enable progression into cytokinesis. CDK1 regulates MKLP1 by phosphorylating its motor domain and thereby inhibiting microtubule binding to the spindle at the wrong stage of the cell cycle (Mishima et al., 2002; Mishima et al., 2004; Nishimura and Yonemura, 2006). Treatment of cells with a CDK-inhibitor, BMI-1026, results in cytokinesis initiation before chromosome separation (Fumihiko Niiya, 2005). Likewise, *Drosophila* cyclin B mutant cells undergo precocious cytokinetic furrowing at an earlier stage in mitosis compared to wild type cells

(Echard and O'Farrell, 2003). *C. elegans* have multiple B-type cyclins that have overlapping functions, and to produce a similar phenotype as CDK1 inhibition, a combination of *cyb-1, cyk-3* (a B3-subfamily member), and *cyb-2.1, cyb-2.2* knockdown is necessary (Monique van der Voet, 2009). An important feature of CDKs in eukaryotes involved in the cell cycle are Thr/Tyr residues that are sites for inhibitory phosphorylation. Although in *C. elegans* there is not much literature about phosphorylation of these sites. It is clear there are many layers to the regulation of CDKs to control their functions through the cell cycle including destruction of cyclins and/or proteins associated with cyclins and activating dephosphorlyation cascades of the CDKs.

While CDK1 is a negative regulator, Plk1 and Aurora B are promoters of cytokinesis. Plk1 is suggested to be an important regulator of Cyclin B and Cdk1 activity. It was first found in *Drosophila*, where loss of Plk1 resulted in abnormal mitosis with cells unable to form a bipolar spindle and caused cell-cycle arrest (Sunkel and Glover, 1988). In mammalian cells, Plk1 overexpression causes multinucleation (Neef et al., 2003). In worms, partial knockdown of PLK-1 results in misaligned chromosomes at the metaphase plate and failure of nuclear envelope breakdown, however cytokinesis still occurs normally (Mohammad M. Rahman, 2015).

Aurora B is also a positive regulator of the cell cycle. Its phosphorylation of microtubule depolymerase mitotic centromere-associated kinesin (MCAK) relocalizes this kinesin (*klp-17* in worms) to kinetochores to ensure appropriate kinetochore attachments to the spindle (Andrews et al., 2004; Lan et al., 2004). Even though Aurora B localizes to the central spindle during anaphase onset, upshifts of an Aurora B temperature sensitive mutant found it actually functions much earlier in the cell cycle, at around the time of nuclear

envelope breakdown and early prometaphase, to support the fidelity of cytokinesis (Davies et al., 2014). In *C. elegans*, *air-2* (Aurora B ortholog) is required for targeting of centralspindlin to the central spindle (Schumacher, 1998b). Aurora B is part of the chromosomal passenger complex (CPC) and Aurora B mutants are unable to complete cytokinesis, show chromosome missegregation, and polar body extrusion defects (Goto et al., 2003; Honda, 2003; Severson, 2000; Terada, 2001). In *C. elegans* AIR-2 mutants show partial contractile ring constriction and chromosome segregation errors (Davies et al., 2014). Together, these kinases CDK1, PLK1, and Aurora B, act in concert to ensure the cell is primed to initiate cytokinesis at the right time.

Rho family GTPases and cytokinesis

Positive regulatory role for Rho during cytokinesis

Rho GTPases play a myriad of roles including actin cytoskeletal organization, cell motility, cell polarity, axon guidance, vesicle trafficking and cell cycle maintenance. They function as molecular switches that cycle between on and off states via positive and negative regulators (Etienne-Manneville and Hall, 2002). A conformational switch occurs via Guanine nucleotide Exchange Factors (GEF) that activate GTPases by catalyzing the exchange of GDP to GTP, and GAPs that inactivate GTPases by inducing GTP hydrolysis (Bos et al., 2007). Additionally, there are Guanine nucleotide-Dissociation Inhibitors (GDIs), which block nucleotide exchange and prevent membrane association (Olofsson, 1999). Five Rho GTPases have been found in worms, of which three: RHO-1 (hereafter referred to as Rho), CED-10/Rac, and CDC-42 are the best characterized.

During cell division, Rho is localized in a band at the cortical zone of the cell equator where it promotes downstream effectors to initiate constriction of the contractile ring (Kamijo et al., 2006; Nishimura et al., 1998; Takaishi et al., 1995; Yonemura et al., 2004; Yuce et al., 2005). This localization is mediated by many regulators including Ect2, Rga3/4, and Plk1 (Matthews, Delabre et al. 2012, Desai et al. 2013). Additionally, Rho functions upstream of f-actin and myosin-II (discussed in more detail later) to recruit them to the contractile ring (Alberts, 2001; Matsumura, 2005; Piekny et al., 2005). Rho's role in cytokinesis was discovered when dividing embryos injected with a dominant negative or constitutively active form of Rho or C3 (anti-Rho antibodies) transferase, failed at cytokinesis (Drechsel et al., 1997; Kishi et al., 1993; Mabuchi and Okuno, 1977). *Drosophila* embryos show cytokinesis defects when expressing mutant Rho or are injected with C3. Likewise, depletion of Rho, RHO-1 in *C. elegans*, results in no cleavage furrow ingression and cytokinesis failure (Canman et al., 2008; Jantsch-Plunger et al., 2000). Hence, Rho is a master regulator of cytokinesis and contractile ring assembly.

Since Rho is a GTPase it requires an activator and inhibitor to regulate its activity. Epithelial cell transforming sequence 2 (Ect2) is the positive regulator of Rho. Disruption of Ect2 shows similar phenotypes to Rho dominant-negative mutants. Using a Rho fret probe, investigators found lower Rho and myosin-II activity at the cortex prior to anaphase when Ect2 was silenced, further confirming a role for it upstream of Rho (Matthews et al., 2012). Knockdown of *pebble*, the Ect2 homolog in *Drosophila*, and a hypomorphic *ect-2* mutant in epidermal cells in *C. elegans* blocks contractile ring assembly, and causes cytokinesis failure (Prokopenko et al., 1999). Ect2 is needed to activate Rho at the cell equator to promote contractile ring ingression. In mammalian and *Drosophila* cells, Ect2 is localized to the

central spindle via recruitment by MgcRacGAP (*RacGAP50C* in flies*)* (Nishimura and Yonemura, 2006; Su et al., 2011). However, in *C. elegans* ECT-2 is cortically enriched (Chan and Nance, 2013). Rho activation is also mediated by other GEFs: Vav3, found in HeLa cells, where overexpression leads to similar cytokinesis defects as Rho overexpression assays (Fujikawa K, 2002). GEF-H1, also found in HeLa cells, mutants displayed blebbing, asymmetric furrowing and increased incidence of cytokinesis failure (Birkenfeld et al., 2007). The GAP RGA-3/-4 is necessary to restrict the zone of Rho activation leading to ectopic activation outside of the cell division plane (Schmutz et al., 2007; Zanin et al., 2013). Knockdown of RGA-3/-4 leads to excessive pseudo-cleavage (a cytokinesis-like furrowing event that does not lead to cell separation), hyper-contractility, membrane ruffling, and ectopic furrowing (Schmutz, Stevens et al. 2007, Zanin, Desai et al. 2013).

Spindle microtubules control a zone of active Rho at the division plane

Even though bundled microtubules at the mitotic spindle have been found to determine the position of the furrow, the molecular mechanisms were still largely a mystery. Experiments using a fluorescent reporter to probe for the small GTPase Rho finally exposed a mechanistic link between microtubules and the furrow (Bement et al., 2005). Investigators found that Rho localized to a narrow zone that corresponded with the division plane (Bement et al., 2005). It did so independently of actin as it still localized correctly in urchin embryos treated with cytochalasin D (used to block actin assembly), suggesting Rho functioned upstream of actin (Bement et al., 2005). However, microtubule disruption did negatively impact the formation of a Rho zone and furrow (Bement et al., 2005). The key experiment tested the role of spindle displacement in the position of the Rho zone. When the spindle was

displaced using a blunt microneedle, the Rho zone and furrow were repositioned, relocating to the location of the misplaced spindle (Bement et al., 2005; Mabuchi I, 1993). This demonstrates the mitotic spindle communicates with the cell cortex via Rho activation to position the division plane and constrict the contractile ring.

Rho effectors: Diaphanous family formins

Rho GTPase family members, and Rho in particular, are important in actin dynamics. Actin can be present in the form of G-actin, as a monomer, or as F-actin where it is part of a linear polymer of G-actin subunits (Schmidt and Hall, 1998). F-actin assembly is an unfavorable and slow event due to the instability and dissociation of actin dimers and trimers (Tobacman and Korn, 1983). Nucleating factors (*e.g.* the Arp2/3 complex, formin proteins, Spire, etc.) are required to initiate assembly of F-actin *in vivo*. Here I will focus on the nucleating factor diaphanous-family formin, which is required for contractile ring constriction.

The actin cytoskeleton is comprised of both linear and branched filament networks that contribute to cell division via contractile ring constriction and cell migration via leading edge protrusion (Pollard et al., 2000; Pruyne et al., 2002). During cytokinesis in metazoan cells, diaphanous-family formins are essential for actin filament assembly (Watanabe et al., 2008). Diaphanous formins were first identified in a *Drosophila* screen looking for spermatogenesis defects where *dia* was found to cause sterility and lethality due to cytokinesis defects (Castrillon DH, 1994). F-actin recruitment appears to be non-muscle myosin II independent as F-actin in COS-7 cells was able to accumulate at the equatorial furrow even in cells where non-muscle myosin II was knocked down (Xuefei Ma, 2012). In NIH 3T3 cells,

anti-mDia-1 antibody injection leads to cytokinesis failure with little furrowing or contractile ring constriction (Tominaga et al., 2000). In *C. elegans,* there are 7 formin-encoding genes, with CYK-1 being the diaphanous-related formin required for cytokinesis (Davies et al., 2014; Severson et al., 2002). In *C. elegans,* CYK-1 localizes to the leading edge of the contractile ring (Swan et al., 1998), and loss of CYK-1 activity results in cytokinesis failure and prevents contractile ring constriction (Davies et al., 2014; Gonczy et al., 2000; Swan et al., 1998). The requirement for diaphanous-family formin in cytokinesis is well conserved throughout eukaryotes.

Diaphanous-family formins contain active domains that promote actin assembly and regulatory domains that control this activity (Alberts, 2001; Watanabe et al., 1999). The C-terminal active region is made up of formin homology 1 (FH1) and FH2 domains (Higgs and Peterson, 2005; Otomo et al., 2005; Pring et al., 2003). The FH1 domain contains a profilin-actin binding site which recruits actin monomers (Paul and Pollard, 2009). The FH2 domain promotes dimerization and association with the barbed (plus) end of an actin filament and is the most conserved domain in formins across phylogeny (Otomo et al., 2005; Xu et al., 2004). Diaphanous-family formins also contain a C-terminal regulatory Diaphanous Autoregulatory Domain (DAD), which interacts with the FH3 (DID) domain at the N-terminus to inhibit actin assembly by the FH2 domain (Alberts, 2001). The auto-inhibitory interactions of the FH3(DID)-DAD domains can be released by the GTPase binding domain (GBD), that is activated by Rho family members such as Rho (Sagot et al., 2002; Watanabe et al., 1999) (Figure 6).

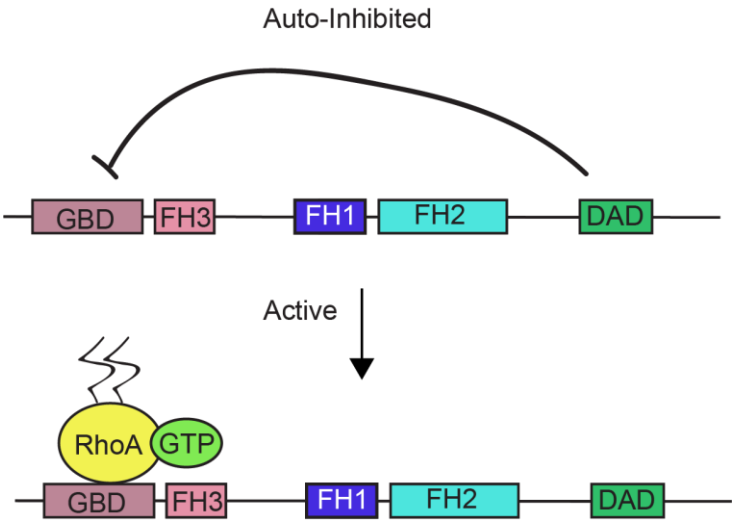

Figure 6: Diaphanous-family formins are activated by Rho family GTPases

Schematic of Diaphanous-family formins, with conserved domains, depicted in the inactive state where the DAD domain inhibits the GBD/DID domain and an active state where Rho binding activates these formins.

Rho effector: Non-Muscle Myosin-II

Non-muscle myosin-II (hereafter myosin-II) is the major motor protein responsible for cytokinesis (Mabuchi and Okuno, 1977). It is a hexamer, made up of 2 myosin heavy chains (MHC), 2 essential light chains (Machacek et al.) and 2 regulatory light chains (RLC) (Tan et al., 1992). The light chains bind myosin-II at the alpha-helical neck region, and are the site of phosphorylations responsible for the activity or inactivity of the head domain. The C-terminal domain of myosin-II is made up of a coiled-coil rod that can dimerize and oligomerize with other myosin molecules, thereby forming short bipolar filaments, much like those found in the thick filaments of muscle tissue. Phosphorylated myosin-II is recruited to the furrow at early anaphase via Rho activation and inhibition of its ATPase activity (Sellers, 1991). CDK1 inhibits myosin ATPase activity by phosphorylating at Ser1, 2, and 9 MLC sites (Bengur et al., 1987). Thus, myosin-II activity in cytokinesis is driven by several phosphorylation events.

Myosin-II was first shown to be essential for cytokinesis in echinoderm blastomeres that were injected with anti-myosin antibodies. While the mitotic cycle was not affected in these blastomeres, cytokinesis was still blocked (Kiehart et al., 1982; Mabuchi and Okuno, 1977). The importance of myosin-II in cytokinesis was further shown in *Dictyostelium* and *S. cerevisiae* (Bi et al., 1998; Zang et al., 1997). Disruption of *spaghetti squash*, a gene that encodes the RLC of non-muscle myosin-II, results in little membrane ingression (Karess et al., 1991). In *C. elegans*, mutants for MLC-4, the homolog for the RLC, also results in loss of membrane ingression (Shelton et al., 1999a). Myo1, the only myosin-II in budding yeast, MHC domain mutants result in abnormal cell division and cell wall organization at the bud neck of *S. cerevisiae*, displaying chain-like growth with attached daughter cells (Bi et al.,

1998; Fang et al., 2010; Lippincott and Li, 1998). Therefore, myosin-II is the major motor protein responsible for cytokinesis (Mabuchi and Okuno, 1977).

While actin and myosin function together to constrict the ring, their localization to the division plane occurs independently. When actin filaments were disrupted in sea urchin embryos using latrunculin A, myosin-II clusters were still able to localize to the division plane (Henson et al., 2017). In S2 cells, myosin-II was found to accumulate at the furrow before F-actin enrichment and was still expressed after Latrunculin A treatment was used to disrupt the actin filaments (Dean et al., 2005). Both in budding and fission yeast, myosin-II ring localization was unaffected by actin depolymerization after formation of the actomyosin ring (Bi et al., 1998; Naqvi et al., 1999). Myosin-II was also still able to localize to the ring even after insult to its actin binding motor domain (Beach and Egelhoff, 2009). Together this evidence supports the notion that myosin-II is recruited in an actin-independent manner (Henson et al., 2017).

Myosin-II is able to mediate its contribution to contractile ring constriction via phosphorylation and dephosphorylation events. Four well-studied upstream myosin-II regulators in mammals involved in phosphorylation of MLC at Ser19 and Thr18 are Rho-kinase inhibitors (Mahlert et al.), Citron kinase, Myosin light chain kinase (MLCK), and myosin phosphatase (MYPT). Mutations in MYPT vary in their degree of severity on cytokinesis depending on the organism. In worms *mel-11*, the MYPT ortholog, results in ectopic furrowing and faster cleavage furrow ingression kinetics with cells still able to complete cytokinesis (Piekny and Mains, 2002).. In *Drosophila*, there doesn't seem to be any effect in cytokinesis (Piekny and Mains, 2002). The precise role of citron at cytokinesis seems to be inconsistent between species as it is not essential in worms, mice or rats, but is required

in several other systems such as *Drosophila* S2 cells, neuronal cells and developing spermatocytes (Bassi ZI, 2011; Cunto et al., 2002; Sonnichsen et al., 2005).

There appears to be a lot of redundancy in the regulation of myosin-II. MLCK is not essential for cytokinesis in all cell types since mice with an MLCK knockout develop fine in-utero and only die shortly after birth (Somlyo et al., 2004). In *C. elegans,* RNAi against calmodulin (a calcium binding messenger protein) and candidate MLCKs, also had no effect on cytokinesis in control or let-502, homolog of ROCK, mutant embryos (Ellen L. Batchelder, 2007). Likewise, the inhibition of ROCK using Y27632 did not result in cytokinesis failure in HeLa cells but did show slower contraction kinetics (Kosako et al., 2000). In *Drosophila,* ROCK mutation phenotypes are limited to specific tissues in the wings and eyes but do not seem to affect the organism overall (Shandala et al., 2004). Mutations in *let-502,* resulted in little or no pseudocleavage and sometimes in cytokinesis failure (Piekny and Mains, 2002). While Rho is involved in recruiting non-muscle myosin-II to the contractile ring, the exact mechanism for how this occurs in *C. elegans,* is still unknown.

Other actomyosin binding proteins and cytokinesis

A number of additional actomyosin binding proteins such as profilin, cofilin, anillin, and septins also play functional roles in the contractile ring. Formin binds profilin, which increases the elongation rate of actin filaments by stimulating actin monomers into filaments via exchange of ADP bound actin to ATP Paul and Pollard (2008). *C. elegans* expresses 3 isoforms of profiling: PFN-1, PFN-2, and PFN-3, all of which are involved in binding actin or manipulating actin dynamics (Polet et al., 2006). Cofilin (*unc-60B in worms)* is involved with actin disassembly by increasing the rate of dissociation of actin monomers at the minus end

via severing and depolymerization, which destabilizes the actin filaments and increases actin turnover (Gunsalus et al., 1995; Mabuchi, 2006; Yamashiro et al., 2005). While these proteins are important in mammalian cells, their function in *C. elegans* is not well defined.

Other important actomyosin cross-linkers in the contractile ring are anillin and septin. The role of anillin in cytokinesis is context dependent. It is important for the structural integrity of the cleavage furrow in HeLa cells and its disruption results in 15-20% cytokinesis defects but is largely dispensable in *C. elegans* (Piekny and Glotzer, 2008; Straight et al., 2005; Zhao and Fang, 2005a). It is a crosslinking protein that binds f-actin, myosin-II, Rho, Cyk-4, and septins (Buttery et al., 2012; Watanabe et al., 2010; Wernike et al., 2014). In *C. elegans, ani-1*, the homolog for anillin, has been implicated in driving asymmetric ingression from one side of the division plane and also plays a role in polar body emission, driving one of the most asymmetric divisions in the cell (Dorn et al., 2010; Maddox et al., 2007). While anillin has many binding partners, with the except for septin, it is not essential for their recruitment to the contractile ring (Field et al., 2005; Maddox et al., 2005).

Like anillins, the requirement for septins is context and organism-dependent. Though important for proliferation in *Drosophila* imaginal tissues and some human cell-types, they are largely not essential for cytokinesis, even though they concentrate at the site of cell division (Adam J. C., 2000; Echard et al., 2004; Fares et al., 1995; Haarer and Pringle, 1987; Kinoshita et al., 1997; Longtine et al., 1996; Maddox et al., 2005; Maddox et al., 2007; Manoj B. Menon, 2015; Neufeld and Rubin, 1994; T.Q. Nguyen, 2000). In *C. elegans* there are only two septins, UNC-59 and UNC-61, while there are many more in other organisms (14 in humans and 5 in flies) (Kinoshita, 2003; Pan et al., 2007). UNC-59 and UNC-61 localize to the leading edge of cleavage furrows but their depletion does not cause gross cytokinetic

defects (Maddox et al., 2007; T.Q. Nguyen, 2000). Overall, the functional contribution of septins in cytokinesis is still elusive.

Other Rho Family GTPases and cytokinesis

Rac negatively regulates cytokinesis

Rac was initially found as a Ras-related C3 botulinum toxin substrate 1 (Didsbury et al., 1989). Since then, it has been implicated in regulating cytoskeletal organization, axonal guidance, cell proliferation, cell migration and transcription. It has also been proposed to negatively regulate constriction of the contractile ring by stimulating activation of the actin-related protein 2/3 (Arp2/3) complex and formation of branched f-actin (Canman et al., 2008). The Arp2/3 complex forms at the leading edge of motile cells where its production of branched filaments generate enough force to push the leading edge forward (Pollard and Borisy, 2003). Rac regulates this activity via WAVE and WASP, which stimulate actin polymerization by the Arp2/3 complex (Pollard and Borisy, 2003; Steffen et al., 2004). It is possible the Arp2/3 complex nucleated branched-actin filaments are less conducive to myosin-II motor-driven constriction than the linear f-actin produced by diaphanous family formins.

As a negative regulator, blocking Rac activity does not cause cytokinesis defects while overexpression of Rac in HeLa and Rat1A cells did cause cytokinesis failure and multinucleation (Dutartre et al., 1996). In HeLa cells, as cytokinesis progressed Rac activity was lower at the site of the division plane and increased at the polar regions of the plasma membrane. Cells expressing a dominant negative mutant of *cyk-4* showed Rac levels remained high at the site of the cytokinetic furrow, supporting evidence for a direct interaction

between CYK-4 and Rac (Yoshizaki et al., 2004). While still contentious, there is additional evidence that Rac activity is inhibited by CYK-4 (discussed more in depth in Chapter 3). In cultured cells and in *Drosophila* mutants, double depletion of *cyk-4* and Rac, or its effectors, largely suppressed the cytokinesis failure phenotype caused from loss of *cyk-4* alone (Bastos et al., 2012; Canman et al., 2008; D'Avino et al., 2004; Loria et al., 2012; Zhuravlev et al., 2017). It has also been proposed that inhibition of Rac leads to a reduction in adhesion at the division plane. Downregulation of Rac binding partners such as ARHGEF7, PAK1, and PAK2 reduced the mutinucleation phenotype in cells with constitutively active Rac (Zuo et al., 2014). A GAP-dead CYK-4 mutant showed more cell substrate adhesion and abnormal adhesion fibers further supporting a role for *cyk-4* in blocking adhesion driven by Rac activity at the division plane (Bastos et al., 2012).

CDC-42 and cytokinesis

Like depletion of Rac, cytokinesis is not negatively affected in the absence of Cdc42 but overexpression assays in Hela cells, using a constitutively active Cdc42, resulted in disoriented F-actin and giant multinucleated cells implicating this GTPase in cytokinesis (Dutartre et al., 1996; Zhu et al., 2011a). Cdc42 was discovered as a cell cycle gene in *S. cerevisiae,* important for proper bud formation and orientation (Johnson and Pringle, 1990). Although loss of Cdc42 did not impact cytokinesis integrity in HeLa cells, they did display a less narrow zone of Rho at the division site and fewer F-actin filaments (Zhu et al., 2011b). In *C. elegans* loss or overexpression of CDC-42 on its own does not cause cytokinesis failure (Jordan et al., 2016). Hyper-activation of Cdc42 hindered cytokinesis in *Xenopus* embryos and rat kidney epithelial cells (Drechsel et al., 1997; Zhu et al., 2011). In *C. elegans* and other

organisms, Cdc42 is enriched asymmetrically, forming a polar cap in the anterior domain (Kumfer et al., 2010). Cdc42 is required for polar body emission in *Xenopus* and mouse oocytes (Maddox et al., 2012; Na and Zernicka-Goetz, 2006). Cdc42 localizes to both the mitotic and central spindle in stained mouse embryos so more direct roles for it in cytokinesis may yet to be discovered (Bielak-Zmijewska et al., 2008). Perhaps related to its potential role in cytokinesis, Cdc42 is also important for cell polarity maintenance during asymmetric cell division (see more below).

Asymmetric cell division

Symmetric verses asymmetric cell divisions

Cytokinesis can result either in a symmetric cell division, resulting in daughter cells that share the same cell fate and/or size, or in a polarized asymmetric cell division, resulting in daughter cells that differ in cell fate or size (Barr and Gruneberg, 2007; Williams and Fuchs, 2013). The *C. elegans* zygote or one-cell embryo, undergoes a polarized asymmetric division, and has been a seminal model system to study how cell polarity and daughter cell asymmetry are regulated. In *C. elegans*, the first polarity cue is triggered by the entry of sperm that contribute their centrioles and determine the posterior end of the embryo (Goldstein and Hird, 1996). Asymmetric divisions are an important way for cells to generate diversity by altering distribution of cytoplasmic components and thereby cell fate.

Because the position of the mitotic spindle determines the position of the contractile ring, it thereby establishes the size of the daughter cells, with a spindle positioned in the middle resulting in equal sized daughter cells and a displaced spindle resulting in asymmetric cells. In one-cell *C. elegans* embryos increased posterior cortical microtubule pulling forces

leads to displacement of the spindle more towards the posterior, which leads to the production of a larger anterior daughter cell and a smaller posterior cell (Gonczy and Hyman, 1996; Grill et al., 2001). This asymmetric spindle positioning is controlled by the cell polarity or PAR proteins (see below)

PAR proteins in cell polarity establishment and maintenance

Asymmetric division requires the PAR proteins (PARtionining defective), which localize to opposite sides of the cell to regulate unequal cytoplasmic and cortical inheritance of the daughter cells (Cabernard et al., 2010; Goldstein and Macara, 2007). The core PARs consist of anterior pars (aPARs; PAR-3, PAR-6, PKC-3, myosin-II, and Cdc42) and posterior pars (pPARs; PAR-1, PAR-2 and LGL-1), so named for their respective localization within the embryo (Rose and Kemphues, 1998). Prior to fertilization, aPARs are distributed equally along the cell membrane, however they become restricted to the anterior upon sperm entry (Boyd, 1996; Guo and Kemphues, 1995; Hoege and Hyman, 2013). Loss of the PAR proteins in *C. elegans* eliminates cell asymmetry, by reducing the pulling forces of the asters to no longer displace the spindle more to the posterior pole, and is a cause of differential cell fate specification between daughter cells, but does not lead to cytokinesis failure on its own.

In *C. elegans,* polarization occurs after fertilization and takes place in two phases: establishment and maintenance. During polarity establishment, the sperm-derived centrosomes (and perhaps asters) trigger the accumulation of PAR-2 and movement of PAR-6/PAR-3/PKC-3, myosin-II, and CDC-42 from the presumptive posterior domain to form an anterior cap (Hehnly and Doxsey, 2012; Munro and Bowerman, 2009). These opposing domains are guided by actomyosin-based cortical and cytoplasmic flows (Cheeks et al., 2004;

Hird and White, 1993; Munro et al., 2004), and are maintained by mutual inhibition at the anterior-posterior aPAR-pPAR boundary (Cuenca et al., 2003). Mutations and chemical treatments that affect myosin-II and/or actin result in mislocalization of the PAR proteins, suggesting that cortical and cytoplasmic flows are dependent on actomyosin contractility and myosin-II (Guo and Kemphues, 1995; Guo and Kemphues, 1996; Munro et al., 2004; Severson and Bowerman, 2003; Shelton et al., 1999a). While the concentration of myosin-II becomes downregulated once the PAR domains are established, there is a notable increase in concentrations of myosin-II*::gfp* that form an anterior-cap. Disruption of myosin-II during establishment results in a completely anteriorized cortex with the posterior PARs excluded from the cortex (Cuenca et al., 2003). In addition, Rho and ECT-2 have also been implicated in polarity establishment. Depletion of Rho or ECT-2 show a reduced accumulation of GFP:PAR-6 at the cortex compared to wild-type embryos, and the signal was never restricted to the anterior cortex (Motegi and Sugimoto 2006). This suggests that Rho and ECT-2 are required for the initial polarization of PAR-6 during polarity establishment.

Polarity maintenance is when the aPAR-pPAR boundary is located at the division plane with the anterior and posterior domains distinguished by mutual inhibition of the PAR proteins, whereby aPARs are required for the localization and restriction of the pPARs and vice versa (Beach and Egelhoff, 2009; Cuenca et al., 2003; Motegi et al., 2011). Mutual inhibition is thought to be accomplished via changes in phosphorylation leading to inhibition of PAR-1 and PAR-2 by atypical protein kinase C (PKC-3), which may change their affinity for the membrane or cortex of the cell if they cross into the anterior boundary (Beatty et al., 2010). After pseudocleavage, *par-2(RNAi)* embryos showed a redistribution of myosin-II fibers over the entire surface and PAR-6 relocalized to the posterior cortex as a result of

changes to the cortical flow (Munro et al., 2004). Therefore, PAR-2 is vital to inhibit myosin-II from the posterior and maintenance of anterior-directed cortical flow to prevent redistribution of anterior PAR proteins. The anterior PARs, PAR-3, PAR-6 and PKC-3 are co-dependent for cortical localization so the loss of even one of the aPARs eliminates pPARs exclusion from the anterior and the entire embryo becomes "posteriorized" (Cheeks et al., 2004; Cuenca et al., 2003). While not required for anterior-posterior polarity establishment, Cdc42 has a conserved role in polarity maintenance. Disruption of Cdc42 blocks the localization of PAR proteins in *C. elegans* embryos; in particular, PAR-3, PAR-6, and PKC-3 are no longer restricted to the anterior (Gotta et al., 2001; Motegi and Sugimoto, 2006) During polarity establishment, *cdc-42(RNAi)* embryos showed normal enrichment of GFP-moe (used to tag the filamentous actin-binding domain) at the anterior and PAR-6 but at polarity maintenance *cdc-42(RNAi)* embryos showed loss of GFP-moe and PAR-6 accumulation, suggesting CDC-42 is not essential during the establishment phase but is essential later (Motegi and Sugimoto, 2006) (Figure 7).

PAR-5 is responsible for maintaining the opposing PAR boundaries, and unlike many other PAR proteins, PAR-5 is symmetrically localized in the early embryo (Morton et al., 2002). In the absence of PAR-5, both aPARs and pPARs become uniformly distributed on the cell cortex (Morton et al., 2002) (see also Chapter 2). PAR-5 is a member of the 14-3-3 family of proteins. 14-3-3 proteins can self-assemble into homodimers and heterodimers (Aitken et al., 2002). As dimers, they can interact and regulate a host of proteins, where they go on to relay signaling cues to regulate protein trafficking, apoptosis, metabolism, cytokinesis, cell-cycle timing, etc. (Wilker et al., 2007). PAR-5 is also a known target of Aurora B during cytokinesis (Basant et al., 2015; Douglas et al., 2010).

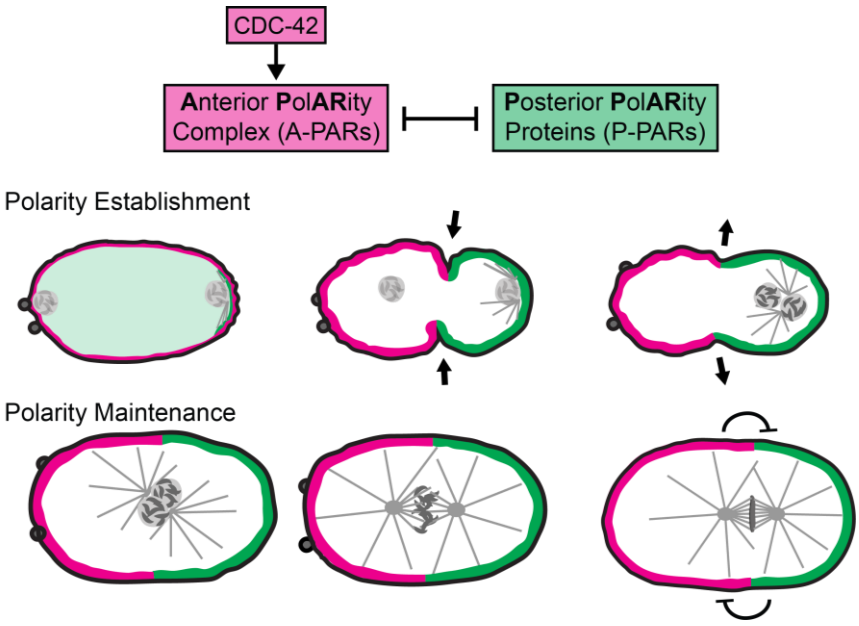

Figure 7: PAR proteins in cell polarity establishment and maintenance.

Schematic of changes to the localization of polarity proteins during polarity establishment and maintenance. At polarity establishment, anterior polarity proteins are localized all along the cortex. As the cell undergoes pseudocleavage, the aPARs become restricted to the anterior cortex and pPARs to the posterior. At polarity maintenance, A-P domains are localized to opposing poles of the cells, maintained via mutual inhibition.

Cytoplasmic asymmetry and the PARs

Downstream of the core PARs are PAR-1 and PAR-4, which are involved in regulating cytoplasmic asymmetries such as the asymmetric distribution of organelles and difference in cell cycle timing. PAR-1 is a serine-threonine kinase that is enriched in the posterior cortex (Boyd et al., 1996; Guo and Kemphues, 1995). *In* vitro, it has been found to phosphorylate PAR-3 (Hoege, 2010). Loss of PAR-1 causes loss of posterior enrichment and uniform distribution of P granules (Kemphues et al., 1988).

PAR-4, also a serine-threonine kinase, is distributed uniformly along the cortex and cytoplasm, so unlike the core PAR proteins, its distribution is not dependent on other PARs (Watts et al., 2000). While loss of PAR-4 also causes cells to lose their asynchronous cell cycle timing and spreads perinuclear RNA granules (P-granules) to all cells, there is little change in the spindle displacement and cell size asymmetry is maintained (Crittenden et al., 1997; Jordan et al., 2016; Kirby et al., 1990). PAR-4 has also been implicated in regulating myosin and furrow positioning during cytokinesis (Benkemoun et al., 2014; Pacquelet et al., 2015). In mammals, LKB1 (mammalian PAR-4) phosphorylates as many as 14 downstream kinases, including PAR-1, and is involved in many processes contributing to cell homeostasis (Alessi et al., 2006).

Polarity proteins are also involved in cell-cycle regulation. To regulate cell cycle progression PAR proteins act through muscle in excess-5/6 (MEX-5/6), two cytoplasmic zinc-finger RNA binding proteins that are distributed in a gradient in the cytoplasm following the A-P axis (Schubert et al., 2000). PAR-1 is largely responsible for the distribution of MEX-5 through phosphorylation and dephosphorylation reactions (Daniels et al., 2010; Tenlen et al., 2008). MEX-5/6 are also important in specifying germline asymmetry and through PAR

polarity proteins, such as PAR-4, maybe be responsible for the exclusive distribution of P-granules to the P2 cell (Schubert et al., 2000). MEX5/6 go on to regulate division timing by binding to PLK-1 and increasing its concentration in the anterior cytoplasm at the one-cell stage (Nishi et al., 2008). Consequently, the anterior AB cell has higher levels of PLK-1 than the posterior P1 cell and goes onto divide approximately two minutes earlier (Budirahardja and Gonczy, 2008, Brauchle, Baumer et al. 2003). As the embryo develops, the asynchronous cell cycle timing is maintained unless polarity proteins are disturbed (Bao, Zhao et al. 2008). In summary, polarity proteins are important in regulating many asymmetrical properties of the cell including inheritance of cytoplasmic components, cell cycle timing, and cell fate.

Cell fate specification and cytokinesis

Cell specific cytokinesis failure

The consequences from cytokinesis failure is not equal across all cell-types. While often it may lead to deleterious repercussions, there are also many cases where cytokinesis failure is programmed to occur. In the literature, there are already many studies that show specific cell-type dysregulation of cytokinesis (Iolascon et al., 2013; Moulding et al., 2007; Vinciguerra et al., 2010). One possibility in why some cells are fated to fail while others are not is that differences in cell "identity" may affect how the cytokinetic machinery drives cell division. Variation in regulatory mechanisms of cytokinesis could be due to factors that are intrinsic or extrinsic to the cell. Intrinsic factors such as cell polarity and RNA granule inheritance have been shown to contribute to robustness of cytokinesis (Cabernard et al., 2010; Jordan et al., 2016). Extrinsic factors such as cell-cell interactions and cell fate

signaling molecules have also been implicated in cytokinesis (Fumoto et al., 2012; Herszterg, 2013).

Notch/Delta signaling and cytokinesis

The Notch/GLP-1 signaling pathway is implicated in many aspects of maintaining homeostasis and cell differentiation (Artavanis-Tsakonas et al., 1999). Notch and most of its ligands are transmembrane proteins that are comprised of many EGF repeats and must be adjacent to the ligand expressing cell to perform its function (Shaya et al., 2017). Synthesized as an inactive precursor, the Notch protein undergoes three different cleavage events in order to become active. The final cleavage event is by γ-secretase, which releases the Notch intracellular domain. It is then translocated into the nucleus to repress or activate gene expression.

Notch is an important gene of interest for its role in oncogenesis and ironically also as a potential tumor suppressor (Rangarajan et al., 2001). Aurora B is necessary for accurate mitosis and may have great potential as a therapeutic agent for cancer though in human cancer cell lines the cells are resistant to Aurora B inhibitors. This resistance is more prevalent in cells with mutations in the Notch1 receptor, which also show an increased chromosome number, potentially implicating a role for Notch in cytokinesis (Moy et al., 2011). γ-secretase is a protease necessary for activating Notch. In studies where Notch1 activity was downregulated in combination with GSIs (γ-secretase inhibitors) the cell lines became more resistant to chemotherapy in the study of T-cell lymphoblastic leukemia (T-ALL) cancer cell lines, while in other studies the combination of treatment has shown to induce cell growth arrest and cell apoptosis. In other studies, the number of multipolar spindles were amplified

when both γ-secretase and microtubule dynamics were perturbed (Singh et al., 2014). In *Drosophila* sensory organ precursors, Notch localizes to the division plane (Coumailleau et al., 2009). Further, in cortical neurons, treatment with Delta, the Notch ligand, is able to induce bundled microtubules (Ferrari-Toninelli et al., 2008). Thus, it is possible that in addition to its many functions, Notch may also be directly involved in cytokinesis.

Wnt signaling and cytokinesis

Like Notch, Wnt/MOM-2 signaling is important for a plethora of cell functions such as cell proliferation, migration, axonal growth, differentiation and polarity. *C. elegans* employ both canonical and non-canonical pathways of Wnt signaling. In the canonical pathway, Wnt binding results in the translocation of BAR-1, a ß-catenin, to the nucleus. In the non-canonical pathway, worms use *wrm-1* as the ß-catenin instead of *bar-1*. Without the Wnt signal, ß-catenin is targeted for ubiquitination and degradation (MacDonald et al., 2009). *C. elegans* have 5 Wnt ligands and 4 Wnt receptors (I will expand on two of these, *mom-2* and *mom-5*, in Chapter 4) (Korswagen, 2002). These signaling proteins are important at the 4-cell stage embryo. In the non-canonical pathway, signaling from *mom-2* (ortholog of Wnt) at the P2 interface to its receptor *mom-5* (ortholog of *Frizzled),* at the EMS cortex, is required for endoderm formation (Goldstein, 1992). Wnt protein function relies on lipid modification (Willert et al., 2003) and cell positioning since it acts as a short-range signal often dependent on neighboring cell contact for its function (Sato et al., 2011; Strand and Micchelli, 2011).

There is some evidence for a link between cytokinesis and Wnt signaling. Cytokinesis proteins Tumbleweed (*Drosophila* homolog of CYK-4) and Pavarotti (homolog of MKLP1) have been found to negatively regulate Wnt activity by inhibiting armadillo (ß-catenin in flies) from activating gene expression at the nuclei of cells at interphase instead of their

traditional expression at the division plane (Jones WM, 2010). In addition, Wnt family members have been found to regulate levels of cytokinesis genes that are involved in human cancer cells (Pandi et al., 2014). In *Drosophila,* Wnt5a localized to the midbody and inhibition of Wnt5a caused cytokinesis failure (Fumoto et al., 2012). In mammalian neuronal cells, Wnt induced axon remodeling invoked changes that are correlated with increased microtubule stability (Salinas, 2007). It may be worthwhile to investigate if Wnt also has a protective role in cytokinesis.

Abscission

Once the contractile ring nears full constriction, the central spindle matures to form the midbody, which serves as a platform for the assembly of abscission proteins (Agromayor and Martin-Serrano, 2013; Fededa and Gerlich, 2012). The midbody, also known as the intracellular bridge, is made up of a condensed antiparallel microtubule array, retaining many contractile ring and central spindle components such as SPD-1, centralspindlin, and the CPC (Glotzer, 2005; Green et al., 2012). While PRC-1 and the CPC associate with the midbody, centralspindlin translocates from the midbody core to another midbody component, the midbody ring (which encircles the core) (Hu, et al. 2012, Elia, et al. 2011). The midbody ring also retains many of the same components involved with contractile ring constriction such as actin, myosin-II, and even septin and anillin (Madaule, et al. 1998; El Amine, et al. 2013; Hu, et al. 2012). To clear what is left of the intercellular bridge/midbody remnant, the cell regulates vesical trafficking and recruits the ESCRT complex to engulf the remainder of the cytokinetic machinery (Bastos and Barr, 2010; Carlton, 2007; Fabbro et al., 2005; Guizetti et al., 2011; Lee et al., 2008; Morita et al., 2007; Schiel et al., 2013; Zhao et al., 2006).

Depletion of TSG-101 (an ESCRT-I subunit) in *C. elegans* blocked recruitment of the endosome sorting complexes required for transport (ESCRT-III) and disrupted membrane internalization and engulfment of the midbody remnant (Konig et al., 2017). In contrast, loss of ESCRT-III assembly in *Drosophila* cells did not impact midbody membrane engulfment (El Amine et al., 2013). Actin is also recognized to play a role in abscission as permeabilized *C. elegans* embryos treated with latrunculin A were unable to normally engulf the midbody remnant (Konig et al., 2017). Remarkably, *C. elegans* embryos depleted of SPD-1 (to disrupt microtubule bundling), still showed midbody ring release, suggesting midbody microtubules are dispensable for abscission (Green, et al. 2013). In *Drosophila* S2 cells, the anillin C terminus links septin and the midbody ring to the plasma membrane while the N terminus shows anillin binding activity toward actin and myosin-II (Kechad A, 2012; Lekomtsev, 2012). In *C. elegans*, inhibition of septin resulted in abnormal midbody/midbody ring release even though ESCRT machinery was still recruited. In either case, abscission is an extremely robust process that likely has many compensatory mechanisms as even in the absence of the ESCRT complex, the cell still completes separation, though the process may be delayed (Green et al., 2013; Konig et al., 2017). Study of abscission is revealing ever more complexity and is an interesting area for future research.

Non-canonical mechanisms of cytokinesis

Traction mediated cytofission

In addition to canonical cytokinesis driven by constriction of an actomyosin ring, some cells have adapted to use different methods to get around the same problem of physically partitioning a cell into two. *Dictyostelium* with an MHC gene deletion still round

up during mitosis and even complete nuclear division but fail at cytokinesis in suspension cultures, resulting in large multinucleate cells (Knecht and Loomis, 1987). However, when grown on an adhesive surface, myosin-II loss does not block division in *Dictyostelium* (Zang et al., 1997). This suggests cells able to brace themselves against a surface to generate tension are able to compensate for the loss of myosin-II. This method of division is known as traction-mediated cytofission (De Lozanne and Spudich, 1987). In epithelial human cell lines that were chemically treated to cause cytokinesis failure, binucleate cells undergoing cytofission show reduced PLK1 and MKLP1 levels and were even able to complete division after treatment with nocodazole. Investigators found that even cells that fail to divide initially but are able to properly segregate chromosomes may undergo interphase cytofission as a means of preserving genomic integrity (Choudhary et al., 2013). Interestingly, in human cells, cytofission was dependent on myosin-II and actin polymerization (Choudhary, Lera et al. 2013). It is possible that in human cells, myosin-II functions more to provide adhesive stress than in *Dictyosteium* cells where reducing myosin-II may increase cell motility (Choudhary et al., 2013). This type of cell division may have broad implications for protecting cells from failed cytokinesis and preventing aneuploidy.

Plant cytokinesis

Unlike in animal cells, plant cells are enclosed by a firm cell wall. These cell walls do not allow for the constriction of a contractile ring due to their rigidity so plants use a different mechanism to divide cells. Instead of a contractile ring, membrane-enclosed vesicles from the Golgi move to the center of the cell where the cell plate grows outward from the division plane until it fuses with the plasma membrane (Jurgens, 2005). The division site is determined by the preprophase band. Like the mitotic apparatus in animal cells, the cell plate consists of

stable microtubule bundles and dynamic microtubules (Murata et al., 2013). These microtubules are arranged in a parallel fashion, oriented to the equator (Euteneuer and McIntosh, 1980). Similar to plant cells, in budding yeast the division plane is marked by a bud-site on the cell cortex (Chant, 1996) and some *S. cerevisiae* strains are able to divide by compensating with unique cell wall deposition in the absence of myosin-II (Bi et al., 1998; Tolliday et al., 2003). The adage, "where there is a will, there is a way" cannot be truer for the various ways cells complete cytokinesis.

Cytokinesis failure and human disease

Cytokinesis failure is causative to human pathologies

When cytokinesis fails, it gives rise to abnormal centrosome and chromosome number, and is thought to be responsible for many human diseases. For example, only mice injected subcutaneously with tetraploid cells developed aneuploid malignancies compared to mice injected with diploid cells (Cunto, Imarisio et al. 2002). X-linked neutropenia is a genetically encoded blood disorder characterized by low numbers of neutrophils as a result of failed cytokinesis (Moulding, Blundell et al. 2007). Cytokinesis failure also has implications for fertility/sterility as *Drosophila* males homozygous for dia1/formin mutations exhibit sterility due to cell division failures in the germline. Females trans-heterozygous for the same mutation display cytokinesis failure in the follicle cell which causes sterility and deposition of eggs with defective eggshells (Castrillon and Wasserman, 1994). In summary, cytokinesis failure has broad impact on human health, as it may contribute to developmental defects, blood disorders, infertility/sterility and cancer (Castrillon and Wasserman, 1994; Cunto et al., 2002; Fujiwara et al., 2005; Liljeholm et al., 2013; Moulding et al., 2007).

Cytokinesis failure in normal tissues

Surprisingly, cytokinesis failure does not always lead to a disease state and in certain tissues occurs during normal development and homeostasis. For example, in humans the adult liver is made up of ~30-40% polyploid cells, which is when a cell contains more than two genomic copies of DNA (Kudryavtsev et al., 1993; Toyoda et al., 2005). Hepatocytes (liver cells) that become polyploid are able to initiate contractile ring ingression but many ultimately regress to form 4N and even 8N cells (Margall-Ducos et al., 2007). In rats, this cytokinesis failure in liver cells is observed once they transition from suckling to weaning (Guidotti et al., 2003). Rats whose insulin/AKT signaling is either disrupted and mice with a homozygous insulin mutation, show a reduction in the formation of binucleated tetraploid cells (Celton-Morizur et al., 2009). The converse experiment, where rats were injected with insulin or a control vehicle, also displayed increased tetraploid hepatocytes compared to control rats. The insulin effect on cytokinesis failure is independent of glucose signaling since rats fed different diet-types that modified glucose levels did not show a change in the formation of binucleated tetraploid hepatocytes. This suggests that in liver cells, insulin plays a role in formation of tetraploid cells (Celton-Morizur et al., 2009). Interestingly, it was recently shown that cytokinesis failure in hepatocytes is protective against tumor formation in a mouse model (Wang et al., 2017).

In other cell types, the mechanism of polyploidization is less clear, but is sometimes due to cytokinesis failure. There is some evidence that polyploidization can be induced by cell stress and injury, particularly in cardiomyocytes, which undergo polyploidization as a result of both endoreplication, where mitosis is inhibited, and multinucleation, when cytokinesis fails (Hixon et al., 2000). For many other tissues that display polyploidy such as

the mammary gland, urothelium, mesothelium, uterine muscles, and Purkinje neurons, the exact mechanism (cytokinesis failure, cell fusion, or endoreplication, etc) that causes ploidy is yet to be determined (Biesterfeld et al., 1994). Interestingly, if the urothelium in rats is exposed to toxins, the superficial layer and its polyploid cells are shed and is replaced completely by diploid cells until a considerable passage of time when polyploid cells and the superficial membrane are restored (R. Marian Hicks, 1976). It would be interesting to learn if cytokinesis failure is also the cause of polyploidy in these systems, as it is not fully understood why some cells are fated to fail while others are not when the same cytokinetic machinery drives cell division in all, and how cells/tissues have adapted to use errors in cytokinesis to their advantage.

Conclusions

Although we do not have a complete understanding of animal cell cytokinesis across organisms and individual cell types, slowly the cytokinesis puzzle is being assembled. We know signals from the metazoan mitotic spindle communicate with the cortex to drive contractile ring constriction. More and more the temporal and spatial regulation of essential cytokinetic proteins are being characterized. Although the puzzle is still incomplete, my thesis work addresses the general areas of Rho GTPases and CYK-4, the role of cell polarity during cytokinesis, and why different cell types may be more or less robust at completing cell division.

Chapter 2. Cortical PAR proteins protect against cytokinesis failure during asymmetric cell division

Part of this chapter has been published in:

Jordan, S.N., Davies, T., **Zhuravlev, Y**., Dumont, J., Shirasu-Hiza, M., and Canman, J.C. (2016). *Cortical PAR polarity proteins promote robust cytokinesis during asymmetric cell division.* J Cell Biol *212*, 39-49.

My contributions to Chapter 2

I conducted the imaging and analysis of cytokinesis in dividing *control*, *formin(ts)*, and *myosin(ts)* one-cell embryos with and without PAR-4 and PAR-5 RNAi (Figure 10, Figure 13) and the imaging and analysis of cytokinesis across a thermal range in dividing *control*, *formin(ts)*, and *myosin(ts)* mutant two-cell embryos with and without RNAi-mediated PAR depletion (Figure 14). Work not published but related to this project begins on page 69, following results and discussion from the article.

My contributions (published manuscript):

I performed the imaging and analysis for par-4 experiments (Figure 10B, C; Figure S 2C, D, & F). My role in this work was to investigate if the downstream PAR protein PAR-4 contributes to contractile ring constriction in this way. Although PAR-4 has previously been implicated as a regulator of myosin-II during cytokinesis in this system, I found that PAR-4 knockdown alone or in combination with *formin(ts)* or *myosin-II(ts)* did not affect cytokinesis, further supporting the positive role for core cortical PAR proteins in cytokinesis (Chartier et al., 2011).

Unpublished results reported here include my investigations on the role of PAR-5 (Figure 13) in the zygote, and the role of PAR-6 and PAR-2 in later cell divisions with and without *formin(ts)* and *myosin-II(ts)* (Figure 14).

Abstract

Cytokinesis, the physical division of one cell into two, is thought to be fundamentally similar in most animal cell divisions, driven by constriction of a contractile ring positioned and controlled solely by the mitotic spindle. During asymmetric cell divisions, the core polarity machinery (PARtitioning defective or PARs) controls the unequal inheritance of key cell fate determinants. Here we show that in asymmetrically dividing *C. elegans* embryos, the cortical PARs (including the small GTPase CDC-42) have an active role in regulating recruitment of a critical component of the contractile ring, filamentous actin (f-actin). We found that the cortical PARs are required for retention of anillin and septin in the anterior pole, cytokinesis proteins that our genetic data suggest act as inhibitors of f-actin at the contractile ring. Together, our results suggest that the cortical PAR proteins coordinate the establishment of cell polarity with the physical process of cytokinesis during asymmetric cell division to ensure the fidelity of daughter cell formation.

Introduction

Cytokinesis, the physical division of one cell into two, occurs trillions of times from fertilization to death, and division failures can have significant consequences including miscarriage, neurological dysfunction, immunological defects, and cancer (Lacroix and Maddox, 2012; Tormos et al., 2015). Cytokinesis is driven by constriction of a contractile ring, composed of formin-nucleated filamentous actin (f-actin) and the motor myosin-II, which is primarily positioned and controlled by the mitotic spindle (Green et al., 2012). Divisions in which the daughter cells 'inherit' equal cytoplasmic and cortical components, and thus the same cell fate and size, are referred to as symmetric. In contrast, many cell

divisions during embryogenesis and in adult stem cells are asymmetric, resulting in daughter cells with different cell fate and/or cell size (Williams and Fuchs, 2013). In metazoans, asymmetric cell division requires G protein-coupled receptors (GPCRs) and the PAR proteins (PARtitioning defective). The PARs are a conserved set of proteins that segregate to opposing poles of the cell during asymmetric cell division and control the unequal inheritance of cytoplasmic and cortical factors (Macara, 2004; Motegi and Seydoux, 2013; Suzuki and Ohno, 2006).

The *C. elegans* single-cell zygote has been a seminal system for understanding the molecular regulation of anterior-posterior (A-P) cell polarity and the PAR proteins (Kemphues et al., 1988). In this system, opposing anterior (aPAR) and posterior (pPAR) cortical PAR domains are formed via two genetically and temporally distinct phases: polarity establishment and polarity maintenance (Cuenca et al., 2003). During polarity establishment, the core cortical aPARs (including the scaffolding proteins PAR-3 and PAR-6, the atypical protein kinase PKC-3, the small GTPase CDC-42) and core pPAR PAR-2 (RING finger and NTPase containing protein) are targeted to opposite sides of the cell via anteriorly directed actomyosin-based cortical flows (Cheeks et al., 2004; Hird and White, 1993; Munro et al., 2004). During polarity maintenance, the aPARs and pPARs remain on opposing sides of the cell cortex forming a distinct A-P boundary near the cell equator via mutual inhibition (for extensive reviews of PARs: (Hoege and Hyman, 2013; Motegi and Seydoux, 2013; Rose and Gonczy, 2014)).

A role for the cortical PARs in cytokinesis was previously thought to be indirect, by controlling spindle length and position (Dechant and Glotzer, 2003). However, emerging evidence suggests that cell polarity has a more active role in cytokinesis, though the

underlying molecular mechanism(s) remain elusive. Perturbations in asymmetrically dividing *Drosophila* neuroblasts revealed that spindle-independent contractile rings can form in association with a GPCR-promoted polarized cap of myosin-II (Cabernard et al., 2010). In *C. elegans*, depletion of PAR-2 enhances contractile ring constriction defects caused by compromised spindle signaling (Dechant and Glotzer, 2003; Verbrugghe and White, 2007). Moreover, both the aPAR and pPAR proteins "track" with the contractile ring during cytokinesis (Pittman and Skop, 2012; Schenk et al., 2010).

Here we show that in the asymmetrically dividing *C. elegans* zygote, cortical A-P polarity protects the cell against cytokinesis failure in the presence of a weakened actomyosin contractile ring. We demonstrate that both the core cortical aPAR (including CDC-42) and pPAR proteins are required for proper f-actin levels at the contractile ring and restrict the localization of two actomyosin binding and crosslinking proteins anillin^{ANI-1} and septin^{UNC-59}. We found that anillin and septin have unexpected inhibitory roles in f-actin accumulation at the contractile ring. Thus we present a model in which cortical PAR proteins protect cytokinesis during asymmetric cell division independent of mitotic spindle length by promoting the anterior retention of anillin and septin away from the contractile ring, thus allowing for robust f-actin accumulation and ring constriction.

Results and Discussion

A synergistic interaction between formin and myosin-II mutants during polarity establishment leads to cytokinesis failure

The f-actin nucleator diaphanous-like formin^{CYK-1} (hereafter formin) and the motor myosin-II^{NMY-2} (hereafter myosin-II) are known to be critical for cytokinesis (Figure S 1A)

(Severson et al., 2002; Shelton et al., 1999b; Swan et al., 1998). Using fast-acting temperature-sensitive (ts) mutants with point mutations in the formin dimerization (FH2) domain, required for actin polymerization, and in the myosin-II neck (S2) domain required for dimerization and head coupling (Davies et al., 2014; Liu et al., 2010), we found that formin and myosin-II are synergistic. At semi-permissive temperatures, where the proteins are perturbed but functional enough to allow cytokinesis (Figure S 1A), 100% of *myosin-II(ts)* and *formin(ts)* single mutant embryos divided successfully, while ~40% of *myosin-II(ts); formin(ts)* double mutant embryos failed to divide, suggesting a synthetic cytokinesis defect (14/35 embryos; Figure 8A; Figure S 1B).

To identify the time of requirement for this synthetic interaction, we used a fluidic device (Davies et al., 2014) to rapidly upshift (<20 sec) *myosin-II(ts); formin(ts)* double mutant embryos to this semi-permissive temperature at precise time-points during cell division. Unexpectedly, we found that this synthetic interaction and cytokinesis failure occurs only when myosin-II and formin are both disrupted well before cytokinesis, during establishment and maintenance of A-P polarity (Figure 8A). Upshift during polarity establishment caused cytokinesis failure in all *myosin-II(ts);formin(ts)* double mutants (7/7). Upshift during polarity maintenance caused an intermediate failure rate (7/22), with all failures seen in earlier upshifts. Upshift after the polarity maintenance phase did not cause cytokinesis failure in any double mutants (0/6). Thus, the synthetic effect is strictly limited to the time period correlated with polarity establishment and maintenance and not during cytokinesis directly.

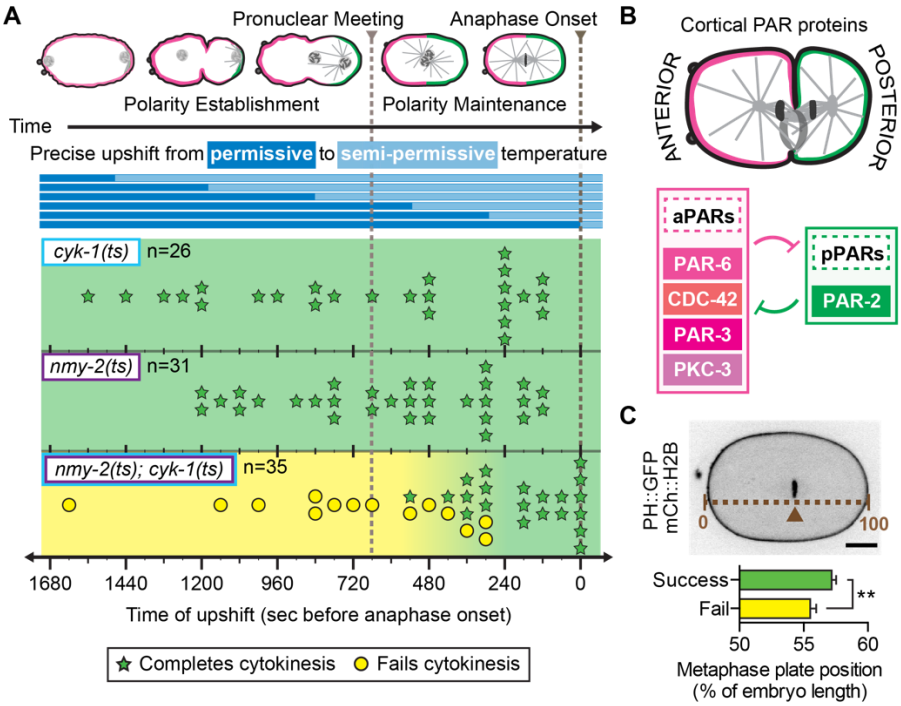

Figure 8: Polarity establishment supports robust cytokinesis

A) Experimental protocol and rapid temperature upshift results. Each symbol (star or circle) represents a single embryo plotted at the time of upshift. B) Schematic of cortical PAR protein localization during asymmetric cell division. C) The metaphase plate in *myosin-II(ts);formin(ts)* embryos that complete cytokinesis (n=21) is positioned more asymmetrically than in those that fail (n=14) (mean ± SD). Scale bar, 10µm. *cyk-1=formin*; *nmy-2=myosin-II.*

Polarity establishment is dependent on myosin-II, but independent of formin activity (Figure S 1C) (Cuenca et al., 2003; Liu et al., 2010; Munro et al., 2004; Velarde et al., 2007). Thus we hypothesized that synthetic cytokinesis failure is due to myosin-II function as a polarity protein, synergizing with an independent formin function. Consistent with this hypothesis, we found that the *myosin-II(ts);formin(ts)* double mutant embryos that failed in cytokinesis were also less polarized, with more centrally located metaphase plates relative to those that succeeded in cytokinesis (Figure 8C). It is unlikely that this early interaction represents a delay in functional inhibition, as both ts mutants are very fast-acting and show a full loss-of-function phenotype within seconds upon upshift to restrictive temperature (Davies et al., 2014). Furthermore, cytokinesis completed successfully when embryos were upshifted to restrictive temperature during polarity establishment then downshifted to permissive temperature prior to anaphase onset (Figure S 1D). Taken together, these results suggest that establishment of A-P polarity (very early in the cell cycle, before NEBD) is required for efficient contractile ring constriction during cytokinesis, a significantly later cell cycle event.

Core cortical PARs are required for cytokinesis when formin activity is weakened

Establishment of A-P polarity requires both core cortical aPAR and pPAR proteins (Figure 8B; Figure 9A). Myosin-II itself is a cortical aPAR, required for polarity establishment and maintenance and localizing to the anterior cortex (Cuenca et al., 2003; Guo and Kemphues, 1996; Liu et al., 2010). To directly test a role for A-P polarity in cytokinesis, we RNAi-depleted five different cortical PAR proteins in either *formin(ts)* or *myosin-II(ts)* mutants to assess these synthetic interactions for cytokinesis function. Depletion of the aPARs (PAR-6, PAR-3, PKC-3, or CDC-42) or pPAR (PAR-2) caused cytokinesis failure in *formin(ts)* embryos at semi-permissive temperature, with little to no contractile ring

constriction (Figure 9B; S3B). In contrast, PAR depletion slowed but did not block cytokinesis in *myosin-II(ts)* embryos at semi-permissive temperature (Figure 9C; S3B). Depletion of each PAR alone, in the absence of another mutation, did not cause cytokinesis failure (Figure 9B-C; S3B), consistent with a synthetic effect. Successful PAR depletion was confirmed by four hallmarks of loss of polarity (see Methods, Figure 9A; S2A-D; S3A). These data suggest that myosin-II and the core cortical PARs act together during A-P polarity establishment to regulate cytokinesis synergistically with formin. That is, the cortical PAR and formin pathways each contribute to cytokinesis and weakening either one alone is not sufficient to cause cytokinesis failure, but weakening both pathways prevents cytokinesis.

Why are both aPARs and pPARs required for robust cytokinesis when formin activity is weakened? One possibility is that cytokinesis in asymmetrically dividing cells requires opposing cortical PAR domains or the A-P polarity boundary, maintained by mutual aPAR and pPAR exclusion. If so, the A-P polarity boundary might act as a special site that facilitates contractile ring assembly and constriction. Indeed, we found that furrow initiation occurred near the A-P polarity boundary (where PAR-6 levels are decreasing and PAR-2 levels begin to increase), suggesting a possible association between the A-P boundary and the initial site of contractile ring assembly (Figure 9D,E)

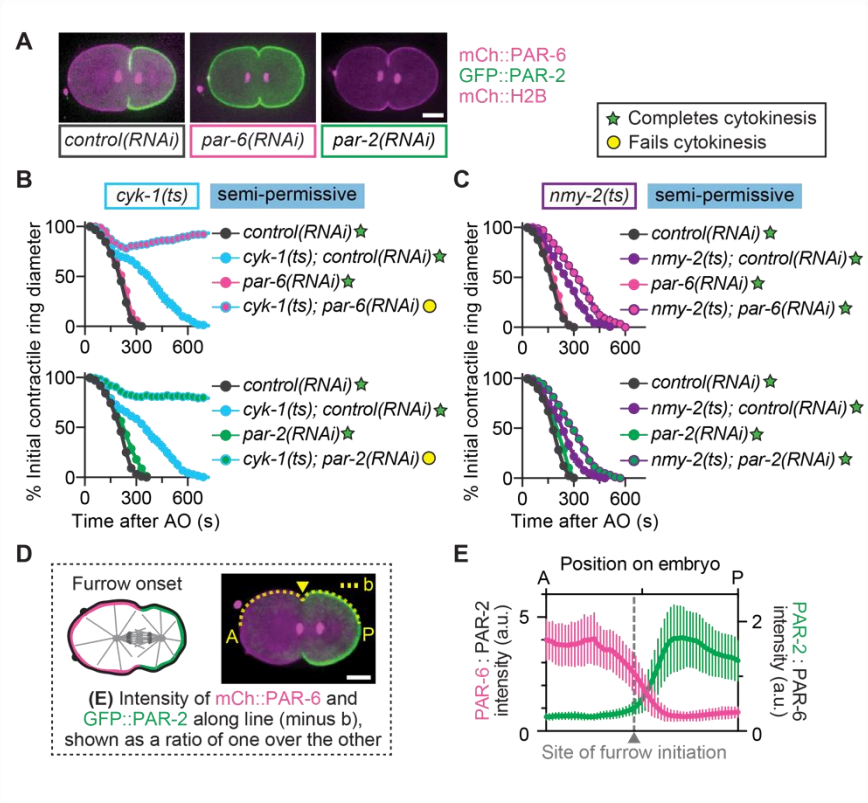

Figure 9: PARs protect against cytokinesis failure when formin activity is reduced

A) RNAi-depletion of cortical PAR proteins disrupts A-P polarity. B,C) Depletion of cortical PAR proteins leads to cytokinesis failure in *formin(ts)* (B) but not *myosin-II(ts)* mutant embryos (C) at semi-permissive temperature (n=10, all conditions, mean ± SEM). D) Schematic of cortical linescan used for analysis in (E). E) The A-P polarity boundary, where PAR-2 levels start to increase relative to PAR-6 levels, coincides with the site of furrow onset (grey line, n=10, mean ± SD). Scale bars, 10µm. AO, anaphase onset. *cyk-1=formin;nmy-2=myosin-II.*

Cytoplasmic polarity and spindle length are not key regulators of cytokinesis when formin activity is compromised

To identify factors downstream of the core cortical PAR proteins during cytokinesis, we first examined PAR-1 and PAR-4, which mediate the asymmetric inheritance of key cytoplasmic components (*e.g.* RNA granules) and differential daughter cell cycle timing (Figure S 2E,F) but are dispensable for cortical A-P polarity in the one-cell embryo (Figure 10A). PAR-1 localizes to the posterior cell cortex (Boyd et al., 1996); PAR-4 localizes uniformly on the cortex (Watts et al., 2000) and has been shown to regulate myosin-II during cytokinesis (Chartier et al., 2011; Pacquelet et al., 2015). We found that depletion of either PAR-1 or PAR-4, alone or in combination with the *formin(ts)* or *myosin-II(ts)* mutation, did not affect cytokinesis (Figure 10B), suggesting that this role in cytokinesis is specific to the core cortical PARs.

It was previously suggested that cortical PARs indirectly regulate cytokinesis by increasing spindle length and astral separation (Dechant and Glotzer, 2003; Lewellyn et al., 2010). We did not find any correlation between reduced spindle length and the success or failure of cytokinesis following cortical PAR depletion (Figure 10C). While PAR-2 depletion decreased spindle length and caused cytokinesis failure in *formin(ts)* mutants, PAR-6 depletion increased spindle length and also caused cytokinesis failure (Figure 10C). Similarly, though PAR-2 depletion in *myosin-II(ts)* mutants led to very short spindles, cytokinesis did not fail with either PAR-2 or PAR-6 depletion in this mutant (Figure 10C). Thus the effects of core cortical PAR proteins on cytokinesis in this system are not due to downstream effects on cytoplasmic factors or reduced spindle length.

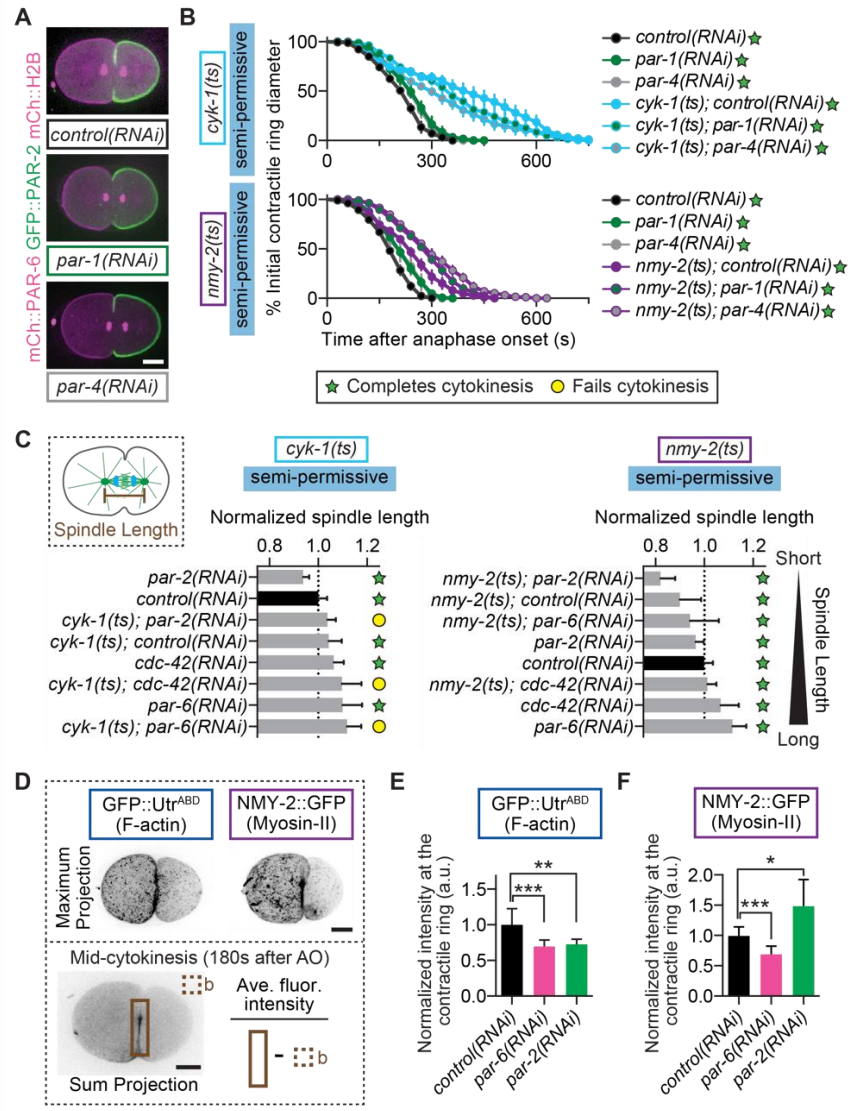

Figure 10: The cortical PAR proteins regulate f-actin in the contractile ring during cytokinesis and not via downstream PAR proteins or spindle length

A) Depletion of neither PAR-1 nor PAR-4 disrupts A-P cortical polarity. B) RNAi- depletion of PAR-1 or PAR-4 does not lead to cytokinesis failure in *formin(ts)* or *myosin-II(ts)* mutant embryos at semi-permissive temperatures (n=10, all conditions, mean ± SEM). C) Spindle lengths for all conditions arranged from shortest to longest at the *formin(ts)* or *myosin-II(ts)* semi-permissive temperature. D) Schematic of region and formula used for analysis shown in (E,F). E) Depletion of PAR-6 or PAR-2 reduces f-actin levels in the contractile ring, relative to controls (*control(RNAi)* n=13, *par-6(RNAi)* n=7, *par-2(RNAi)* n=7, mean ± SD). F) Depletion of PAR-6 or PAR-2 has opposing effects on myosin-II levels in the contractile ring, relative to controls (*control(RNAi)* n=13, *par-6(RNAi)* n=7, *par-2(RNAi)* n=7, mean ± SD). Scale bars, 10μm. AO, anaphase onset. *cyk-1=formin*;*nmy-2=myosin-II*.

The core cortical PAR proteins are required for normal f-actin accumulation in the contractile ring

Because the myosin-II/cortical PAR pathway shows a synthetic interaction with the formin pathway during cytokinesis and a major function of formin is actin polymerization, we next tested whether the core cortical PAR proteins regulate f-actin levels in the contractile ring, using GFP-tagged reporters to monitor f-actin and myosin-II (Figure 10D). Depletion of either PAR-6 or PAR-2 alone led to a 30% and 27% reduction, respectively, in f-actin levels at the contractile ring (Figure 10E), consistent with their synthetic cytokinesis failure phenotypes. Effects on myosin-II levels were inconsistent between PAR-6 and PAR-2, as depletion of PAR-6 led to a 31% decrease and PAR-2 led to a 48% increase in myosin-II levels in the contractile ring (Figure 10F), as expected from their opposing effects on global cortical myosin-II levels (Munro et al., 2004). These data suggest that both the cortical aPAR and pPAR proteins promote normal f-actin levels at the contractile ring in asymmetrically dividing cells and that this function is synthetic with compromised formin activity during cytokinesis.

The cortical PARs mediate the anterior retention of anillin and septin and restrict their targeting to the contractile ring

How do the PARs regulate f-actin levels at the contractile ring? The anterior of the early embryo is enriched for several actomyosin binding and regulatory proteins (Munro et al., 2004). Starting from a list of genes that genetically interact with the cortical PARs (Fievet et al., 2013), we next identified asymmetric (anterior) enrichment of two actomyosin-binding and crosslinking proteins implicated in cytokinesis: septin^{UNC-59} (hereafter septin) and

anillin^{ANI-1} (hereafter anillin) (Figure 11A-C; S3C-D) (Bridges and Gladfelter, 2015; Field et al., 2005; Maddox et al., 2007; Oegema et al., 2000; Straight et al., 2005). We found that this anterior localization of septin and anillin is dependent on the cortical PARs (Figure 11A-C; S3C-D). That is, depletion of PAR-6 or PAR-2 led to a decrease in anterior enrichment and increase in posterior enrichment of GFP::septin and GFP::anillin during metaphase (Figure 11A-C; S3C-D). During furrow onset, septin and anillin remained polarized in control embryos (Figure S 3E-F). In contrast, PAR-6 or PAR-2 depletion decreased the polarization of septin and anillin and increased their levels at the contractile ring both at furrow onset (Figure S 3E-F) and during ring constriction (37% and 42% increases in septin; 29% and 21% increases in anillin, after PAR-6 and PAR-2 depletion, respectively) (Figure 11A, D-E). Importantly, depletion of neither septin nor anillin disrupted A-P polarity (by PAR-6 and PAR-2 distribution), suggesting these proteins are downstream of the cortical PARs (Figure 11F). Thus, the core cortical PARs are required for the asymmetric anterior localization of both septin and anillin (Figure 11G) and to restrict their accumulation at the contractile ring during cytokinesis.

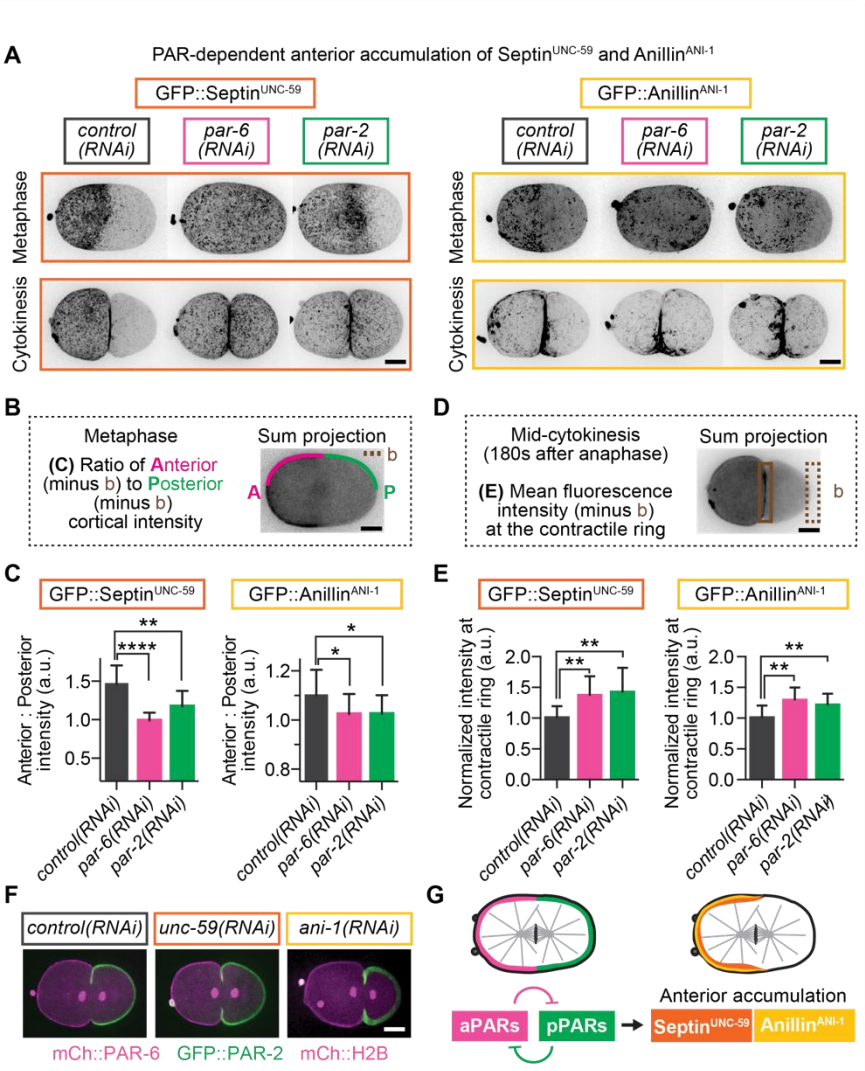

Figure 11: PAR proteins are required to retain septin and anillin in the cell anterior away from the contractile ring

A) Representative images of maximum projections of GFP::septin^{UNC-59} and GFP::anillin^{ANI-1} at metaphase and during cytokinesis, with and without A-P polarity. B) Schematic of A and P cortical linescans used for analysis shown in (C). C) Ratio of anterior to posterior cortical fluorescence of septin and anillin with and without PAR-6 and PAR-2 depletion (n≥10, all conditions, mean ± SD). D) Schematic of region and formula used for analysis shown in (E). E) Septin and anillin levels in the contractile ring increase following disruption of A-P polarity. F) Depletion of septin or anillin does not disrupt A-P polarity. G) Anterior enrichment of septin and anillin is PAR-dependent, but not vice versa. Scale bars, 10µm. *ani-1=anillin*; *unc-59=septin*.

Septin and anillin negatively regulate f-actin levels in the contractile ring

Since we found that the core cortical PARs modulate f-actin levels at the contractile ring and are also required to spatially restrict septin and anillin, we next tested whether septin and anillin also modulate f-actin and/or myosin-II levels in the contractile ring. Unexpectedly, RNAi-mediated depletion of either septin or anillin led to increased f-actin levels in the contractile ring (20% and 19% respectively; Figure 12A,B), suggesting that these two proteins inhibit f-actin accumulation. As previously published, depletion of septin or anillin led to a 24% increase or no change (respectively) in myosin-II levels in the ring (Lewellyn et al., 2011; Maddox et al., 2007) (Figure 12A,C). These results demonstrate that PAR-6 and PAR-2 have opposite effects on spindle length and myosin-II localization but similar effects on f-actin, septin, and anillin levels in the contractile ring during cytokinesis. These results further suggest that septin and anillin function as negative regulators of f-actin accumulation at the contractile ring during cytokinesis and their PAR-dependent anterior polar retention allows proper f-actin accumulation at the ring during asymmetric cell division.

Depletion of septin and anillin suppresses cytokinesis failure in formin mutants with and without the cortical PARs

We finally predicted that, if loss of cortical PAR proteins enhances cytokinesis failure in formin mutants by increasing the levels of septin and anillin in the contractile ring, then depletion of septin and/or anillin should rescue cytokinesis failure in *formin(ts)* mutants lacking A-P polarity. Consistent with this prediction, we found that depletion of septin completely rescued cytokinesis failure in *formin(ts);par-6(RNAi)* and *formin(ts);par-2(RNAi)* zygotes, even at semi-restrictive temperature when *formin(ts)* mutants alone fail in cytokinesis

(Figure 12D; S1A). These results suggest that the synthetic interaction between loss of formin activity and loss of PAR proteins is dependent on septin. Thus, the major contribution of the cortical PARs to cytokinesis may be to inhibit septin, since in the absence of septin the PARs are dispensable. Indeed, depletion of septin or anillin rescues cytokinesis failure in *formin(ts)* mutants but not in *myosin-II(ts)* mutants (Figure 12E-F). While depletion of septin (but not anillin) led to increased contractile ring constriction in *myosin-II(ts)* embryos at semi-restrictive temperature, cytokinesis ultimately failed in 100% of embryos (Figure 12F). This is consistent with the increase in contractile ring myosin-II levels observed following septin (but not anillin) depletion (Figure 12C). Taken together, our results suggest a model in which opposing cortical aPAR and pPAR proteins promote robust cytokinesis during asymmetric cell division by mediating the localization of septin and anillin to the cell anterior (Figure 12G). Further experiments will be necessary to determine if this is a direct or indirect effect.

While we were initially surprised by the inhibitory role for anillin and septin during cytokinesis, there is little consensus for a positive regulatory role for these proteins in cell division. Anillin homologs are not required for contractile ring assembly and constriction in many systems, including budding yeast (Norden et al., 2006), fission yeast (Chang et al., 1996), many *C. elegans* cell types (Maddox et al., 2007), some cells in *Drosophila* (Field et al., 2005; O'Farrell and Kylsten, 2008), zebrafish ganglion cell progenitors (Paolini et al., 2015), and even HeLa cells, in which loss of anillin causes cytokinesis failure in only 15-50% of cells (Piekny and Glotzer, 2008; Straight et al., 2005). The septins, originally identified in the asymmetrically dividing budding yeast, are required in that system for mother-daughter cell separation but not for actomyosin contractile ring constriction (Wloka et al., 2011). Septins are also dispensable for most cytokinetic events in fission yeast (Wu et al., 2010),

worms (Maddox et al., 2007; Nguyen et al., 2000), some *Drosophila* cell types (Field et al., 2008), and in many human cell types (Menon and Gaestel, 2015). In fact, ring constriction is faster without the septins in some systems (Lewellyn et al., 2011; Wloka et al., 2011). Anillin and septin have also both been implicated in regulating the asymmetry of contractile ring constriction within the division plane (Maddox et al., 2007). This role is quite different than the PAR-dependent asymmetry in daughter cell fate and size that we describe here. Our data suggest that, at least in asymmetrically dividing *C. elegans* embryos, anillin and septin function as negative regulators of contractile ring assembly and constriction, perhaps due to their ability to cross-link f-actin and/or myosin-II and thus increase drag or filament severing, or reduce filament turnover.

Two classic hallmarks of cancer progression are the loss of cell polarity and defects in cytokinesis (Davoli and de Lange, 2011; Ganem et al., 2007; Halaoui and McCaffrey, 2015). Here we demonstrate that during asymmetric cell division the PAR proteins actively promote robust contractile ring constriction during cytokinesis. This regulation might help protect against division errors and protect the fidelity of critical asymmetric cell divisions, such as in proliferating stem cells. Our work also suggests that the loss of cell polarity increases the incidence of cytokinesis failure and thus could be a cause, rather than an effect, of cancer development.

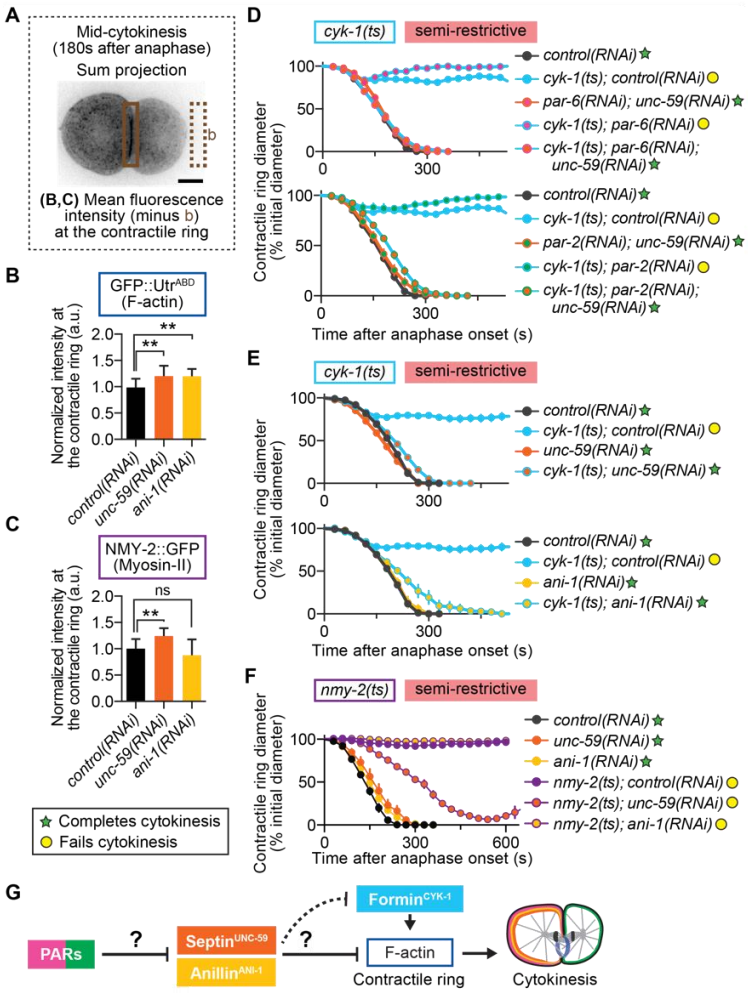

Figure 12: Septin and anillin restrict contractile ring f-actin levels and negatively regulate cytokinesis

A) Schematic of region and formula used for analysis shown in (B,C). B) Depletion of septin and anillin increased f-actin levels in the contractile ring, whereas C) only septin depletion increased myosin-II levels in the ring (n≥10, all conditions, mean ± SD). D) Depletion of septin suppresses cytokinesis failure in *formin(ts)* mutant embryos at semi-restrictive temperature, even when A-P polarity is simultaneously disrupted (*control(RNAi)* n=9, *cyk-1(ts);control(RNAi)* n=11, *par-6(RNAi);unc-59(RNAi)* n=11, *cyk-1(ts);par-6(RNAi)* n=3, *cyk-1(ts);par-6(RNAi);unc-59(RNAi)* n=12, *par-2(RNAi);unc-59(RNAi)* n=10, *cyk-1(ts);par-2(RNAi)* n=4, *cyk-1(ts); par-2(RNAi); unc-59(RNAi)* n=12, mean ± SEM). E) Depletion of septin and anillin suppresses cytokinesis failure in *formin(ts)* mutant embryos at semi-restrictive temperature (n=10, all conditions, mean ± SEM). F) RNAi-mediated depletion of neither anillin nor septin suppresses cytokinesis failure in *myosin-II(ts)* mutant embryos at semi-restrictive temperature (n≥8, all conditions, mean ± SEM). G) In our genetic model, PAR proteins inhibit septin and anillin localization in the contractile ring by promoting their anterior retention. This prevents septin and anillin from inhibiting f-actin and thereby promotes robust cytokinesis. Scale bar, 10µm. *cyk-1=formin*; *nmy-2=myosin-II*; *ani-1=anillin*; *unc-59=septin*.

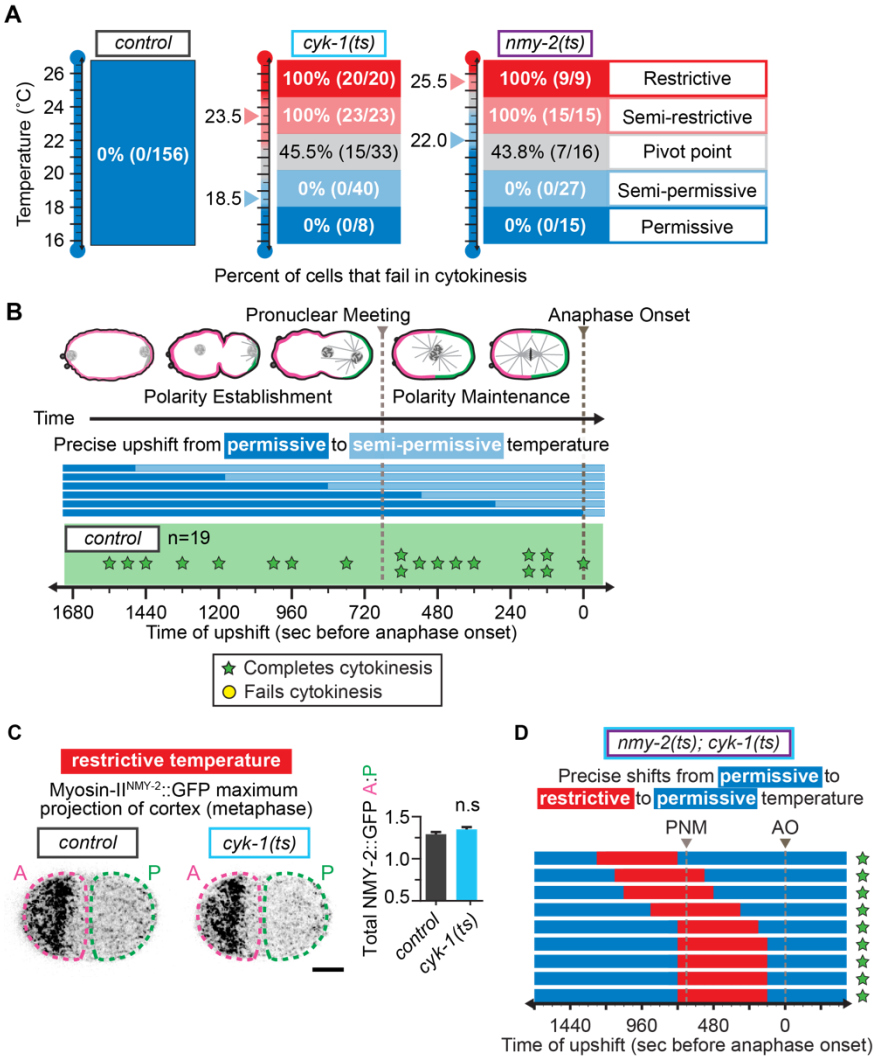

Figure S 1: ts mutants allow tuning of specific protein functions that are necessary for cytokinesis.

A) Temperature response tables for control, *formin(ts)*, and *myosin-II(ts)* embryos. Formin and myosin-II fast-acting ts mutants have tunable constriction defects, dependent on temperature. B) Control embryos complete cytokinesis when upshifted to semi-permissive temperature prior to cytokinesis. C) At fully restrictive temperature, *formin(ts)* embryos successfully polarize myosin-II (NMY-2::GFP) in an anterior cap prior to cytokinesis. D) Double *myosin-II(ts);formin(ts)* mutant embryos complete cytokinesis when temporarily upshifted to restrictive temperature and returned to fully permissive temperature before anaphase onset, indicating that these ts mutant phenotypes are reversible. Scale bar, 10µm. *cyk-1=formin*; *nmy-2=myosin-II*.

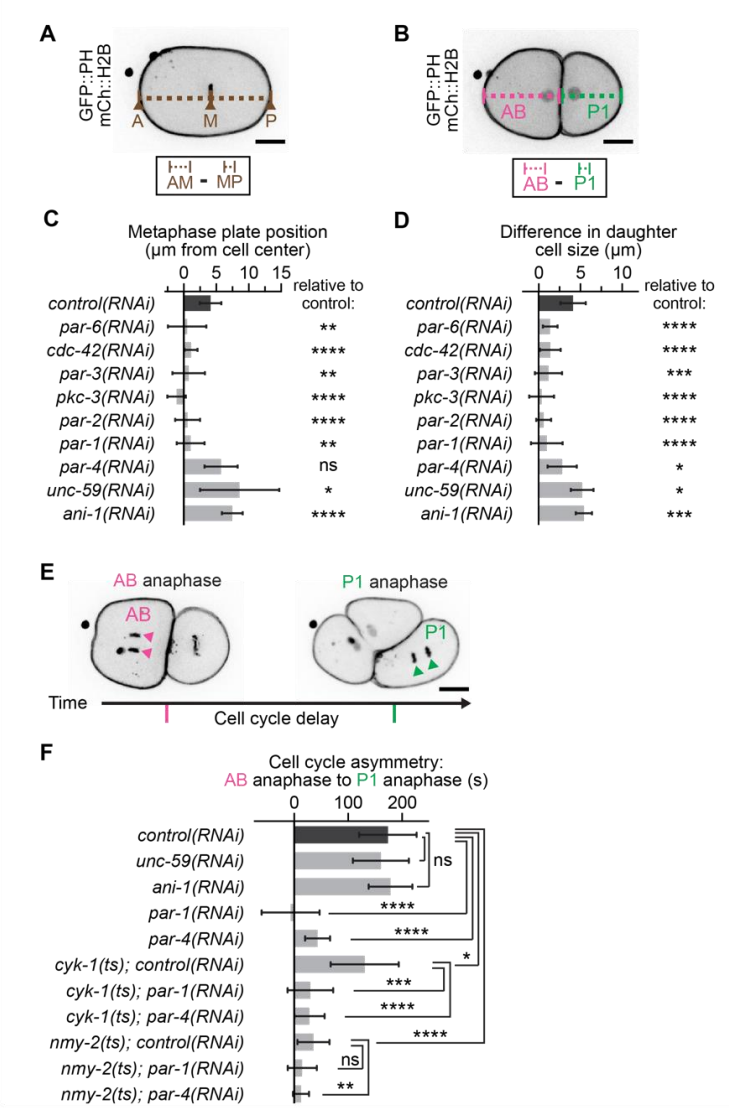

Figure S 2: Successful RNAi-mediated knockdown of PAR proteins was confirmed using hallmarks of the loss of polarity.

A) Metaphase plate position in RNAi-depleted embryos was measured immediately prior to anaphase onset by calculating the deviation in position of the metaphase plate from the cell center (at 0µm) towards the anterior (negative change) or posterior (positive change). B) Daughter cell size asymmetry was measured immediately following contractile ring closure. Asymmetric division is indicated by an increased difference in daughter cell length (when AB>P1). C) Metaphase plate position for RNAi-depleted embryos. D) Daughter cell size asymmetry for RNAi-depleted embryos. E) Successful depletion of cytoplasmic polarity regulators (PAR-1 and PAR-4) was determined by measuring the loss of the cell cycle delay between anaphase onset in the AB blastomere and anaphase onset in the P1 blastomere. In control embryos, there is a significant delay between the two cell cycles; this difference is lost upon disruption of cytoplasmic polarity. F) Difference in time between anaphase of AB and anaphase of P1. All data shown as mean ± SD. Scale bars, 10µm. NOTE: *cyk-1=formin*; *nmy-2=myosin-II*; *unc-59=septin; ani-1=anillin*.

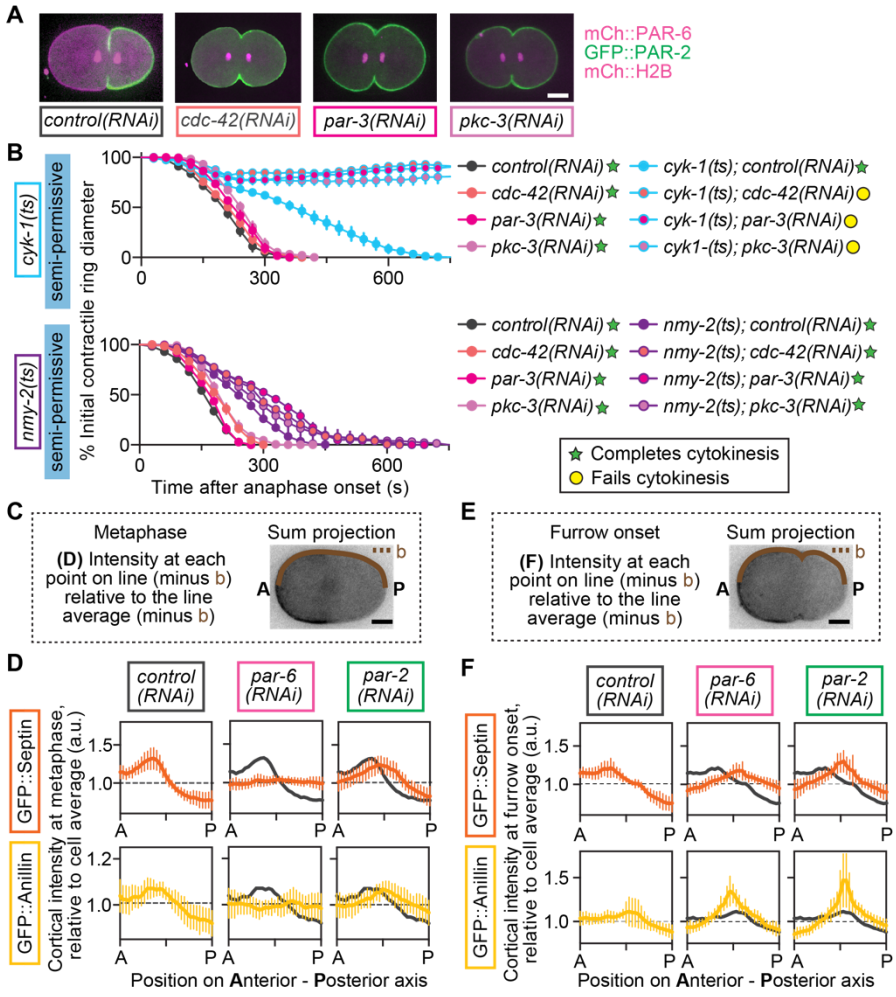

Figure S 3: Cortical PAR proteins regulate cytokinesis and sequester septin and anillin in the cell anterior.

A) Depletion of the aPARs CDC-42, PAR-3, and PKC-3 results in an expansion of the posterior PAR PAR-2 into the entire cell cortex. B) RNAi-mediated depletion of cortical aPAR proteins (CDC-42, PAR-3, or PKC-3) leads to cytokinesis failure in *formin(ts)* but not *myosin-II(ts)* mutant embryos at semi-permissive temperature (n≥9, all conditions, mean ± SEM). C) Schematic of linescan taken for quantifications in (D) to measure reporter localization. D) At metaphase, septin and anillin are enriched in the cell anterior in a PAR-dependent manner (n≥10, all conditions, mean ± SD). Mean from *control(RNAi)* is displayed for reference. E) Schematic of linescan taken for quantifications in (F) to quantify reporter localization. F) At furrow onset, septin and anillin are enriched in the cell anterior in a PAR-dependent manner (n≥10, all conditions, mean ± SD). Mean from *control(RNAi)* is displayed for reference. Scale bars, 10µm. NOTE: *cyk-1=formin*; *nmy-2=myosin-II*.

Strain	Genotype
OD95	*unc-119(ed3)* ltIs38 [pAA1; pie-1/GFP::PH(PLC1delta1); unc-119 (+)]III; ltIs37 [pAA64; pie-1/m-CHERRY::his-58; unc-119(+)]IV*
JCC146	*cyk-1(or596ts) unc-119(ed3)* ltIs38 [pAA1; pie-1/GFP::PH(PLC1delta1); unc-119(+)]III; ltIs37 [pAA64; pie-1/mCHERRY::his-58; unc-119(+)]IV*
JCC192	*nmy-2(ne3409ts) dpy-5**I; unc-119(ed3)* ltIs38 [pAA1; pie-1/GFP::PH(PLC1delta1); unc-119(+)]III; ltIs37 [pAA64; pie-1/mCHERRY::his-58; unc-119(+)]IV*
JCC212	*nmy-2(ne3409ts) dpy-5**I; cyk-1(or596ts) unc-119(ed3)* ltIs38 [pAA1; pie-1/GFP::PH(PLC1delta1); unc-119(+)]III; ltIs37 [pAA64; pie-1/mCHERRY::his-58; unc-119(+)]IV*
JCC744	*unc-119(ed3)*III; ddIs25 [GFP::F58B6.3;unc-119(+)]; ddIs26 [mCherry::T26E3.3;unc-119(+)]; ltIs37 [pAA64; pie-1/mCHERRY::his-58; unc-119(+)]IV*
JCC719	*mgSi3[cb-unc-119(+); GFP:UTROPHIN]II; unc-119(ed3)*III; ltIs37 [pAA64; pie-1/mCHERRY::his-58; unc-119(+)]IV*
JCC541	*unc-119(ed3)*III; ltIs37 [pAA64; pie-1/mCHERRY::his-58; unc-119 (+)] IV; zuIs45[nmy-2::NMY-2::GFP; unc-119(+)]V*
JCC559	*cyk-1(or596ts) unc-119(ed3)*III; ltIs37 [pAA64; pie-1/mCHERRY::his-58; unc-119(+)] IV; zuIs45[nmy-2::NMY-2::GFP; unc-119(+)]V*
JCC425	*unc-119(ed3)*III; ltIs37 [pAA64; pie-1/mCHERRY::his-58; unc-119(+)] IV; ltIs20 [pASM10; pie-1:GFP::unc-59; unc-119(+)]*
OD159	*unc-119(ed3)*III; ltIs86 [pASM65; pie-1:ani-1(fl cDNA)::GFP; unc-119(+)]*

*The *unc-119(ed3)* mutation was present in the parental strains but has not been directly sequenced in these strains to determine if the *unc-119* gene is mutated.
**The exact *dpy-5* allele is unknown but presumed to be *e61*, as published in (Carvalho *et al.* 2009. *Cell*. 137:936-37).

Table S 1: Strain names and genotypes.

Strain names and genotypes used in this study

Plasmid	Gene(s)	Oligo 1	Oligo 2	Template	Cloning vector
pJC165	*par-1 (H39E23.1)*	gcgcgACTAGTttgctgattttggattttcg	gcgcgACTAGTgctgatcctgcagtgattgat	N2 cDNA	L4440 (empty vector)
pJC317	*par-2 (F58B6.3)*	gcgcgACTAGTcggccgctctagaactagtat	gcgcgACTAGTtcctgcagcccgggggat	N2 cDNA	L4440
pJC166	*pkc-3 (F09E5.1)*	gcgcgACTAGTcgtctccgacatcattagagg	gcgcgACTAGTgattcggtctggaagcaaga	N2 cDNA	L4440
pJC186	*par-4 (Y59A8B.14)*	gcgcgACTAGTgggccgtcaaaattatgaaat	gcgcgACTAGTaggccttgatcctctggg	N2 cDNA	L4440
pJC132	*ani-1 (Y49E10.19)*	gcgcgACTAGTactccagtgcattttcaccc	gcgcgACTAGTgacgatgatgatgatgtcgc	N2 cDNA	L4440
pJC43	*par-3 (F54E7.3)*	Acquired from Ahringer library (Clone # III-3A01)			
pJC56	*par-6 (T26E3.3)*	Acquired from Ahringer library (Clone # I-6M10)			
pJC53	*cdc-42 (R07G3.1)*	Acquired from Ahringer library (Clone # II-5P13)			
pJC55	*unc-59 (W09C5.2)*	Acquired from Ahringer library (Clone # I-6N04)			
pJC319	*par-2 (F58B6.3)* and *unc-59 (W09C5.2)*	gcgcgGAATTCcggccgctctagaactagtat	gcgcgGAATTCtcctgcagcccgggggat	pJC317 (par-2)	pJC55 (unc-59)
pJC318	*par-6 (T26E3.3)* and *unc-59 (W09C5.2)*	gcgcgGAATTCgaaaaatccaaattttca	gcgcgGAATTCttaacgatttttgagctgt	pJC56 (par-6)	pJC55 (unc-59)

Table S 2: Feeding RNAi constructs.

Plasmid names, targeted genes for RNAi experiments, oligos used to generate RNAi feeding construct and DNA template used or Ahringer library (Kamath and Ahringer, 2003; Kamath et al., 2003) clone number, and cloning vectors used in this study.

Results and Discussion not published in the paper

Opposing polarity domains may contribute to the fidelity of cytokinesis

As we found both the opposing aPAR and pPAR proteins (which overlap at the division plane) were required to protect against cytokinesis failure in the *formin(ts)* mutant, we were also interested to see if the presence of opposing domains itself is a contributing factor in cell division. To address this, we used *PAR-5(RNAi),* which is responsible for the exclusion of opposing polarity proteins and results in the entire cortex being occupied by both aPARs and pPARs (Morton et al., 2002). If the presence of both aPARs and pPARs is contributing to cytokinesis, then use of *PAR-5(RNAi)* in our sensitized mutants should show rescue of ingression. *formin(ts);PAR-5(RNAi)* embryos still exhibited little furrow ingression and ultimately 10 out of 10 embryos failed in cytokinesis (Figure 13A,C). Further, *myosin-II(ts);PAR-5(RNAi)* embryos showed enhancement with 3/8 embryos failing to divide compared to all embryos completing cytokinesis in *myosin-II(ts)* at SP (Figure 13B-C).

Even so, from this we cannot conclude that the overlap or opposing zone of aPAR and pPAR proteins is not an ingredient required for PAR-mediated protection of cytokinesis because PAR-5 is one of two 14-3-3 proteins in *C. elegans*, which are proteins that regulate many aspects of cell homeostasis. *(Aristizabal-Corrales et al., 2013)*. As a consequence of 14-3-3 loss, cap-dependent translation-- normally suppressed during mitosis, is not inhibited and cytokinesis fails, which we cannot rule out as a reason for why we see enhanced failure here.

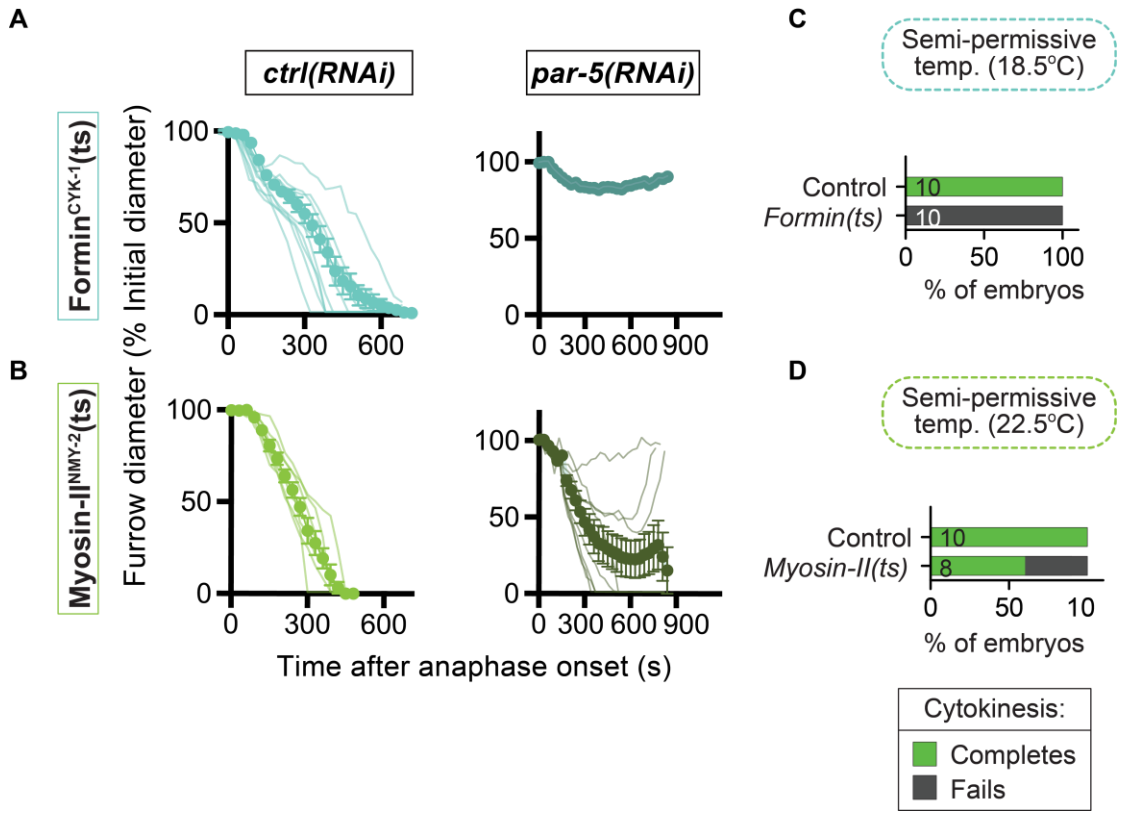

Figure 13: Loss of PAR-5 does not rescue cytokinesis failure in CR weakened ts strains

A, B) Kinetic analysis of contractile ring constriction in *formin(ts)* and *myosin(ts)* mutant 1-cell embryos with and without PAR-5, dividing at semi-permissive temperatures (18.5ºC) (A) and semi-permissive (22.5ºC) (B) temperature. Graphs show the mean ring diameter over time, with all replicates for the in a more transparent shade of the same dark blue. Error bars represent the SEM. C, D) Cytokinesis failure and success rates for different genotypes.

Requirement for "core" cytokinetic proteins may be cell and PAR-dependent

Cytokinesis is not equal across all tissue types such as in the liver and heart where incomplete cytokinesis occurs intentionally (Margall-Ducos et al., 2007). This propelled us to study how differences in cell "identity" affect the ability of the cytokinetic machinery to drive cell division. I went on to study the differential regulation of cytokinesis in the 4-to-8 cell *C. elegans* embryo. Using conditional, temperature-sensitive (ts) mutants of the core cytokinetic machinery (*formin, myosin-II*) to selectively weaken specific proteins that function in cytokinesis and bypass the first and second rounds of division, we have found that cytokinesis is differentially regulated in the 4-to-8 cell embryo. I also investigated the contribution of PAR proteins in these mutants. At the four-cell stage in the *C. elegans* embryo, there are two cells that undergo an asymmetric division (EMS and P2), and two cells that undergo a symmetric cell division (ABa and ABp). At this stage, each daughter cell is programmed to form a unique cell fate and lineage, which are specified to form the hypodermis, nervous system, pharynx and the germ-line from their descendants (Riddle et al., 1997). This cell fate specification is mediated by conserved signaling molecules Delta/Notch, and Wnt/Frizzled, some of which also control the orientation of PAR proteins (Arata et al., 2010). The fates of the blastomere sisters are conditional on their cell-contacts within the embryo, which also go on to effect cell polarity.

To begin, I set out to find the pivot temperature, the temperature at which I observe equal cytokinesis failure and completion, for *formin* and *myosin-II* mutants. In the one-cell embryo at the restrictive temperature 26ºC, no contractile ring constriction is observed for myosin-II or formin mutants (Davies et al., 2014) but there was no published data on the cytokinetic phenotype if the mutants were disrupted at later cell divisions. By upshifting the

embryos from permissive to a range of temperatures, I could determine if and how the requirement for myosin-II or formin varies between the different cell types.

To find the pivot temperatures, I performed time-lapse image analysis of cytokinesis in the four-cell *C. elegans* embryo, under *control(RNAi)* or PAR knockdown conditions at temperatures ranging from approximately 19ºC-26ºC using a device dubbed the Therminator. The Therminator is a fluidic device made in the lab that is able to shift between cold and warm temperatures in ~ 17s. In doing so, it rapidly inactivates protein function of temperature sensitive mutants during live imaging of cells (Davies et al., 2014). Then I went on test if PARs protect against cytokinesis failure in a multicellular embryo in the sensitized genetic mutants by searching for suppressors or enhancers of cytokinesis. Given the results of polarity's role in cytokinesis in the one-cell zygote, I expected the EMS and P2 daughter cells to be more protected against cytokinesis failure than ABa and ABp because they establish opposing polarity domains while the latter are non-polarized.

PAR activity was disrupted using feeding RNAi against PAR-6 and/or PAR-2 function (Figure 14). I found for formin the pivot temperature of ABa would be between 20ºC and 22ºC, given the failure phenotype (only 1/7 or 14.3% complete at 22 ºC) (Figure 14C). The pivot temperature for ABp appears to be higher, at around 23ºC where 4/9 (~44%) of embryos complete cytokinesis. EMS and P2 exhibit a much higher pivot temperature than ABa and ABp and more so even than the zygote (Davies et al., 2014). EMS may have less requirement for formin than even P2 cells as no failure is seen even at 25ºC and some embryos still complete even at 26ºC (though there are few n's at this temperature). For P2 the pivot temperature appears to be ~25ºC with 5/8 (~63%) of embryos completing cytokinesis. At 26 ºC 3/4 embryos are still able to complete cytokinesis but given the small number of

embryos observed, a greater n would likely yield to the observance of more cytokinesis failure at this temperature.

Upon knockdown of PAR-6 in the *formin(ts)* mutants, I observed some enhancement of the failure phenotype in EMS and P2 cells (Figure 14C). It is difficult to conclude the effect of PAR-6 RNAi on ABa and ABp cells given the few n's, but there does not appear to be much enhancement. For the ABa cell in the *formin(ts);par-6(RNAi)* condition, fewer cells fail at 23 ºC (6/7 or 86% complete cytokinesis) than in the *formin(ts)* alone where 8/9 (~89%) of embryos fail to divide at the same temperature. Even so, this is already a much higher pivot point than observed at the 1-cell embryo, where all embryos exhibit cytokinesis failure at 23.5ºC (and needless to say at the restrictive 26ºC) whereas the EMS and P2 cell still show embryos completing cytokinesis at 25ºC and 26ºC. Based on this limited data, it seems PAR-6 may have a protective role in cytokinesis for the EMS and P2 cell but not in the ABa or ABp cell. It is also possible, that PAR-6 function may be slightly less advantageous for ABp given that PAR-6 knockdown causes more cells (5/7) to complete cytokinesis than in *formin(ts)* mutants alone (4/9) at the same temperature (though again more n's would be necessary to draw any big conclusions).

In regards to the effect of PAR-2 depletion it seems that ABp cells have a better resistance than ABa cells as 0/8 cells fail to divide at 23 ºC while 4/8 (50%) ABa cells fail at this same temperature (Figure 14E). Surprisingly, only 4/7 (57%) of P2 cells completed cytokinesis at 23 ºC while all 7/7 (100%) of EMS cells divided. This may suggest that the P2 cell is more sensitive to the loss of posterior polarity proteins than the EMS cell.

The requirement for myosin-II, unlike for formin, appears to be equally necessary for all 4 cell types. At 24ºC, ABa divides successfully 52% of the time and ABp divides 68%

while at 25ºC all cells fail so 24ºC- 24.5ºC is likely the pivot point (Figure 14A). This is similar to what is observed in the C. elegans zygote (Davies et al., 2014). Unexpectedly, EMS and P2 show more sensitivity to loss of myosin than ABa and ABp, with 7/8 (~88%) failing to divide at 24ºC. Since all embryos complete cytokinesis at 22ºC the pivot temperature is likely around 23ºC. It seems that myosin function is important for cytokinesis for all 4 cells, and particularly so for the EMS and P2 cells to divide.

Although double mutants *myosin-II(ts);par-6(RNAi)* were only observed at 3 temperatures, already an enhancement in the failure phenotype is present given that all cell-types begin to show some failure at 22ºC whereas in *myosin-II(ts)* mutants alone generally failure is only observed at 24ºC and above (with the 1 anomaly of an ABa cell that fails at 20 ºC) (Figure 14B). This suggests that perhaps PAR-6 continues to have a protective role in cytokinesis even later in development.

In the anterior blastomere daughter cells, ABa and ABp, the requirement for formin was similar as in the zygote while EMS and P2 display protection against cytokinesis failure and need a much higher upshift in temperature before the cells fail to divide. It is possible this may have something to do with how these cells divide. One similarity between EMS and P2 is they divide asymmetrically, unlike ABa and ABp cells. Further, the position of EMS and P2 within their lineage may be another reason they are more robust at completing cytokinesis even in the absence of formin, though this same reasoning would not apply for the loss of myosin. ABa and ABp are downstream of their mother AB founder cell whereas EMS and P2 are upstream of their founder cells E, MS and P4. As such, these cells may afford more protection to better guarantee chances for the formation of their founder cell descendants.

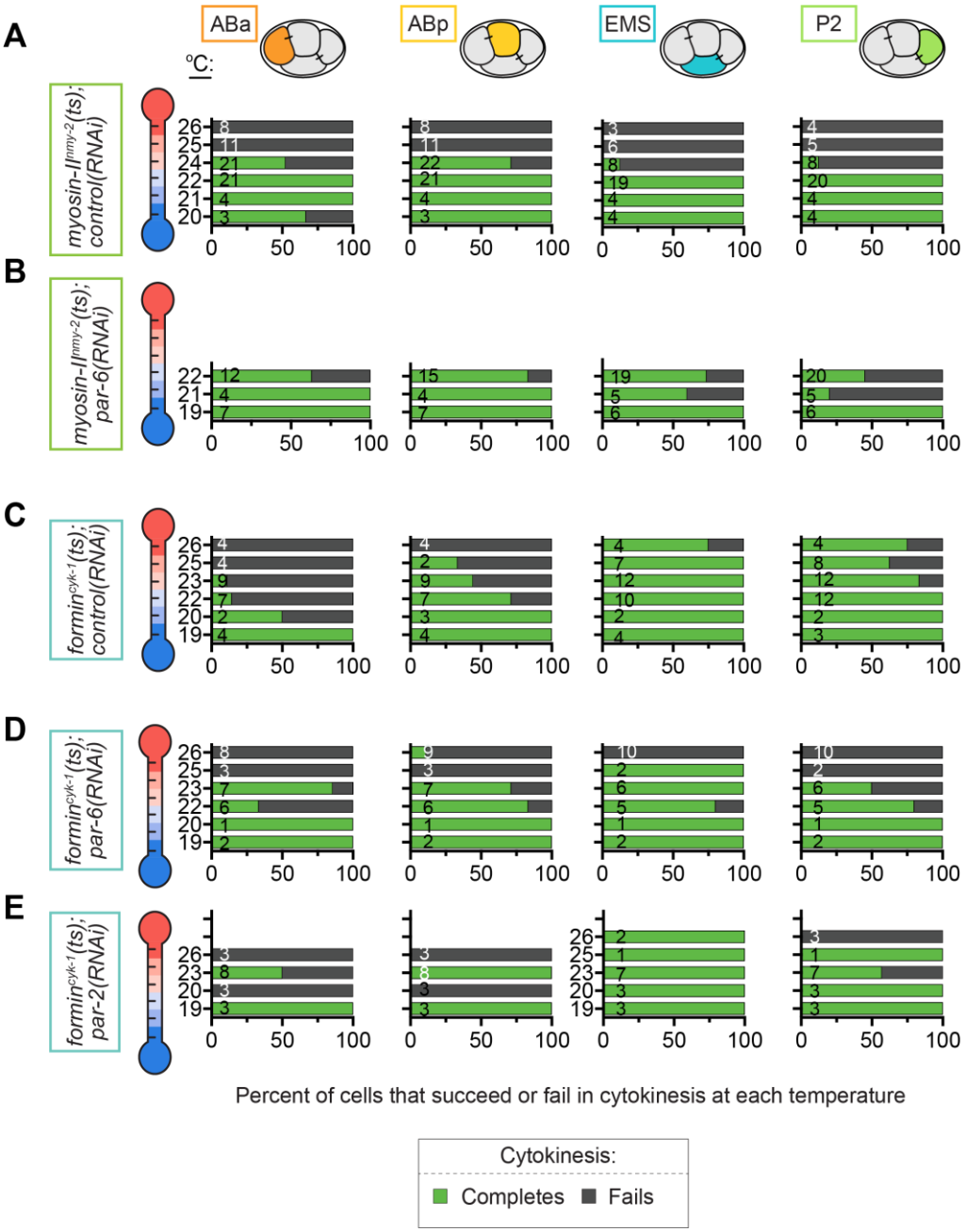

Figure 14: Requirement of myosin-II and formin with and without PARs

A) *Contro(RNAi);myosin-II*$^{NMY-2}$*(ts),* B) *PAR-6(RNAi);myosin-II*$^{NMY-2}$*(ts)* C) *Contro(RNAi);formin*$^{CYK-1}$*(ts),* D) *PAR-6(RNAi);formin*$^{CYK-1}$*(ts)* E) *PAR-2(RNAi);formin*$^{CYK-1}$*(ts)* mutant embryos were upshifted to specific temperatures and the cytokinetic outcome of each blastomere was scored. The percent of cells exhibiting each cytokinetic phenotype at the indicated temperature is plotted for each cell type and genotype.

A major caveat is that knockdown of PAR proteins via RNAi precludes polarity establishment during critical points of development that could go on to define the essential fate of the cell. If the fate of the cells is not conserved then it is difficult to interpret much of this data and the reason for the differential cytokinesis phenotypes. While the differences in the requirement for myosin-II and formin has gone on to be investigated by another member of the lab, the effect of PARs in conjunction with loss of these proteins can still be probed further. Some things that would have to be accounted for again are the fate of the cells. There are intrinsic regulatory mechanisms besides polarity and cell-cycle differences that can be attributed to different fates. For instance, P1 cell descendants inherit P-granules and CAR-1 (Pitt et al., 2000; Schisa et al., 2001; Strome and Wood, 1982). Observing if there are any differences in typical spindle alignment in EMS and P2 where EMS typically divides along the A-P axis while P2 divides dorsal to ventral axis may be one solution to examining if cell identity is still present (Evans et al., 1994; Priess and Thomson, 1987). If these intrinsic fate characteristics are not maintained when PARs are depleted so early on with feeding RNAi, another option, albeit much more difficult, would be to make or look for temperature sensitive PAR mutants whose semi-restrictive/restrictive temperature would optimally be less than or the same as for the other cytokinetic mutants so PAR proteins could be depleted at specific stages of interest. Perhaps also, the difference in requirement is tethered to the fate of the cell's descendants such that certain cells that eventually become [X] have a higher or lower requirement for a given protein (explored more in Chapter 4).

One thing is certain, the different cell-specific requirements for formin and myosin-II points to the importance of investigating classically required cytokinetic protein functions beyond the 1-cell stage.

Materials and Methods

Strain maintenance

Caenorhabditis elegans were maintained on standard NGM plates seeded with OP50 *E. coli*, as described (Brenner, 1974). Strain names and genotypes used in this study can be found in Table S 1. Amy Maddox (University of North Carolina; Chapel Hill, NC, USA) provided the strains OD159 [GFP::ANI-1] and OD26 [GFP::UNC-59], the latter of which was crossed with a strain containing the histone marker ltIs37[pAA64; pie-1/mCHERRY::his-58; unc-119 (+)] to generate JCC425. Michael Glotzer (University of Chicago; Chicago, IL, USA) provided a strain containing the f-actin marker mgSi3[tb-unc-119(+) GFP::Utrophin], which was crossed with a strain containing the histone marker ltIs37[pAA64; pie-1/mCHERRY::his-58; unc-119 (+)] to generate JCC719.

Temperature control

Control and temperature-sensitive (ts) strains were maintained in an incubator (Crittenden et al.) at permissive temperature (16.0˚C ± 0.5˚C), except JCC744, JCC719, JCC541, JCC425, and OD159, which were maintained at room temperature to prevent silencing of fluorescent reporters. Live imaging was performed in a room with homeostatic temperature control, set to the desired temperature at least one hour prior to the experiment. The temperature of the specimen was continuously monitored using three thermometers, attached directly to the objective lens with a glue gun. Where denoted throughout the paper, room temperatures were as follows: *formin(ts)* semi-permissive temperature (18.5˚C ± 0.5˚C); *formin(ts)* semi-restrictive temperature (23.5˚C ± 0.5˚C); *myosin-II(ts)* semi-permissive temperature (22.0˚C ± 0.5˚C); *myosin-II(ts)* semi-restrictive temperature (25.5˚C ± 0.5˚C);

fully restrictive temperature (26.5˚C ± 0.5˚C). During Therminator experiments (Figure 8A; S1B,D), the room was maintained at the *formin(ts)* semi-permissive temperature (18.5˚C ± 0.5˚C) (Davies et al., 2014).

Rapid temperature shifts

Rapid temperature shifts were performed using a custom-built fluidic system called the Therminator (Davies et al., 2014) (Bioptechs) with one water/isopropanol bath maintained at permissive temperature (16.0˚C ± 0.5˚C) and a second bath at the semi-permissive temperature (18.5˚C ± 0.5˚C; Figure 8A; S1B) or restrictive temperature (26.5˚C ± 0.5˚C; Figure S 1D). A switch mechanism determines which water bath supplies liquid for the chamber above the specimen. Forced heat convection from the flow chamber to the glass barrier directly above the specimen chamber rapidly shifts the sample temperature.

Live-cell imaging

Young gravid hermaphrodites were dissected in 16˚C M9 buffer (Brenner, 1974) and mounted on a thin, 2% agar pad, as previously described (Davies et al., 2014; Gonczy et al., 1999). Embryos were filmed using a Yokagawa CSU-10 spinning disc confocal with Borealis (Spectral Applied Research) on a Nikon Ti inverted microscope with a 60x 1.4 N.A. oil-immersion PlanApochromat objective with 2x2 binning on a Hamamatsu Orca-R2 CCD camera. During temperature shift experiments, a 20x 0.75 N.A. dry objective was used. Z-sectioning was done with a Piezo-driven motorized stage (Applied Scientific Instrumentation) and focus was maintained using Perfect Focus (Nikon) prior to each Z-series acquisition. An acousto-optic tunable filter was used to select the excitation light of two 100mW lasers for excitation at 491 and 561nm for eGFP and mCherry, respectively (Spectral Applied

Research), and a filter-wheel was used for emission wavelength selection (Sutter Instruments). The system was controlled by Metamorph software (Molecular Devices).

A central DIC image and a through-cell fluorescent Z-series were collected every 30s to measure contractile ring dynamics (7 x 2.0μm steps; Figure 9B,C; Figure 10B; Figure 12D-F; S1A; S3B) or every 60s for Therminator upshifts (5 x 2.0μm steps; Figure 8A; S1B,D), and measurement of fluorescent reporter accumulation in the cell poles and contractile ring (11 x 2.5μm steps; Figure 9D,E; Figure 10D-F; Figure 11B-E; Figure 12A-C; Figure S 3C-F). 3 x 1.0μm steps were acquired at the cell cortex for Figure S 1C.

Image analysis

Metamorph and Image J software were used for all data analysis. Metaphase plate positions were measured 30s prior to anaphase onset. In Figure 8C, positions are shown relative to the A-P axis, with the anterior pole being 0% and the posterior pole 100%. In Figure S 2A,C, the distance between the posterior pole and the metaphase plate was subtracted from the distance between the anterior pole and the metaphase plate. Positions reflect displacement of the metaphase plate from the cell center (0μm).

Contractile ring diameter was measured at the cell equator from anaphase onset until, in the case of cytokinesis completion, anaphase of the subsequent cell cycle, or, in the case of cytokinesis failure, until the contractile ring had completely regressed and the next cell cycle began in the aneuploid cell. The ring diameter was measured as the shortest distance between the furrow tips, using a fluorescent marker targeted to the plasma membrane (PH::GFP, pleckstrin homology domain; (Audhya et al., 2005)). For each time point, the Z plane at which the ring diameter was widest was used for this measurement. Contractile ring diameter

was plotted as a percentage of the initial diameter (at metaphase) as a function of time. Anaphase onset was determined using a fluorescent histone marker (mCherry::Histone2B; (Audhya et al., 2007)) and was set as the first time point at which distinct sister chromatids became visible.

Cortical localization of fluorescent markers (GFP::anillin^{ANI-1}, GFP::septin^{UNC-59}) (Maddox et al., 2007) was measured at metaphase (one frame prior to anaphase onset) and furrow onset (one frame prior to formation of a "double membrane furrow", ~60s after anaphase onset). A sum projection of 7 central planes was generated and the mean fluorescence was measured along a linescan tracing the cortex from anterior to posterior pole. The mean fluorescence was measured outside of the cell and subtracted from the cortical fluorescence. Values along the cortical linescan were then normalized to the line average for that cell; that is, a homogeneous cortex would have a value of 1 at all points. In Figure 9D-E, the mean fluorescence of the two polarity markers (mCh::PAR-6 and GFP::PAR-2) (Schonegg et al., 2007) was measured similarly but are shown as a ratio of one to the other, rather than being normalized to the line average. Fluorescence values around polar bodies were removed from linescans. Polarized accumulation of GFP::anillin^{ANI-1} and GFP::septin^{UNC-59} (Figure 11B-C) was calculated at metaphase as a ratio of the mean fluorescence in the anterior half over the posterior half of the embryo.

Accumulation of contractile ring markers (GFP::Utrophin^{ABD}, myosin-II^{NMY-2}::GFP, GFP::septin^{UNC-59}, GFP::anillin^{ANI-1}) (Burkel et al., 2007; Maddox et al., 2007; Munro et al., 2004; Tse et al., 2012) was measured 180s after anaphase onset from a through-cell Z-series sum projection (11 planes, encompassing entire cell). The mean fluorescence was measured in a 65μm^2 region that encompassed the contractile ring. The mean fluorescence of an

equivalent background region was measured outside of the cell and subtracted from the mean ring fluorescence. Intensities were then normalized to the contractile ring of *control(RNAi)* embryos imaged on the same day.

Daughter cell size asymmetry was measured at the time of contractile ring closure (0% initial diameter) and is shown as a ratio of the AB (anterior daughter cell) length to the P1 (posterior daughter cell) length. Cell cycle asymmetry was measured as the difference in time from anaphase onset in AB to the time of anaphase onset in P1. Spindle lengths were measured 150s after anaphase onset, using transmitted light (differential interference contrast, DIC) to visualize the spindle poles. Distances were normalized to the spindle length of controls at the same temperature.

RNAi

Exonic sequences from the desired gene were cloned into the multiple cloning site of the L4440 vector using standard cloning techniques and then transformed into HT115 *E. coli* using $CaCl_2$ transformation, as described (Timmons et al., 2001). RNAi primers and template DNA for each gene are listed in Table S 2. When available, RNAi constructs were obtained directly from the Ahringer RNAi library (Kamath and Ahringer, 2003). For double RNAi constructs (*par-6; unc-59* and *par-2; unc-59*), exonic sequences for either *par-6* or *par-2* were cloned into the multiple cloning site of pJC55 (L4440 containing *unc-59*), which was linearized via EcoRI digestion.

RNAi feeding bacteria were grown in Luria Broth with ampicillin (100 µg/mL) for 8-16 hours at 32˚C. 300 µL of this culture was plated on RNAi plates: NGM agar plates (Brenner, 1974) supplemented with 50µg/mL ampicillin and 1mM IPTG. These plates were

allowed to dry and grow at 32˚C for 24-48 hours. L1 worms were plated on RNAi plates and then incubated at 16˚C for 72 hours prior to filming. Successful RNAi-mediated knockdown of PAR proteins was confirmed using four hallmarks of the loss of polarity (Bossinger and Cowan, 2012): 1) reduced spindle displacement at metaphase, 2) loss of daughter cell size asymmetry following division, 3) high embryonic lethality, and 4) mislocalized fluorescent reporters for the anterior (mCh::PAR-6) and posterior (GFP::PAR-2) domains, and/or loss of cell cycle asynchrony in the AB/P1 cell divisions (see Figure S 2).

Statistical Analysis

Unpaired two-tailed t-tests were conducted using Graphpad Prism software. *indicates $p<0.05$; **indicates $p<0.005$; ***indicates $p<0.0005$; and ****indicates $p<0.0001$.

Experimental Procedures for experiments not published in the paper

Temperature control

myosin-II(ts);par-5(RNAi) was imaged at its semi-permissive temperature of 22.5ºC and *formin(ts);par-5(RNAi)* was kept at its semi-permissive temperature of 18.5ºC. A range of temperatures were used for the *formin(ts), myosin-II(ts)* with *control*, *par-6,* and *par-2* RNAi. For *myosin-II(ts)* 20ºC-26ºC was observed for all blastomeres at the four-cell stage. For *myosin-II(ts);par-6(RNAi*) only 19ºC, 21ºC, and 22ºC temperatures were filmed. For *formin(ts)* and *formin(ts);par-6(RNAi)* 19ºC-26ºC (with the exception of no cells at 24ºC) were observed. *formin(ts);par-2(RNAi)* was imaged at 19ºC, 20ºC, 23ºC and 26ºC.

PAR-5 (M117.2.2) RNAi: pJC 132 F: gcgcg**actagt**aaaatgtccgataccgtgga

R: gcgcg**actagt**agaaaaatggaagatggggg

Acknowledgements

We thank all Canman, Shirasu-Hiza, and Dumont lab members for support; Gregg Gundersen, Clare Waterman, Sriramkumar Sundaramoorthy, and Andy Kummel for critical reading; Natalia Spica, Isaiah Thomas, and Vandana Chand for lab assistance; Jennifer Waters for microscopy consultation; and Amy Maddox, Michael Glotzer, and the Caenorhabditis Genetics Center for worm strains. Authors have no competing financial interests. ANR-09-RPDOC-005-01, FRM-AJE201112, and the Emergence program from Mairie de Paris (JD); NIH-R01-GM105775 and NIH-R01-AG045842 (MSH); and NIH-DP2-OD008773 to (JCC).

Chapter 3. CYK-4 regulates Rac, but not Rho, during cytokinesis

Most of this chapter has been published in

Yelena Zhuravlev, Sophia M. Hirsch, Shawn N. Jordan, Julien Dumont, Mimi Shirasu-Hiza, and Julie C. Canman. *CYK-4 regulates Rac, but not Rho, during cytokinesis.* MBoC. March, 2017

Preface/Author contributions

Publication of this research is thanks to the contribution of people in the author's list and acknowledgement section. SNJ, JCC, and I conceived and conducted all of the experiments. SMH, SNJ, JD, MSH, JCC, and I made intellectual contributions and wrote the manuscript; and JCC and I made all the figures. More specifically, SMH contributed to the experiments and analysis used in Figure 20, where she investigated if CDC-42 was another target of Cyk-4 by looking at strains with and without CYK-4, Rac, CDC-42 and combinations thereof. Julie Canman also contributed experiments and analysis used in Figure 20, where she explored the contribution of paternal requirement of Cyk-4 by looking at brood size and viability. SNJ imaged some of the *cyk-4(ts);Rac(RNAi)* strains that were used for analysis in Figure 15. All unpublished results and discussion related to this project begin on page 115.

Abstract

Cytokinesis is driven by constriction of an actomyosin contractile ring that is controlled by Rho family small GTPases. Rho, activated by the Guanine-nucleotide Exchange Factor (GEF) ECT-2, is upstream of both myosin-II activation and diaphanous formin-mediated filamentous actin (f-actin) assembly, which drive ring constriction. The role for Rac and its regulators is more controversial but, based on the finding that Rac inactivation can rescue cytokinesis failure when the GTPase Activating Protein (GAP) CYK-4 is disrupted, Rac activity was proposed to be inhibitory to contractile ring constriction and thus specifically inactivated by CYK-4 at the division plane. An alternative model proposes that Rac inactivation generally rescues cytokinesis failure by reducing cortical tension, thus making it easier for the cell to divide when ring constriction is compromised. In this alternative model, CYK-4 was instead proposed to activate Rho by binding ECT-2. Using a combination of time-lapse *in vivo* single-cell analysis and *C. elegans* genetics, our evidence does not support this alternative model. First, we found that Rac disruption does not generally rescue cytokinesis failure: inhibition of Rac specifically rescues cytokinesis failure due to disruption of CYK-4 or ECT-2 but does not rescue cytokinesis failure due to disruption of two other contractile ring components, the Rho effectors diaphanous formin or myosin-II. Second, if CYK-4 regulates cytokinesis through Rho rather than Rac, then CYK-4 inhibition should decrease levels of downstream targets of Rho. Inconsistent with this, we found no change in the levels of f-actin or myosin-II at the division plane when CYK-4 GAP activity was reduced, suggesting that CYK-4 is not upstream of ECT-2/Rho activation. Instead, we found that the rescue of cytokinesis in CYK-4 mutants by Rac inactivation was Cdc42-dependent.

Together our data suggest that CYK-4 GAP activity opposes Rac (and perhaps Cdc42) during cytokinesis.

Introduction

Rho family small GTPases (Rho, Rac, and Cdc42) function as molecular switches: when GDP-bound, they are inactive and when GTP-bound, they interact with cytoskeletal effectors to choreograph the cell shape changes required for complex cellular events such as cell motility, phagocytosis, and cytokinesis (Hall, 2012; Jordan and Canman, 2012; Mao and Finnemann, 2015; Ridley, 2015). Cytokinesis, the physical division of one cell into two, is driven by constriction of an actomyosin contractile ring, directed to form at the division plane after anaphase onset via Rho family GTPase signaling. In most animal cells, assembly and constriction of the actomyosin contractile ring is downstream of Rho (Bement et al., 2005; Kamijo et al., 2006; O'Connell et al., 1999), which is activated at the division plane by the Guanine-nucleotide Exchange Factor (GEF) ECT-2 (epithelial cell transforming-2), a human oncogene (D'Avino et al., 2015; Kamijo et al., 2006; Kimura et al., 2000; Tatsumoto et al., 1999). Once activated, Rho promotes both filamentous actin (f-actin) nucleation by a diaphanous-family formin (CYK-1 in *C. elegans*, hereafter formin) and non-muscle myosin-II motor activation (NMY-2 in *C. elegans*, hereafter myosin-II), which drive contractile ring assembly and power ring constriction (for review see (D'Avino et al., 2015; Green et al., 2012; Pollard, 2010)). Rho activation during cytokinesis is opposed by the GTPase Activating Protein (GAP) MP-GAP (RGA-3/4 in *C. elegans*), which promotes Rho's hydrolysis of GTP to GDP (Zanin et al., 2013).

The role(s) for the Rho family GTPase Rac and the Rac GAP CYK-4 during cytokinesis is still under debate. CYK-4 (HsCYK4/MgcRacGAP in humans, RacGAP50c in flies, hereafter CYK-4) is essential for cytokinesis in nearly all cell types (Goldstein et al., 2005; Hirose et al., 2001; Jantsch-Plunger et al., 2000), forms a complex called Centralspindlin with the kinesin MKLP-1/ZEN-4 (Mishima et al., 2002; Pavicic-Kaltenbrunner et al., 2007), and has been proposed to both inhibit Rac activation and promote Rho activation at the division plane via its GAP domain (Bastos et al., 2012; Canman et al., 2008; Cannet et al., 2014; D'Avino et al., 2004; Jantsch-Plunger et al., 2000; Loria et al., 2012; Miller and Bement, 2009; Zhang and Glotzer, 2015). *In vitro*, CYK-4 inactivates Rac and Cdc42 by promoting GTP hydrolysis, but has little effect on the activity of Rho (Bastos et al., 2012; Jantsch-Plunger et al., 2000; Toure et al., 1998). *In vivo*, CYK-4 has been proposed to inhibit Rac activity (Bastos et al., 2012; Canman et al., 2008; Cannet et al., 2014; D'Avino et al., 2004; Yoshizaki et al., 2004), promote Rho-GTP turnover (or flux) (Miller and Bement, 2009), and promote the activation of Rho by stimulating the GEF activity of ECT-2 during cytokinesis (Loria et al., 2012; Tse et al., 2012; Zhang and Glotzer, 2015; Zhao and Fang, 2005b). Thus, currently, there is no consensus view on the mechanisms by which CYK-4 and/or Rac activity regulate cytokinesis.

To support the model in which CYK-4 negatively regulates Rac during cytokinesis, in worms, flies, and cultured human cells, mutational disruption of the CYK-4 GAP domain leads to cytokinesis failure that can be rescued by reducing Rac activity (Bastos et al., 2012; Canman et al., 2008; Cannet et al., 2014; D'Avino et al., 2004). Cytokinesis failure in CYK-4 GAP-domain mutants can also be rescued by depletion of the Arp2/3 complex, a Rac effector and branched f-actin nucleator in worms and cultured mammalian cells (Canman et al., 2008;

Cannet et al., 2014). Moreover, in cultured mammalian cells, cytokinesis failure caused by CYK-4 GAP disruption can be rescued by depleting Rac effectors that promote cell substrate attachment such as PAK1 and ARHGEF7 (Bastos et al., 2012) and the upstream Rac GEF Trio (Cannet et al., 2014). Thus, CYK-4 GAP-mediated inactivation of Rac at the division plane has been proposed to function in parallel to Rho activation to allow contractile ring constriction and promote efficient cytokinesis.

In contrast, CYK-4 has also been proposed to function during cytokinesis through the promotion of Rho activation by facilitating GTP-turnover (flux) or by activating the Rho GEF ECT-2 (Loria et al., 2012; Miller and Bement, 2009; Tse et al., 2012; Zhang and Glotzer, 2015; Zhao and Fang, 2005b). Although *in vitro* CYK-4 is not effective at promoting the GTP-turnover of Rho (Bastos et al., 2012; Jantsch-Plunger et al., 2000; Toure et al., 1998), *in vivo* mutations in the GAP domain have a strong effect on the width and stability of the zone of active GTP-bound Rho at the division plane in *Xenopus* embryos (Miller and Bement, 2009). This could be due to a direct effect on Rho activation, or an indirect effect by modulating other Rho family members that compete for effectors and upstream regulators such as GAPs, GEFs, and GDIs (*e.g.* (Boulter et al., 2010; Garcia-Mata et al., 2011; Machacek et al., 2009; Tatsumoto et al., 1999)). CYK-4 has also been proposed to promote Rho activation by stimulating the Rho GEF ECT-2 (Zhang and Glotzer, 2015; Zhao and Fang, 2005b). This hypothesis was based on the findings that CYK-4/MgcRacGAP can bind ECT-2 (Burkard et al., 2009; Somers and Saint, 2003; Wolfe et al., 2009; Yuce et al., 2005; Zhang and Glotzer, 2015) and that mutational disruption of the CYK-4 GAP domain can be suppressed by hyperactivating mutations in the ECT-2 GEF domain (Zhang and Glotzer, 2015). The same group also reported that CYK-4 disruption prevents the enrichment of f-

actin and myosin-II at the division plane, which would be expected if CYK-4 activates ECT-2 and thus Rho activity during cytokinesis (Loria et al., 2012). However, other studies could not confirm that CYK-4 GAP disruption leads to decreased levels of myosin-II at the division plane (Canman et al., 2008; Zhang and Glotzer, 2015). Moreover, *in vitro* analysis found no change in ECT-2 GEF activity towards Rho in the presence or absence of CYK-4 (Zhang and Glotzer, 2015), although this negative result cannot rule out that additional factors may be needed. Thus, while CYK-4 has been proposed to play an essential role in ECT-2 and Rho activation, much of the evidence for this model is indirect.

Furthermore, in models that support a role for CYK-4 in Rho activation via ECT-2 (Loria et al., 2012; Zhang and Glotzer, 2015), the finding that cytokinesis failure resulting from CYK-4 GAP disruption can be rescued by Rac inactivation is attributed to a general or "bypass" role for Rac (Loria et al., 2012) in regulating cortical tension and opposing contractile ring constriction, as was found in *Dictyostelium* (Zhang and Robinson, 2005). Support for this model relies on the finding that reducing Rac activity could also rescue cytokinesis failure in a hypomorphic *ect-2(ts)* mutant background (Loria et al., 2012). Yet, *in vitro* ECT-2 GEF activity can activate both Rho and Rac (Tatsumoto et al., 1999); thus, Rac depletion might rescue cytokinesis when ECT-2 activity is weakened by simply reducing competition with Rho for the GEF domain. Moreover, Rac disruption does not rescue cytokinesis failure when Aurora B kinase activity is compromised, which also regulates contractile ring constriction in a pathway parallel to CYK-4 during cytokinesis (Lewellyn et al., 2011). Thus, a general role for Rac in opposing contractile ring constriction in animal cells is not well supported.

The role for Cdc42 in animal cell cytokinesis is also controversial. Cdc42 is essential for polar body emission during meiotic cytokinesis in frog and murine embryos (Ma et al., 2006; Wang et al., 2013; Zhang et al., 2008). However, disruption of Cdc42 does not block mitotic cytokinesis in most metazoan systems (Gotta et al., 2001; Jordan et al., 2016; Zhu et al., 2011b). Injection of constitutively active or dominant negative forms of Cdc42 at very high levels (µM range) can disrupt mitotic cytokinesis in frog embryos (Drechsel et al., 1997), and expression of constitutively active Cdc42 in dividing mammalian cultured cells leads to the assembly of a broader contractile ring but does not block cytokinesis (Zhu et al., 2011b). In asymmetrically dividing *C. elegans* embryos, Cdc42 regulates cell polarity and is required for robust contractile ring f-actin assembly, and its depletion leads to synthetic cytokinesis failure in embryos from a temperature-sensitive diaphanous-related formin mutant (Jordan et al., 2016). Hence, Cdc42 likely participates in animal cell cytokinesis but is not an essential player.

Here we examine the roles of Rac and the GAP CYK-4 in cytokinesis in the early *C. elegans* embryo. We found that, as was shown previously, Rac inactivation rescued cytokinesis failure in a CYK-4 GAP mutant and to a lesser extent in a hypomorphic ECT-2 mutant. Rac disruption did not rescue the rate of contractile ring constriction in CYK-4 or ECT-2 mutants, and we found Rac disruption-mediated rescue of cytokinesis failure in CYK-4 mutants was dependent on Cdc42. We did not find evidence that Rac activity generally opposes contractile ring constriction, as Rac inactivation did not rescue the rate of cytokinesis failure in embryos with mutations in the Rho effectors diaphanous formin or the motor myosin-II. Furthermore, we found that disrupting CYK-4 activity did not lead to a reduction in the total levels of contractile ring f-actin or myosin-II at the division plane, indicating that

CYK-4 is unlikely to act upstream of ECT-2-mediated activation of Rho. Instead we propose that, at least in the early *C. elegans* embryo, ECT-2 activity may promote Rac activation, and thus in part negatively regulate cytokinesis. Together, our data supports a model in which CYK-4 functions to inhibit Rac activity (and potentially Cdc42) and does not participate directly in Rho activation; our data also do not suggest a non-specific or bypass role for Rac in opposing contractile ring constriction.

Results

We first sought to confirm that cytokinesis failure due to mutational disruption of the CYK-4 GAP domain could be rescued by reducing Rac activity. To do this, we performed time-lapse image analysis of cytokinesis in the 1-cell *C. elegans* embryo, with and without Rac disruption, in a temperature-sensitive CYK-4 GAP-domain mutant (E448K) background (Canman et al., 2008), hereafter *cyk-4(ts)*. Imaging was done at the semi-restrictive temperature (24ºC) where contractile ring ingression progresses further in *cyk-4(ts)* mutant embryos than at fully restrictive temperature, but cytokinesis fails 100% of the time in the *cyk-4(ts)* mutant alone (Figure 15A and B). Rac activity was disrupted in two ways: 1) with feeding RNAi and 2) with a loss-of-function (lof) Rac/CED-10 GTPase mutant (G60R; *ced-10(n3246)*, hereafter *Rac(G60R)* (Cabello et al., 2014; Reddien and Horvitz, 2000; Sun et al., 2012)) that, based on an identical G60R mutation in the closely related KRas, renders the small GTPase stuck in the GTP-bound state but unable to interact with effectors, GAPs, or GEFs (Gremer et al., 2011). As expected, 100% of control, *control(RNAi)*, *Rac(RNAi)*, and *Rac(G60R)* single mutant embryos successfully completed cytokinesis (16/16, 10/10, 12/12, and 12/12 embryos divide respectively), whereas 100% of *cyk-4(ts)* and *cyk-4(ts);*

control(RNAi) embryos failed in cytokinesis at this temperature (0/12 and 0/12 embryos divide respectively; Figure 15A and B). In contrast, cytokinesis was significantly rescued (Fisher's and Barnard's exact tests, p-values in Table S 5) in *cyk-4(ts);Rac(RNAi)* and *cyk-4(ts);Rac(G60R)* double mutant embryos (8/10 embryos divide for both genotypes; Figure 15A and B). To test if this rescue is conserved in other cell divisions, we also investigated if Rac disruption could rescue cytokinesis failure in the AB and P1 blastomeres of 2-cell *cyk-4(ts)* embryos (Figure S 4C). We found that both AB and P1 blastomeres fail cytokinesis in *cyk-4(ts)* 2-cell embryos at a lower rate than in 1-cell embryos (4/19 AB cells and 12/20 of P1 cells divide at semi-restrictive temperature, 25.5ºC in this case) (Figure S 4C). Nonetheless, cytokinesis failure was significantly rescued (Fisher's and Barnard's exact tests, p-values in Table S 5) in both blastomeres of *cyk-4(ts)*; *Rac(G60R)* double mutant 2-cell embryos (12/14 AB cells and 16/16 P1 cells divide successfully) (Figure S 4C). Thus, Rac inhibition rescues cytokinesis failure due to mutational disruption of the CYK-4 GAP-domain in both 1-cell and 2-cell *C. elegans* embryos. This result supports a model in which CYK-4 GAP activity inhibits Rac activation during cytokinesis, but does not rule out the possibility that Rac is a general inhibitor of contractile ring constriction (Figure 15D).

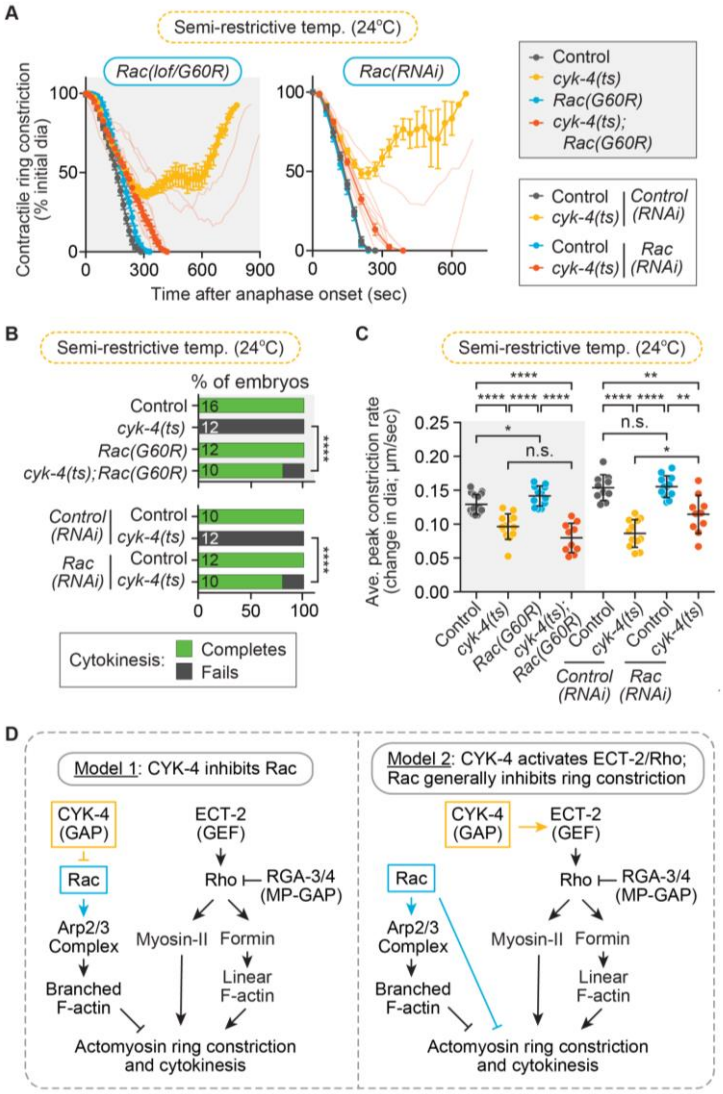

Figure 15: Rac disruption rescues cytokinesis failure in a CYK-4 GAP mutant

A) Kinetic analysis of contractile ring constriction in control and *cyk-4(ts)* mutant 1-cell embryos at semi-restrictive temperature (24ºC) with and without *Rac(lof/G60R)* (left) and *Rac(RNAi)* (Calvert et al.). Graphs show the mean ring diameter over time, with all replicates for the *cyk-4(ts);Rac(G60R or RNAi)* shown in the background in a more transparent shade of the same orange. Error bars represent the SEM. B) Cytokinesis failure and success rates for different genotypes in (A). The number of embryos per genotype is indicated on each individual bar; p-values were obtained by both Fisher's and Barnard's exact tests (Table S 5). C) Average peak rate of contractile ring constriction, plotted as the change in diameter (µm/sec; see Methods section on image analysis). Error bars represent the SD; p-values were obtained by an unpaired, two-tailed student's t-test (Table S 5). D) Current genetic models for the function of CYK-4 and Rac during cytokinesis.

We next sought to determine if Rac disruption can also rescue the slowed rate of contractile ring constriction observed in 1-cell *cyk-4(ts)* embryos. Rac disruption by RNAi or the G60R mutation either did not significantly change or only mildly increased the rate of contractile ring constriction in both control and *cyk-4(ts)* embryos (Figure 15C; unpaired student's t-test, p-values in Table S 5). Thus, Rac disruption rescues the extent of contractile ring constriction but overall does not significantly rescue the rate of ring constriction in *cyk-4(ts)* mutants (Table S 5 ; see also (Loria et al., 2012)). This result suggests that CYK-4 (and/or Rac) could play an independent role in regulating the rate of ring constriction, potentially by further activating ECT-2 (and thus Rho) at the division plane as has been proposed in this system (Figure 15D) (Tse et al., 2012; Zhang and Glotzer, 2015). This result could also support a model in which Rac disruption rescues cytokinesis in *cyk-4(ts)* mutant embryos via a non-specific or "bypass" pathway (e.g. (Loria et al., 2012; Zhang and Glotzer, 2015)).

The main argument proposed against Rac as a specific target of CYK-4 is two-fold: first, that Rac is a general inhibitor of ring constriction and its depletion might non-specifically rescue cytokinesis failure; and second, that CYK-4's true target is ECT-2. In the first part of the argument, Rac disruption has been proposed to allow successful cytokinesis in *cyk-4(ts)* embryos via a "bypass" mechanism that generally reduces cortical tension and makes it easier to complete cytokinesis when the contractile ring is weakened (Loria et al., 2012) (Figure 15D). We set out to resolve if Rac disruption can generally rescue cytokinesis failure when ring constriction is weakened, by combining *Rac(RNAi)* or *Rac(lof)* with other mutants in the ECT-2/Rho pathway that would also compromise the integrity of the contractile ring. If disrupting Rac generally facilitates contractile ring constriction, then

Rac(lof) should rescue cytokinesis failure when downstream targets of ECT-2/Rho are disrupted to weaken the contractile ring. Thus, we next tested if Rac disruption could rescue cytokinesis failure in a fast-acting *ts* mutant that affects the *C. elegans* diaphanous-related formin actin-nucleator CYK-1 (hereafter *formin(ts)*), which is required to nucleate f-actin in the contractile ring and is activated downstream of Rho (Davies et al., 2014; Jordan and Canman, 2012; Jordan et al., 2016) (Figure 15D). For this experiment, *formin(ts)* 1-cell embryos were imaged at the semi-restrictive temperature (23.5ºC), at which *formin(ts)* mutants alone can undergo partial contractile ring constriction but fail in cytokinesis 100% of the time (0/11 embryos divide; Figure 16A and C) (Jordan et al., 2016). Importantly, at this semi-restrictive temperature, cytokinesis failure in *formin(ts)* embryos can be fully rescued by depletion of other negative regulators of contractile ring constriction (*e.g.* septin (Jordan et al., 2016)). We found that at this temperature, *formin(ts); Rac(G60R)* mutants still failed in cytokinesis 100% of the time (0/10 embryos divide) and underwent even less contractile ring constriction than in the *formin(ts)* mutant alone (Figure 16A and C). This result suggests that disrupting Rac activity does not significantly rescue cytokinesis failure in *formin(ts)* mutant embryos (Fisher's and Barnard's exact tests, p-values in Table S 5). We next examined whether Rac disruption could enhance the rate of cytokinesis failure in *formin(ts)* mutant embryos at the semi-permissive temperature (18.5ºC), at which all *formin(ts)* mutant embryos successfully complete cytokinesis (13/13 embryos divide; Figure 16B and D) (Jordan et al., 2016). At semi-permissive temperature, *formin(ts); Rac(G60R)* embryos exhibited mild cytokinesis failure (10/12 embryos divide; Figure 16B and D), though this was not statistically significant (Fisher's and Barnard's exact tests, p-values in Table S 5). The rate of contractile ring constriction was significantly slower in *formin(ts)* mutant embryos than in

control embryos at both semi-restrictive and semi-permissive temperatures, but this rate was not affected by the *Rac(G60R)* mutation (Figure 16E and F; unpaired student's test, Table S 5). Thus, perturbing Rac activity does not rescue cytokinesis failure when the contractile ring is weakened by reduced formin/CYK-1 activity.

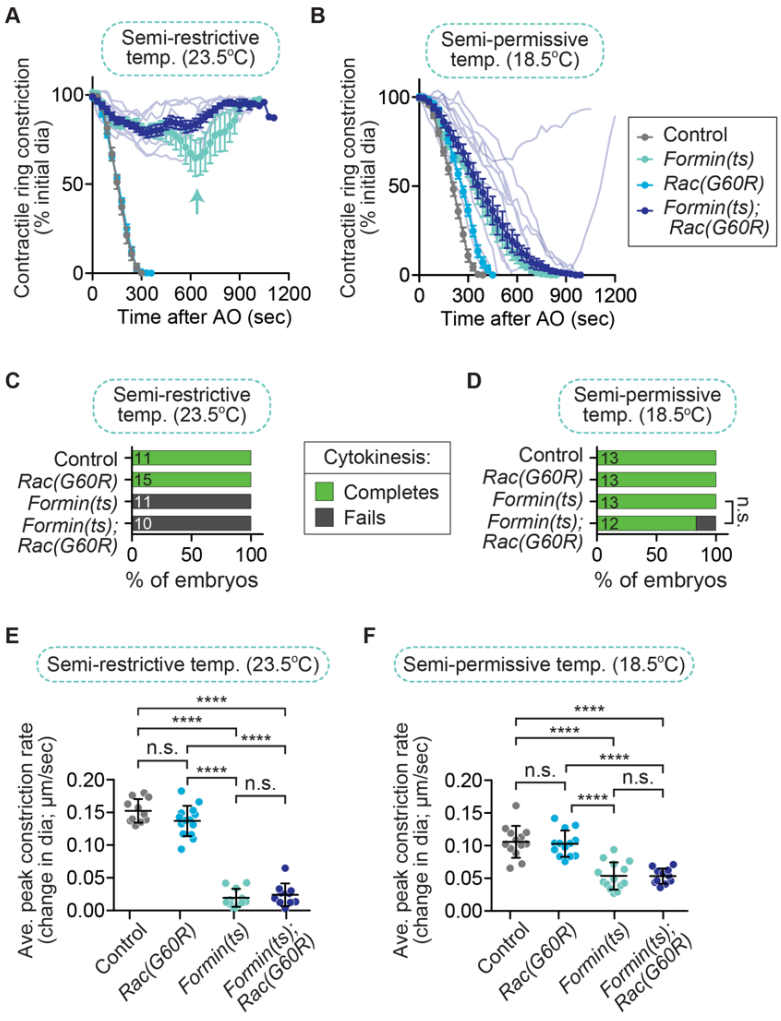

Figure 16: Rac disruption does not rescue cytokinesis failure in formin(ts) embryos

A, B) Kinetic analysis of contractile ring constriction in control and *formin(ts)* mutant 1-cell embryos with and without *Rac(G60R)*, dividing at semi-restrictive (23.5ºC) (A) and semi-permissive (18.5ºC) (B) temperature. Graphs show the mean ring diameter over time, with all replicates for the *formin(ts);Rac(G60R*) double mutant in a more transparent shade of the same dark blue. Error bars represent the SEM. The aqua arrow in (A) shows the more persistent attempt at contractile ring constriction seen in *formin(ts)* single mutant embryos but not in *formin(ts);Rac(G60R)* double mutant embryos. AO=anaphase onset. C, D) Cytokinesis failure and success rates for different genotypes at semi-restrictive (C) and semi-permissive (D) temperature. The number of embryos per genotype is indicated on each individual bar; p-values were obtained by both Fisher's and Barnard's exact tests (Table S 5). E, F) Average peak rate of contractile ring constriction, plotted as the change in diameter (µm/sec) when the rate of ingression peaks from ~90-50% ring constriction (or the point of maximum contractile ring constriction when embryos did not constrict to 50% of the initial cell diameter) at semi-restrictive (E) and semi-permissive (F) temperature. Error bars represent the SD; p-values were obtained by an unpaired, two-tailed student's t-test (Table S 5). n.s.=p≥0.05; ****=p<0.0001.

We next tested if Rac disruption could rescue cytokinesis failure when the actin-based motor non-muscle myosin-II (NMY-2) is weakened, which drives contractile ring constriction downstream of Rho (Figure 15D). For this experiment, we used a fast-acting *myosin-II(ts)* allele (Davies et al., 2014; Liu et al., 2010) and imaged at the semi-restrictive temperature (25.5ºC), at which *myosin-II(ts)* single mutant 1-cell embryos can undergo some contractile ring constriction but fail in cytokinesis 100% of the time (0/13 embryos divide; Figure 17A and C) (Jordan et al., 2016). Using the *Rac(G60R)* mutation, we found that at this temperature all *myosin-II(ts);Rac(G60R)* embryos fail in cytokinesis (0/10 embryos divide), and undergo reduced contractile ring constriction relative to the *myosin-II(ts)* mutants alone Figure 17A and C). This result suggests that disrupting Rac activity does not significantly change the rate of cytokinesis failure in *myosin-II(ts)* mutant embryos (Fisher's and Barnard's exact tests, p-values in Table S 5). We next examined the effect of Rac disruption on *myosin-II(ts)* mutant embryos at the semi-permissive temperature (22.5ºC), where the *myosin-II(ts)* mutant embryos undergo contractile ring constriction more slowly, but cytokinesis is always successful (13/13 embryos divide; Figure 17B and D) (Jordan et al., 2016). At semi-permissive temperature, most *myosin-II(ts);Rac(G60R)* embryos complete cytokinesis (9/10 embryos divide; Figure 17B and D). We also found that the rate of contractile ring constriction was significantly slower in *myosin-II(ts)* mutant embryos than in control embryos at both semi-restrictive and semi-permissive temperatures, and this constriction rate was not affected by the *Rac(G60R)* mutation (Figure 17E and F; unpaired student's test, Table S 5). Thus, perturbing Rac activity does not significantly rescue cytokinesis failure or the rate of contractile ring constriction when myosin-II activity is weakened (Table S 5). Together with a lack of rescue upon Rac disruption when formin (Figure 16) or Aurora B (Lewellyn et al.,

2011) activity is weakened, these data suggest that Rac disruption is not a simple bypass mechanism that facilitates completion of contractile ring constriction. Instead, our and others' genetic results suggest that Rac disruption specifically suppresses cytokinesis failure when CYK-4 (or ECT-2) is reduced (Bastos et al., 2012; Canman et al., 2008; Cannet et al., 2014; D'Avino et al., 2004; Loria et al., 2012).

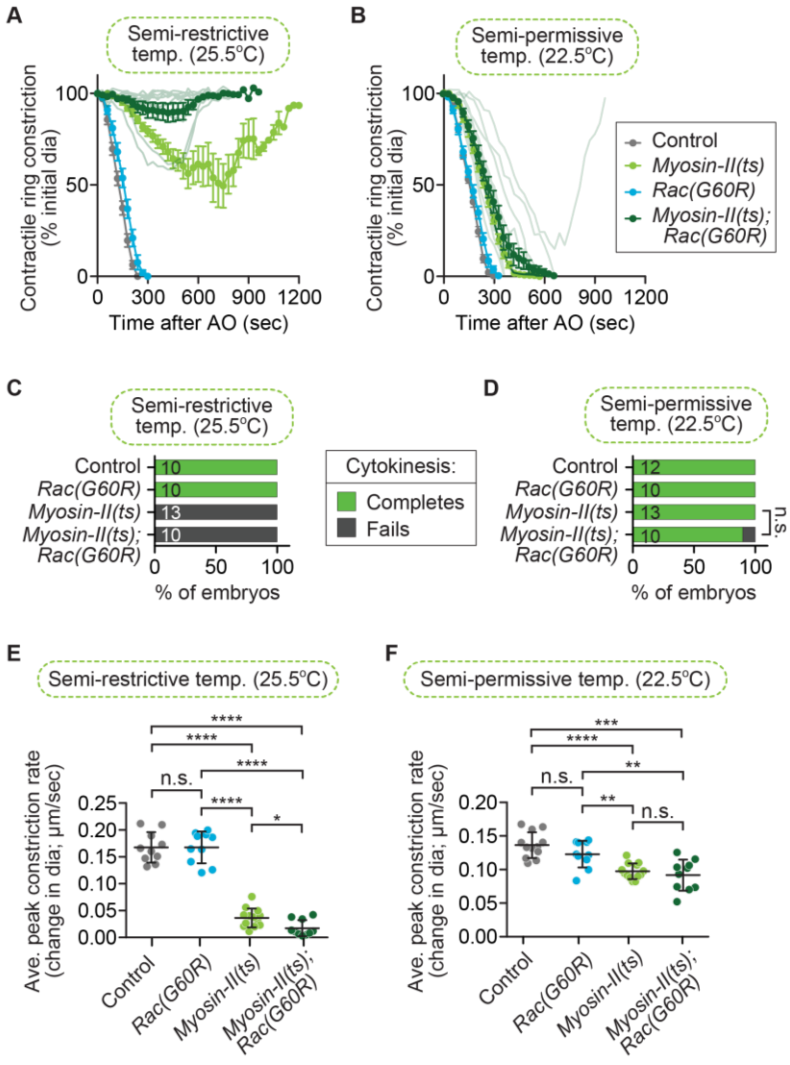

Figure 17: Rac disruption does not rescue cytokinesis failure in myosin-II(ts) embryos

A, B) Kinetic analysis of contractile ring constriction in control and *myosin-II(ts)* mutant 1-cell embryos with and without *Rac(G60R)*, dividing at semi-restrictive (25.5ºC) (A) and semi-permissive (22.5ºC) (B) temperature. Graphs show the mean ring diameter over time, with all replicates for the *myosin-II(ts);Rac(G60R*) double mutant in a more transparent shade of forest green. Error bars represent the SEM. C, D) Cytokinesis failure and success rates for different genotypes at semi-restrictive (C) and semi-permissive (D) temperature. The number of embryos per genotype is indicated on each individual bar; p-values were obtained by both Fisher's and Barnard's exact tests (Table S 5). E, F) Average peak rate of contractile ring constriction, plotted as the change in diameter (µm/sec) at semi-restrictive (E) and semi-permissive (F) temperature. Error bars represent the SD; p-values were obtained by an unpaired, two-tailed student's t-test (Table S 5). AO=anaphase onset. n.s.=p≥0.05; *=p<0.05; **=p<0.01; ***=p<0.001; ****=p<0.0001.

To support the hypothesis that Rac disruption rescues cytokinesis failure via a non-specific mechanism, it was reported that Rac inhibition was also able to rescue cytokinesis failure of a slow-acting *ect-2* allele (*ax751ts)* (hereafter *ect-2(ts)*) (Loria et al., 2012); we next sought to confirm this result. Loria and colleagues reported that *ect-2(ts)* mutant 1-cell embryos fail in cytokinesis at a high frequency (~97%) following a prolonged (8+ hours) upshift to restrictive temperature and that this cytokinesis failure rate was reduced to ~35% in *ect-2(ts);Rac(V190G)* double mutant embryos (Loria et al., 2012). This hypomorphic *ect-2(ts)* mutation is not a fast-acting ts allele and results from a single residue substitution in the PH domain of ECT-2 (Zonies et al., 2010). Moreover, embryos from this *ect(ts)* allele were first published to have a low frequency of cytokinesis failure after prolonged upshift to restrictive temperature, although the precise cytokinesis failure rate frequency was not reported (Zonies et al., 2010). We determined the rate of cytokinesis failure in this *ect-2(ts)* mutant background by monitoring the success or failure of cytokinesis in 1-cell embryos following prolonged upshifts (12+ hours) of *ect-2(ts)* mutants to the restrictive temperature (26ºC). In our hands, 1-cell embryos from this *ect-2(ts)* mutant failed in cytokinesis at a rate of only 38% (8/13 embryos divide; Figure 18A and C). *ect-2(ts)* mutant embryos that failed in cytokinesis exhibited a significantly slower rate of contractile ring constriction than *ect-2(ts)* mutant embryos that successfully completed cytokinesis, but the overall rate of contractile ring constriction in *ect-2(ts)* mutants was unchanged by *Rac(RNAi)* (Figure 18B; unpaired student's t-test, Table S 5). While the rate of cytokinesis failure in *ect-2(ts)* mutant embryos was low, in agreement with the results of (Zonies et al., 2010), we confirmed that cytokinesis failure could be partially suppressed by Rac disruption (Loria et al., 2012), as *ect-2(ts);Rac(RNAi)* embryos failed in cytokinesis at a rate of 17% (10/12 embryos divide; Figure

18A and C). Based on either a Fisher's exact test or a Barnard's exact test, this rescue was not statistically significant (p-values in Table S 5). We also investigated whether Rac disruption could rescue cytokinesis failure in the AB and P1 blastomeres of 2-cell *ect-2(ts)* embryos with and without Rac depletion (Figure 18E). We found that 100% of both AB and P1 blastomeres successfully completed cytokinesis in *ect-2(ts);control(RNAi)* and *ect(ts);Rac(RNAi)* embryos, even after a 12-hour upshift to restrictive temperature (12/12 of both AB and P1 cells divide in *ect-2(ts);control(RNAi)* embryos; 14/14 AB cells and 16/16 P1 cells divide in *ect-2(ts);Rac(RNAi)* 2-cell embryos, respectively; Figure 18E). The lack of cytokinesis failure in 2-cell *ect-2(ts)* embryos is likely due to the hypomorphic nature of this allele (Zonies et al., 2010), although we cannot rule out the possibility that ECT-2 may play less of a role during cytokinesis in 2-cell embryos than it does in 1-cell embryos. Thus, our data suggests that depletion of Rac by RNAi can partially rescue cytokinesis failure in 1-cell embryos from *ect-2(ts)* mutants, though this rescue is not statistically significant (Table S 5).

Because we saw a lower rate of cytokinesis failure in the *ect-2(ts)* mutant and a lower rate of rescue following Rac disruption by RNAi than observed by Loria and colleagues, we obtained the strains used by these researchers to test if there could be strain variation between two labs. We found that their *ect-2(ts)* mutants still failed in cytokinesis at a lower rate in our hands when upshifted to restrictive temperature for at least 12 hours (48% or 25/48 embryos divide here vs ~97% in Loria *et al.*; Figure 18D), again more similar to the low cytokinesis failure rate of this mutant strain originally reported by Zonies and colleagues (Zonies et al., 2010). We also confirmed that the rate of cytokinesis failure was partially rescued in *ect-2(ts);Rac(V190G)* double mutants (14/19 embryos divide; Figure 18D). Similar to *ect-2(ts)* 1-cell embryos, this rescue in *ect-2(ts)* 2-cell embryos was not statistically significant (Fisher's

and Barnard's exact tests, p-values in Table S 5). *Rac(V190G)* is a mild loss-of-function allele (*n1993*) that affects the CAAX box and thus likely affects Rac association with the plasma membrane (Kinsella et al., 1991; Reddien and Horvitz, 2000; Roberts et al., 2008; Shakir et al., 2006; Steffen et al., 2013). Although we do not observe the same high rate of cytokinesis failure in the *ect-2(ts)* mutant after prolonged upshifts to restrictive temperature as reported (Loria et al., 2012), possibly due to environmental effects, we observed a similar rescue of cytokinesis failure rates in *ect-2(ts);Rac(RNAi)* and *ect-2(ts);Rac(V190G)* embryos. Thus, reducing Rac activity can partially rescue cytokinesis failure when ECT-2 activity is compromised, although to a lesser extent than in *cyk-4(ts)* mutants (*e.g.* Figure 15 and (Canman et al., 2008; Loria et al., 2012) and not to statistically significant levels (Table S 5).

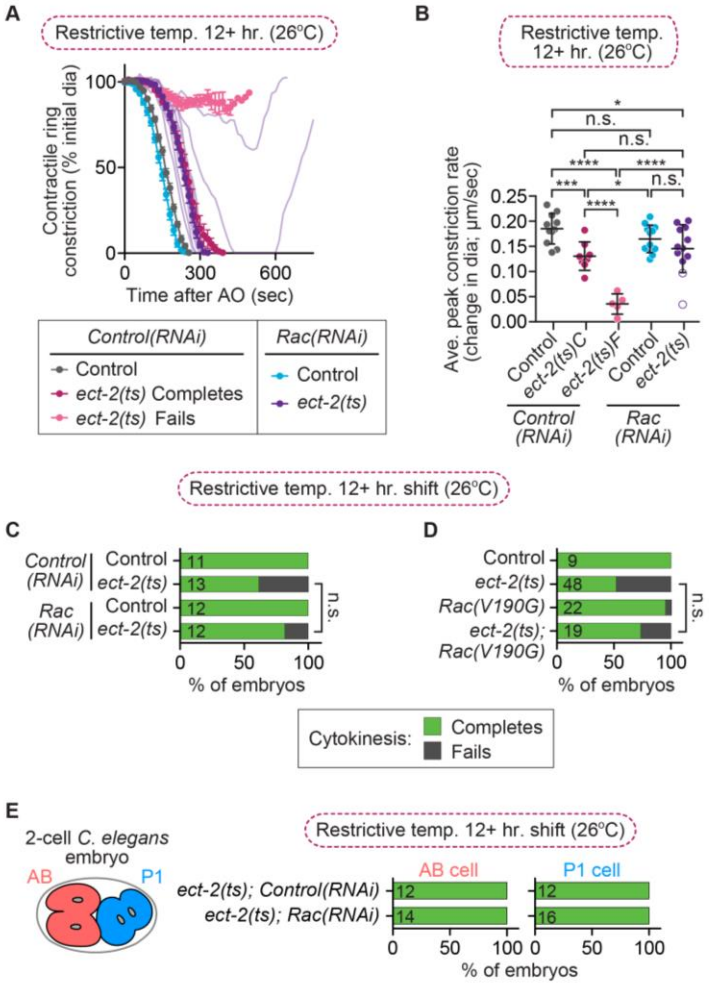

Figure 18: Rac disruption partially rescues cytokinesis failure in ect-2(ts) embryos

A) Kinetic analysis of contractile ring constriction in control and *ect-2(ts)* mutant 1-cell embryos at restrictive temperature (26ºC) with and without *Rac(RNAi).* Graph shows the mean ring diameter over time, with all replicates for the *ect-2(ts);Rac(RNAi*) double mutant in a more transparent shade of deep purple. Error bars represent the SEM. AO=anaphase onset. B) Average rate of peak contractile ring constriction, plotted as the change in diameter (µm/sec) for embryos in (A). C=cytokinesis completes; F=cytokinesis fails. The white dots with a purple outline represent the *ect-2(ts);Rac(RNAi)* embryos that failed in cytokinesis. Error bars represent the SD; p-values were obtained by an unpaired, two-tailed student's t-test (Table S 5). C) Cytokinesis failure and success rates for the embryos represented in (A). D) Cytokinesis failure and success rates for 1-cell embryos from *ect-2(ts)* mutant strains obtained from the authors of Loria *et al.* (2012). (C, D) The number of embryos per genotype is indicated on each individual bar; p-values were obtained by both Fisher's and Barnard's exact tests (Table S 5). E) Schematic of the *C. elegans* 2-cell embryo and graphs showing cytokinesis failure and success rates in the AB and P1 cell divisions for *ect-2(ts)* mutant embryos with or without *Rac(RNAi).* n.s.=p≥0.05; *=p<0.05; **=p<0.01; ***=p<0.001; ****=p<0.0001.

The second part of the argument against Rac as a specific target of CYK-4 is that the main target of CYK-4 is ECT-2, which then activates Rho. This is largely based on the findings that 1) CYK-4 and ECT-2 from various species can interact in biochemical assays (Burkard et al., 2009; Kim et al., 2014; Somers and Saint, 2003; Wolfe et al., 2009; Yuce et al., 2005; Zhang and Glotzer, 2015; Zou et al., 2014), and 2) a *C. elegans* gain-of-function ECT-2 mutation can rescue cytokinesis failure caused by a loss-of-function CYK-4 GAP mutation (Figure 15D) (Zhang and Glotzer, 2015). If CYK-4 is upstream of ECT-2, then reducing CYK-4 activity should lead to a reduction in ECT-2-mediated Rho activation and Rho effector accumulation at the division plane. To test this, we quantified the levels of downstream Rho targets GFP::myosin-II (GFP::NMY-2; (Munro et al., 2004)) and a reporter for filamentous actin (f-actin), GFP::Utrophin^{ABD} (GFP::Utr^{ABD}) (Burkel et al., 2007; Tse et al., 2012) at the division plane during cytokinesis in 1-cell embryos at 150 seconds after anaphase onset. At this time point, most control, but not *cyk-4(ts)*, embryos have formed a double membrane at the furrow tip or initiated "furrow involution" (Lewellyn et al., 2010) (Figure S 4A and B), as contractile rings in *cyk-4(ts)* embryos are less constricted than controls (Figure 15A and C).

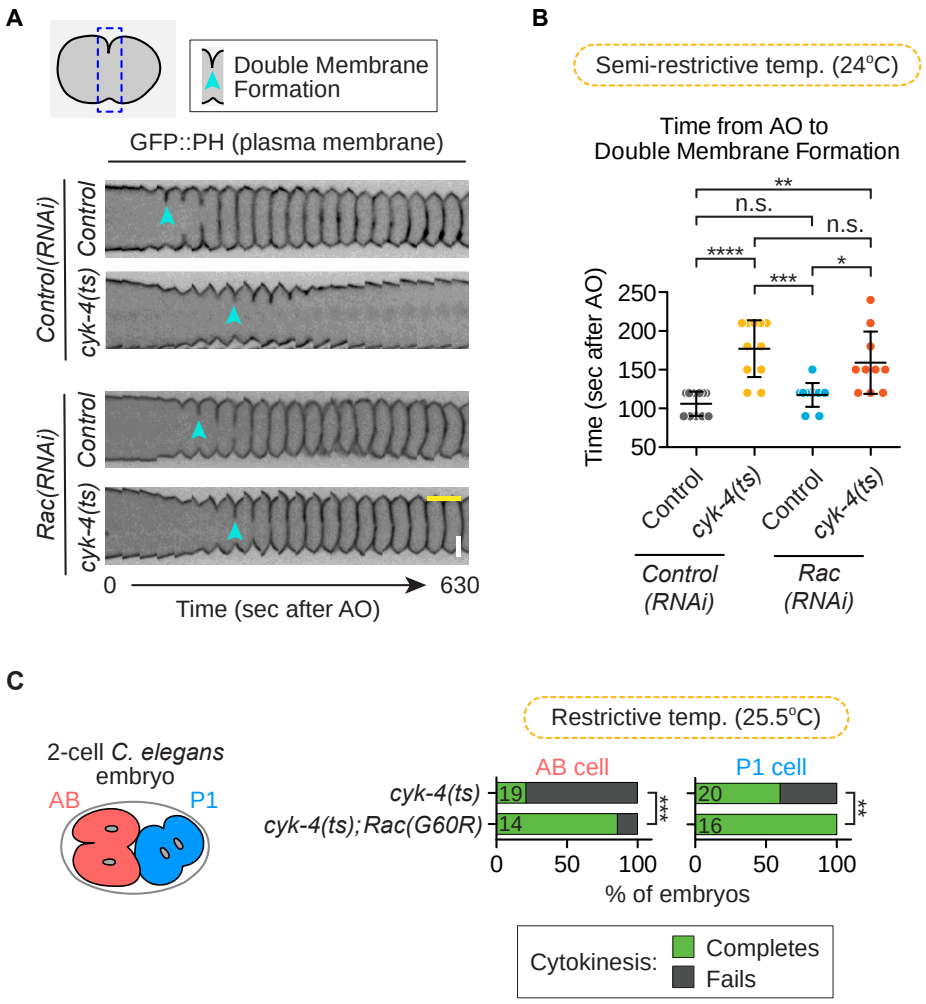

Figure S 4: cyk-4(ts) mutant embryos take longer to form a double membrane and fail in cytokinesis at the 2-cell stage via a Rac-dependent mechanism

A) Time-lapse montage of the division plane region over time during cytokinesis in control and *cyk-4(ts)* mutant 1-cell embryos with and without *Rac(RNAi).* The plasma membrane is labeled with GFP::PH. B) Analysis of the time from anaphase onset to double membrane formation in embryos from the genotypes shown. All of the controls but only a few *cyk-4(ts)* mutant embryos have formed a double membrane at 150 sec post-AO due to the slower rate of contractile ring constriction in *cyk-4(ts)* mutants (*e.g.* Figure 15A and C). Error bars represent the SD; p-values were obtained by an unpaired, two-tailed t-test (Table S 5). C) Schematic of the 2-cell *C. elegans* embryo indicating the anterior AB and posterior P1 cells; and bar graph showing cytokinesis completion/failure rates of AB and P1 cells in *cyk-4(ts)* mutant 2-cell embryos with or without *Rac(G60R)* at restrictive temperature. The number of embryos per genotype is indicated on each individual bar; p-values were obtained by both Fisher's and Barnard's exact tests (Table S 5). AO=anaphase onset. n.s.=p>0.05; *=p<0.05; **=p<0.01; ***=p<0.001; ****=p<0.0001. Scale bars: yellow=60 sec, white=10 μm.

We found no significant difference in the levels of GFP::myosin-II or GFP::Utr^{ABD} at the division plane in *cyk-4(ts)* mutants relative to control embryos during this early stage of contractile ring constriction (Figure 19A-C). Although in *cyk-4(ts)* embryos contractile ring f-actin appeared to be less tightly bundled, likely due to the reduced constriction rate in *cyk-4(ts)* embryos relative to in controls (Figure 15A and C), the total levels of f-actin at the division plane did not significantly differ from those in controls (Figure 19B and D; Table S 5). Thus, the levels of f-actin and myosin-II, two downstream effectors of ECT-2 and Rho activation (Figure 15D and S2), are not significantly changed at the contractile ring upon functional disruption of CYK-4 GAP activity (unpaired student's t-test; Table S 5). This result suggests that CYK-4 is not upstream of ECT-2/Rho activation but does not exclude the possibility that ECT-2 is upstream of another function of CYK-4, such as modulation of Rac activity, or that CYK-4 may regulate another small GTPase (*e.g.* Cdc42).

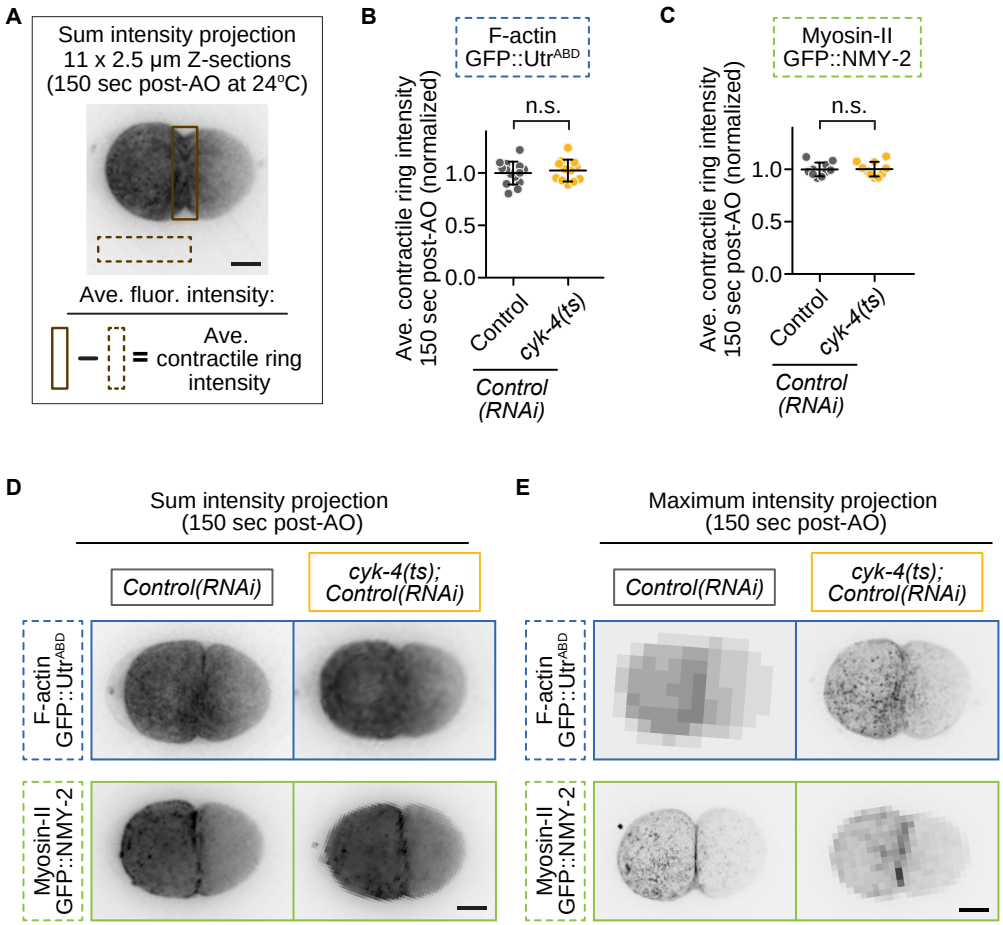

Figure 19: Downstream targets of Rho, f-actin and myosin-II, are not reduced at the division plane in cyk-4(ts) mutants

A) Schematic of how quantitative image analysis was performed for (B) and (C). B, C) Quantification of contractile ring levels of (B) f-actin (GFP::Utr^{ABD}) and (C) myosin-II (NMY-2::GFP) at 150 sec post-AO at semi-restrictive temperature (24ºC). Error bars represent the SD; p-values were obtained by an unpaired, two-tailed student's t-test (Table S 5). D) Representative sum projections of f-actin (GFP::Utr^{ABD}) and myosin-II (NMY-2::GFP) in control and *cyk-4(ts)* embryos at 150 sec post-AO. E) Representative higher Z-resolution maximum projections of f-actin and myosin-II at 150 sec post-AO. AO=Anaphase onset. Scale bars=10 µm. n.s.=p≥0.05.

The above results, as well as the finding that we did not rescue the reduced rate of contractile ring constriction in *cyk-4(ts)* mutants by disrupting Rac activity (Figure 15C), could indicate a secondary positive role for CYK-4 or Rac during cytokinesis. In support of a possible positive role for Rac in cytokinesis, we saw a slight (though non-significant) enhancement of cytokinesis failure following depletion of Rac in both *formin(ts)* and *myosin-II(ts)* mutant embryos. However, Rac depletion on its own did not lead to any delays or obvious defects in cytokinesis in most of our experiments (Figure 15- Figure 18). *In vitro*, CYK-4 can also promote the GTP hydrolysis of Cdc42 (CDC-42 in *C. elegans*, hereafter Cdc42) (Bastos et al., 2012; Jantsch-Plunger et al., 2000; Toure et al., 1998). Thus, it is possible that CYK-4 GAP activity may also regulate Cdc42 during cell division. Depletion of Cdc42 by RNAi leads to a short but reproducible delay in the onset of contractile ring constriction (Jordan et al., 2016). At this early stage of *C. elegans* development, Cdc42 plays an essential role in maintaining anterior-posterior polarity, which leads to asymmetric cell division and results in a larger anterior and smaller posterior blastomere (Aceto et al., 2006; Gotta et al., 2001; Kay and Hunter, 2001; Motegi and Sugimoto, 2006; Schonegg and Hyman, 2006). CYK-4 was also proposed to play a critical role in regulating cell polarity in the early embryo by functioning within the sperm to trigger polarity establishment upon fertilization (Jenkins et al., 2006). However, we do not observe a dramatic increase in embryonic lethality or decrease in brood size when the sole sperm used for fertilization is homozygous for the *cyk-4(ts)* mutation, even at restrictive temperature, which would be expected if CYK-4 GAP activity plays this essential role in cell polarity (Figure 20A); unpaired student's t-test, Table S 5). Furthermore, we do not see a significant loss in the asymmetric position of the site of furrowing or daughter cell size in *cyk-4(ts)* single mutant embryos (Figure 20; unpaired

student's t-test, Table S 5). Thus, if CYK-4 regulates Cdc42 in this system, it is likely not a major player in anterior-posterior cell polarity.

We recently identified a role for Cdc42 during cytokinesis in promoting the robustness of contractile ring constriction (Jordan et al., 2016). One possibility is that CYK-4 regulates Cdc42 specifically during cytokinesis. We tested whether disrupting Cdc42 by RNAi could further rescue the rate of cytokinesis failure in 1-cell *cyk-4(ts);Rac(lof) d*ouble mutant embryos. To ensure that we were able to obtain sufficient embryos from all genetic backgrounds, we used a partial Cdc42 depletion that reduced but did not eliminate cell polarity, as evidenced by the significant reduction in anterior to posterior daughter size asymmetry (Figure 20B; unpaired student's t-test, Table S 5). *cdc42(RNAi)* did not significantly change the success rate or constriction kinetics of cytokinesis in *control*, *Rac(G60R)*, or *cyk-4(ts)* embryos and, as expected, *cyk-4(ts);Rac(G60R);control(RNAi)* embryos only failed in cytokinesis 30% of the time (12/15 embryos divide; Figure 20C and D; Table S 5). In contrast, *cyk-4(ts);Rac(G60R);Cdc42(RNAi)* triple embryos failed in cytokinesis 100% of the time (0/11 embryos divide; Figure 20C and D). Thus, Cdc42 depletion significantly enhances the rate of cytokinesis failure relative to *cyk-4(ts);Rac(G60R);control(RNAi)* embryos (Fisher's and Barnard's exact tests, Table S 5), indicating that the rescue of cytokinesis failure in *cyk-4(ts)* mutants following Rac disruption is dependent on Cdc42. This is consistent with a role for CYK-4 in regulating Cdc42 during cytokinesis although, due to the known role of Cdc42 and the PAR polarity proteins in cytokinesis (Jordan et al., 2016) and lack of an effect of *cdc42(RNAi)* on cytokinesis in the cyk-4(ts) mutant, it is difficult to draw any firm conclusions (Figure 20C and D). In summary, our data support a model in which the predominant role for CYK-4's GAP activity

during cytokinesis is to downregulate Rac to allow for timely contractile ring constriction, at least in C. elegans 1- and 2-cell embryos (Figure S 5).

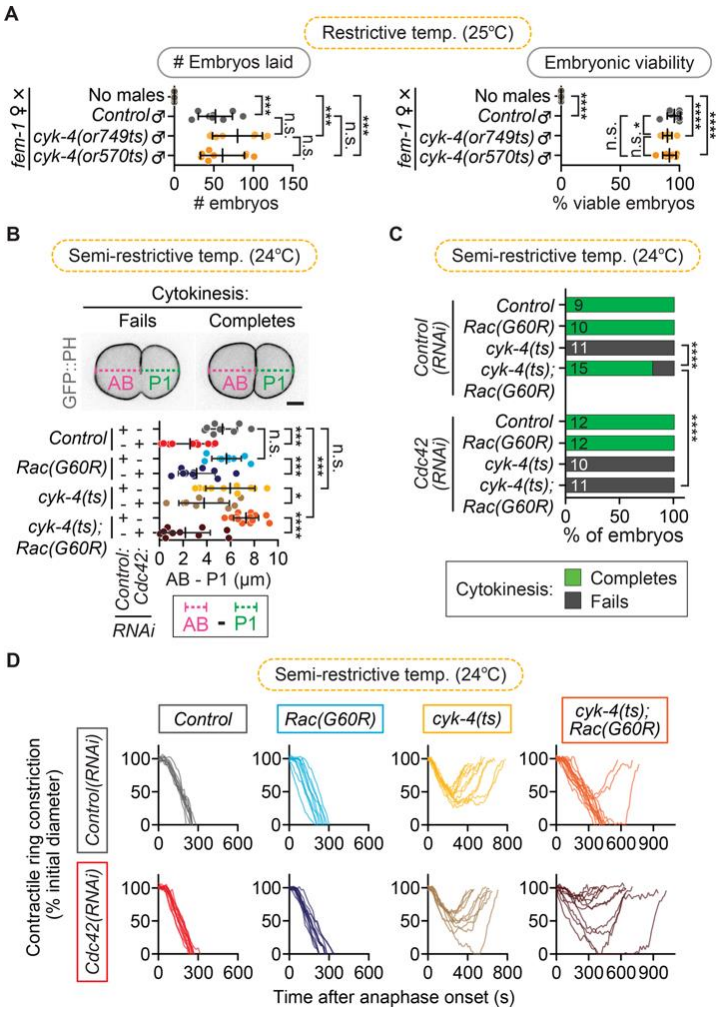

Figure 20: cyk-4(ts); Rac(G60R) fail in cytokinesis when Cdc42 is depleted

(A) Paternal requirement test for sperm-supplied CYK-4 GAP activity in ~24-30-hour brood size (left) and embryonic viability (Calvert et al.) when *cyk-4(ts)* males are mated with non-sperm producing feminized *fem-1(hc17ts)* hermaphrodites at restrictive temperature (25ºC). The low embryonic lethality rate indicates sperm supplied CYK-4 GAP activity is not essential to establish and/or maintain cell polarity. Error bars represent the SD; p-values were obtained by an unpaired, two-tailed student's t-test (Table S 5). B) Asymmetry of furrow position in 1-cell embryos (when cytokinesis fails) or of AB vs P1 daughter cell size (when cytokinesis completes) among different genotypes used in (D). Error bars represent the SD; p-values were obtained by an unpaired, two-tailed student's t-test (Table S 5). C) Cytokinesis failure and success rates for different genotypes in (D). The number of embryos per genotype is indicated on each individual bar; p-values were obtained by both Fisher's and Barnard's exact tests (Table S 5). D) Kinetic analysis of contractile ring constriction in control, *cyk-4(ts)*, *Rac(G60R)*, and *cyk-4(ts);Rac(G60R)* double mutant 1-cell embryos with and without *Cdc42(RNAi)* at semi-restrictive temperature (24ºC). Embryos from each genotype are plotted on individual graphs to make it easier to see and traces for all individual embryos are shown. Scale bar=10 µm. n.s.=p>0.05; *=p<0.05; **=p<0.01; ***=p<0.001; ****=p<0.0001.

Discussion

This work addressed the role of CYK-4 and the Rho family small GTPase Rac in cytokinesis. Our results confirmed that, as was previously found, Rac inactivation partially rescued the rate of cytokinesis failure in a CYK-4 GAP mutant and a hypomorphic ECT-2 mutant (Bastos et al., 2012; Canman et al., 2008; Cannet et al., 2014; Loria et al., 2012; Zhang and Glotzer, 2015). However, we did not find evidence that Rac inhibition is a non-specific "bypass" mechanism that generally facilitates contractile ring constriction, as has been proposed by others (Loria et al., 2012). While Rac disruption did not rescue the rate of contractile ring constriction in *cyk-4(ts)* mutants, suggestive of another role for CYK-4 (or Rac) in cytokinesis, we did not find a role for CYK-4 upstream of ECT-2-mediated activation of Rho. We also did not find evidence that Rac activity changes the rate of or generally opposes contractile ring constriction; Rac inactivation did not rescue cytokinesis failure in strains with mutations in the Rho effectors diaphanous formin/CYK-1 or myosin-II/NMY-2. Furthermore, we found that disrupting CYK-4 GAP activity did not affect the levels of f-actin or myosin-II in the contractile ring, indicating that CYK-4 is unlikely to act upstream of ECT-2-mediated activation of Rho. Our data instead suggests that CYK-4 negatively regulates Rac (and potentially Cdc42) during cytokinesis (Figure S 5).

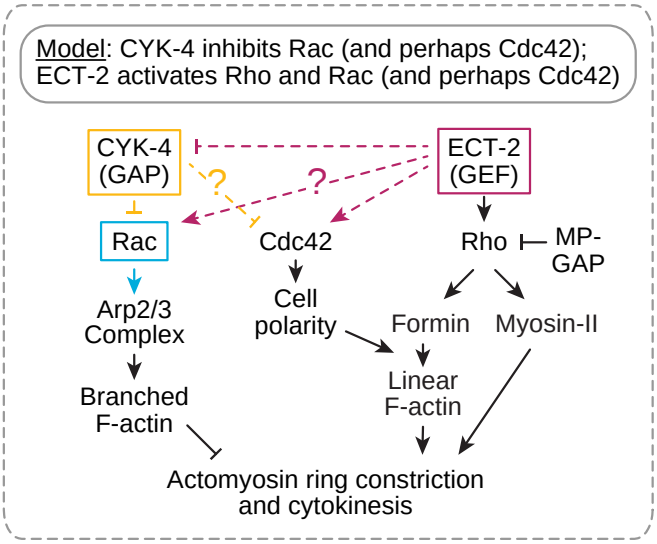

Figure S 5: Genetic model for Rho family GTPase signaling during cytokinesis

Revised genetic model for the molecular regulation of Rho family small GTPases during cytokinesis. Note: We cannot rule out a role for ECT-2 in regulating Rac and/or CYK-4 activity. We also cannot rule out a role for ECT-2 and/or CYK-4 in regulating Cdc42 activity.

There are at least three possible explanations for the mild rescue of ECT-2-mediated cytokinesis failure by loss of Rac: 1) Rac is a general suppressor of cytokinesis when the contractile ring is weakened as was proposed (Loria et al., 2012; Zhang and Glotzer, 2015), although our data showing a lack of rescue resulting from Rac disruption in *formin(ts)* and *myosin-II(ts)* mutants argue against this model; 2) Rac and Rho are mutually inhibitory and/or compete for binding partners (*e.g.* RhoGDIs, GEFs, GAPs, or effectors) so that perturbing Rac activity promotes more Rho activity, as can occur in other cell contexts (*e.g.* (Boulter et al., 2010; Garcia-Mata et al., 2011; Machacek et al., 2009)); or 3) the GEF activity of ECT-2 promotes Rac activation during cytokinesis either directly or via CYK-4 (Figure S 5), which is inhibitory to contractile ring constriction. *In vitro*, ECT-2 was found in one study to be an even more potent GEF for Rac and Cdc42 than Rho (Tatsumoto et al., 1999); therefore, this is indeed a possibility. This would explain why disruption of Rac activity can rescue cytokinesis failure in both *cyk-4(ts)* and to some extent in *ect-2(ts)* mutant embryos, but not *formin(ts)* or *myosin-II(ts)* embryos. Thus, we propose that, in addition to its positive role in cytokinesis via Rho activation, ECT-2 (alone or through CYK-4) may function in a negative regulatory feedback loop to spatiotemporally control Rac activity and/or GTPase flux during cytokinesis (Figure S 5).

Our results on Rho-effector levels in the contractile ring after CYK-4 disruption are in conflict with the results reported by Loria and colleagues (Loria et al., 2012), but in agreement with previous analyses of the effect of CYK-4/Centralspindlin disruption on myosin-II targeting to the contractile ring during ring constriction (Canman et al., 2008; Lewellyn et al., 2011), including myosin-II analysis presented in a more recent publication from the same lab that published the Loria *et al.* paper (Zhang and Glotzer, 2015). One

possible difference between these studies is the method used to quantify fluorescence intensity in the contractile ring. Loria and colleagues quantified the levels within a region of interest (Gilliane Maton) around the division plane from the maximum projected images of 5 x 2.5 µm central Z-sections, applied a threshold with a minimal value of 1.25x the background intensity, and then integrated and normalized to the background (Loria et al., 2012). Here we quantified the signal in a ROI around the entire division plane from the sum projected images from 11 x 2.5 µm Z-sections, subtracted the sum projected background signal from an identical sized ROI, then normalized to the levels in control embryos (Figure 19). While our analysis reflects all of the GFP signal in the contractile ring, the arbitrary thresholding and maximum projections used in the other analysis would decrease detection of more diffuse cytoskeletal signal in the contractile ring. In the case of *cyk-4(ts)* mutants, a more diffuse signal would be expected due to the reduced rate of contractile ring constriction (Figure 15C) and thus likely reduced rate of actomyosin bundling. Furthermore, limiting analysis to only 5 x 2.5 µm central Z-sections during imaging (Loria et al., 2012) (vs 11 x 2.5 µm here; *C. elegans* embryos are ~25-30 µm in diameter) would be more likely to miss regions of the equatorial cell cortex that contain peak levels of contractile ring proteins especially early in cytokinesis, as contractile ring constriction itself is asymmetric in this system and initiates from a single position along the equatorial cell cortex (Maddox et al., 2007).

We also found that rescue of *cyk-4(ts)* GAP-defective mutants by Rac depletion is Cdc42-dependent. This could represent a role for CYK-4 in regulating Cdc42 activity during cell polarity maintenance and/or cytokinesis, or could represent general Rho family imbalance due to Cdc42-mediated competition for inhibitory Rho family effectors and/or regulators (*e.g.*

GDIs) (Boulter et al., 2010; Garcia-Mata et al., 2011; Machacek et al., 2009; Tatsumoto et al., 1999). Cdc42 hyper-activation was found to inhibit the formation of a focused band of f-actin in the contractile ring in HeLa cells (Zhu et al., 2011b), yet depletion of Cdc42 does not block contractile ring constriction in HeLa cells or in *C. elegans* embryos (Jordan et al., 2016; Zhu et al., 2011b). In the early *C. elegans* embryo, Cdc42 plays an important role in maintaining anterior-posterior polarity (Gotta et al., 2001; Kay and Hunter, 2001) and we recently identified a role for Cdc42 (via a collaboration with the PAR polarity proteins) in promoting f-actin accumulation in the contractile ring (Jordan et al., 2016). Thus, it is possible that CYK-4 may regulate this function of Cdc42 during polarity maintenance. Sperm-supplied CYK-4 has also been implicated in regulating anterior-posterior (A-P) cell polarity in *C. elegans* embryos (Jenkins et al., 2006), but we see either no difference or only a mildly significant difference in embryonic lethality and no significant difference in brood size when homozygous *cyk-4(ts)* males were mated with genetically feminized worms (*fem-1* mutant) at restrictive temperature, as would be expected if A-P polarity was grossly disrupted. Furthermore, in *cyk-4(ts)* single mutants, we do not see a change in two strong indicators of a polarity disruption: 1) asymmetric cleavage furrow position along the A-P axis and 2) daughter size asymmetry (Figure 20). We do, however, see a significantly more posteriorized furrow position in *cyk-4(ts);Rac(lof)* double mutants (Figure 20). This is a similar phenotype to that seen following depletion of the Cdc42 GAP CHIN-1 (CHimaerIN), known to be a regulator of Cdc42 during cell polarity maintenance in this system (Beatty et al., 2013; Kumfer et al., 2010). Nevertheless, enhancement of cytokinesis failure alone cannot confirm a role for CYK-4 in Cdc42 regulation during contractile ring constriction. Taken together,

our data support a model in which, at least in the early *C. elegans* embryo, CYK-4 functions to inhibit Rac activity and does not participate directly in Rho activation (Figure S 5).

Additional results and discussion (not in published manuscript)

Ect-2 and Rac/CED-10 in general embryo quality

In Zhuravlev et al (2017), we found that Rac inhibition showed an insignificant rescue of cytokinesis failure in *ect-2(lof)* embryo. Initially, we hypothesized that perhaps the slight rescue could be due to a general rescue of embryo quality due to the known roles for worm ECT-2 in germline structural maintenance (Green et al., 2011) and cell polarity establishment (Zonies et al., 2010). Normally, *C. elegans* embryos are 30 x 50 μm (or a length to width ratio of ~1.7) (Riddle et al., 1997) ovoids, but when the structure and polarity of the syncytial gonad is perturbed, embryos differ in size and shape, and often become rounder. Thus, to test if Rac suppressed the germline roles for ECT-2, I quantified the length to width ratio of embryos from *control*, *Rac(G60R)*, *etc-2(ts)*, *ect-2(ts);Rac(V190G)* worms after 16 hours at restrictive temperature (Figure 21). *Control* strains produced the embryos with the greatest length to width ratio (1.8 +/- .019; (Figure 21). The *ect-2(ts);Rac(V190G)* double mutant hermaphrodites exhibited the smallest length to width ratio, significantly less than the single *ect-2(ts)* mutant alone and thus were the most round (1.4 +/- .027 vs 1.6 +/- .018, respectively; Figure 21). *Rac(G60R)* mutant embryos exhibited a significantly smaller length to width ratio (1.5 +/- .033) than control (1.8 +/- .019) and *ect-2(ts)* mutant embryos, (1.6 +/- .018) but was not significantly different from that of *ect-2(ts);Rac(V190G)* (1.4 +/- .027) embryos (Figure 21). Thus, Rac disruption seems to reduce embryo quality and increase roundness, but this is not likely the mechanism of partial cytokinesis rescue in *ect-2(ts)* mutant embryos.

One caveat to our analysis of the role for Rac in embryo quality/germline structure is the *Rac(V190G)* mutant strain versus the *Rac(G60R)* used in the double mutant are not the same. As previously mentioned, the *Rac(V190G)* is a milder loss-of-function allele (*n1993*) that likely affects Rac's association with the plasma membrane rather than its GTPase activity as with *Rac(G60R)* (Kinsella et al., 1991; Reddien and Horvitz, 2000; Roberts et al., 2008; Shakir et al., 2006; Steffen et al., 2013). In the future, it would be important to determine if *Rac(RNAi)* similarly affects embryo shape and size. Rac/CED-10 is known to play a role in apoptotic cell corpse engulfment (Reddien and Horvitz, 2000) a process that also regulates embryo quality control, thus it would also be interesting to determine if disruption of other genes required in the apoptotic pathway lead to similar changes in the size and shape of embryos.

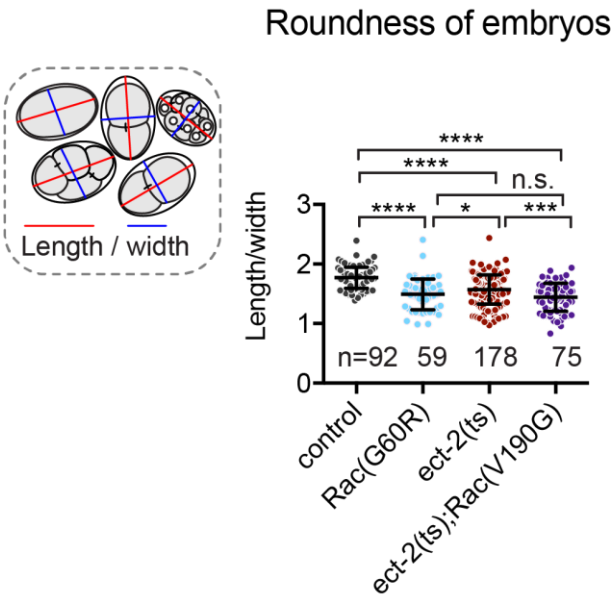

Figure 21: Length to width ratio with or without Rac and/or Ect2

Length to width ratio for embryos of the indicated genotype. Error bars are in SD. n.s.=p≥0.05; *=p<0.05; **=p<0.01; ***=p<0.001; ****=p<0.0001.

CYK-4 and Anillin/ANI-1 in cytokinesis

Since Rac largely rescues the cytokinesis failure phenotype in *cyk-4(ts)* mutants but not the rate of contractile ring constriction it suggests the possibility of another role for CYK-4 during cytokinesis. The *Drosophila* orthologue of CYK-4, RacGAP50c, has been shown to bind to the F-actin crosslinking protein anillin (ANI-1 in worms) (D'Avino et al., 2008; Gregory et al., 2008; Piekny and Maddox, 2010). In the *C. elegans* embryo, ANI-1 is not required for cytokinesis, and has recently been shown to negatively regulate F-actin levels at the contractile ring (Jordan et al., 2016; Maddox et al., 2007). Thus, one possibility is that CYK-4 is required to regulate ANI-1. To test this, I examined if knockdown of *ani-1* in combination with *cyk-4* and *Rac* disruption could rescue the slower rate of ingression. Fewer *cyk-4(ts);Rac(G60);ani-1(RNAi)* embryos failed in cytokinesis than *cyk-4(ts);Rac(G60)* double mutants (14% or 2/14 versus 40% or 4/10, respectively). I also observed that *cyk-4(ts);ani-1(RNAi)* embryos displayed more extensive contractile ring constriction than *cyk-4(ts)* mutants alone, I saw no rescue of the rate of contractile ring constriction in the triple mutant and only a very mild rescue of the rate of contractile ring constriction in *cyk-4(ts);ani-1(RNAi)* versus in *cyk-4(ts)* mutants alone (Figure 22). Thus, if CYK-4 is required to regulate ANI-1 during cytokinesis, this cannot explain the reduced rate of contractile ring constriction in *cyk-4(ts)* mutant embryos.

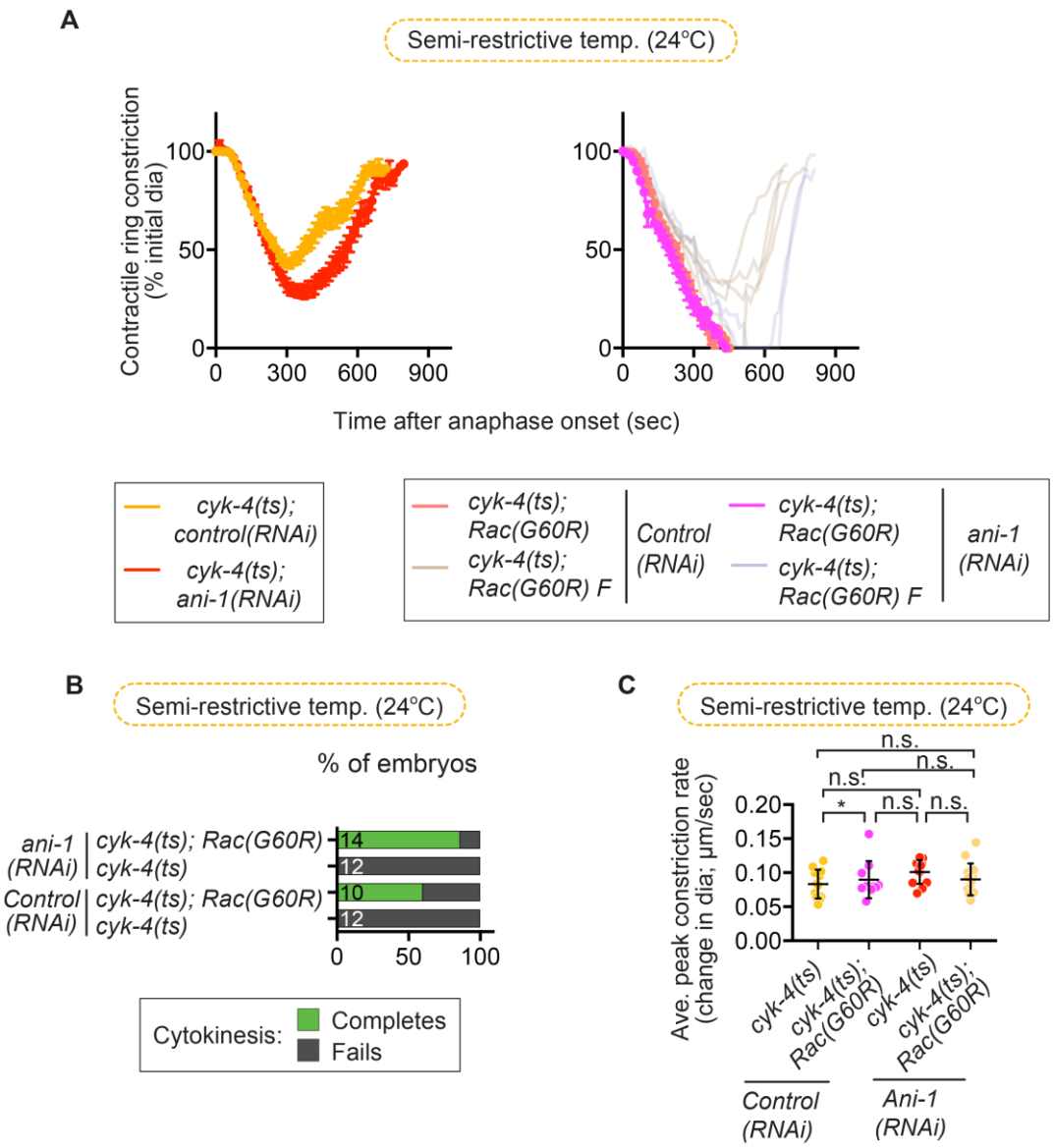

Figure 22 Anillin depletion does not rescue rate of ingression in cyk-4(ts) mutants

A) Kinetic analysis of contractile ring constriction in control and *cyk-4(ts)* mutant and *cyk-4(ts);Rac(G60R)* 1-cell embryos at semi-restrictive temperature (24ºC) with and without *ani(RNAi).* Left and Right graph shows the mean ring diameter over time, with all replicates for *cyk-4(ts);Rac(G60R)* double mutants in a more transparent shade of brown for *control(RNAi)* or purple for *ani-1(RNAi)* conditions. Error bars represent the SEM. B) Cytokinesis failure and success rates for 1-cell embryos per genotype indicated. C) Average rate of peak contractile ring constriction, plotted as the change in diameter (µm/sec) for embryos in (A). n.s.=p≥0.05; *=p<0.05; **=p<0.01; ***=p<0.001; ****=p<0.0001.

Cdc42 and cytokinesis: A role for the Cdc42 GAP Chimerin/CHIN-1?

The small GTPase Cdc42 is required for anterior-posterior cell polarity maintenance in the asymmetrically dividing *C. elegans* one-cell embryo. In Zhuravlev et al 2017, we saw a more posteriorized furrow position in *cyk-4(ts);Rac(G60R)* and enhanced cytokinesis failure in *cyk-4(ts);Rac(G60R);Cdc42(RNAi)*. This is a phenotype previously found associated with disruption of the Cdc42 GAP CHIN-1/Chimerin. Thus, I next tested whether CYK-4 might cooperate with CHIN-1 to regulate Cdc42 during cytokinesis. Loss of CHIN-1 leads to hyperactivation of CDC-42 without altering the distribution of anterior or posterior polarity proteins (Kumfer et al., 2010). *cyk-4(ts);Rac(G60R);chin-1(RNAi)* at semi-restrictive temperature resulted in cytokinesis failure in 3/19 (~16%) embryos compared to 1/8 (~13%) embryos in *cyk-4(ts);Rac(G60R);control(RNAi)* (Figure 23). Although the triple mutant appears to still be more posteriorized than controls, there was a lot of variability. Additionally, *chin-1(RNAi)* on its own did not show significant posteriorization compared to controls, though the RNAi treatment likely worked given the enhanced failure phenotype observed.

Previously, a colleague in the lab found that cytokinesis failure in *formin(ts) (cyk-1)* mutants was enhanced by *Cdc42(RNAi)* but rescued by *chin-1(RNAi)*. Since I saw enhancement of cytokinesis failure in *cyk-4(ts)* mutants with both CDC-42 and CHIN-1 knockdowns (Figure 23), I was interested to look at what the genetic interaction between *cyk-4(ts)* and *cyk-1(ts)* would yield during cytokinesis and whether it would enhance failure even at the semi-permissive temperature where both mutants are able to complete cytokinesis on their own. Very preliminary data suggests that *cyk-4(ts);cyk-1(ts)* enhances the rate of cytokinesis failure with 3/4 embryos failing to complete cytokinesis. This result provides further support for a model in which the Formin/CYK-1 and CYK-4 function in parallel

pathways during cytokinesis (Figure 15D). Further information will be needed to determine how CHIN-1 contributes to cell division, but this result suggests that it is possible Cdc42 may contribute to more than one pathway during cytokinesis.

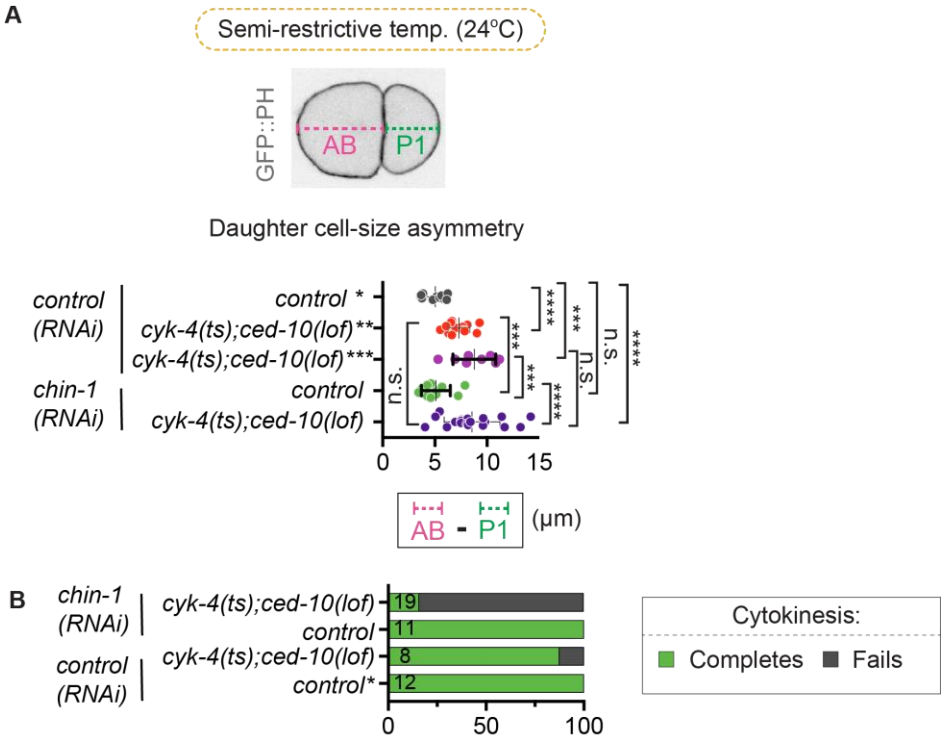

Figure 23: Chin-1 enhances cytokinesis failure in *cyk-4(ts);Rac(G60R)*

A) AB vs P1 asymmetry measurement for daughter cell size in 1-cell embryos. Measurements were taken one time point following contractile ring closure or the timepoint at which the ring was most ingressed. Asymmetric division is indicated by an increased difference in daughter cell length (when AB>P1). B) Completion and failure rates for genotypes indicated. All data shown as mean ± SD. n.s.=p≥0.05; *=p<0.05; **=p<0.01; ***=p<0.001; ****=p<0.0001
For starred genotypes in A) * and **means data shown is the same as from figure 6 in Zhuravlev et al 2017.
*** is new data collected for this experiment.

CYK-4 and ECT-2 continued

To argue that CYK-4 is unlikely to be an activator of ECT-2, we showed that levels of downstream Rho effectors are not reduced in *cyk-4(ts)* mutants. However, given that the GFP::Utr^{ABD} levels in *cyk-4(ts);control(RNAi)* were not statistically significant from *GFP::Utr^{ABD};control(RNAi)* but still looked strikingly different by eye, I performed the same analysis again using decreasing sizes of regions of interest, as it could very well be possible that the rectangular ROI used in Zhuravlev et al 2017 was too big. If so, this would dilute signal with the background in the control strains and could be a reason for why I observed no statistical difference between the control and experimental strain. To address this potential issue, I used 5 different rectangular ROI widths of 5, 10, 20, 30 and 38 pixels, and found in all cases that the levels were not significantly different in either GFP::myosin-II or GFP::Utr^{ABD} with or without *cyk-4(ts)* at semi-restrictive temperature (Figure 24).

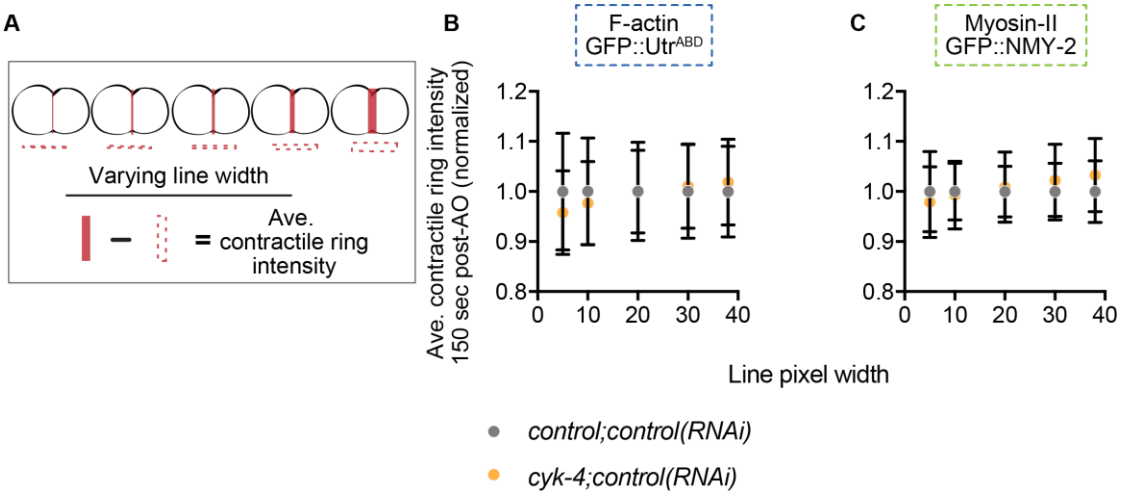

Figure 24: Even with a smaller ROI downstream targets of Rho, f-actin and myosin-II, are not reduced at the division plane in *cyk-4(ts)* mutants

A) Schematic depicting different rectangle ROIs used subtracted from a background of the same size ROI. B-C) Quantification of contractile ring levels of f-actin (GFP::Utr^{ABD} and myosin-II with or without *cyk-4(ts)* at 150 sec post AO using a pixel width of various sizes as indicated. Error bars represent the SD.

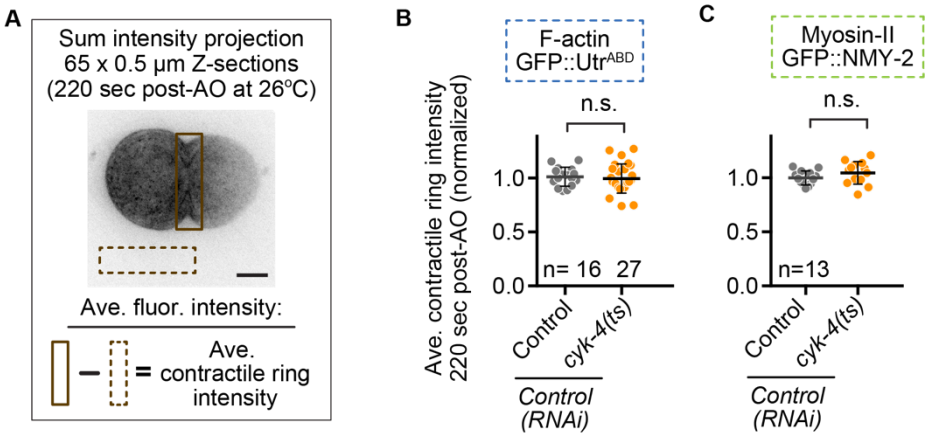

Figure 25: F-actin and myosin-II levels are not reduced at the division plane in *cyk-4(ts)* mutants even at 220 sec

A) Schematic of how quantitative image analysis was performed for (B) and (C). B, C) Quantification of contractile ring levels of (B) f-actin (GFP::Utr^{ABD}) and (C) myosin-II (NMY-2::GFP) at 220 sec post-AO at restrictive temperature (26ºC). Error bars represent the SD; p-values were obtained by an unpaired, two-tailed student's t-test.

Additionally, the 150 sec time point chosen for our previous analysis could be too early during ring constriction to show any change in levels of GFP::myosin-II or GFP::Utr^{ABD} given that contractile rings in controls are still ~71% (average of ~21µm) open at this time point, while in *cyk-4(ts)* strains the rings are ~82% (average of ~27µm) open (Figure S 4). At 220 sec *cyk-4(ts)* mutants are much more open than controls, averaging 17 µm whereas controls are nearly completely closed averaging ~1.5 µm. Generally, at 220 sec the *cyk-4(ts)* strain is not yet regressing so I chose to look at GFP::Utr^{ABD} and GFP::myosin-II levels here to see if the drastic difference of ring openness and thus contractile ring dynamics would yield a statistical difference. Also, here I imaged at the fully restrictive (26ºC) temperature to make sure there is no residual CYK-4 GAP activity that may be contributing to the signal. Surprisingly, even though the controls are so much further along in ingression than the *cyk-4(ts)* mutants, I still found no statistical difference in GFP::Utr^{ABD} levels at 220 sec (Figure 25). Ideally, we would look at a mutant whose levels of GFP::myosin-II and/or GFP::Utr^{ABD} we would expect to be reduced as a negative control but this wasn't done in this study. Ideally, both strains would be analyzed at different time points but approximately similar rates of ingression to test if here the levels of GFP::Utr^{ABD} and GFP::myosin-II show differences with or without CYK-4.

These additional experiments confirm that Rho-effector levels in the contractile ring are not significantly changed with depletion of CYK-4, using smaller regions of interest and looking at a later time of contractile ring ingression, the opposite of what would be expected if CYK-4 were an activator of ECT-2/Rho. We also found that hyper-activation of CDC-42 enhanced cytokinesis failure, much like the result from depletion of CDC-42. It is possible that CYK-4 requires a precise balance of CDC-42 activity. Further, while it seems CYK-4

functions independently of ANI-1, we did see more rescue and deeper ingression in ANI-1 knocked down double mutants. In summary, the search for other targets of CYK-4 is not over but we have shown that CYK-4 specifically inhibits Rac activity and is unlikely to contribute to Rho activation.

Strain	Genotype
N2	*wild-type (ancestral)*
OD95	*unc-119(ed3)* ltIs38[pAA1; pie-1::eGFP::PH(PLC1delta1) unc-119(+)]III; ltIs37[pAA64; pie-1::mCherry::his-58 unc-119(+)]IV*
JCC176	*unc-119(ed3)* ltIs38[pAA1; pie-1::eGFP::PH(PLC1delta1) unc-119(+)]III; ced-10(n3246)IV*
OD239	*cyk-4(or749ts) unc-119(ed3)* ltIs38[pAA1; pie-1::eGFP::PH(PLC1delta1) unc-119(+)]III; ltIs37[pAA64; pie-1::mCherry::his-58 unc-119(+)]IV*
JCC146	*cyk-1(or596ts) unc-119(ed3)* ltIs38[pAA1; pie-1::eGFP::PH(PLC1delta1) unc-119(+)]III; ltIs37 [pAA64; pie-1::mCherry::his-58 unc-119(+)]IV*
JCC177	*cyk-1(or596ts) unc-119(ed3)* ltIs38[pAA1; pie-1::eGFP::PH(PLC1delta1) unc-119(+)]III; ced-10(n3246)IV*
JCC192	*nmy-2(ne3409ts) dpy-5**; unc-119(ed3)* ltIs38[pAA1; pie-1::eGFP::PH(PLC1delta1) unc-119(+)]III; ltIs37[pAA64; pie-1::mCherry::his-58 unc-119(+)]IV*
JCC203	*nmy-2(ne3409ts), dpy-5**I; unc-119(ed3)* ltIs38[pAA1; pie-1::eGFP::PH(PLC1delta1) unc-119(+)]III; ced-10(n3246)IV*
JCC925	*ect-2(ax751ts)II; unc-119(ed3)*, ltIs38 [pAA1; pie-1::eGFP::PH(PLC1delta1) unc-119(+)]III*
JH2754	*ect-2(ax751ts)II*
MG592	*ect-2(ax751ts)II; ced-10(n1993)IV*
MT5013	*ced-10(n1993)IV*
JCC719	*mgSi3[cb-unc-119(+) eGFP:utrophin]II; unc-119(ed3)*III; ltIs37[pAA64; pie-1::mCherry::his-58 unc-119(+)]IV*
JCC765	*mgSi3[cb-unc-119(+) eGFP:utrophin]II; unc-119(ed3)* cyk-4(or749ts)III; ltIs37 [pAA64; pie-1::mCherry::his-58 unc-119(+)]IV*
JCC541	*unc-119(ed3)*III; ltIs37 [pAA64; pie-1::mCherry::his-58; unc-119(+)]IV; zuIs45[nmy-2::nmy-2::eGFP unc-119(+)]V*
OD235	*unc-119(ed3)* cyk-4(or749ts)III; zuIs45[nmy-2::nmy-2::eGFP unc-119(+)]V.*
JCC178	*unc-119(ed3)* cyk-4(or749ts) ltIs38[pAA1; pie-1::eGFP::PH(PLC1delta1) unc-119(+)]III; ced-10(n3246)IV*
BA17	*fem-1(hc17)IV*
OD227	*cyk-4(or749ts)III*
EU1303	*cyk-4(or570ts)III*

*The *unc-119(ed3)* mutation was present in the parental strains but has not been directly sequenced in these strains to determine if the *unc-119* gene is mutated.

Table S 3: Feeding RNAi constructs

Strain names and genotypes used in this study

Plasmid	Gene(s)	Oligo 1 (5'-3')	Oligo 2 (5'-3')	Template	Cloning vector
pJC90	*ced-10 (C09G12.8)*	GCGCG**AAGCTT** TCAAATGTGTCGTCGTTGGT	GCGCG**AAGCTT** GATCGCCTCATCGAAAACTTG	N2 cDNA	L4440 (empty vector)
pJC53	*cdc-42 (R07G3.1)*	Acquired from Ahringer library (Clone # II-5P13)			

Table S 4: Strain names and genotype

Plasmid names, targeted genes for RNAi experiments, oligos used to generate RNAi feeding construct and DNA template used or Ahringer library (Kamath and Ahringer, 2003; Kamath et al., 2003) clone number, and cloning vectors used in this study.

Figure (within the manuscript):			Strains to be compared: Fisher's exact test			
15B	# of embryos		Control	Rac(G60R)	cyk-4(ts)	cyk-4(ts); Rac(G60R)
cyk-4(ts) cytokinesis completion rate with and without Rac(G60R) at semi-restrictive temp	16	Control		1	<.0001	<.0001
	12	Rac(G60R)			<.0001	<.0001
	13	cyk-4(ts)				0.0001
	10	cyk-4(ts);Rac(G60R)				

			Strains to be compared: Fisher's exact test			
cyk-4(ts) cytokinesis completion rate with and without Rac(RNAi) at semi-restrictive temp	# of embryos		Control(RNAi)	Rac(RNAi)	cyk-4(ts); Control(RNAi)	cyk-4(ts); Rac(RNAi)
	10	Control(RNAi)		1	<.0001	<.0001
	12	Rac(RNAi)			<.0001	<.0001
	12	cyk-4(ts);Control(RNAi)				0.0001
	10	cyk-4(ts);Rac(RNAi)				
			Strains to be compared: Barnard's exact test			
	# of embryos		Control	Rac(G60R)	cyk-4(ts)	cyk-4(ts); Rac(G60R)
cyk-4(ts) cytokinesis completion rate with and without Rac(G60R) at semi-restrictive temp	16	Control		1	<.0001	<.0001
	12	Rac(G60R)			<.0001	<.0001
	13	cyk-4(ts)				<.0001
	10	cyk-4(ts);Rac(G60R)				
			Strains to be compared: Barnard's exact test			
	# of embryos		Control(RNAi)	Rac(RNAi)	cyk-4(ts); Control(RNAi)	cyk-4(ts); Rac(RNAi)
cyk-4(ts) cytokinesis completion rate with and without Rac(RNAi)at semi-restrictive temp	10	Control(RNAi)		1	<.0001	<.0001
	12	Rac(RNAi)			<.0001	<.0001
	12	cyk-4(ts);Control(RNAi)				<.0001
	10	cyk-4(ts);Rac(RNAi)				
			Strains to be compared: Unpaired, two-tailed student's t-test			
	# of embryos		Control	Rac(G60R)	cyk-4(ts)	cyk-4(ts); Rac(G60R)
cyk-4(ts) contractile ring constriction rates with and witho Rac(G60R) or Rac(RNAi) at semi-restrictive temp	16	Control		0.0359	<.0001	<.0001
	12	Rac(G60R)			<.0001	<.0001
	13	cyk-4(ts)				0.0687
	10	cyk-4(ts);Rac(G60R)				
			Strains to be compared: Unpaired, two-tailed student's t-test			
15C	# of embryos		Control(RNAi)	Rac(RNAi)	cyk-4(ts); Control(RNAi)	cyk-4(ts); Rac(RNAi)
cyk-4(ts) contractile ring constriction rates with and witho Rac(G60R) or Rac(RNAi) at semi-restrictive temp	10	Control(RNAi)		0.0735	<.0001	<.0001
	12	Rac(RNAi)			<.0001	0.0012
	12	cyk-4(ts);Control(RNAi)				0.0177
	10	cyk-4(ts);Rac(RNAi)				
			Strains to be compared: Fisher's exact test			
16D	# of embryos		Control	Rac(G60R)	cyk-1(ts)	cyk-1(ts); Rac(G60R)
formin/cyk-1(ts) cytokinesis completion rate with and without Rac(G60R) at semi-permissive temp	13	Control		1	1	1
	13	Rac(G60R)			1	1
	13	cyk-1(ts)				0.22
	12	cyk-1(ts);Rac(G60R)				
			Strains to be compared: Barnard's exact test			
	# of embryos		Control	Rac(G60R)	cyk-1(ts)	cyk-1(ts); Rac(G60R)
formin/cyk-1(ts) cytokinesis completion rate with and without Rac(G60R) at semi-permissive temp	13	Control		1	1	1
	13	Rac(G60R)			1	1
	13	cyk-1(ts)				0.116554
	12	cyk-1(ts);Rac(G60R)				
			Strains to be compared: Unpaired, two-tailed student's t-test			
16E	# of embryos		Control	Rac(G60R)	cyk-1(ts)	cyk-1(ts); Rac(G60R)
formin/cyk-1(ts) contractile ring constriction rates with an without Rac(G60R) at semi-restrictive temp	11	Control		0.0735	<.0001	<.0001
	15	Rac(G60R)			<.0001	<.0001
	11	cyk-1(ts)				0.4925
	10	cyk-1(ts);Rac(G60R)				
			Strains to be compared: Unpaired, two-tailed student's t-test			
16F	# of embryos		Control	Rac(G60R)	cyk-1(ts)	cyk-1(ts); Rac(G60R)
formin/cyk-1(ts) contractile ring constriction rates with an without Rac(G60R) at semi-permissive temp	13	Control		0.7396	<.0001	<.0001
	13	Rac(G60R)			<.0001	<.0001
	13	cyk-1(ts)				0.9645
	12	cyk-1(ts);Rac(G60R)				
			Strains to be compared: Fisher's exact test			
17D	# of embryos		Control	Rac(G60R)	nmy-2(ts)	nmy-2(ts); Rac(G60R)
myosin-II/nmy-2(ts) cytokinesis completion rate with and without Rac(G60R) at semi-permissive temp	10	Control		1	1	1
	10	Rac(G60R)			1	1
	13	nmy-2(ts)				0.4348
	10	nmy-2(ts);Rac(G60R)				
			Strains to be compared: Barnard's exact test			
	# of embryos		Control	Rac(G60R)	nmy-2(ts)	nmy-2(ts); Rac(G60R)
myosin-II/nmy-2(ts) cytokinesis completion rate with and without Rac(G60R) at semi-permissive temp	10	Control		1	1	1
	10	Rac(G60R)			1	1
	13	nmy-2(ts)				0.278902
	10	nmy-2(ts);Rac(G60R)				
			Strains to be compared: Unpaired, two-tailed student's t-test			
17E	# of embryos		Control	Rac(G60R)	nmy-2(ts)	nmy-2(ts); Rac(G60R)
myosin-II/nmy-2(ts) contractile ring constriction rates with and without Rac(G60R) at semi-restrictive temp	10	Control		0.933	<.0001	<.0001
	10	Rac(G60R)			<.0001	<.0001
	13	nmy-2(ts)				0.01
	10	nmy-2(ts);Rac(G60R)				
			Strains to be compared: Unpaired, two-tailed student's t-test			
17F	# of embryos		Control	Rac(G60R)	nmy-2(ts)	nmy-2(ts); Rac(G60R)
myosin-II/nmy-2(ts) contractile ring constriction rates with and without Rac(G60R) at semi-permissive temp	12	Control	134	0.128	<.0001	0.0001
	10	Rac(G60R)			0.003	0.0047
	13	nmy-2(ts)				0.4866
	10	nmy-2(ts);Rac(G60R)				

18B	# of embryos		Control(RNAi)	Rac(RNAi)	ect-2(ts); Control(RNAi) Completes cytokinesis	ect-2(ts); Control(RNAi) Fails cytokinesis	ect-2(ts); Rac(RNAi)
ect-2(ts) contractile ring constriction rates with and witho Rac(RNAi) long shift at restrictive temp	11	Control(RNAi)		0.1082	0.001	<.0001	0.0269
	12	Rac(RNAi)			0.0166	<.0001	0.2393
	8	ect-2(ts); Control(RNAi) Completes cytokinesis				<.0001	0.3883
	5	ect-2(ts); Control(RNAi) Fails cytokinesis					<.0001
	12	ect-2(ts);Rac(RNAi)					

18C	# of embryos		Control(RNAi)	Rac(RNAi)	ect-2(ts); Control(RNAi)	ect-2(ts); Rac(RNAi)
ect-2(ts) cytokinesis completion rate with and without Rac(RNAi) at restrictive temp (GFP::PH domain; mCherry::H2B)	11	Control(RNAi)		1	0.0411	0.4783
	12	Rac(RNAi)			0.0391	0.4783
	12	ect-2(ts); Control(RNAi)				0.3783
	12	ect-2(ts);Rac(RNAi)				
			Strains to be compared: Barnard's exact test			
	# of embryos		Control(RNAi)	Rac(RNAi)	ect-2(ts); Control(RNAi)	ect-2(ts); Rac(RNAi)
ect-2(ts) cytokinesis completion rate with and without Rac(RNAi) at restrictive temp (GFP::PH domain; mCherry::H2B)	11	Control(RNAi)		1	0.019718	0.13817
	12	Rac(RNAi)			0.017417	0.125521
	12	ect-2(ts); Control(RNAi)				0.140907
	12	ect-2(ts);Rac(RNAi)				
			Strains to be compared: Fisher's exact test			

18D	# of embryos		Control(RNAi)	Rac(RNAi)	ect-2(ts); Control(RNAi)	ect-2(ts); Rac(RNAi)
ect-2(ts) cytokinesis completion rate with and without Rac(RNAi) at restrictive temp (no markers)	11	Control(RNAi)		1	0.0078	0.144
	12	Rac(RNAi)			0.0001	0.0155
	12	ect-2(ts); Control(RNAi)				0.1689
	12	ect-2(ts);Rac(RNAi)				
			Strains to be compared: Barnard's exact test			
	# of embryos		Control(RNAi)	Rac(RNAi)	ect-2(ts); Control(RNAi)	ect-2(ts); Rac(RNAi)
ect-2(ts) cytokinesis completion rate with and without Rac(RNAi) at restrictive temp (no markers)	11	Control(RNAi)		0.544659	0.005152	0.083613
	12	Rac(RNAi)			0.000384	0.065114
	12	ect-2(ts); Control(RNAi)				0.072989
	12	ect-2(ts);Rac(RNAi)				
			Strains to be compared: Unpaire two-tailed student's t-test			

19B	# of embryos		Control(RNAi)	cyk-4ts); Control(RNAi)
Contractile ring GFP::utrophin (f-actin) levels in control a cyk-4(ts) embryos at 150sec post-AO at semi-restrictive temperature	14	Control(RNAi)		0.5609
	12	cyk-4(ts);Control(RNAi)		
			Strains to be compared: Unpaire two-tailed student's t-test	

19C	# of embryos		Control(RNAi)	cyk-4ts); Control(RNAi)
Contractile ring GFP::NMY-2 (myosin-II) levels in contro cyk-4(ts) embryos at 150 sec post-AO at semi-restrictiv temperature	10	Control(RNAi)		0.9214
	10	cyk-4(ts);Control(RNAi)		
			Strains to be compared: Unpaired, two-tailed student's t-test	

20A	# of embryo /# of worms		fem1 no males	fem1 x N2 males	fem1 x cyk-4(or570ts) males	fem1 x cyk-4(or749ts) males
Brood size- paternal requirement test	0/8	fem1		0.0003	0.0005	0.0002
	416/8	fem1 x N2			0.4844	0.0603
	640/8	fem1 x cyk-4(or570)				0.2241
	488/8	fem1 x cyk-4(or749)				
			Strains to be compared: Unpaired, two-tailed student's t-test			
	# of viable embryos /# of worms		fem1 no males	fem1 x N2 males	fem1 x cyk-4(or570ts) males	fem1 x cyk-4(or749ts) males
Embryonic viability- paternal requirement test	0/8	fem1		<.0001	<.0001	<.0001
	401/8	fem1 x N2			0.1742	0.0378
	573/8	fem1 x cyk-4(or570)				0.2241
	446/8	fem1 x cyk-4(or749)				

20D	# of embryos		Control; Control(RNAi)	Control; cdc-42(RNAi)	Rac(G60R); Control(RNAi)	Rac(G60R); cdc-42(RNAi)	cyk-4(ts); Control(RNAi)	cyk-4(ts); cdc-42(RNAi)	cyk-4(ts); Rac(G60R); Control(RNAi)	cyk-4(ts); Rac(G60R); cdc-42(RNAi)
cyk-4(ts) contractile ring constriction rates with and withe cdc-42(RNAi) and Rac(G60R) at semi-restrictive temp	9	Control; Control(RNAi)		0.6044	0.0684	0.5681	<0.0001	0.0001	<0.0001	<0.0001
	10	Control; cdc-42(RNAi)			0.1249	0.8598	<0.0001	<0.0001	0.1249	0.8598
	10	Rac(G60R); Control(RNAi)				0.2485	<0.0001	0.0001	<0.0001	0.0001
	12	Rac(G60R); cdc-42(RNAi)					0.0001	0.0001	<0.0001	<0.0001
	12	cyk-4(ts); Control(RNAi)						0.6835	0.4894	0.0433
	10	cyk-4(ts); cdc-42(RNAi)							0.984	0.1046
	10	cyk-4(ts); Rac(G60R); Control(RNAi)								0.0751
	15	cyk-4(ts); Rac(G60R); cdc-42(RNAi)								
		Strains to be compared: Unpaired, two-tailed student's t-test								
20B	# of embryos		Control; Control(RNAi)	Control; cdc-42(RNAi)	Rac(G60R); Control(RNAi)	Rac(G60R); cdc-42(RNAi)	cyk-4(ts); Control(RNAi)	cyk-4(ts); cdc-42(RNAi)	cyk-4(ts); Rac(G60R); Control(RNAi)	cyk-4(ts); Rac(G60R); cdc-42(RNAi)
Difference in daughter cell size; AB- P1	9	Control; Control(RNAi)		0.0003	0.5537	0.0017	0.4053	0.0621	0.0003	0.0006
	10	Control; cdc-42(RNAi)			<0.0001	0.4068	0.0003	0.1526	<0.0001	0.6046
	10	Rac(G60R); Control(RNAi)				0.0005	0.6865	0.0262	0.0017	0.0002
	12	Rac(G60R); cdc-42(RNAi)					0.0012	0.4246	<0.0001	0.2285
	12	cyk-4(ts); Control(RNAi)						0.0273	0.0419	0.0004
	10	cyk-4(ts); cdc-42(RNAi)							<0.0001	0.1023
	10	cyk-4(ts); Rac(G60R); Control(RNAi)								<0.0001
	15	cyk-4(ts); Rac(G60R); cdc-42(RNAi)								
		Strains to be compared: Fisher's exact test								
20C	# of embryos		Control; Control(RNAi)	Control; cdc-42(RNAi)	Rac(G60R); Control(RNAi)	Rac(G60R); cdc-42(RNAi)	cyk-4(ts); Control(RNAi)	cyk-4(ts); cdc-42(RNAi)	cyk-4(ts); Rac(G60R); Control(RNAi)	cyk-4(ts); Rac(G60R); cdc-42(RNAi)
cyk-4(ts) cytokinesis completion rates with and without Rac(G60R) and with and without cdc-42(RNAi) at semi-perimissive temperature	9	Control; Control(RNAi)		1	1	1	<0.0001	<0.0001	0.2663	<0.0001
	10	Control; cdc-42(RNAi)			1	1	<0.0001	<0.0001	0.2308	<0.0001
	10	Rac(G60R); Control(RNAi)				1	<0.0001	<0.0001	0.25	<0.0001
	12	Rac(G60R); cdc-42(RNAi)					<0.0001	<0.0001	0.2308	<0.0001
	12	cyk-4(ts); Control(RNAi)						1	<0.0001	1
	10	cyk-4(ts); cdc-42(RNAi)							<0.0001	1
	10	cyk-4(ts); Rac(G60R); Control(RNAi)								<0.0001
	15	cyk-4(ts); Rac(G60R); cdc-42(RNAi)								
		Strains to be compared: Barnard's exact test								
	# of embryos		Control; Control(RNAi)	Control; cdc-42(RNAi)	Rac(G60R); Control(RNAi)	Rac(G60R); cdc-42(RNAi)	cyk-4(ts); Control(RNAi)	cyk-4(ts); cdc-42(RNAi)	cyk-4(ts); Rac(G60R); Control(RNAi)	cyk-4(ts); Rac(G60R); cdc-42(RNAi)
cyk-4(ts) cytokinesis completion rates with and without Rac(G60R) and with and without cdc-42(RNAi) at semi-perimissive temperature	9	Control; Control(RNAi)		1	1	1	<0.0001	<0.0001	0.117741	<0.0001
	10	Control; cdc-42(RNAi)			1	1	<0.0001	<0.0001	0.103254	<0.0001
	10	Rac(G60R); Control(RNAi)				1	<0.0001	<0.0001	0.112572	<0.0001
	12	Rac(G60R); cdc-42(RNAi)					<0.0001	<0.0001	0.103254	<0.0001
	12	cyk-4(ts); Control(RNAi)						1	<0.0001	1
	10	cyk-4(ts); cdc-42(RNAi)							<0.0001	1
	10	cyk-4(ts); Rac(G60R); Control(RNAi)								<0.0001
	15	cyk-4(ts); Rac(G60R); cdc-42(RNAi)								

Supplementary Figure:		Strains to be compared: Fisher's exact test		
S4D	# of embryos		cyk-4(ts)	cyk-4ts); Rac(RNAi)
2-cell embryo cyk-4(ts) AB cell cytokinesis completion ra at restrictive temp	19	cyk-4(ts)		0.0004
	14	cyk-4(ts); Rac(RNAi)		
		Strains to be compared: Fisher's exact test		
	# of embryos		cyk-4(ts)	cyk-4ts); Rac(RNAi)
2-cell embryo cyk-4(ts) P1 cell cytokinesis completion ra at restrictive temp	20	cyk-4(ts)		0.0046
	16	cyk-4(ts); Rac(RNAi)		
		Strains to be compared: Barnard's exact test		
	# of embryos		cyk-4(ts)	cyk-4ts); Rac(RNAi)
2-cell embryo cyk-4(ts) AB cell cytokinesis completion ra at restrictive temp	19	cyk-4(ts)		0.000121
	14	cyk-4(ts); Rac(RNAi)		
		Strains to be compared: Barnard's exact test		
	# of embryos		cyk-4(ts)	cyk-4ts); Rac(RNAi)
2-cell embryo cyk-4(ts) P1 cell cytokinesis completion ra at restrictive temp	20	cyk-4(ts)		0.005581
	16	cyk-4(ts); Rac(RNAi)		

Table S 5: P values for all data in publication

Exact p-values for all figures in publication.

Materials and Methods

Strain maintenance

Caenorhabditis elegans were kept on standard NGM plates seeded with OP50 *E. coli* bacteria, as described (Brenner, 1974). All strain names and genotypes used in this study are listed in Table S 4.

Temperature control

All control and temperature-sensitive (ts) strains were raised in an incubator (Crittenden et al.) kept at permissive temperature (16 ± 0.5ºC) and all fast-acting ts strains were also dissected in cooled (~16ºC) M9 buffer (3 g KH_2PO_4, 6 g Na_2HPO_4, 5 g NaCl, 1 mL 1 M $MgSO_4$, H_2O to 1 L and sterilized by autoclaving) until just before the 1-cell or 2-cell division. For the non-fast-acting *ect-2(ts)* experiments (Figure 18), worms were raised at permissive temperature (16ºC) until the L4 stage at which time they were moved to a 26ºC incubator (Crittenden et al.) overnight for at least 12 hours and dissected in a warmed room (~26ºC) in ~26ºC M9 buffer (Brenner, 1974).

Live-cell imaging was performed in a thermally-controlled room. Room temperature was monitored with two thermometers attached directly to the objective, and another thermometer attached to the stage via a glue gun to monitor the temperature of the specimen during filming. Wherever mentioned throughout this article, experimental temperatures were calculated by averaging the values from the two thermometers attached to the objective and were as follows: *cyk-4(ts)* semi-restrictive (24.0 ± 0.5ºC); *ect-2(ts)* restrictive (26.0 ± 0.5ºC*); formin(ts)* semi-permissive temperature (18.5 ± 0.5ºC); *formin(ts)* semi-restrictive temperature (23.5 ± 0.5ºC); *myosin-II(ts)* semi-permissive temperature (22.5 ± 0.5ºC); *myosin-II(ts)* semi-restrictive temperature (25.5 ± 0.5ºC). Temperatures are defined for each individual mutant

allele as follows: permissive temperature=all ts embryos complete cytokinesis with kinetics most similar to non-ts controls; semi-permissive temperature=highest temperature at which all ts embryos complete cytokinesis; semi-restrictive temperature=lowest temperature at which all ts embryos fail in cytokinesis; and restrictive temperature=all embryos fail in cytokinesis with a null-like phenotype (aside from the *ect-2(ts)* mutant that often divides successfully even at the restrictive temperature of 26ºC).

Live-cell imaging

Single-cell embryos were mounted on a 2% agar pad as described previously (Gonczy et al., 1999; Jordan et al., 2016). Imaging was performed on a Nikon Ti inverted microscope with 40x 1.3 N.A. and 60x 1.4 N.A. oil-immersion PlanApochromat objectives using a Yokagawa CSU-10 spinning disc confocal equipped with Borealis (Spectral Applied Research) and a Hamamatsu Orca ER camera. Z-sectioning was done with a Piezo-driven motorized stage (Applied Scientific Instrumentation) and focus was maintained using Perfect Focus (Nikon) prior to each Z-series acquisition. Solid-state 150 mW lasers were used for excitation at 488 and 561 nm for eGFP and mCherry respectively (Spectral Applied Research), and a filter-wheel was used for emission wavelength selection (Sutter Instruments). The imaging system was controlled by Metamorph software (Molecular Devices).

A central, transmitted light image and through-cell GFP and mCherry fluorescent Z-series were collected every 15 sec or 30 sec to measure ingression kinetics (see below). For data presented in Figure 15-Figure 18, Figure 20 and S1, embryos were imaged with the 40x 1.3 N.A. oil objective with 2 x 2 binning and 100 msec exposures. Laser power was tuned to

20% for the 488 nm laser and 50% for the 561 nm laser (except for Figure 20, where we look at the effect of *Cdc42(RNAi)* on cytokinesis in *cyk-4(ts)* embryos with and without *Rac(G60R)*), the 561 nm laser intensity was 70%). For data presented in Figures 15, 17, and 18 (*cyk-4(ts)* kinetics with and without *Rac(G60R)* or *Rac(RNAi)*;*cyk-1(ts)* kinetics with and without *Rac(G60R)*; and *nmy-2(ts)* kinetics with and without *Rac(G60R)*), the same imaging parameters were used except embryos were imaged every 30 sec. Z-sectioning was as follows: 13 x 2 μm steps (Figure 15-Figure 18, Figure S 4C and Figure 20B-D) with the exception of a few embryos filmed using 7 x 2 μm steps in Figure 16 and Figure 17 at the semi-restrictive temperature, where the contractile ring closes in the central Z-plane. The embryos imaged using 7 x 2 μm steps were acquired with the 60x 1.4 N.A. oil objective 2 x 2 binning (Figure 16, Figure 17). For analysis of the contractile ring levels of GFP::myosin-II (GFP::NMY-2 (Munro et al., 2004)) and GFP::Utrophin^{ABD} (GFP::Utr^{ABD}), a reporter for f-actin (Burkel et al., 2007; Tse et al., 2012), a single 11 x 2.5 μm or 65 x 0.5 μm Z-section image stack (see also below in image analysis section) was taken 150 sec after anaphase onset using a 60x 1.4 N.A. oil-immersion PlanApochromat objective with 2 x 2 binning on a Hamamatsu Orca ER camera and 150 mW 488 nm and 561 nm lasers at 50% laser power intensity with 100 msec exposures (Figure 19). For the 220 sec a 65 x 0.5 μm Z-section image stack was taken 220 sec after anaphase onset otherwise using the same parameters as for 150sec. For brood quality experiments a 25 x1 μm Z-section image stack was taken with the 20x air objective with 1 x1 binning and just the DIC channel. Only 1 time point was imaged with multiple stages to capture as many embryos per field as possible. Prior to imaging worms were kept at 26 ºC for over 12 hours.

Image analysis

Metamorph (Molecular Devices) and FIJI (ImageJ) software were used for all data analysis (Schindelin et al., 2012; Schindelin et al., 2015). Contractile ring constriction was measured from the time of metaphase (time point immediately prior to anaphase onset) until anaphase onset of the next division, or in the case of cytokinesis failure, until complete contractile ring regression. The contractile ring diameter was measured at each time point in the z-section where the ring was most open and displayed as a percentage of the initial diameter over time. The rate of ingression is plotted as the μm/sec when the rate of ingression peaks from ~90-50% of the initial cell diameter. When embryos did not ingress to 50% of the initial cell diameter, the point of deepest contractile ring constriction was used (Figure 15-Figure 18). Where histone markers were not available (in strains with *Rac(lof)* and *cyk-4(ts);GFP::NMY-2*), anaphase onset was determined by transmitted light.

The levels of f-actin and myosin-II (GFP::Utrophin^{ABD} and GFP::myosin-II^{NMY-2}) in the contractile ring in *cyk-4(ts)* embryos (at semi-restrictive temperature, 24ºC) were calculated as follows: All 11 x 2.5 μm Z-stacks were sum projected using FIJI (Figure 19B-D). A region of fixed size (195 x 38 pixels) surrounding the entire division plane was used to measure the average pixel intensity and measurements from a region of the same size in a nearby background area, outside of the embryo, was subtracted for each individual embryo as is schematized in Figure 19A. These data were normalized to controls and plotted as the average intensity at 150 sec post-anaphase onset (Figure 19B-D). Where higher resolution images are shown (Figure 19E), a 65 x 0.5 μm Z-section stack acquired at 150 sec post-anaphase onset and a maximum projection image for all 65 Z-sections was generated using FIJI (FIJI is just Image J) (Schindelin et al., 2012; Schindelin et al., 2015).

The asymmetric differences in daughter cell size were calculated by measuring the length of the newly formed AB (anterior) and P1 (posterior) blastomeres using the time point immediately following completion of cytokinesis (Figure 20 showing *cyk-4(ts)* with and without *Rac(G60R)* and *Cdc42(RNAi*)). The length of the posterior P1 cell was subtracted from the length of the anterior AB cell. Cell size measurement was done using a single central plane from the 488 nm GFP channel. When embryos failed to complete cytokinesis, a similar measurement was taken using the distance from the anterior and posterior poles to the cleavage furrow at the time of maximum contractile ring constriction. Analysis of the time from anaphase onset to double membrane formation in Figure S 4 was done using the same embryos in Figure 15A (kinetics of cytokinesis in *cyk-4(ts)* mutant embryos with and without *Rac(RNAi)*). For the 220 sec images the region of interest was 364 x 40 pixels, otherwise image analysis was performed the same way as for 150 sec.

Embryonic viability and brood size

fem-1(hc17ts) hermaphrodites were raised at 25ºC to feminize them (by blocking sperm production), then singled as L4s onto individual mating plates (35 mm NGM agar plates seeded with 10 µL of OP50 (Brenner, 1974)). *cyk-4(ts)* males were also raised at 25ºC from the ~L3/L4 stage. 7 males per genotype (except for the no male controls) were added to each plate containing a single hermaphrodite and allowed to mate for ~15 hours at 25ºC. To ensure the *fem-1(hc17ts)* hermaphrodites were feminized (and thus sterile) we did not add males to one set of *fem-1(ts)* hermaphrodites (no male controls). The adults from each individual cross were transferred twice to a new plate every ~10 hours (after laying ~50 embryos). The number of viable progeny and dead embryos per feminized hermaphrodite

(Figure 20A) was quantified for two plates per cross (representing ~24-30 hours of egg laying) 24 hours after transferring off the adults (to allow all embryos to hatch) using a digital counting pen (Burkard et al.) on a Nikon dissecting microscope

Feeding RNAi

All primers and DNA template used for RNAi experiments are listed in Table S 3. Cloning was performed by inserting the *Rac/ced-10* sequence into the L4440 vector using standard cloning protocols and then transformed into HT115 *E. coli (Timmons et al., 2001).* The empty L4440 vector in HT115 cells was used as a control. RNAi feeding bacteria were inoculated in Luria Broth with 100 µg/mL ampicillin for either 7 hours at 37ºC or 16 hours at 32ºC. 300 µL of this culture was plated on RNAi plates (NGM agar plates (Brenner, 1974) supplemented with 50 µg/mL ampicillin and 1 mM IPTG). After drying, the plates were grown at 32ºC for 24-48 hours. L1 worms were transferred onto RNAi plates and then grown at 16ºC until young adulthood when they were dissected to obtain the embryos. RNAi knockdown for *Rac/ced-10* was confirmed by 1) observing deeper furrowing during pseudocleavage, and 2) completion of cytokinesis in *cyk-4(ts)* mutant embryos at its semi-restrictive temperature (24 ± 0.5ºC). Confirmation of Cdc42 (CDC-42) knockdown was confirmed by assaying embryonic lethality and loss of cell division asymmetry (Figure 20B).

Statistical Analysis

Unpaired student's t-tests were conducted using Graphpad Prism software. n.s.=$p \geq 0.05$, *=$p < 0.05$, **=$p < 0.01$, ***=$p < 0.001$, and ****=$p < 0.0001$. Error bars for traces of cell diameter over time during cytokinesis represent SEM. Error bars for contractile ring

constriction rates, myosin-II and f-actin levels, embryonic lethality, brood size, and asymmetry of furrow position represent the SD. Statistics for cytokinesis completion/failure bar graphs used a two-tailed Fisher's exact test, but this analysis was also done with a Barnard's exact test (Table S 5: P values for all data in publication). See also statistical analysis in Table S 5 for all p-values.

Experimental procedures for unpublished data

Image analysis

The levels of f-actin and myosin-II (GFP::Utrophin^{ABD} and GFP::myosin-II^{NMY-2}) in the contractile ring in *cyk-4(ts)* embryos (at semi-restrictive temperature, 24ºC) were calculated as follows: All 11 x 2.5 μm Z-stacks were sum projected using FIJI(Schindelin et al., 2012; Schindelin et al., 2015). A region of 5,10, 20, 30 and 38 pixels surrounding the entire division plane was used to measure the average pixel intensity and measurements from a region of the same size in a nearby background area, outside of the embryo, was subtracted for each individual embryo as is schematized in Figure 19A at 150sec. These data were normalized to controls and plotted as the average intensity at 150 sec post-anaphase onset (Figure 19B-D). Analysis of f-actin and myosin-II (GFP::Utrophin^{ABD} and GFP::myosin-II^{NMY-2}) levels in the contractile ring at 220 sec was performed the same as in Zhuravlev et al 2017 (Figure 19).

Brood quality analysis

For brood quality experiments length and width were measured using metamorph where a line at the equator of the cell spanned from the anterior/dorsal most point of the

eggshell to the posterior/ventral most point. This measurement was done irrespective of the developmental stage of the embryo for all conditions. The middle/most in focus slice was used for the measurements.

Feeding RNAi

Ani-1 (Y49E10.19) RNAi; pjc132*:* F:gcgcg**actagt**actccagtgcattttcaccc

R:gcgcg**actagt**gacgatgatgatgatgtcgc

Acknowledgments

We thank all members of the Canman, Dumont, and Shirasu-Hiza labs for their support; Natalia Spica, Isaiah Thomas, Carrie Walsh, Benjamin Leslie-Pringle, Samrawit Solomon, Vandana Chand, Amanda Smith, and Nancy Quinn for lab assistance; Christian Garcia for confirming the *cyk-4(ts);Rac(RNAi)* cytokinesis rescue; Elizabeth Stivison for her eyelashes for use in clustering embryos; and Paul Maddox and Vincent Boudreau for help in quantifying the levels of cytokinetic f-actin and myosin-II by a different method. We thank Jennifer Waters (Nikon Imaging Center at Harvard Medical School) for microscopy consultation. We are grateful to Michael Glotzer, Bruce Bowerman, and the *Caenorhabditis* Genomics Center for worm strains and Oliver Hobert for the *Cdc42(RNAi)* plasmid. This work was funded by: ANR-09-RPDOC-005-01 (JD); FRM-AJE201112 (JD); the Emergence program from Mairie de Paris (JD); NIH-R01-GM105775 (MSH); NIH-R01-AG045842 (MSH); NIH-R01GM117407 (JCC); and NIH-DP2-OD008773 (JCC).

Chapter 4. The short and happy life of Notch/glp-1, Delta/APX-1, and Wnt/MOM-2 signalling in cytokinesis

None of this chapter has been previously published.

My contributions to Chapter 4

I conducted all of the experiments and analysis for all figures in this chapter.

Abstract

Although fundamental elements of cytokinesis are common across much of metazoan phylogeny, it is clear that cytokinesis itself shows a great deal of diversity from one species to the next, and even within a multicellular organism, from one tissue to the next. For example, genetic inhibition of central spindle assembly in worms and flies disrupts cytokinesis in some cell types, but not in others (Verbrugghe and White, 2007). Moreover, in humans, hypomorphic mutations in the core cytokinesis signaling proteins often lead to tissue and/or cell-type specific diseases, such as with X-linked neutropenia that only affects neutrophil cells, or congenital dyserythropoietic anemia type II, which affects only erythroblasts (Heimpel et al., 2003). Using a SPD-1 mutant, which results in disruption of the central spindle, as a sensitized genetic background, we found a differential failure pattern at the 4-cell stage (Verbrugghe and White, 2004). At this stage, the fate of each blastomere is already decided via conserved signaling molecules such as Notch and Wnt (Mickey et al., 1996; Rocheleau et al., 1997; Thorpe et al., 1997). We found that the P2 cell was always protected against cell division failure while the ABa cell nearly always failed to complete cytokinesis. The other cell-types, ABp and EMS showed a more intermediate failure pattern. Given the differences observed for ABa and ABp, sibling cells that are identical until a signal from P2 changes the fate of ABp, we hypothesized that cell fate may be a critical factor in cell division integrity. The P2 cell expresses Delta and Wnt, which specifies the ABp and a progeny of the EMS cell respectively. I investigated if Notch/Wnt signaling is able to shield the ABp/EMS cell from cytokinesis failure by making a double mutant strain of *spd-1(ts);glp-1(ts)* and *spd-1(ts);mom-2(ts).* While initially results were promising, we found too much variability with *spd-1(oj5)* making it an unreliable mutant to use as our sensitized background. Our

preliminary data suggests that loss of Delta or Notch signaling does not appear to affect the failure rate of the ABp cell.

Introduction

During cell division, the segregation of the chromosomes and specification of the division plane are coordinated by mitotic spindle microtubules. When the chromosomes begin to separate during anaphase, an antiparallel array of microtubules assembles between them at the division plane, called the central spindle. This assembly is dependent on the microtubule bundling protein SPD-1 (the *C. elegans* homolog of vertebrate PRC1, Fascetto in *Drosophila*), and depletion of this protein leads to cytokinesis failure in cultured mammalian and *Drosophila* cells (Jiang et al., 1998). In the small roundworm *Caenorhabditis elegans, spd-1* mutants also fail in cytokinesis, however not all divisions in the early embryo are equally affected. In fact, the first two rounds of cell division occur successfully, despite the absence of bundled central spindle microtubules (Verbrugghe and White, 2004).

While PRC1 is essential for cytokinesis in transformed mammalian cultured cells, SPD-1 (the *C. elegans* homolog) is necessary for integrity of the central spindle but not for cytokinesis success in early embryonic cell divisions. Rather, disrupting SPD-1 activity results in the failure of cytokinesis in specific cell lineages. *spd-1(oj5ts)* is a temperature sensitive maternal-effect mutation that results in embryonic lethality at the restrictive temperature (26°C) while at the permissive temperature (16°C) adults produce normal and viable young. In the absence of *spd-1* there is no detectable central spindle. When *spd-1* mutant embryos are filmed at the restrictive temperature during the four-to-eight-cell transition a differential failure pattern is observed (Verbrugghe and White, 2004).

At this four-to-eight-cell stage there is also a difference in signaling that occurs for the AB progeny due to the location of the cells, with ABa being the most anteriorly positioned cell (Figure 26). The fates of the blastomere sisters are conditional on their positions within the embryo. This is because the Delta/APX-1-expressing P2 cell signal specifically activates Notch/GLP-1 in the ABp cell due to the cell positioning of the early embryo (Priess and Thomson, 1987). Although both ABa and ABp have the Notch/GLP-1 receptor, physical contact is crucial because the P2 signal, Delta/APX-1, and the Notch/GLP-1 receptor is membrane bound. In experiments where the positions of ABa and ABp are switched, with ABa in direct contact with P2, the cell fates are likewise switched: ABa goes on to adopt the ABp fate while ABp adopts the fate of ABa; confirming immunofluorescence analysis which revealed that both sisters express Notch/GLP-1 and both could respond to Delta/APX-1 (Shelton and Bowerman, 1996).

During the four-cell stage, physical contact with P2 is also crucial for another blastomere: the EMS cell. When EMS is isolated from P2 there is no gut differentiation and this cannot be rescued when an experimentally isolated EMS is recombined with either ABp or ABa. EMS divides to form the MS and E daughter cells. In the absence of P2 contact, both cells will take on the MS-like fate (Goldstein, 1992). When P2 is experimentally moved to contact the other side of the EMS blastomere, gut differentiation occurs in the daughter closest to P2, suggesting all of EMS can respond to P2's signal. It has been shown that the signal on P2's membrane is the Wnt/MOM-2 ligand and the receptor on EMS is Frizzled/MOM-5 (Goldstein, 1992).

Although Wnts are secreted signaling morphogens, they are poorly mobile and often contact-dependent due to posttranslational modifications (Strand and Micchelli, 2011). Once

the Wnt/MOM-2 ligand binds to its receptor, Frizzled/MOM-5, the destruction complex (APC/APR-1 PRY-1/GSK-3) dissociates and β-catenin/WRM-1 is no longer degraded. Instead, it translocates into the nucleus of the posterior cell (that was polarized by P2) where it associates with the armadillo-repeat protein, SYS-1, to export TCF/POP-1 from the nucleus; thereby activating the expression of repressed genes. The polarization of EMS by P2 induces the endodermal fate along with rotating its mitotic spindle 90 degrees to lie along the A/P axis. Importantly, this orientation does not rely on gene transcription, implying Wnt signaling is directly involved in targeting the cytoskeleton (Goldstein, 1995; Schlesinger et al., 1999; Walston et al., 2004).

In *C. elegans* there are three β-catenin genes that fulfill separate functions in the Wnt pathway. In the EMS cell, the β-catenin used is β-catenin/WRM-1. Because this pathway is still reliant on WRM-1 as a central player, but not on BAR-1 (the mammalian β-catenin ortholog) it is considered a non-canonical variant. There is evidence for Wnt/MOM-2 pathway components contributing to functions outside cell fate such as mitotic spindle orientation and reorganization of the cytoskeleton. Wnt/MOM-2 pathway proteins are necessary for reorientation of the mitotic spindles depending on the cortical status of β-catenin/WRM-1 (Goldstein, 1995; Schlesinger et al., 1999; Walston et al., 2004). Similarly, Frizzled/MOM-5 and members of the destruction complex are involved in actin cytoskeletal rearrangements in the gonadal arms. WNT-7a, one of the 19 vertebrate members of the Wnt family, has been shown to participate in neuronal cytoskeleton regulation as it results in increased growth cone size and axonal branching (Hall, 2000; Lucas and Salinas, 1997; Salinas, 2007).

Here we examined the potential role cell fate determinants may play in the outcome of cytokinesis by creating double mutants to disrupt SPD-1 and/or Notch/GLP-1, Delta/APX-1,

Wnt/MOM-2 function. We found, as was shown previously, *spd-1* mutants result in a differential failure pattern, however we saw the majority of failure occur in the ABa cell-type and not EMS (Verbrugghe and White, 2004; Verbrugghe and White, 2007). Surprisingly, disruption of *spd-1(ts);glp-1(ts)* and *spd-1(ts);apx-1(ts)* did not enhance cytokinesis failure in the ABp progeny. Furthermore, while it seemed that the EMS blastomere displayed increased cell division failure upon double knockdown: *spd-1(ts);mom-2(ts),* we found too much variability in the *spd-1* mutant on its own, making interpretation of data difficult and unreliable.

Results

Loss of SPD-1 results in differential cytokinesis failure in the 4-cell embryo

Loss of SPD-1 disrupts the integrity of the central spindle, but only leads to cytokinesis failure in some of the cells. I have successfully replicated previous experiments that show the *spd-1* mutant strain results in differential failure of daughter cells in the 4-to-8 cell stage, with ABa failing ~100% of the time, ABp and EMS failing ~20% of the time, and the P2 cell never failing to divide (with substantial caveats, see more below). Of particular interest is the failure of ABa in light of the success of the ABp blastomere. Both are the products of a symmetric division from their AB mother cell and are initially equivalent (Figure 26) (Bowerman et al., 1992; Mango et al., 1994; Mickey et al., 1996; Moskowitz et al., 1994; Shelton and Bowerman, 1996). Why then, is one more susceptible to failure when the two cells are born identical from a symmetric cell division? One possible explanation for why two cells with equal potential express differential failure patterns is that one possesses a protective advantage based on inter-cellular signaling. In the ABp cell there is a well-

characterized Notch/GLP-1 - Delta/APX-1 signaling cascade that determines cell fate, which is absent in ABa (Priess and Thomson, 1987).

To test if Notch/GLP-1-Delta/APX-1 signaling shields ABp from the cytokinesis failure of the ABa cell, a colleague disrupted Delta/APX-1 activity in the *spd-1* background. He found Delta/APX-1 knockdown lead to a 5-fold increase in failure specifically in the ABp cell, thus I first set out to confirm this result with a *spd-1(ts);glp-1(ts)* mutant. We would expect if ABp is being protected by Delta/Notch signaling then disrupting this signal by using a double mutant of either *apx-1(ts)*; *spd-1(ts)* and/or either *glp-1(ts)*;*spd-1(ts)* should cause an increase in cytokinesis failure.

Unexpectedly, *spd-1(ts);glp-1(ts)* showed no increase in ABp failure and some suppression of failure in EMS. This suggests either that Delta/APX-1 works through a different Notch/GLP-1 receptor that is also present at the early four–cell embryo (though no other Notch is reported in the literature at this stage), that it may somehow function independently of Notch/GLP-1, or that something was wrong with the original data.

Due to the unexpected results from *spd-1(ts);glp-1(ts),* I refilmed *spd-1(ts);apx-1(ts)* to certify the ABp failure was still consistent. However, I was unable to replicate the 100% failure pattern for ABp following *spd-1(ts);apx-1(ts)* co-inactivation found by another lab member. Instead, my results recapitulated similar data to the *spd-1(ts)* phenotype alone with regular 100% failure in ABa, 32% failure in ABp, 21% failure in EMS and no failure for P2. This suggests ABp division is unlikely to be protected by Notch/GLP-1 and Delta/APX-1.

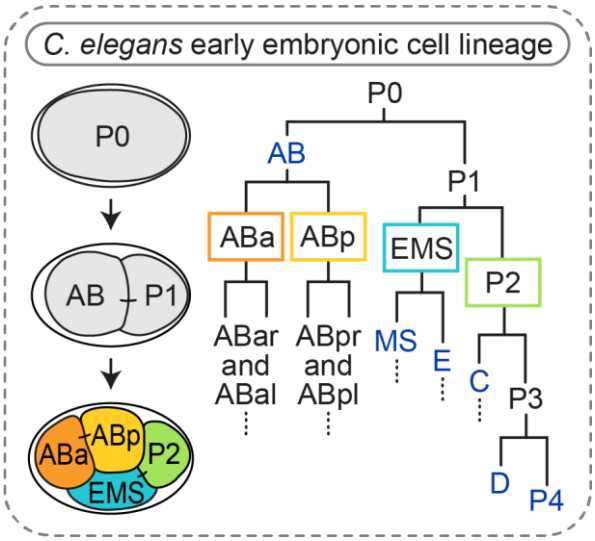

Figure 26: Embryonic lineage

Embryonic lineage map showing the identity and division patterning that occurs during the early blastomere divisions in *C. elegans* embryos. Founder cells AB, E, MS, C, D, and P4 are in dark blue.

EMS, like ABp, is also in direct contact with P2 suggesting the signal from the MOM-2 ligand of P2 to the Frizzled/MOM-5 receptor of EMS may be responsible for the low failure rate of this cell. *spd-1(ts);mom-2(RNAi)* mutants resulted in increased failure of the EMS daughter cell, with 52% unable to complete cytokinesis while the failure of the remaining blastomeres was unchanged (Table 1). *spd-1(ts);mom-2(ts)* mutants also showed increased failure of the EMS daughter cell, with 70% unable to complete division. In addition, an increased failure in ABp, that was not observed with RNAi depletion, was found in the double knockdown with over 1.5-fold increase (Table 1). As previously shown, only the P2 cell successfully divided each time. Because *spd-1(ts);mom-2(ts)* was shown to enhance EMS failure we hypothesized other components in the Wnt pathway may also play a reinforcing role in these cytokinetic events.

I tested if the known downstream targets of Wnt-mediated cell-fate specification contribute to the robustness of cytokinesis. To this end, I generated *spd-1(ts);wrm-1(ts)* double mutants. As it functions more downstream, if the *spd-1(ts);wrm-1(ts)* double mutant also shows more failure of EMS, it would suggest it plays an important role earlier in division. However, if EMS division failure remains unchanged it suggests only Wnt/MOM-2 and possibly Frizzled/MOM-5 are involved in generating stability for the EMS cell.

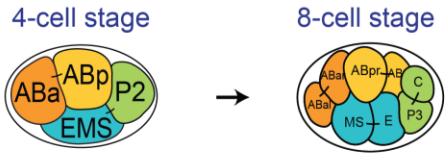

%of Failed Division

25.5°C±0.5°C

Strain	ABa	ABp	EMS	P2	N
spd-1(oj5ts); glp-1(ql273ts)	93	19	15	0	42
glp-1(ql273ts)	0	0	0	0	4
spd-1(oj5ts)	100	14	15	0	36
spd-1(oj5ts); apx-1(zu347ts)	100	32	21	0	19
apx-1(zu347ts)	0	0	0	0	20
control(RNAi)	0	0	0	0	4
spd-1(oj5ts); mom-2(ne2626ts)	95	54	70	0	80
mom-2(ne2626ts)	0	0	0	0	14
spd-1(oj5ts)	95	21	34	0	38
spd-1(oj5ts); control(RNAi)	100	18	18	0	17
spd-1(oj5ts); mom-2(RNAi)	100	13	57	0	23
spd-1(oj5ts); control(RNAi)	100	29	79	0	14
spd-1(oj5ts); wrm-1(RNAi)	88	59	59	0	17
spd-1(oj5ts); wrm-1(ne1982)	100	20	60	0	10
wrm-1(ne1982)	0	0	0	0	3
spd-1(oj5ts)	100	25	75	0	4

Table 1: Reported percentage cytokinesis failures corresponding to respective blastomeres in each condition.

Observed cytokinesis failure percentages for indicated strains. Same color coding in strains represents grouped experiments for the purposes of this study.

In *spd-1(ts);wrm-1(ts)* we observed 60 % of EMS blastomeres fail to divide. Here we also began to notice more failure in the *spd-1(ts)* alone. In *spd-1(ts);wrm-1(RNAi),* this issue became especially apparent with EMS cells failing 59% while *spd-1(ts)* EMS cells failed even more at 79%. Additionally, ABp failure increased to 59% in *spd-1(ts);wrm-1(RNAi)* compared to *spd-1(ts)* where it failed at its regular 20%. This increase of background EMS failure complicates the interpretation within this line of double mutants and brings to doubt any results gathered with the *spd-(ts)* used as the sensitized background.

spd-1(ts) mutant embryos exhibit inconsistent cytokinesis failure phenotypes

The increase in failure observed for ABp and EMS in *spd-1(ts)* were a cause for concern given that the enhancement of the double mutant is taken in context with the failure pattern in the single mutant, previously presumed to be stable and show reproducible cytokinesis success/failure rates for ABa, ABp, EMS, and P2. I therefore revisited all my previous data for this strain and found that on different days there were varying failures for the ABp and EMS cell types. To address this concern, we isolated 6 individual hermaphrodites and filmed their progeny. We observed inconsistent failure patterns in the different isolates (Figure 27). This suggests our *spd-1(ts)* may have some background mutation(s) interfering with cytokinesis and/or cell fate specification. However, the mutant was outcrossed 6x prior to imaging, so any mutation would likely be tightly linked, and thus I have dropped this project for the time being. In the future, I would like to test if *spd-1(RNAi)* or CRISPR *spd-1(ts)* has a differential effect on cytokinesis in individual cells within the 4-to-8 cell embryo to bypass this concern.

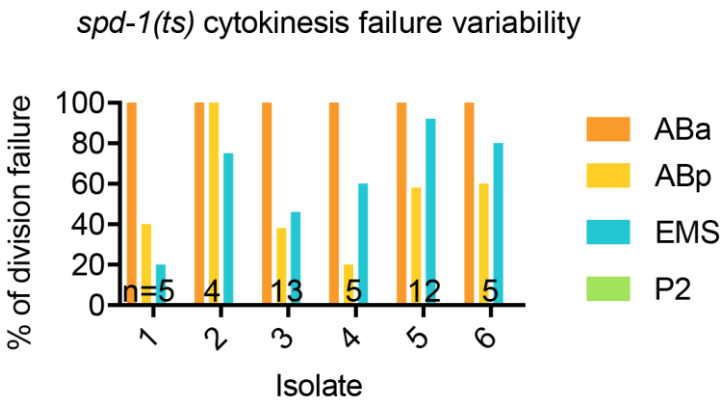

Figure 27: *spd-1(ts)* isolates exhibit variability in cytokinesis failure phenotypes

Percent of cytokinesis failure for indicated blastomeres in different isolates of *spd-1(ts)* strains.

Discussion

We found loss of NOTCH/GLP-1 and Delta/APX-1 in our *spd-1(ts)* background likely had no impact on the low failure rate of the ABp blastomere, suggesting the variation in cell division success is not due to P2 polarizing the cell using these signals. Unfortunately, my results here suggest that little can actually even be drawn from the data because of the isolate-specific variability in failure of the other cell types in the *spd-1(ts)* alone.

What about ABa makes it more likely to fail to divide and P2 more likely to complete cytokinesis?

Importantly, while patterns for EMS and ABp in *spd-1(ts)* are unpredictable, the extreme values (~100% failure for ABa and 0% failure for P2) remain consistent. It is to these that I would like to focus my attention, in particular to study what about P2 makes it so robust at cell division? With ABa and P2 there are differences in cell fate, cell size and even polarity. P2 is a germ line cell; it's the smallest cell in the embryo and prior to division is able to establish anterior and posterior polarity domains.

In contrast, what about the ABa cell makes it so sensitive to cell division? A crucial experiment would be to rescue ABa failure, where we consistently see ~100% failure in the *spd-1* background. One way to do this may be to remove the egg shell and experimentally move a P2 cell to contact the ABa cell verses the ABp cell and monitor the success or failure of cytokinesis. Assuming the manipulation is done successfully the switch should result in the ABa cell completing cytokinesis at its new contact with P2 while the ABp cell should fail to divide. Alternatively, an additional P2 cell from another embryo can be positioned by the ABa cell that still has its original contacts to see if here both ABa and ABp show lower cytokinesis

failure. This could help determine if perhaps it is signaling from P2 or something about the cell-cell junction that could be the protective force. Another point to consider regarding neighboring cells is how compression may factor into robustness of cytokinesis. For example, the ABp cell divides in between other cells, so perhaps squeezing or pressure from those cells effect the outcome of cytokinesis completion.

Investigation of these unequal division failures, depending on cell fate, may alter the current simple understanding that all cell division engages similar mechanisms. Ultimately, this research will inform personalized approaches to treating proliferative disorders, such as cancer, based on the context of Notch and Wnt signaling pathway activation.

Strain	Genotype
OD95	*unc-119(ed3)* ltIs38[pAA1; pie-1::eGFP::PH(PLC1delta1) unc-119(+)]III; ltIs37[pAA64; pie-1::mCherry::his-58 unc-119(+)]IV*
JCC242	*spd-1(oj5) I; unc-119(ed3) III?; ltIs38 [pAA1; pie-1/GFP::PH(PLC1delta1); unc-119 (+)] III; ltIs37 [pAA64; pie-1/mCHERRY::his-58; unc-119 (+)] IV*
JCC860	*unc-119(ed3)III?; jccSi1[Pmex-5::GFP-PH::tbb2 3'UTR] cb-unc-119(+)] II; ltIs37 [pAA64; pie-1/mCHERRY::his-58; unc-119 (+)] IV; mom-2(ne2626) V.*
JCC864	*spd-1(oj5) I; unc-119(ed3)III?; jccSi1[Pmex-5::GFP-PH::tbb2 3'UTR] cb-unc-119(+)] II; glp-1(q231ts)III;jccSi1[Pmex-5::GFP-PH::tbb2 3'UTR] cb-unc-119(+)] II; ltIs37 [pAA64; pie-1/mCHERRY::his-58; unc-119 (+)] IV; ltIs37 [pAA64; pie-1/mCHERRY::his-58; unc-119 (+)] IV.*
JCC618	*apx-1(zu347); V. [unc-119(ed3) III?; ltIs38 [pAA1; pie-1/GFP::PH(PLC1delta1); unc-119 (+)] III]; unc-119(ed3)III?; ltIs37 [pAA64; pie-1/mCHERRY::his-58; unc-119 (+)] IV*
JCC641	*spd-1(oj5) I. apx-1 (zu347) V. unc-119(ed3) III?; ltIs38 [pAA1; pie-1/GFP::PH(PLC1delta1); unc-119 (+)] III. unc-119(ed3) III?; ltIs37 [pAA64; pie-1/mCHERRY::his-58; unc-119 (+)] IV*
JCC865	*spd-1(oj5) I;unc-119(ed3)III?; jccSi1[Pmex-5::GFP-PH::tbb2 3'UTR] cb-unc-119(+)] II; ltIs37 [pAA64; pie-1/mCHERRY::his-58; unc-119 (+)] IV; mom-2(ne2626) V*
JCC893	*wrm-1(ne1982) III. ; unc-119 (+)] III; ltIs37 [pAA64; pie-1/mCHERRY::his-58; unc-119 (+)] IV; unc-119(ed3)III?; jccSi1[Pmex-5::GFP-PH::tbb2 3'UTR] cb-unc-119(+)] II; ltIs37 [pAA64; pie-1/mCHERRY::his-58; unc-119 (+)] IV.*
JCC907	*spd-1(oj5) I; jccSi1[Pmex-5::GFP-PH::tbb2 3'UTR] cb-unc-119(+)] II; wrm-1(ne1982) III. ; unc-119 (+)] III; ltIs37 [pAA64; pie-1/mCHERRY::his-58; unc-119 (+)] IV; unc-119(ed3)III?;*
JCC855	*glp-1(q231ts)III; jccSi1[Pmex-5::GFP-PH::tbb2 3'UTR] cb-unc-119(+)] II; ltIs37 [pAA64; pie-1/mCHERRY::his-58; unc-119 (+)] IV.*

*The *unc-119(ed3)* mutation was present in the parental strains but has not been directly sequenced in these strains to determine if the *unc-119* gene is mutated.

Table S 6: Strain names and genotype

Strain names and genotypes used in this study.

Plasmid	Gene(s)	Oligo 1 (5'-3')	Oligo 2 (5'-3')	Template	Cloning vector
pJC246	*wrm-1 (B0336.1)*	GCGCG**ACTAGT**T GATCAGTGAGAATGCCGAC	GCGCG**ACTAGT**TGTACCCGC ACAAAGATTCA	N2 cDNA	L4440 (empty vector)
pJC248	*mom-2 (F38E1.7)*	GCGCG**ACTAGT**GGACGTC GCCTTCTTGTTAAT	GCGCG**ACTAGT**TGCGACAGT GACAAGATCAA	N2 cDNA	L4440 (empty vector)

Table S 7: RNAi feeding constructs

Plasmid names, targeted genes for RNAi experiments, oligos used to generate RNAi feeding construct and DNA template used or Ahringer library (Kamath and Ahringer, 2003; Kamath et al., 2003) clone number, and cloning vectors used in this study.

Materials and Methods

Strain maintenance

Caenorhabditis elegans were kept on standard NGM plates seeded with OP50 *E. coli* bacteria, as described (Brenner, 1974).

Temperature control

All control and temperature-sensitive (ts) strains were raised in an incubator (Crittenden et al.) kept at permissive temperature (16 ± 0.5ºC) and all fast-acting ts strains were also dissected in cooled (~16ºC) M9 buffer (Brenner, 1974) until just before the 2-cell division.

Live-cell imaging was performed in a thermally-controlled room. Room temperature was monitored with two thermometers attached directly to the objective, and another thermometer attached to the stage via a glue gun to monitor the temperature of the specimen during filming. Wherever mentioned throughout this article, experimental temperatures were calculated by averaging the values from the two thermometers attached to the objective and were as follows: restrictive (26.0 ± 0.5ºC).

Live-cell imaging

Single-cell embryos were mounted on a 2% agar pad as described previously (Gonczy et al., 1999; Jordan et al., 2016). Imaging was performed on a Nikon Ti inverted microscope with 40x 1.3 N.A. and 60x 1.4 N.A. oil-immersion PlanApochromat objectives using a Yokagawa CSU-10 spinning disc confocal equipped with Borealis (Spectral Applied Research) and a Hamamatsu Orca ER camera. Z-sectioning was done with a Piezo-driven

motorized stage (Applied Scientific Instrumentation) and focus was maintained using Perfect Focus (Nikon) prior to each Z-series acquisition. Solid-state 150 mW lasers were used for excitation at 488 and 561 nm for eGFP and mCherry respectively (Spectral Applied Research), and a filter-wheel was used for emission wavelength selection (Sutter Instruments). The imaging system was controlled by Metamorph software (Molecular Devices).

Image analysis

Metamorph (Molecular Devices) and FIJI (ImageJ) software were used for all data analysis to view failure or completion of cytokinesis (Schindelin et al., 2012; Schindelin et al., 2015).

Feeding RNAi

All primers and DNA template used for RNAi experiments are listed in Table S5-6. The empty L4440 vector in HT115 cells was used as a control. RNAi feeding bacteria were inoculated in Luria Broth with 100 µg/mL ampicillin for either 7 hours at 37ºC or 16 hours at 32ºC. 300 µL of this culture was plated on RNAi plates (NGM agar plates (Brenner, 1974) supplemented with 50 µg/mL ampicillin and 1 mM IPTG). After drying, the plates were grown at 32ºC for 24-48 hours. L1 worms were transferred onto RNAi plates and then grown at 16ºC until young adulthood when they were dissected to obtain the embryos. RNAi knockdown for *mom-2* and *wrm-1* was confirmed by embryonic lethality.

Chapter 5. Discussion

None of this chapter has been previously published.

My contributions to Chapter 5

I, thanks to the mentorship and discussions with Julie Canman, Shawn Jordan and Tim Davies, came up with the future directions presented here.

Discussion

Orchestrating successful cell division involves the coordination of intricate and complex processes. Through my doctoral investigations, I probed the interactions and nuances at play during cell division. In Chapter 2, I contributed to work that found polarity proteins contribute to cytokinesis fidelity. In Chapter 3, I clarified and expanded on key genetic interactions that were contested in the literature. In Chapter 4, I began investigations into the differential regulation of cytokinesis in different cells. Here, I will discuss more in depth what I have learned through my graduate work and present potential future avenues of study that could be pursued.

CYK-4 GAP activity inhibits Rac to promote cytokinesis completion: understanding the GTPase milieu

In Chapter 3, I showed that CYK-4 specifically inhibits Rac activity as loss of Rac is able to suppress *cyk-4(ts)* cytokinesis failure, and also showed that Rac does not act as a global suppressor of cytokinesis. Additionally, I demonstrated that CYK-4 is unlikely to activate ECT-2 as there was no reduction in levels of downstream Rho effectors in *cyk-4(ts)* mutants. Furthermore, the ability to suppress cytokinesis failure due to loss of Rac appeared to be dependent on CDC-42 activity, though we later found even over-activating CDC-42 using a *chin-1(RNAi),* also did not suppress cell division failure in *cyk-4(ts);Rac(G60R)* mutants.

GTPases do not function in isolation but involve a lot of crosstalk with other GTPases, activators (GEFs), and inhibitors (GAPs). However, many of the biochemical approaches to study the specificity of CYK-4 and its GAP domain have not taken this into consideration when performing GTPase assays. While my paper attempts a genetic approach to settle the CYK-4 – Rac debate, a biochemical tactic is essential to answer the many remaining questions. Previous studies looked at CYK-4 and each GTPase alone but that is not enough to get a clear idea of how these proteins function. Conducting a GTP hydrolysis assay in which Rac, Cdc42, Rho, CYK-4, ZEN-4, and ECT-2 are screened against a panel of GAP domain proteins alone and also in duplicate, triplicate, etc. would help address the issue. This would illuminate how certain complexes affect GTPase regulation, if there is competition among certain GTPases that affects their function, and if certain proteins have more specificity for other proteins and how that is maintained/altered in the presence of different regulators.

Visually distinguishing between linear f-actin and branched f-actin

Our model, that CYK-4 specifically inhibits Rac activity, predicts that loss of CYK-4 should result in increased branched f-actin since Rac would no longer be inhibited (Figure 15D). Unfortunately, there is currently no probe that could distinguish between linear and branched f-actin. Even so, we do observe ARP2/3-dependent puncta of actin with our Utrophin::GFP strain. Either we could code a program or perform careful analysis by eye to determine if the number of puncta varies with loss or gain of Rac with or without CYK-4. In the literature, platinum replica EM has been shown to distinguish between branched and linear f-actin so perhaps this is another road worth pursuing (Korobova and Svitkina, 2010). I would expect that in the *cyk-4(ts)* condition there would be more branched f-actin than in the

control cells as Rac would be free to recruit the arp2/3 complex. When Rac is also inactivated in *cyk-4(ts);Rac(G60R)* mutant embryos, this ectopic branched f-actin would be lost.

For this model to be correct, the increase in f-actin likely acts to inhibit cytokinesis by two non-exclusive mechanisms, 1) by forming local actin structures that are refractory to cytokinesis, and 2) by competing for G-actin subunits which would reduce formation of productive linear f-actin filaments, especially at the contractile ring. To further test this model, it will be interested to look at Rac overexpression with and without CYK-4. I would expect that even with CYK-4, if Rac is overexpressed we may begin to see cytokinesis failure as the increase in Rac is available to drive ARP2/3 activation and formation of branched f-actin, which our model predicts inhibits cytokinesis.

Does CYK-4 have additional targets?

In addition to targeting Rac, previous work has suggested that CYK-4 may also act as GAP on other GTPases, including CDC-42 (Bastos et al., 2012; Jantsch-Plunger et al., 2000; Toure et al., 1998). However, in Chapter 3, I show that both knockdown and over-activation of CDC-42 resulted in enhanced cytokinesis failure of *cyk-4(ts);Rac(G60R*) double mutants. This suggests that any role of CYK-4 inactivated CDC-42 is too complex to be understood in this system with current available tools.

Since loss of ANI-1, Rac, and CDC-42 did not restore the rate of ingression in CYK-4 mutants the search for the other target(s) continues. SPD-1 mutants result in a chromosomes "flying" apart phenotype where chromosome separation is accelerated due to having no central spindle and thereby weaker resistance against pulling forces (Verbrugghe and White, 2007). Given this and previous studies that have shown PRC1/SPD-1 binds to CYK-4, I

wonder if *cyk-4(ts);spd-1(RNAi)* or *cyk-4(ts);spd-1(RNAi);Rac(G60R),* could possibly rescue the rate of ingression at least in the one-cell embryo where SPD-1 is not required for cytokinesis completion. If so, it would suggest that CYK-4 functions somewhat independently of the central spindle.

Does loss of Rac free up more Ect-2 to act on Rho?

In work shown above and in Zhuravlev et al, we found a statistically insignificant rescue of cytokinesis failure in *ect-2(lof);Rac(G60R).* Since Ect2 is able to act on all 3 GTPases (Rho, Rac, and Cdc42) perhaps loss of Rac frees up any remaining Ect2, thereby accounting for the slight rescue we see in Figure 18. To test this, we could look at the intensity of GFP::Utrophin^{ABD} and GFP::myosin-II^{NMY-2} at the ring, as was done for CYK-4, either using double mutants or the Ect2 mutant with Rac(RNAi). If loss of Rac does result in more Ect2 able to act on Rho then I would predict to see higher intensity levels of GFP::Utrophin^{ABD} and GFP::myosin-II^{NMY-2}in *ect-2(lof);Rac(RNAi)* after 12 hours at the restrictive temperature compared to an *ect-2(lof)* strain. To do this experiment I would first have to make sure that the intensity levels in the mutant strain are comparable to control marked strains left at the permissive temperature.

Cell fate-dependent protection against cytokinesis failure

Using other temperature sensitive mutants to explore differences in cytokinesis completion in later cell divisions.

At the end of Chapter 2 and in Chapter 4, I explore how different blastomeres vary in their cytokinesis outcomes and cytokinetic protein requirements. Although I found that using SPD-1 exhibited too much inconsistency to use as a sensitized background we could remake

the strain using CRISPR to get rid of the background mutation that was likely the cause of the variability. In accompaniment, we have other temperature sensitive mutants in the lab that also exhibit differential failure patterns that could be used to probe whether Notch and Wnt may be playing a protective role. Based on the upshifts in Chapter 2, the *formin(ts)* mutant background may be promising to pursue given the increased cytokinesis completion of the EMS blastomere versus AB progeny at the same temperature. The *formin(ts)* mutant has a point mutation in the FH2 domain, which prevents processive actin polymerization (Davies et al., 2014). Could depletion of Wnt and/or Frizzled in *formin(ts)* mutant embryos result in increased EMS failure? One easy method to test if EMS is being protected via signaling from the P2 cell is to remove the eggshell and isolate the blastomeres. In this context does EMS still complete cytokinesis in the same frequency as EMS in the intact embryo? If not, it suggests that in the EMS cell integrity of cytokinesis is maintained via extrinsic signaling, possibly through the Wnt/Frizzled pathway, which depends on cell-cell contact.

Why is the P2 blastomere so protected against cytokinesis failure?

It is of particular interest how robust the P2 cell appears, having consistently shown no failure in all of the *spd-1(ts)* mutants and also less failure in *formin-1(ts)* embryos. Why is P2 more resilient against cytokinesis perturbation? Because the P2 cell gives rise to the germline it may be under more selective pressure to adopt additional protective mechanisms to guard against cytokinesis failure. In such a case, germline specific factors such as P granules or CAR-1, may promote fidelity of cytokinesis. P2 is also the transmitter of two signals that break symmetry, the Delta/*apx-1* ligand and the Frizzled/*mom-5* receptor. A-P polarity may also somehow contribute to cytokinetic robustness given that both EMS and P2 divide

asymmetrically unlike ABa and ABp. Unfortunately, studying the effect of polarity on cytokinesis in a multicellular context is fraught with difficulty as no fast acting temperature sensitive polarity mutants are available, and using RNAi would globally disrupt the polarity and asymmetric cell division, voiding cell identities.

Conclusions

"Be fruitful and multiply," is apt to describe cytokinesis. Utilizing varied and often redundant mechanisms, cells have stacked the odds in their favor to ensure the completion of their division. Through crosstalk, functional redundancies, and overall complexity the integrity of this process is maintained. Through my PhD, I have contributed to research where polarity impacts cytokinesis outcomes, explored novel cytokinetic mechanisms such as cell fate, and added support for the argument that CYK-4 directly inhibits Rac activity. It is an exciting time in science for cytokinesis, as improved imaging and technology can answer long-standing questions in the field and application of this research for clinical therapies is ripe with opportunity.

Reference List

1 Aceto, D., M. Beers, and K.J. Kemphues. 2006. Interaction of Par-6 with Cdc-42 Is Required for Maintenance but Not Establishment of Par Asymmetry in C. Elegans. *Dev Biol*. 299:386-397.

2 Adam J. C., P.J.R., Peifer M. E. 2000. Evidence for Functional Differentiation among Drosophila Septins in Cytokinesis and Cellularization. *Molecular Biology of the Cell*. 11:3123-3125.

3 Adams, R.R., A.A. Tavares, A. Salzberg, H.J. Bellen, and D.M. Glover. 1998. Pavarotti Encodes a Kinesin-Like Protein Required to Organize the Central Spindle and Contractile Ring for Cytokinesis. *Genes Dev*. 12:1483-1494.

4 Agromayor, M., and J. Martin-Serrano. 2013. Knowing When to Cut and Run: Mechanisms That Control Cytokinetic Abscission. *Trends Cell Biol*. 23:433-441.

5 Aitken, A., H. Baxter, T. Dubois, S. Clokie, S. Mackie, K. Mitchell, A. Peden, and E. Zemlickova. 2002. Specificity of 14-3-3 Isoform Dimer Interactions and Phosphorylation. *Biochem Soc Trans*. 30:351-360.

6 Alberts, A.S. 2001. Identification of a Carboxyl-Terminal Diaphanous-Related Formin Homology Protein Autoregulatory Domain. *J Biol Chem*. 276:2824-2830.

7 Alessi, D.R., K. Sakamoto, and J.R. Bayascas. 2006. Lkb1-Dependent Signaling Pathways. *Annu Rev Biochem*. 75:137-163.

8 Alsop, G.B., and D. Zhang. 2003. Microtubules Are the Only Structural Constituent of the Spindle Apparatus Required for Induction of Cell Cleavage. *J Cell Biol*. 162:383-390.

9 Andrews, P.D., Y. Ovechkina, N. Morrice, M. Wagenbach, K. Duncan, L. Wordeman, and J.R. Swedlow. 2004. Aurora B Regulates Mcak at the Mitotic Centromere. *Dev Cell*. 6:253-268.

10 Arata, Y., J.Y. Lee, B. Goldstein, and H. Sawa. 2010. Extracellular Control of Par Protein Localization During Asymmetric Cell Division in the C. Elegans Embryo. *Development*. 137:3337-3345.

11 Aristizabal-Corrales, D., S. Schwartz, Jr., and J. Ceron. 2013. Par-5 Is a Party Hub in the Germline: Multitask Proteins in Development and Disease. *Worm*. 2:e21834.

12 Artavanis-Tsakonas, S., M.D. Rand, and R.J. Lake. 1999. Notch Signaling: Cell Fate Control and Signal Integration in Development. *Science*. 284:770-776.

13 Audhya, A., A. Desai, and K. Oegema. 2007. A Role for Rab5 in Structuring the Endoplasmic Reticulum. *J Cell Biol*. 178:43-56.

14 Audhya, A., F. Hyndman, I.X. McLeod, A.S. Maddox, J.R. Yates, 3rd, A. Desai, and K. Oegema. 2005. A Complex Containing the Sm Protein Car-1 and the Rna Helicase Cgh-1 Is Required for Embryonic Cytokinesis in Caenorhabditis Elegans. *J Cell Biol*. 171:267-279.

15 Balasubramanian, M.K., E. Bi, and M. Glotzer. 2004. Comparative Analysis of Cytokinesis in Budding Yeast, Fission Yeast and Animal Cells. *Curr Biol*. 14:R806-818.

16 Ban, R., Y. Irino, K. Fukami, and H. Tanaka. 2004. Human Mitotic Spindle-Associated Protein Prc1 Inhibits Mgcracgap Activity toward Cdc42 During the Metaphase. *J Biol Chem*. 279:16394-16402.

17 Barr, F.A., and U. Gruneberg. 2007. Cytokinesis: Placing and Making the Final Cut. *Cell*. 131:847-860.

18 Baruni, J.K., E.M. Munro, and G. von Dassow. 2008. Cytokinetic Furrowing in Toroidal, Binucleate and Anucleate Cells in C. Elegans Embryos. *J Cell Sci*. 121:306-316.

19 Basant, A., S. Lekomtsev, Y.C. Tse, D. Zhang, K.M. Longhini, M. Petronczki, and M. Glotzer. 2015. Aurora B Kinase Promotes Cytokinesis by Inducing Centralspindlin Oligomers That Associate with the Plasma Membrane. *Dev Cell*. 33:204-215.

20 Bassi ZI, V.K., Capalbo L, Gregory S, Montembault E, Glover DM, D'Avino PP. 2011. Sticky/Citron Kinase Maintains Proper Rhoa Localization at the Cleavage Site During Cytokinesis. *Cell Biology*. 195:595-603.

21 Basto, R., J. Lau, T. Vinogradova, A. Gardiol, C.G. Woods, A. Khodjakov, and J.W. Raff. 2006. Flies without Centrioles. *Cell*. 125:1375-1386.

22 Bastos, R.N., and F.A. Barr. 2010. Plk1 Negatively Regulates Cep55 Recruitment to the Midbody to Ensure Orderly Abscission. *J Cell Biol*. 191:751-760.

23 Bastos, R.N., X. Penate, M. Bates, D. Hammond, and F.A. Barr. 2012. Cyk4 Inhibits Rac1-Dependent Pak1 and Arhgef7 Effector Pathways During Cytokinesis. *J Cell Biol*. 198:865-880.

24 Beach, J.R., and T.T. Egelhoff. 2009. Myosin Ii Recruitment During Cytokinesis Independent of Centralspindlin-Mediated Phosphorylation. *J Biol Chem*. 284:27377-27383.

25 Beatty, A., D. Morton, and K. Kemphues. 2010. The C. Elegans Homolog of Drosophila Lethal Giant Larvae Functions Redundantly with Par-2 to Maintain Polarity in the Early Embryo. *Development*. 137:3995-4004.

26 Beatty, A., D.G. Morton, and K. Kemphues. 2013. Par-2, Lgl-1 and the Cdc-42 Gap Chin-1 Act in Distinct Pathways to Maintain Polarity in the C. Elegans Embryo. *Development*. 140:2005-2014.

27 Bell, L.G.E. 1962. Some Mechanisms Involved in Cell Division. *Nature*. 193:190-191.

28 Bement, W.M., H.A. Benink, and G. von Dassow. 2005. A Microtubule-Dependent Zone of Active Rhoa During Cleavage Plane Specification. *J Cell Biol*. 170:91-101.

29 Bengur, A.R., E.A. Robinson, E. Appella, and J.R. Sellers. 1987. Sequence of the Sites Phosphorylated by Protein Kinase C in the Smooth Muscle Myosin Light Chain. *J Biol Chem*. 262:7613-7617.

30 Benkemoun, L., C. Descoteaux, N.T. Chartier, L. Pintard, and J.C. Labbe. 2014. Par-4/Lkb1 Regulates DNA Replication During Asynchronous Division of the Early C. Elegans Embryo. *J Cell Biol*. 205:447-455.

31 Bi, E., P. Maddox, D.J. Lew, E.D. Salmon, J.N. McMillan, E. Yeh, and J.R. Pringle. 1998. Involvement of an Actomyosin Contractile Ring in Saccharomyces Cerevisiae Cytokinesis. *J Cell Biol*. 142:1301-1312.

32 Bielak-Zmijewska, A., A. Kolano, K. Szczepanska, M. Maleszewski, and E. Borsuk. 2008. Cdc42 Protein Acts Upstream of Iqgap1 and Regulates Cytokinesis in Mouse Oocytes and Embryos. *Dev Biol*. 322:21-32.

33 Biesterfeld, S., K. Gerres, G. Fischer-Wein, and A. Bocking. 1994. Polyploidy in Non-Neoplastic Tissues. *J Clin Pathol*. 47:38-42.

34 Birkenfeld, J., P. Nalbant, B.P. Bohl, O. Pertz, K.M. Hahn, and G.M. Bokoch. 2007. Gef-H1 Modulates Localized Rhoa Activation During Cytokinesis under the Control of Mitotic Kinases. *Dev Cell*. 12:699-712.

35 Bos, J.L., H. Rehmann, and A. Wittinghofer. 2007. Gefs and Gaps: Critical Elements in the Control of Small G Proteins. *Cell*. 129:865-877.

36 Bossinger, O., and C.R. Cowan. 2012. Methods in Cell Biology: Analysis of Cell Polarity in C. Elegans Embryos. *Methods Cell Biol*. 107:207-238.

37 Boulter, E., R. Garcia-Mata, C. Guilluy, A. Dubash, G. Rossi, P.J. Brennwald, and K. Burridge. 2010. Regulation of Rho Gtpase Crosstalk, Degradation and Activity by Rhogdi1. *Nat Cell Biol*. 12:477-483.

38 Bowerman, B., F.E. Tax, J.H. Thomas, and J.R. Priess. 1992. Cell Interactions Involved in Development of the Bilaterally Symmetrical Intestinal Valve Cells During Embryogenesis in Caenorhabditis Elegans. *Development*. 116:1113-1122.

39 Boyd, L., S. Guo, D. Levitan, D.T. Stinchcomb, and K.J. Kemphues. 1996. Par-2 Is Asymmetrically Distributed and Promotes Association of P Granules and Par-1 with the Cortex in C. Elegans Embryos. *Development*. 122:3075-3084.

40 Boyd, L., Guo, S. , Levitan, D. , Stinchcomb, D. T. & Kemphues, K. J. 1996. Par-2 Is Asymmetrically Distributed and Promotes Association of P Granules and Par-1 with the Cortex in C. Elegans Embryos. *Development*. 122:3075-3084.

41 Brenner, S. 1974. The Genetics of Caenorhabditis Elegans. *Genetics*. 77:71-94.

42 Bridges, A.A., and A.S. Gladfelter. 2015. Septin Form and Function at the Cell Cortex. *J Biol Chem*. 290:17173-17180.

43 Bringmann, H., and A.A. Hyman. 2005. A Cytokinesis Furrow Is Positioned by Two Consecutive Signals. *Nature*. 436:731-734.

44 Budirahardja, Y., and P. Gonczy. 2008. Plk-1 Asymmetry Contributes to Asynchronous Cell Division of C. Elegans Embryos. *Development*. 135:1303-1313.

45 Burkard, M.E., J. Maciejowski, V. Rodriguez-Bravo, M. Repka, D.M. Lowery, K.R. Clauser, C. Zhang, K.M. Shokat, S.A. Carr, M.B. Yaffe, and P.V. Jallepalli. 2009. Plk1 Self-Organization and Priming Phosphorylation of Hscyk-4 at the Spindle Midzone Regulate the Onset of Division in Human Cells. *PLoS Biol*. 7:e1000111.

46 Burkard, M.E., C.L. Randall, S. Larochelle, C. Zhang, K.M. Shokat, R.P. Fisher, and P.V. Jallepalli. 2007. Chemical Genetics Reveals the Requirement for Polo-Like Kinase 1 Activity in Positioning Rhoa and Triggering Cytokinesis in Human Cells. *Proc Natl Acad Sci U S A*. 104:4383-4388.

47 Burkel, B.M., G. von Dassow, and W.M. Bement. 2007. Versatile Fluorescent Probes for Actin Filaments Based on the Actin-Binding Domain of Utrophin. *Cell Motil Cytoskeleton*. 64:822-832.

48 Buttery, S.M., K. Kono, E. Stokasimov, and D. Pellman. 2012. Regulation of the Formin Bnr1 by Septins Anda Mark/Par1-Family Septin-Associated Kinase. *Mol Biol Cell*. 23:4041-4053.

49 Cabello, J., J. Samann, E. Gomez-Orte, T. Erazo, A. Coppa, A. Pujol, I. Bussing, B. Schulze, J.M. Lizcano, I. Ferrer, R. Baumeister, and E. Dalfo. 2014. Pdr-1/Hparkin Negatively Regulates the Phagocytosis of Apoptotic Cell Corpses in Caenorhabditis Elegans. *Cell Death Dis*. 5:e1120.

50 Cabernard, C., K.E. Prehoda, and C.Q. Doe. 2010. A Spindle-Independent Cleavage Furrow Positioning Pathway. *Nature*. 467:91-94.

51 Calvert, M.E., G.D. Wright, F.Y. Leong, K.H. Chiam, Y. Chen, G. Jedd, and M.K. Balasubramanian. 2011. Myosin Concentration Underlies Cell Size-Dependent Scalability of Actomyosin Ring Constriction. *J Cell Biol*. 195:799-813.

52 Canman, J.C., L.A. Cameron, P.S. Maddox, A. Straight, J.S. Tirnauer, T.J. Mitchison, G. Fang, T.M. Kapoor, and E.D. Salmon. 2003. Determining the Position of the Cell Division Plane. *Nature*. 424:1074-1078.

53 Canman, J.C., D.B. Hoffman, and E.D. Salmon. 2000. The Role of Pre- and Post-Anaphase Microtubules in the Cytokinesis Phase of the Cell Cycle. *Curr Biol*. 10:611-614.

54 Canman, J.C., L. Lewellyn, K. Laband, S.J. Smerdon, A. Desai, B. Bowerman, and K. Oegema. 2008. Inhibition of Rac by the Gap Activity of Centralspindlin Is Essential for Cytokinesis. *Science*. 322:1543-1546.

55 Cannet, A., S. Schmidt, B. Delaval, and A. Debant. 2014. Identification of a Mitotic Rac-Gef, Trio, That Counteracts Mgcracgap Function During Cytokinesis. *Mol Biol Cell*. 25:4063-4071.

56 Cao, L.G., and Y.L. Wang. 1996. Signals from the Spindle Midzone Are Required for the Stimulation of Cytokinesis in Cultured Epithelial Cells. *Mol Biol Cell*. 7:225-232.

57 Carlton, J.G., Martin-Serrano, J. 2007. Parallels between Cytokinesis and Retroviral Budding: A Role for the Escrt Machinery. *Science*:1908-1912.

58 Carlton, J.G.C., A. Caballe, M. Agromayor, M. Kloc, J. Martin-Serrano. 2012. Escrt-Iii Governs the Aurora B-Mediated Abscission Checkpoint through Chmp4c. *Science*. 336:220-225.

59 Carvalho, A., A. Desai, and K. Oegema. 2009. Structural Memory in the Contractile Ring Makes the Duration of Cytokinesis Independent of Cell Size. *Cell*. 137:926-937.

60 Castagnetti, S., S. Oliferenko, and P. Nurse. 2010. Fission Yeast Cells Undergo Nuclear Division in the Absence of Spindle Microtubules. *PLoS Biol*. 8:e1000512.

61 Castrillon, D.H., and S.A. Wasserman. 1994. Diaphanous Is Required for Cytokinesis in Drosophila and Shares Domains of Similarity with the Products of the Limb Deformity Gene. *Development*. 120:3367-3377.

62 Castrillon DH, W.S. 1994. Diaphanous Is Required for Cytokinesis in Drosophila and Shares Domains of Similarity with the Products of the Limb Deformity Gene. *Development*. 120:3367-3377.

63 Celton-Morizur, S., G. Merlen, D. Couton, G. Margall-Ducos, and C. Desdouets. 2009. The Insulin/Akt Pathway Controls a Specific Cell Division Program That Leads to Generation of Binucleated Tetraploid Liver Cells in Rodents. *Journal of Clinical Investigation*. 119:1880-1887.

64 Chan, E., and J. Nance. 2013. Mechanisms of Cdc-42 Activation During Contact-Induced Cell Polarization. *J Cell Sci*. 126:1692-1702.

65 Chang, F., A. Woollard, and P. Nurse. 1996. Isolation and Characterization of Fission Yeast Mutants Defective in the Assembly and Placement of the Contractile Actin Ring. *J Cell Sci*. 109 (Pt 1):131-142.

66 Chant, J. 1996. Generation of Cell Polarity in Yeast. *Current Opinion in Cell Biology*. 8:557-565.

67 Chartier, N.T., D.P. Salazar Ospina, L. Benkemoun, M. Mayer, S.W. Grill, A.S. Maddox, and J.C. Labbe. 2011. Par-4/Lkb1 Mobilizes Nonmuscle Myosin through Anillin to Regulate C. Elegans Embryonic Polarization and Cytokinesis. *Curr Biol*. 21:259-269.

68 Cheeks, R.J., J.C. Canman, W.N. Gabriel, N. Meyer, S. Strome, and B. Goldstein. 2004. C. Elegans Par Proteins Function by Mobilizing and Stabilizing Asymmetrically Localized Protein Complexes. *Curr Biol*. 14:851-862.

69 Choudhary, A., R.F. Lera, M.L. Martowicz, K. Oxendine, J.J. Laffin, B.A. Weaver, and M.E. Burkard. 2013. Interphase Cytofission Maintains Genomic Integrity of Human Cells after Failed Cytokinesis. *Proc Natl Acad Sci U S A*. 110:13026-13031.

70 Coumailleau, F., M. Furthauer, J.A. Knoblich, and M. Gonzalez-Gaitan. 2009. Directional Delta and Notch Trafficking in Sara Endosomes During Asymmetric Cell Division. *Nature*. 458:1051-1055.

71 Cristiana Mollinari, J.-P.K., Wei Jiang, Guy Schoehn, Tony Hunter, and Robert L. Margolis. 2002. Prc1 Is a Microtubule Binding and Bundling Protein Essential to Maintain the Mitotic Spindle Midzone. *Journal of Cell Biology*. 157:1175-1186.

72 Crittenden, S.L., D. Rudel, J. Binder, T.C. Evans, and J. Kimble. 1997. Genes Required for Glp-1 Asymmetry in the Early Caenorhabditis Elegans Embryo. *Dev Biol*. 181:36-46.

73 Cuenca, A.A., A. Schetter, D. Aceto, K. Kemphues, and G. Seydoux. 2003. Polarization of the C. Elegans Zygote Proceeds Via Distinct Establishment and Maintenance Phases. *Development*. 130:1255-1265.

74 Cunto, F.D., S. Imarisio, P. Camera, C. Boitani, F. Altruda, and L. Silengo. 2002. Essential Role of Citron Kinase in Cytokinesis of Spermatogenic Precursors. *J Cell Sci*. 115:4819-4826.

75 D'Avino, P.P., M.G. Giansanti, and M. Petronczki. 2015. Cytokinesis in Animal Cells. *Cold Spring Harb Perspect Biol*. 7:a015834.

76 D'Avino, P.P., M.S. Savoian, and D.M. Glover. 2004. Mutations in Sticky Lead to Defective Organization of the Contractile Ring During Cytokinesis and Are Enhanced by Rho and Suppressed by Rac. *J Cell Biol*. 166:61-71.

77 D'Avino, P.P., T. Takeda, L. Capalbo, W. Zhang, K.S. Lilley, E.D. Laue, and D.M. Glover. 2008. Interaction between Anillin and Racgap50c Connects the Actomyosin Contractile Ring with Spindle Microtubules at the Cell Division Site. *J Cell Sci*. 121:1151-1158.

78 Daniels, B.R., T.M. Dobrowsky, E.M. Perkins, S.X. Sun, and D. Wirtz. 2010. Mex-5 Enrichment in the C. Elegans Early Embryo Mediated by Differential Diffusion. *Development*. 137:2579-2585.

79 Davies, T., S.N. Jordan, V. Chand, J.A. Sees, K. Laband, A.X. Carvalho, M. Shirasu-Hiza, D.R. Kovar, J. Dumont, and J.C. Canman. 2014. High-Resolution Temporal Analysis Reveals a Functional Timeline for the Molecular Regulation of Cytokinesis. *Dev Cell*. 30:209-223.

80 Davies, T., N. Kodera, G.S. Kaminski Schierle, E. Rees, M. Erdelyi, C.F. Kaminski, T. Ando, and M. Mishima. 2015. Cyk4 Promotes Antiparallel Microtubule Bundling by Optimizing Mklp1 Neck Conformation. *PLoS Biol*. 13:e1002121.

81 Davoli, T., and T. de Lange. 2011. The Causes and Consequences of Polyploidy in Normal Development and Cancer. *Annu Rev Cell Dev Biol*. 27:585-610.

82 De Lozanne, A., and J.A. Spudich. 1987. Disruption of the Dictyostelium Myosin Heavy Chain Gene by Homologous Recombination. *Science*. 236:1086-1091.

83 Dean, S.O., S.L. Rogers, N. Stuurman, R.D. Vale, and J.A. Spudich. 2005. Distinct Pathways Control Recruitment and Maintenance of Myosin Ii at the Cleavage Furrow During Cytokinesis. *Proc Natl Acad Sci U S A*. 102:13473-13478.

84 Dechant, R., and M. Glotzer. 2003. Centrosome Separation and Central Spindle Assembly Act in Redundant Pathways That Regulate Microtubule Density and Trigger Cleavage Furrow Formation. *Dev Cell*. 4:333-344.

85 Desai, A., H.W. Deacon, C.E. Walczak, and T.J. Mitchison. 1997. A Method That Allows the Assembly of Kinetochore Components onto Chromosomes Condensed in Clarified Xenopus Egg Extracts. *Proc Natl Acad Sci U S A*. 94:12378-12383.

86 Devore, J.J., G.W. Conrad, and R. Rappaport. 1989. A Model for Astral Stimulation of Cytokinesis in Animal Cells. *J Cell Biol*. 109:2225-2232.

87 Didsbury, J., R.F. Weber, G.M. Bokoch, T. Evans, and R. Snyderman. 1989. Rac, a Novel Ras-Related Family of Proteins That Are Botulinum Toxin Substrates. *J Biol Chem*. 264:16378-16382.

88 Dorn, J.F., L. Zhang, V. Paradis, D. Edoh-Bedi, S. Jusu, P.S. Maddox, and A.S. Maddox. 2010. Actomyosin Tube Formation in Polar Body Cytokinesis Requires Anillin in C. Elegans. *Curr Biol*. 20:2046-2051.

89 Douglas, M.E., T. Davies, N. Joseph, and M. Mishima. 2010. Aurora B and 14-3-3 Coordinately Regulate Clustering of Centralspindlin During Cytokinesis. *Curr Biol*. 20:927-933.

90 Drechsel, D.N., A.A. Hyman, A. Hall, and M. Glotzer. 1997. A Requirement for Rho and Cdc42 During Cytokinesis in Xenopus Embryos. *Curr Biol*. 7:12-23.

91 Dutartre, H., J. Davoust, J.P. Gorvel, and P. Chavrier. 1996. Cytokinesis Arrest and Redistribution of Actin-Cytoskeleton Regulatory Components in Cells Expressing the Rho Gtpase Cdc42hs. *J Cell Sci*. 109 (Pt 2):367-377.

92 Echard, A., G.R. Hickson, E. Foley, and P.H. O'Farrell. 2004. Terminal Cytokinesis Events Uncovered after an Rnai Screen. *Curr Biol*. 14:1685-1693.

93 Echard, A., and P.H. O'Farrell. 2003. The Degradation of Two Mitotic Cyclins Contributes to the Timing of Cytokinesis. *Curr Biol*. 13:373-383.

94 El Amine, N., A. Kechad, S. Jananji, and G.R. Hickson. 2013. Opposing Actions of Septins and Sticky on Anillin Promote the Transition from Contractile to Midbody Ring. *J Cell Biol*. 203:487-504.

95 Ellen L. Batchelder, C.L.T.V., Jeffery D. Hardin, and John G. White. 2007. Cytokinesis Is Not Controlled by Calmodulin or Myosin Light Chain Kinase in the Caenorhabditis Elegans Early Embryo. *FEBS Lett*. 22:4337-4341.

96 Etienne-Manneville, S., and A. Hall. 2002. Rho Gtpases in Cell Biology. *Nature*. 420:629-635.

97 Euteneuer, U., and J.R. McIntosh. 1980. Polarity of Midbody and Phragmoplast Microtubules. *J Cell Biol*. 87:509-515.

98 Evans, T.C., S.L. Crittenden, V. Kodoyianni, and J. Kimble. 1994. Translational Control of Maternal Glp-1 Mrna Establishes an Asymmetry in the C. Elegans Embryo. *Cell*. 77:183-194.

99 Fabbro, M., B.B. Zhou, M. Takahashi, B. Sarcevic, P. Lal, M.E. Graham, B.G. Gabrielli, P.J. Robinson, E.A. Nigg, Y. Ono, and K.K. Khanna. 2005. Cdk1/Erk2- and Plk1-Dependent Phosphorylation of a Centrosome Protein, Cep55, Is Required for Its Recruitment to Midbody and Cytokinesis. *Dev Cell*. 9:477-488.

100 Fang, X., J. Luo, R. Nishihama, C. Wloka, C. Dravis, M. Travaglia, M. Iwase, E.A. Vallen, and E. Bi. 2010. Biphasic Targeting and Cleavage Furrow Ingression Directed by the Tail of a Myosin Ii. *J Cell Biol*. 191:1333-1350.

101 Fares, H., M. Peifer, and J.R. Pringle. 1995. Localization and Possible Functions of Drosophila Septins. *Mol Biol Cell*. 6:1843-1859.

102 Fededa, J.P., and D.W. Gerlich. 2012. Molecular Control of Animal Cell Cytokinesis. *Nat Cell Biol*. 14:440-447.

103 Ferrari-Toninelli, G., S.A. Bonini, P. Bettinsoli, D. Uberti, and M. Memo. 2008. Microtubule Stabilizing Effect of Notch Activation in Primary Cortical Neurons. *Neuroscience*. 154:946-952.

104 Field, C., A.S. Maddox, J.R. Pringle, and K. Oegema. 2008. Septins in the Metazoan Model Systems *Drosophila Melanogaster* and *Caenorhabditis Elegans*. *The Septins*:147-168.

105 Field, C.M., M. Coughlin, S. Doberstein, T. Marty, and W. Sullivan. 2005. Characterization of Anillin Mutants Reveals Essential Roles in Septin Localization and Plasma Membrane Integrity. *Development*. 132:2849-2860.

106 Fievet, B.T., J. Rodriguez, S. Naganathan, C. Lee, E. Zeiser, T. Ishidate, M. Shirayama, S. Grill, and J. Ahringer. 2013. Systematic Genetic Interaction Screens

Uncover Cell Polarity Regulators and Functional Redundancy. *Nat Cell Biol*. 15:103-112.

107 Foe, V.E., and G. von Dassow. 2008. Stable and Dynamic Microtubules Coordinately Shape the Myosin Activation Zone During Cytokinetic Furrow Formation. *J Cell Biol*. 183:457-470.

108 Fujikawa K, I.Y., Sakai M, Koyama Y, Nishi S, Funada R, Alt FW, Swat W. 2002. Vav3 Is Regulated During the Cell Cycle and Effects Cell Division. *Proc Natl Acad Sci USA*. 99:4313-4318.

109 Fujiwara, T., M. Bandi, M. Nitta, E.V. Ivanova, R.T. Bronson, and D. Pellman. 2005. Cytokinesis Failure Generating Tetraploids Promotes Tumorigenesis in P53-Null Cells. *Nature*. 437:1043-1047.

110 Fumihiko Niiya, X.X., Kyung S. Lee, Hiroki Inoue and Toru Miki. 2005. Inhibition of Cyclin-Dependent Kinase 1 Induces Cytokinesis without Chromosome Segregation in an Ect2 and Mgcracgap-Dependent Manner. *Journal of Biological Chemistry*. 280:36502-36509.

111 Fumoto, K., K. Kikuchi, H. Gon, and A. Kikuchi. 2012. Wnt5a Signaling Controls Cytokinesis by Correctly Positioning Escrt-Iii at the Midbody. *Journal of Cell Science*. 125:4822-4832.

112 Ganem, N.J., Z. Storchova, and D. Pellman. 2007. Tetraploidy, Aneuploidy and Cancer. *Curr Opin Genet Dev*. 17:157-162.

113 Garcia-Mata, R., E. Boulter, and K. Burridge. 2011. The 'Invisible Hand': Regulation of Rho Gtpases by Rhogdis. *Nat Rev Mol Cell Biol*. 12:493-504.

114 George von Dassow, K.J.C.V., Ann L. Miller, Jenny R. Sider, William M. Bement. 2009. Action at a Distance During Cytokinesis. *JCB*. 187.

115 Gilliane Maton, F.E., Benjamin Lacroix, Marine Stefanutti, Kimberley Laband, Tiffany Lieury, Taekyung Kim, Julien Espeut, Julie C. Canman, Julien Dumont. 2015. Kinetochore Components Are Required for Central Spindle Assembly. *Nature Cell Biology*. 17:697-705.

116 Glotzer, M. 2005. The Molecular Requirements for Cytokinesis. *Science*. 307:1735-1739.

117 Glotzer, M. 2009. The 3ms of Central Spindle Assembly: Microtubules, Motors and Maps. *Nat Rev Mol Cell Biol*. 10:9-20.

118 Goldstein, A.Y., Y.N. Jan, and L. Luo. 2005. Function and Regulation of Tumbleweed (Racgap50c) in Neuroblast Proliferation and Neuronal Morphogenesis. *Proc Natl Acad Sci U S A*. 102:3834-3839.

119 Goldstein, B. 1992. Induction of Gut in Caenorhabditis Elegans Embryos. *Nature*. 357:255-257.

120 Goldstein, B. 1995. Cell Contacts Orient Some Cell Division Axes in the Caenorhabditis Elegans Embryo. *Journal of Cell Biology*. 129:1071-1080.

121 Goldstein, B., and S.N. Hird. 1996. Specification of the Anteroposterior Axis in Caenorhabditis Elegans. *Development*. 122:1467-1474.

122 Goldstein, B., and I.G. Macara. 2007. The Par Proteins: Fundamental Players in Animal Cell Polarization. *Dev Cell*. 13:609-622.

123 Gonczy, P., C. Echeverri, K. Oegema, A. Coulson, S.J. Jones, R.R. Copley, J. Duperon, J. Oegema, M. Brehm, E. Cassin, E. Hannak, M. Kirkham, S. Pichler, K. Flohrs, A. Goessen, S. Leidel, A.M. Alleaume, C. Martin, N. Ozlu, P. Bork, and A.A. Hyman. 2000. Functional Genomic Analysis of Cell Division in C. Elegans Using Rnai of Genes on Chromosome Iii. *Nature*. 408:331-336.

124 Gonczy, P., and A.A. Hyman. 1996. Cortical Domains and the Mechanisms of Asymmetric Cell Division. *Trends Cell Biol*. 6:382-387.

125 Gonczy, P., H. Schnabel, T. Kaletta, A.D. Amores, T. Hyman, and R. Schnabel. 1999. Dissection of Cell Division Processes in the One Cell Stage Caenorhabditis Elegans Embryo by Mutational Analysis. *J Cell Biol*. 144:927-946.

126 Goto, H., Y. Yasui, A. Kawajiri, E.A. Nigg, Y. Terada, M. Tatsuka, K. Nagata, and M. Inagaki. 2003. Aurora-B Regulates the Cleavage Furrow-Specific Vimentin Phosphorylation in the Cytokinetic Process. *J Biol Chem*. 278:8526-8530.

127 Gotta, M., M.C. Abraham, and J. Ahringer. 2001. Cdc-42 Controls Early Cell Polarity and Spindle Orientation in C. Elegans. *Curr Biol*. 11:482-488.

128 Green, R.A., H.L. Kao, A. Audhya, S. Arur, J.R. Mayers, H.N. Fridolfsson, M. Schulman, S. Schloissnig, S. Niessen, K. Laband, S. Wang, D.A. Starr, A.A. Hyman, T. Schedl, A. Desai, F. Piano, K.C. Gunsalus, and K. Oegema. 2011. A High-Resolution C. Elegans Essential Gene Network Based on Phenotypic Profiling of a Complex Tissue. *Cell*. 145:470-482.

129 Green, R.A., J.R. Mayers, S. Wang, L. Lewellyn, A. Desai, A. Audhya, and K. Oegema. 2013. The Midbody Ring Scaffolds the Abscission Machinery in the Absence of Midbody Microtubules. *J Cell Biol*. 203:505-520.

130 Green, R.A., E. Paluch, and K. Oegema. 2012. Cytokinesis in Animal Cells. *Annu Rev Cell Dev Biol*. 28:29-58.

131 Gregory, S.L., S. Ebrahimi, J. Milverton, W.M. Jones, A. Bejsovec, and R. Saint. 2008. Cell Division Requires a Direct Link between Microtubule-Bound Racgap and Anillin in the Contractile Ring. *Curr Biol*. 18:25-29.

132 Gremer, L., T. Merbitz-Zahradnik, R. Dvorsky, I.C. Cirstea, C.P. Kratz, M. Zenker, A. Wittinghofer, and M.R. Ahmadian. 2011. Germline Kras Mutations Cause Aberrant Biochemical and Physical Properties Leading to Developmental Disorders. *Hum Mutat*. 32:33-43.

133 Grill, S.W., P. Gonczy, E.H. Stelzer, and A.A. Hyman. 2001. Polarity Controls Forces Governing Asymmetric Spindle Positioning in the Caenorhabditis Elegans Embryo. *Nature*. 409:630-633.

134 Guidotti, J.E., O. Bregerie, A. Robert, P. Debey, C. Brechot, and C. Desdouets. 2003. Liver Cell Polyploidization: A Pivotal Role for Binuclear Hepatocytes. *J Biol Chem*. 278:19095-19101.

135 Guizetti, J., L. Schermelleh, J. Mantler, S. Maar, I. Poser, H. Leonhardt, T. Muller-Reichert, and D.W. Gerlich. 2011. Cortical Constriction During Abscission Involves Helices of Escrt-Iii-Dependent Filaments. *Science*. 331:1616-1620.

136 Gunsalus, K.C., S. Bonaccorsi, E. Williams, F. Verni, M. Gatti, and M.L. Goldberg. 1995. Mutations in Twinstar, a Drosophila Gene Encoding a Cofilin/Adf Homologue,

Result in Defects in Centrosome Migration and Cytokinesis. *J Cell Biol*. 131:1243-1259.

137 Guo, S., and K.J. Kemphues. 1995. Par-1, a Gene Required for Establishing Polarity in C. Elegans Embryos, Encodes a Putative Ser/Thr Kinase That Is Asymmetrically Distributed. *Cell*. 81:611-620.

138 Guo, S., and K.J. Kemphues. 1996. A Non-Muscle Myosin Required for Embryonic Polarity in Caenorhabditis Elegans. *Nature*. 382:455-458.

139 Guse, A., M. Mishima, and M. Glotzer. 2005. Phosphorylation of Zen-4/Mklp1 by Aurora B Regulates Completion of Cytokinesis. *Curr Biol*. 15:778-786.

140 Haarer, B.K., and J.R. Pringle. 1987. Immunofluorescence Localization of the Saccharomyces Cerevisiae Cdc12 Gene Product to the Vicinity of the 10-Nm Filaments in the Mother-Bud Neck. *Mol Cell Biol*. 7:3678-3687.

141 Halaoui, R., and L. McCaffrey. 2015. Rewiring Cell Polarity Signaling in Cancer. *Oncogene*. 34:939-950.

142 Hall, A. 2012. Rho Family Gtpases. *Biochem Soc Trans*. 40:1378-1382.

143 Hall, A.C., et al. 2000. Axonal Remodeling and Synaptic Differentiation in the Cerebellum Is Regulated by Wnt-7a Signaling. . *Cell*. 100:525-535.

144 Hamaguchi, Y. 1975. Microinjection of Colchicine into Sea-Urchin Eggs. *Development Growth & Differentiation*. 17:111-117.

145 Hehnly, H., and S. Doxsey. 2012. Polarity Sets the Stage for Cytokinesis. *Mol Biol Cell*. 23:7-11.

146 Heimpel, H., V. Anselstetter, L. Chrobak, J. Denecke, B. Einsiedler, K. Gallmeier, A. Griesshammer, T. Marquardt, G. Janka-Schaub, M. Kron, and E. Kohne. 2003. Congenital Dyserythropoietic Anemia Type Ii: Epidemiology, Clinical Appearance, and Prognosis Based on Long-Term Observation. *Blood*. 102:4576-4581.

147 Henson, J.H., C.E. Ditzler, A. Germain, P.M. Irwin, E.T. Vogt, S. Yang, X. Wu, and C.B. Shuster. 2017. The Ultrastructural Organization of Actin and Myosin Ii Filaments

in the Contractile Ring: New Support for an Old Model of Cytokinesis. *Mol Biol Cell*. 28:613-623.

148 Herszterg, S., Leibfried, A., Bosveld, F., Martin, C. & Bellaiche, Y. . 2013. Interplay between the Dividing Cell and Its Neighbors Regulates Adherens Junction Formation During Cytokinesis in Epithelial Tissue. *Dev Cell*. 24:256-270.

149 Higgs, H.N., and K.J. Peterson. 2005. Phylogenetic Analysis of the Formin Homology 2 Domain. *Mol Biol Cell*. 16:1-13.

150 Hiramoto, Y. 1956. Cell Division without Mitotic Apparatus in Sea Urchin Eggs. *Experimental Cell Research*:630-636.

151 Hiramoto, Y. 1970. Rheological Properties of Sea Urchin Eggs. *Biorheology*. 6:201-234.

152 Hird, S.N., and J.G. White. 1993. Cortical and Cytoplasmic Flow Polarity in Early Embryonic Cells of Caenorhabditis Elegans. *J Cell Biol*. 121:1343-1355.

153 Hirose, K., T. Kawashima, I. Iwamoto, T. Nosaka, and T. Kitamura. 2001. Mgcracgap Is Involved in Cytokinesis through Associating with Mitotic Spindle and Midbody. *J Biol Chem*. 276:5821-5828.

154 Hixon, M.L., C. Obejero-Paz, C. Muro-Cacho, M.W. Wagner, E. Millie, J. Nagy, T.J. Hassold, and A. Gualberto. 2000. Cks1 Mediates Vascular Smooth Muscle Cell Polyploidization. *J Biol Chem*. 275:40434-40442.

155 Hoege, C., and A.A. Hyman. 2013. Principles of Par Polarity in Caenorhabditis Elegans Embryos. *Nat Rev Mol Cell Biol*. 14:315-322.

156 Hoege, C.e.a. 2010. Lgl Can Partition the Cortex of One-Cell Caenorhabditis Elegans Embryos into Two Domains. *Curr. Biol.* 20:1296-1303.

157 Honda, R., R. Korner, and E.A. Nigg. 2003. Exploring the Functional Interactions between Aurora B, Incenp, and Survivin in Mitosis. *Molecular Biology of the Cell*. 14:3325-3341.

158 Iolascon, A., H. Heimpel, A. Wahlin, and H. Tamary. 2013. Congenital Dyserythropoietic Anemias: Molecular Insights and Diagnostic Approach. *Blood*. 122:2162-2166.

159 Jantsch-Plunger, V., P. Gonczy, A. Romano, H. Schnabel, D. Hamill, R. Schnabel, A.A. Hyman, and M. Glotzer. 2000. Cyk-4: A Rho Family Gtpase Activating Protein (Gap) Required for Central Spindle Formation and Cytokinesis. *J Cell Biol*. 149:1391-1404.

160 Jenkins, N., J.R. Saam, and S.E. Mango. 2006. Cyk-4/Gap Provides a Localized Cue to Initiate Anteroposterior Polarity Upon Fertilization. *Science*. 313:1298-1301.

161 Jiang, W., G. Jimenez, N.J. Wells, T.J. Hope, G.M. Wahl, T. Hunter, and R. Fukunaga. 1998. Prc1: A Human Mitotic Spindle-Associated Cdk Substrate Protein Required for Cytokinesis. *Mol Cell*. 2:877-885.

162 Johnson, D.I., and J.R. Pringle. 1990. Molecular Characterization of Cdc42, a Saccharomyces Cerevisiae Gene Involved in the Development of Cell Polarity. *J Cell Biol*. 111:143-152.

163 Jones WM, C.A., Zavortink M, Saint R, Bejsovec A. 2010. Cytokinesis Proteins Tum and Pav Have a Nuclear Role in Wnt Regulation. *Journal of Cell Science*. 123:2179-2189.

164 Jordan, S.N., and J.C. Canman. 2012. Rho Gtpases in Animal Cell Cytokinesis: An Occupation by the One Percent. *Cytoskeleton (Hoboken)*. 69:919-930.

165 Jordan, S.N., T. Davies, Y. Zhuravlev, J. Dumont, M. Shirasu-Hiza, and J.C. Canman. 2016. Cortical Par Polarity Proteins Promote Robust Cytokinesis During Asymmetric Cell Division. *J Cell Biol*. 212:39-49.

166 Jurgens, G. 2005. Cytokinesis in Higher Plants. *Annu Rev Plant Biol*. 56:281-299.

167 Kamath, R.S., and J. Ahringer. 2003. Genome-Wide Rnai Screening in Caenorhabditis Elegans. *Methods*. 30:313-321.

168 Kamath, R.S., A.G. Fraser, Y. Dong, G. Poulin, R. Durbin, M. Gotta, A. Kanapin, N. Le Bot, S. Moreno, M. Sohrmann, D.P. Welchman, P. Zipperlen, and J. Ahringer.

2003. Systematic Functional Analysis of the Caenorhabditis Elegans Genome Using Rnai. *Nature*. 421:231-237.

169 Kamijo, K., N. Ohara, M. Abe, T. Uchimura, H. Hosoya, J.S. Lee, and T. Miki. 2006. Dissecting the Role of Rho-Mediated Signaling in Contractile Ring Formation. *Mol Biol Cell*. 17:43-55.

170 Karess, R.E., X.J. Chang, K.A. Edwards, S. Kulkarni, I. Aguilera, and D.P. Kiehart. 1991. The Regulatory Light Chain of Nonmuscle Myosin Is Encoded by Spaghetti-Squash, a Gene Required for Cytokinesis in Drosophila. *Cell*. 65:1177-1189.

171 Kawamura, K. 1960. Studies on Cytokinesis in Neuroblasts of the Grasshopper, Chortophaga Viridifasciata (De Geer). I. Formation and Behavior of the Mitotic Apparatus. *Exp Cell Res*. 21:1-18.

172 Kawamura, K. 1977. Microdissection Studies on the Dividing Neuroblast of the Grasshopper, with Special Refernece to the Mechanism of Unequal Cytokinesis. *Experimental Cell Research*. 106:127-137

.

173 Kay, A.J., and C.P. Hunter. 2001. Cdc-42 Regulates Par Protein Localization and Function to Control Cellular and Embryonic Polarity in C. Elegans. *Curr Biol*. 11:474-481.

174 Kemphues, K.J., J.R. Priess, D.G. Morton, and N.S. Cheng. 1988. Identification of Genes Required for Cytoplasmic Localization in Early C. Elegans Embryos. *Cell*. 52:311-320.

175 Khodjakov, A., Cole RW., Oakley BR., Rieder CL. 2000. Centrosome-Independent Mitotic Spindle Formation in Vertebrates. *Curr Biol*. 10:59-67.

176 Kiehart, D.P., I. Mabuchi, and S. Inoue. 1982. Evidence That Myosin Does Not Contribute to Force Production in Chromosome Movement. *J Cell Biol*. 94:165-178.

177 Kim, H., F. Guo, S. Brahma, Y. Xing, and M.E. Burkard. 2014. Centralspindlin Assembly and 2 Phosphorylations on Mgcracgap by Polo-Like Kinase 1 Initiate Ect2 Binding in Early Cytokinesis. *Cell Cycle*. 13:2952-2961.

178 Kimura, K., T. Tsuji, Y. Takada, T. Miki, and S. Narumiya. 2000. Accumulation of Gtp-Bound Rhoa During Cytokinesis and a Critical Role of Ect2 in This Accumulation. *J Biol Chem*. 275:17233-17236.

179 Kinoshita, M. 2003. Assembly of Mammalian Septins. *J Biochem*. 134:491-496.

180 Kinoshita, M., S. Kumar, A. Mizoguchi, C. Ide, A. Kinoshita, T. Haraguchi, Y. Hiraoka, and M. Noda. 1997. Nedd5, a Mammalian Septin, Is a Novel Cytoskeletal Component Interacting with Actin-Based Structures. *Genes Dev*. 11:1535-1547.

181 Kinsella, B.T., R.A. Erdman, and W.A. Maltese. 1991. Carboxyl-Terminal Isoprenylation of Ras-Related Gtp-Binding Proteins Encoded by Rac1, Rac2, and Rala. *J Biol Chem*. 266:9786-9794.

182 Kirby, C., M. Kusch, and K. Kemphues. 1990. Mutations in the Par Genes of Caenorhabditis Elegans Affect Cytoplasmic Reorganization During the First Cell Cycle. *Dev Biol*. 142:203-215.

183 Kishi, K., T. Sasaki, S. Kuroda, T. Itoh, and Y. Takai. 1993. Regulation of Cytoplasmic Division of Xenopus Embryo by Rho P21 and Its Inhibitory Gdp/Gtp Exchange Protein (Rho Gdi). *J Cell Biol*. 120:1187-1195.

184 Knecht, D.A., and W.F. Loomis. 1987. Antisense Rna Inactivation of Myosin Heavy Chain Gene Expression in Dictyostelium Discoideum. *Science*. 236:1081-1086.

185 Konig, J., E.B. Frankel, A. Audhya, and T. Muller-Reichert. 2017. Membrane Remodeling During Embryonic Abscission in Caenorhabditis Elegans. *J Cell Biol*. 216:1277-1286.

186 Korobova, F., and T. Svitkina. 2010. Molecular Architecture of Synaptic Actin Cytoskeleton in Hippocampal Neurons Reveals a Mechanism of Dendritic Spine Morphogenesis. *Mol Biol Cell*. 21:165-176.

187 Korswagen, H.C. 2002. Canonical and Non-Canonical Wnt Signaling Pathways in Caenorhabditis Elegans: Variations on a Common Signaling Theme. *Bioessays*. 24:801-810.

188 Kosako, H., T. Yoshida, F. Matsumura, T. Ishizaki, S. Narumiya, and M. Inagaki. 2000. Rho-Kinase/Rock Is Involved in Cytokinesis through the Phosphorylation of

Myosin Light Chain and Not Ezrin/Radixin/Moesin Proteins at the Cleavage Furrow. *Oncogene*. 19:6059-6064.

189 Kudryavtsev, B.N., M.V. Kudryavtseva, G.A. Sakuta, and G.I. Stein. 1993. Human Hepatocyte Polyploidization Kinetics in the Course of Life Cycle. *Virchows Arch B Cell Pathol Incl Mol Pathol*. 64:387-393.

190 Kumfer, K.T., S.J. Cook, J.M. Squirrell, K.W. Eliceiri, N. Peel, K.F. O'Connell, and J.G. White. 2010. Cgef-1 and Chin-1 Regulate Cdc-42 Activity During Asymmetric Division in the Caenorhabditis Elegans Embryo. *Mol Biol Cell*. 21:266-277.

191 Kurasawa, Y., W.C. Earnshaw, Y. Mochizuki, N. Dohmae, and K. Todokoro. 2004. Essential Roles of Kif4 and Its Binding Partner Prc1 in Organized Central Spindle Midzone Formation. *EMBO J*. 23:3237-3248.

192 Kwan, K.M., and M.W. Kirschner. 2005. A Microtubule-Binding Rho-Gef Controls Cell Morphology During Convergent Extension of Xenopus Laevis. *Development*. 132:4599-4610.

193 Lacroix, B., and A.S. Maddox. 2012. Cytokinesis, Ploidy and Aneuploidy. *J Pathol*. 226:338-351.

194 Lan, W., X. Zhang, S.L. Kline-Smith, S.E. Rosasco, G.A. Barrett-Wilt, J. Shabanowitz, D.F. Hunt, C.E. Walczak, and P.T. Stukenberg. 2004. Aurora B Phosphorylates Centromeric Mcak and Regulates Its Localization and Microtubule Depolymerization Activity. *Curr Biol*. 14:273-286.

195 Lee, H.H., N. Elia, R. Ghirlando, J. Lippincott-Schwartz, and J.H. Hurley. 2008. Midbody Targeting of the Escrt Machinery by a Noncanonical Coiled Coil in Cep55. *Science*. 322:576-580.

196 Lekomtsev, S., K.C. Su, V.E. Pye, K. Blight, S. Sundaramoorthy, T. Takaki, L.M. Collinson, P. Cherepanov, N. Divecha, and M. Petronczki. 2012. Centralspindlin Links the Mitotic Spindle to the Plasma Membrane During Cytokinesis. *Nature*. 492:276-279.

197 Lewellyn, L., A. Carvalho, A. Desai, A.S. Maddox, and K. Oegema. 2011. The Chromosomal Passenger Complex and Centralspindlin Independently Contribute to Contractile Ring Assembly. *J Cell Biol*. 193:155-169.

198 Lewellyn, L., J. Dumont, A. Desai, and K. Oegema. 2010. Analyzing the Effects of Delaying Aster Separation on Furrow Formation During Cytokinesis in the Caenorhabditis Elegans Embryo. *Mol Biol Cell*. 21:50-62.

199 Liljeholm, M., A.F. Irvine, A.L. Vikberg, A. Norberg, S. Month, H. Sandstrom, A. Wahlin, M. Mishima, and I. Golovleva. 2013. Congenital Dyserythropoietic Anemia Type Iii (Cda Iii) Is Caused by a Mutation in Kinesin Family Member, Kif23. *Blood*. 121:4791-4799.

200 Lippincott, J., and R. Li. 1998. Sequential Assembly of Myosin Ii, an Iqgap-Like Protein, and Filamentous Actin to a Ring Structure Involved in Budding Yeast Cytokinesis. *J Cell Biol*. 140:355-366.

201 Liu, J., L.L. Maduzia, M. Shirayama, and C.C. Mello. 2010. Nmy-2 Maintains Cellular Asymmetry and Cell Boundaries, and Promotes a Src-Dependent Asymmetric Cell Division. *Dev Biol*. 339:366-373.

202 Longtine, M.S., D.J. DeMarini, M.L. Valencik, O.S. Al-Awar, H. Fares, C. De Virgilio, and J.R. Pringle. 1996. The Septins: Roles in Cytokinesis and Other Processes. *Curr Opin Cell Biol*. 8:106-119.

203 Loria, A., K.M. Longhini, and M. Glotzer. 2012. The Rhogap Domain of Cyk-4 Has an Essential Role in Rhoa Activation. *Curr Biol*. 22:213-219.

204 Lucas, F.R., and P.C. Salinas. 1997. Wnt-7a Induces Axonal Remodeling and Increases Synapsin I Levels in Cerebellar Neurons. *Dev Biol*. 192:31-44.

205 Ma, C., H.A. Benink, D. Cheng, V. Montplaisir, L. Wang, Y. Xi, P.P. Zheng, W.M. Bement, and X.J. Liu. 2006. Cdc42 Activation Couples Spindle Positioning to First Polar Body Formation in Oocyte Maturation. *Curr Biol*. 16:214-220.

206 Mabuchi, I. 1994. Cleavage Furrow: Timing of Emergence of Contractile Ring Actin Filaments and Establishment of the Contractile Ring by Filament Bundling in Sea Urchin Eggs. *J Cell Sci*. 107 (Pt 7):1853-1862.

207 Mabuchi I, H.Y., Fujimoto H, Morii N, Mishima M, Narumiya S. . 1993. A Rho-Like Protein Is Involved in the Organisation of the Contractile Ring in Dividing Sand Dollar Eggs. *Zygote*. 1:325- 331.

208 Mabuchi, I., and M. Okuno. 1977. The Effect of Myosin Antibody on the Division of Starfish Blastomeres. *J Cell Biol*. 74:251-263.

209 Mabuchi, K.N.a.I. 2006. Actin-Depolymerizing Protein Adf1 Is Required for Formation and Maintenance of the Contractile Ring During Cytokinesis in Fission Yeast. *MBoC*. 17:1933-1945.

210 Macara, I.G. 2004. Par Proteins: Partners in Polarization. *Curr Biol*. 14:R160-162.

211 MacDonald, B.T., K. Tamai, and X. He. 2009. Wnt/Beta-Catenin Signaling: Components, Mechanisms, and Diseases. *Dev Cell*. 17:9-26.

212 Machacek, M., L. Hodgson, C. Welch, H. Elliott, O. Pertz, P. Nalbant, A. Abell, G.L. Johnson, K.M. Hahn, and G. Danuser. 2009. Coordination of Rho Gtpase Activities During Cell Protrusion. *Nature*. 461:99-103.

213 Maddox, A.S., J. Azoury, and J. Dumont. 2012. Polar Body Cytokinesis. *Cytoskeleton (Hoboken)*. 69:855-868.

214 Maddox, A.S., B. Habermann, A. Desai, and K. Oegema. 2005. Distinct Roles for Two C. Elegans Anillins in the Gonad and Early Embryo. *Development*. 132:2837-2848.

215 Maddox, A.S., L. Lewellyn, A. Desai, and K. Oegema. 2007. Anillin and the Septins Promote Asymmetric Ingression of the Cytokinetic Furrow. *Dev Cell*. 12:827-835.

216 Mahlert, M., L. Leveleki, A. Hlubek, B. Sandrock, and M. Bolker. 2006. Rac1 and Cdc42 Regulate Hyphal Growth and Cytokinesis in the Dimorphic Fungus Ustilago Maydis. *Mol Microbiol*. 59:567-578.

217 Mango, S.E., C.J. Thorpe, P.R. Martin, S.H. Chamberlain, and B. Bowerman. 1994. Two Maternal Genes, Apx-1 and Pie-1, Are Required to Distinguish the Fates of Equivalent Blastomeres in the Early Caenorhabditis Elegans Embryo. *Development*. 120:2305-2315.

218 Manoj B. Menon, M.G. 2015. Sep(T)Arate or Not – How Some Cells Take Septin-Independent Routes through Cytokinesis. *J Cell Sci*. 128:1877-1886.

219 Mao, Y., and S.C. Finnemann. 2015. Regulation of Phagocytosis by Rho Gtpases. *Small GTPases*. 6:89-99.

220 Margall-Ducos, G., S. Celton-Morizur, D. Couton, O. Bregerie, and C. Desdouets. 2007. Liver Tetraploidization Is Controlled by a New Process of Incomplete Cytokinesis. *J Cell Sci*. 120:3633-3639.

221 Mastronarde, D.N., K.L. McDonald, R. Ding, and J.R. McIntosh. 1993. Interpolar Spindle Microtubules in Ptk Cells. *J Cell Biol*. 123:1475-1489.

222 Matsumura, F. 2005. Regulation of Myosin Ii During Cytokinesis in Higher Eukaryotes. *Trends Cell Biol*. 15:371-377.

223 Matthews, H.K., U. Delabre, J.L. Rohn, J. Guck, P. Kunda, and B. Baum. 2012. Changes in Ect2 Localization Couple Actomyosin-Dependent Cell Shape Changes to Mitotic Progression. *Dev Cell*. 23:371-383.

224 Maupin, P., and T.D. Pollard. 1986. Arrangement of Actin Filaments and Myosin-Like Filaments in the Contractile Ring and of Actin-Like Filaments in the Mitotic Spindle of Dividing Hela Cells. *J Ultrastruct Mol Struct Res*. 94:92-103.

225 Megraw TL, K.L., Kaufman TC. 2001. Zygotic Development without Functional Mitotic Centrosomes. *Current Biology*. 11:116-120.

226 Menon, M.B., and M. Gaestel. 2015. Sep(T)Arate or Not - How Some Cells Take Septin-Independent Routes through Cytokinesis. *J Cell Sci*. 128:1877-1886.

227 Mickey, K.M., C.C. Mello, M.K. Montgomery, A. Fire, and J.R. Priess. 1996. An Inductive Interaction in 4-Cell Stage C. Elegans Embryos Involves Apx-1 Expression in the Signalling Cell. *Development*. 122:1791-1798.

228 Miller, A.L., and W.M. Bement. 2009. Regulation of Cytokinesis by Rho Gtpase Flux. *Nat Cell Biol*. 11:71-77.

229 Mishima, M., S. Kaitna, and M. Glotzer. 2002. Central Spindle Assembly and Cytokinesis Require a Kinesin-Like Protein/Rhogap Complex with Microtubule Bundling Activity. *Dev Cell*. 2:41-54.

230 Mishima, M., Kaitna S, Glotzer M. 2002. Demonstration That Cyk-4 and Mklp1 Form an Evolutionarily Conserved Complex Required for Central Spindle Assembly. *Dev Cell*. 2:41-54.

231 Mishima, M., V. Pavicic, U. Gruneberg, E.A. Nigg, and M. Glotzer. 2004. Cell Cycle Regulation of Central Spindle Assembly. *Nature*. 430:908-913.

232 Mitchison, T., and M. Kirschner. 1984. Dynamic Instability of Microtubule Growth. *Nature*. 312:237-242.

233 Mohammad M. Rahman, M.M., Kiyomi Kaneshiro, Brandon Lee, Susan Strome, Thomas Müller-Reichert, and Orna Cohen-Fixa. 2015. Caenorhabditis Elegans Polo-Like Kinase Plk-1 Is Required for Merging Parental Genomes into a Single Nucleus. *Molecular Biology of the Cell*. 26:4718-4735.

234 Monique van der Voet, M.A.L., Dayalan G. Srinivasan, Karen L. Bennett, and Sander van den Heuvel. 2009. C. Elegans Mitotic Cyclins Have Distinct as Well as Overlapping Functions in Chromosome Segregation. *Cell Cycle*. 24:4091-4102.

235 Morita, E., V. Sandrin, H.Y. Chung, S.G. Morham, S.P. Gygi, C.K. Rodesch, and W.I. Sundquist. 2007. Human Escrt and Alix Proteins Interact with Proteins of the Midbody and Function in Cytokinesis. *EMBO J*. 26:4215-4227.

236 Morton, D.G., D.C. Shakes, S. Nugent, D. Dichoso, W. Wang, A. Golden, and K.J. Kemphues. 2002. The Caenorhabditis Elegans Par-5 Gene Encodes a 14-3-3 Protein Required for Cellular Asymmetry in the Early Embryo. *Dev Biol*. 241:47-58.

237 Moskowitz, I.P., S.B. Gendreau, and J.H. Rothman. 1994. Combinatorial Specification of Blastomere Identity by Glp-1-Dependent Cellular Interactions in the Nematode Caenorhabditis Elegans. *Development*. 120:3325-3338.

238 Motegi, F., and G. Seydoux. 2013. The Par Network: Redundancy and Robustness in a Symmetry-Breaking System. *Philos Trans R Soc Lond B Biol Sci*. 368:20130010.

239 Motegi, F., and A. Sugimoto. 2006. Sequential Functioning of the Ect-2 Rhogef, Rho-1 and Cdc-42 Establishes Cell Polarity in Caenorhabditis Elegans Embryos. *Nat Cell Biol*. 8:978-985.

240 Motegi, F., S. Zonies, Y. Hao, A.A. Cuenca, E. Griffin, and G. Seydoux. 2011. Microtubules Induce Self-Organization of Polarized Par Domains in Caenorhabditis Elegans Zygotes. *Nat Cell Biol*. 13:1361-1367.

241 Moulding, D.A., M.P. Blundell, D.G. Spiller, M.R. White, G.O. Cory, Y. Calle, H. Kempski, J. Sinclair, P.J. Ancliff, C. Kinnon, G.E. Jones, and A.J. Thrasher. 2007. Unregulated Actin Polymerization by Wasp Causes Defects of Mitosis and Cytokinesis in X-Linked Neutropenia. *J Exp Med*. 204:2213-2224.

242 Moy, C., C.A. Oleykowski, R. Plant, J. Greshock, J.P. Jing, K. Bachman, M.A. Hardwicke, R. Wooster, and Y. Degenhardt. 2011. High Chromosome Number in Hematological Cancer Cell Lines Is a Negative Predictor of Response to the Inhibition of Aurora B and C by Gsk1070916. *Journal of Translational Medicine*. 9.

243 Munro, E., and B. Bowerman. 2009. Cellular Symmetry Breaking During Caenorhabditis Elegans Development. *Cold Spring Harb Perspect Biol*. 1:a003400.

244 Munro, E., J. Nance, and J.R. Priess. 2004. Cortical Flows Powered by Asymmetrical Contraction Transport Par Proteins to Establish and Maintain Anterior-Posterior Polarity in the Early C. Elegans Embryo. *Dev Cell*. 7:413-424.

245 Murata, T., T. Sano, M. Sasabe, S. Nonaka, T. Higashiyama, S. Hasezawa, Y. Machida, and M. Hasebe. 2013. Mechanism of Microtubule Array Expansion in the Cytokinetic Phragmoplast. *Nat Commun*. 4:1967.

246 Murthy, K., Wadsworth, P. 2005. Myosin-Ii-Dependent Localization and Dynamics of F-Actin During Cytokinesis. *Curr Biol*. 15:724-731.

247 Na, J., and M. Zernicka-Goetz. 2006. Asymmetric Positioning and Organization of the Meiotic Spindle of Mouse Oocytes Requires Cdc42 Function. *Curr Biol*. 16:1249-1254.

248 Naqvi, N.I., K. Eng, K.L. Gould, and M.K. Balasubramanian. 1999. Evidence for F-Actin-Dependent and -Independent Mechanisms Involved in Assembly and Stability of the Medial Actomyosin Ring in Fission Yeast. *EMBO J*. 18:854-862.

249 Neef, R., C. Preisinger, J. Sutcliffe, R. Kopajtich, E.A. Nigg, T.U. Mayer, and F.A. Barr. 2003. Phosphorylation of Mitotic Kinesin-Like Protein 2 by Polo-Like Kinase 1 Is Required for Cytokinesis. *J Cell Biol*. 162:863-875.

250 Neufeld, T.P., and G.M. Rubin. 1994. The Drosophila Peanut Gene Is Required for Cytokinesis and Encodes a Protein Similar to Yeast Putative Bud Neck Filament Proteins. *Cell*. 77:371-379.

251 Nguyen, T.Q., H. Sawa, H. Okano, and J.G. White. 2000. The C. Elegans Septin Genes, Unc-59 and Unc-61, Are Required for Normal Postembryonic Cytokineses and Morphogenesis but Have No Essential Function in Embryogenesis. *J Cell Sci*. 113 Pt 21:3825-3837.

252 Nishi, Y., E. Rogers, S.M. Robertson, and R. Lin. 2008. Polo Kinases Regulate C. Elegans Embryonic Polarity Via Binding to Dyrk2-Primed Mex-5 and Mex-6. *Development*. 135:687-697.

253 Nishimura, Y., K. Nakano, and I. Mabuchi. 1998. Localization of Rho Gtpase in Sea Urchin Eggs. *FEBS Lett*. 441:121-126.

254 Nishimura, Y., and S. Yonemura. 2006. Centralspindlin Regulates Ect2 and Rhoa Accumulation at the Equatorial Cortex During Cytokinesis. *J Cell Sci*. 119:104-114.

255 Norden, C., M. Mendoza, J. Dobbelaere, C.V. Kotwaliwale, S. Biggins, and Y. Barral. 2006. The Nocut Pathway Links Completion of Cytokinesis to Spindle Midzone Function to Prevent Chromosome Breakage. *Cell*. 125:85-98.

256 O'Connell, C.B., S.P. Wheatley, S. Ahmed, and Y.L. Wang. 1999. The Small Gtp-Binding Protein Rho Regulates Cortical Activities in Cultured Cells During Division. *J Cell Biol*. 144:305-313.

257 O'Farrell, F., and P. Kylsten. 2008. Drosophila Anillin Is Unequally Required During Asymmetric Cell Divisions of the Pns. *Biochem Biophys Res Commun*. 369:407-413.

258 Oegema, K., M.S. Savoian, T.J. Mitchison, and C.M. Field. 2000. Functional Analysis of a Human Homologue of the Drosophila Actin Binding Protein Anillin Suggests a Role in Cytokinesis. *J Cell Biol*. 150:539-552.

259 Oliferenko, S., T.G. Chew, and M.K. Balasubramanian. 2009. Positioning Cytokinesis. *Genes Dev*. 23:660-674.

260 Olofsson, B. 1999. Rho Guanine Dissociation Inhibitors: Pivotal Molecules in Cellular Signalling. *Cell Signal*. 11:545-554.

261 Otomo, T., D.R. Tomchick, C. Otomo, S.C. Panchal, M. Machius, and M.K. Rosen. 2005. Structural Basis of Actin Filament Nucleation and Processive Capping by a Formin Homology 2 Domain. *Nature*. 433:488-494.

262 Pacquelet, A., P. Uhart, J.P. Tassan, and G. Michaux. 2015. Par-4 and Anillin Regulate Myosin to Coordinate Spindle and Furrow Position During Asymmetric Division. *J Cell Biol*. 210:1085-1099.

263 Pan, F., R.L. Malmberg, and M. Momany. 2007. Analysis of Septins across Kingdoms Reveals Orthology and New Motifs. *BMC Evol Biol*. 7:103.

264 Pandi, N.S., M. Manimuthu, P. Harunipriya, M. Murugesan, G.V. Asha, and S. Rajendran. 2014. In Silico Analysis of Expression Pattern of a Wnt/Beta-Catenin Responsive Gene Anln in Gastric Cancer. *Gene*. 545:23-29.

265 Paolini, A., A.L. Duchemin, S. Albadri, E. Patzel, D. Bornhorst, P. Gonzalez Avalos, S. Lemke, A. Machate, M. Brand, S. Sel, V. Di Donato, F. Del Bene, F.R. Zolessi, M. Ramialison, and L. Poggi. 2015. Asymmetric Inheritance of the Apical Domain and Self-Renewal of Retinal Ganglion Cell Progenitors Depend on Anillin Function. *Development*. 142:832-839.

266 Paul, A.S., and T.D. Pollard. 2008. The Role of the Fh1 Domain and Profilin in Formin-Mediated Actin-Filament Elongation and Nucleation. *Curr Biol*. 18:9-19.

267 Paul, A.S., and T.D. Pollard. 2009. Energetic Requirements for Processive Elongation of Actin Filaments by Fh1fh2-Formins. *J Biol Chem*. 284:12533-12540.

268 Pavicic-Kaltenbrunner, V., M. Mishima, and M. Glotzer. 2007. Cooperative Assembly of Cyk-4/Mgcracgap and Zen-4/Mklp1 to Form the Centralspindlin Complex. *Mol Biol Cell*. 18:4992-5003.

269 Pelham, R.J., and F. Chang. 2002. Actin Dynamics in the Contractile Ring During Cytokinesis in Fission Yeast. *Nature*. 419:82-86.

270 Piekny, A., M. Werner, and M. Glotzer. 2005. Cytokinesis: Welcome to the Rho Zone. *Trends Cell Biol*. 15:651-658.

271 Piekny, A.J., and M. Glotzer. 2008. Anillin Is a Scaffold Protein That Links Rhoa, Actin, and Myosin During Cytokinesis. *Curr Biol*. 18:30-36.

272 Piekny, A.J., and A.S. Maddox. 2010. The Myriad Roles of Anillin During Cytokinesis. *Semin Cell Dev Biol*. 21:881-891.

273 Piekny, A.J., and P.E. Mains. 2002. Rho-Binding Kinase (Let-502) and Myosin Phosphatase (Mel-11) Regulate Cytokinesis in the Early Caenorhabditis Elegans Embryo. *J Cell Sci*. 115:2271-2282.

274 Pitt, J.N., J.A. Schisa, and J.R. Priess. 2000. P Granules in the Germ Cells of Caenorhabditis Elegans Adults Are Associated with Clusters of Nuclear Pores and Contain Rna. *Dev Biol*. 219:315-333.

275 Pittman, K.J., and A.R. Skop. 2012. Anterior Par Proteins Function During Cytokinesis and Maintain Dyn-1 at the Cleavage Furrow in Caenorhabditis Elegans. *Cytoskeleton (Hoboken)*. 69:826-839.

276 Polet, D., A. Lambrechts, K. Ono, A. Mah, F. Peelman, J. Vandekerckhove, D.L. Baillie, C. Ampe, and S. Ono. 2006. Caenorhabditis Elegans Expresses Three Functional Profilins in a Tissue-Specific Manner. *Cell Motil Cytoskeleton*. 63:14-28.

277 Pollard, T.D. 2010. Mechanics of Cytokinesis in Eukaryotes. *Curr Opin Cell Biol*. 22:50-56.

278 Pollard, T.D., L. Blanchoin, and R.D. Mullins. 2000. Molecular Mechanisms Controlling Actin Filament Dynamics in Nonmuscle Cells. *Annu Rev Biophys Biomol Struct*. 29:545-576.

279 Pollard, T.D., and G.G. Borisy. 2003. Cellular Motility Driven by Assembly and Disassembly of Actin Filaments. *Cell*. 112:453-465.

280 Powers, J., O. Bossinger, D. Rose, S. Strome, and W. Saxton. 1998. A Nematode Kinesin Required for Cleavage Furrow Advancement. *Curr Biol*. 8:1133-1136.

281 Powers, J., D.J. Rose, A. Saunders, S. Dunkelbarger, S. Strome, and W.M. Saxton. 2004. Loss of Klp-19 Polar Ejection Force Causes Misorientation and Missegregation of Holocentric Chromosomes. *J Cell Biol*. 166:991-1001.

282 Priess, J.R., and J.N. Thomson. 1987. Cellular Interactions in Early C. Elegans Embryos. *Cell*. 48:241-250.

283 Pring, M., M. Evangelista, C. Boone, C. Yang, and S.H. Zigmond. 2003. Mechanism of Formin-Induced Nucleation of Actin Filaments. *Biochemistry*. 42:486-496.

284 Prokopenko, S.N., A. Brumby, L. O'Keefe, L. Prior, Y. He, R. Saint, and H.J. Bellen. 1999. A Putative Exchange Factor for Rho1 Gtpase Is Required for Initiation of Cytokinesis in Drosophila. *Genes Dev*. 13:2301-2314.

285 Pruyne, D., M. Evangelista, C. Yang, E. Bi, S. Zigmond, A. Bretscher, and C. Boone. 2002. Role of Formins in Actin Assembly: Nucleation and Barbed-End Association. *Science*. 297:612-615.

286 R. Marian Hicks, J.S.J.W. 1976. Membrane Changes During Urothelial Hyperplasia and Neoplasia'. *Cancer Research*. 36:2502-2507.

287 Raich, W.B., A.N. Moran, J.H. Rothman, and J. Hardin. 1998. Cytokinesis and Midzone Microtubule Organization in Caenorhabditis Elegans Require the Kinesin-Like Protein Zen-4. *Mol Biol Cell*. 9:2037-2049.

288 Rangarajan, A., C. Talora, R. Okuyama, M. Nicolas, C. Mammucari, H. Oh, J.C. Aster, S. Krishna, D. Metzger, P. Chambon, L. Miele, M. Aguet, F. Radtke, and G.P. Dotto. 2001. Notch Signaling Is a Direct Determinant of Keratinocyte Growth Arrest and Entry into Differentiation. *EMBO J*. 20:3427-3436.

289 Rappaport, R. 1961. Experiments Concerning the Cleavage Stimulus in Sand Dollar Eggs. *J Exp Zool*. 148:81-89.

290 Rappaport, R. 1969. Aster-Equatorial Surface Relations and Furrow Establishment. *J Exp Zool*. 171:59-68.

291 Rappaport, R. 1971. Cytokinesis in Animal Cells. *Int Rev Cytol*. 31:169-213.

292 Rappaport, R. 1975. Establishment and Organization of the Cleavage Stimulus in Sand Dollar Eggs. *Molecules and Cell Movement*:287-303.

293 Rappaport, R. 1981. Cytokinesis: Cleavage Furrow Establishment in Cylindrical Sand Dollar Eggs. *J. Exp. Zool.* 217:365-375.

294 Rappaport, R. 1985. Repeated Furrow Formation from a Single Mitotic Apparatus in Cylindrical Sand Dollar Eggs. *The Journal of Experimental Zoology*:247-253.

295 Rappaport, R. 1986. Establishment of the Mechanism of Cytokinesis in Animal Cells. *Int Rev Cytol*. 105:245-281.

296 Rappaport, R. 1988. Surface Behavior in Artificially Constricted Sand Dollar Eggs and Egg Fragments *The Journal of Experimental Zoology*. 246:253-257.

297 Rappaport, R. 1991. Enhancement of Aster-Induced Furrowing Activity by a Factor Associated with the Nucleus. *Journal of Experimental Zoology*. 257:87-95.

298 Rappaport, R., and B.N. Rappaport. 1974. Establishment of Cleavage Furrows by the Mitotic Spindle. *J Exp Zool*. 189:189-196.

299 Reddien, P.W., and H.R. Horvitz. 2000. Ced-2/Crkii and Ced-10/Rac Control Phagocytosis and Cell Migration in Caenorhabditis Elegans. *Nat Cell Biol*. 2:131-136.

300 Riddle, D.L., T. Blumenthal, B.J. Meyer, and J.R. Priess. 1997. Introduction to C. Elegans. *In* C. Elegans Ii. D.L. Riddle, T. Blumenthal, B.J. Meyer, and J.R. Priess, editors, Cold Spring Harbor (NY).

301 Ridley, A.J. 2015. Rho Gtpase Signalling in Cell Migration. *Curr Opin Cell Biol*. 36:103-112.

302 Ris, H. 1949. The Anaphase Movement of Chromosomes in the Spermatocytes of the Grasshopper. *Biol Bull*. 96:90-106.

303 Roberts, P.J., N. Mitin, P.J. Keller, E.J. Chenette, J.P. Madigan, R.O. Currin, A.D. Cox, O. Wilson, P. Kirschmeier, and C.J. Der. 2008. Rho Family Gtpase Modification and Dependence on Caax Motif-Signaled Posttranslational Modification. *J Biol Chem*. 283:25150-25163.

304 Rocheleau, C.E., W.D. Downs, R. Lin, C. Wittmann, Y. Bei, Y.H. Cha, M. Ali, J.R. Priess, and C.C. Mello. 1997. Wnt Signaling and an Apc-Related Gene Specify Endoderm in Early C. Elegans Embryos. *Cell*. 90:707-716.

305 Rose, L., and P. Gonczy. 2014. Polarity Establishment, Asymmetric Division and Segregation of Fate Determinants in Early C. Elegans Embryos. *WormBook*:1-43.

306 Rose, L.S., and K. Kemphues. 1998. The Let-99 Gene Is Required for Proper Spindle Orientation During Cleavage of the C. Elegans Embryo. *Development*. 125:1337-1346.

307 Sagot, I., A.A. Rodal, J. Moseley, B.L. Goode, and D. Pellman. 2002. An Actin Nucleation Mechanism Mediated by Bni1 and Profilin. *Nat Cell Biol*. 4:626-631.

308 Salinas, P.C. 2007. Modulation of the Microtubule Cytoskeleton: A Role for a Divergent Canonical Wnt Pathway. *Trends Cell Biol*. 17:333-342.

309 Sanger, J.M., and J.W. Sanger. 1980. Banding and Polarity of Actin Filaments in Interphase and Cleaving Cells. *J Cell Biol*. 86:568-575.

310 Sato, T., J.H. van Es, H.J. Snippert, D.E. Stange, R.G. Vries, M. van den Born, N. Barker, N.F. Shroyer, M. van de Wetering, and H. Clevers. 2011. Paneth Cells Constitute the Niche for Lgr5 Stem Cells in Intestinal Crypts. *Nature*. 469:415-418.

311 Schenk, C., H. Bringmann, A.A. Hyman, and C.R. Cowan. 2010. Cortical Domain Correction Repositions the Polarity Boundary to Match the Cytokinesis Furrow in C. Elegans Embryos. *Development*. 137:1743-1753.

312 Schiel, J.A., C. Childs, and R. Prekeris. 2013. Endocytic Transport and Cytokinesis: From Regulation of the Cytoskeleton to Midbody Inheritance. *Trends Cell Biol*. 23:319-327.

313 Schindelin, J., I. Arganda-Carreras, E. Frise, V. Kaynig, M. Longair, T. Pietzsch, S. Preibisch, C. Rueden, S. Saalfeld, B. Schmid, J.Y. Tinevez, D.J. White, V. Hartenstein, K. Eliceiri, P. Tomancak, and A. Cardona. 2012. Fiji: An Open-Source Platform for Biological-Image Analysis. *Nat Methods*. 9:676-682.

314 Schindelin, J., C.T. Rueden, M.C. Hiner, and K.W. Eliceiri. 2015. The Imagej Ecosystem: An Open Platform for Biomedical Image Analysis. *Mol Reprod Dev*. 82:518-529.

315 Schisa, J.A., J.N. Pitt, and J.R. Priess. 2001. Analysis of Rna Associated with P Granules in Germ Cells of C. Elegans Adults. *Development*. 128:1287-1298.

316 Schlesinger, A., C.A. Shelton, J.N. Maloof, M. Meneghini, and B. Bowerman. 1999. Wnt Pathway Components Orient a Mitotic Spindle in the Early Caenorhabditis Elegans Embryo without Requiring Gene Transcription in the Responding Cell. *Genes Dev*. 13:2028-2038.

317 Schmidt, A., and M.N. Hall. 1998. Signaling to the Actin Cytoskeleton. *Annu Rev Cell Dev Biol*. 14:305-338.

318 Schmutz, C., J. Stevens, and A. Spang. 2007. Functions of the Novel Rhogap Proteins Rga-3 and Rga-4 in the Germ Line and in the Early Embryo of C. Elegans. *Development*. 134:3495-3505.

319 Schonegg, S., A.T. Constantinescu, C. Hoege, and A.A. Hyman. 2007. The Rho Gtpase-Activating Proteins Rga-3 and Rga-4 Are Required to Set the Initial Size of Par Domains in Caenorhabditis Elegans One-Cell Embryos. *Proc Natl Acad Sci U S A*. 104:14976-14981.

320 Schonegg, S., and A.A. Hyman. 2006. Cdc-42 and Rho-1 Coordinate Acto-Myosin Contractility and Par Protein Localization During Polarity Establishment in C. Elegans Embryos. *Development*. 133:3507-3516.

321 Schroeder, T.E. 1972. The Contractile Ring. Ii. Determining Its Brief Existence, Volumetric Changes, and Vital Role in Cleaving Arbacia Eggs. *J Cell Biol*. 53:419-434.

322 Schubert, C.M., R. Lin, C.J. de Vries, R.H. Plasterk, and J.R. Priess. 2000. Mex-5 and Mex-6 Function to Establish Soma/Germline Asymmetry in Early C. Elegans Embryos. *Mol Cell*. 5:671-682.

323 Schumacher, J.M., Golden, A., and Donovan, P. J. . 1998b. Air-2, an Aurora/Ipl1-Related Protein Kinase Associated with Chromosomes and Midbody Microtubules Is Required for Polar Body Extrusion and Cytokinesis in Caenorhabditis Elegans Embryos. *J. Cell Biol.* 143:1635-1646.

324 Sellers, J.R. 1991. Regulation of Cytoplasmic and Smooth Muscle Myosin. *Curr Opin Cell Biol*. 3:98-104.

325 Severson, A.F., D.L. Baillie, and B. Bowerman. 2002. A Formin Homology Protein and a Profilin Are Required for Cytokinesis and Arp2/3-Independent Assembly of Cortical Microfilaments in C. Elegans. *Curr Biol*. 12:2066-2075.

326 Severson, A.F., and B. Bowerman. 2003. Myosin and the Par Proteins Polarize Microfilament-Dependent Forces That Shape and Position Mitotic Spindles in Caenorhabditis Elegans. *J Cell Biol*. 161:21-26.

327 Severson, A.F., Hamill, D. R., Carter, J. C., Schumacher, J., and Bowerman, B. . 2000. The Aurora-Related Kinase Air-2 Recruits Zen-4/Cemklp1 to the Mitotic Spindle at Metaphase and Is Required for Cytokinesis. . *Curr Biol*. 10:1162-1171.

328 Shakir, M.A., J.S. Gill, and E.A. Lundquist. 2006. Interactions of Unc-34 Enabled with Rac Gtpases and the Nik Kinase Mig-15 in Caenorhabditis Elegans Axon Pathfinding and Neuronal Migration. *Genetics*. 172:893-913.

329 Shandala, T., S.L. Gregory, H.E. Dalton, M. Smallhorn, and R. Saint. 2004. Citron Kinase Is an Essential Effector of the Pbl-Activated Rho Signalling Pathway in Drosophila Melanogaster. *Development*. 131:5053-5063.

330 Shaya, O., U. Binshtok, M. Hersch, D. Rivkin, S. Weinreb, L. Amir-Zilberstein, B. Khamaisi, O. Oppenheim, R.A. Desai, R.J. Goodyear, G.P. Richardson, C.S. Chen, and D. Sprinzak. 2017. Cell-Cell Contact Area Affects Notch Signaling and Notch-Dependent Patterning. *Dev Cell*. 40:505-511 e506.

331 Shelton, C., A.,, J.C. Carter, C. Ellis G, and B. Bowerman. 1999a. The Nonmuscle Myosin Regulatory Light Chain Gene Mlc-4 Is Required for Cytokinesis, Anterior-Posterior Polarity, and Body Morphology During Caenorhabditis Elegans Embryogenesis. *The Journal of Cell Biology*. 146:439.

332 Shelton, C.A., and B. Bowerman. 1996. Time-Dependent Responses to Glp-1-Mediated Inductions in Early C. Elegans Embryos. *Development*. 122:2043-2050.

333 Shelton, C.A., J.C. Carter, G.C. Ellis, and B. Bowerman. 1999b. The Nonmuscle Myosin Regulatory Light Chain Gene Mlc-4 Is Required for Cytokinesis, Anterior-Posterior Polarity, and Body Morphology During Caenorhabditis Elegans Embryogenesis. *J Cell Biol*. 146:439-451.

334 Shuster, C.B., and D.R. Burgess. 2002. Transitions Regulating the Timing of Cytokinesis in Embryonic Cells. *Curr Biol*. 12:854-858.

335 Singh, A., M.C. Zapata, Y.S. Choi, and S.O. Yoon. 2014. Gsi Promotes Vincristine-Induced Apoptosis by Enhancing Multi-Polar Spindle Formation. *Cell Cycle*. 13:157-166.

336 Somers, W.G., and R. Saint. 2003. A Rhogef and Rho Family Gtpase-Activating Protein Complex Links the Contractile Ring to Cortical Microtubules at the Onset of Cytokinesis. *Dev Cell*. 4:29-39.

337 Somlyo, A.V., H. Wang, N. Choudhury, A.S. Khromov, M. Majesky, G.K. Owens, and A.P. Somlyo. 2004. Myosin Light Chain Kinase Knockout. *J Muscle Res Cell Motil*. 25:241-242.

338 Sonnichsen, B., L.B. Koski, A. Walsh, P. Marschall, B. Neumann, M. Brehm, A.M. Alleaume, J. Artelt, P. Bettencourt, E. Cassin, M. Hewitson, C. Holz, M. Khan, S. Lazik, C. Martin, B. Nitzsche, M. Ruer, J. Stamford, M. Winzi, R. Heinkel, M. Roder, J. Finell, H. Hantsch, S.J. Jones, M. Jones, F. Piano, K.C. Gunsalus, K. Oegema, P. Gonczy, A. Coulson, A.A. Hyman, and C.J. Echeverri. 2005. Full-Genome Rnai Profiling of Early Embryogenesis in Caenorhabditis Elegans. *Nature*. 434:462-469.

339 Stark, B.C., T.E. Sladewski, L.W. Pollard, and M. Lord. 2010. Tropomyosin and Myosin-Ii Cellular Levels Promote Actomyosin Ring Assembly in Fission Yeast. *Mol Biol Cell*. 21:989-1000.

340 Steffen, A., M. Ladwein, G.A. Dimchev, A. Hein, L. Schwenkmezger, S. Arens, K.I. Ladwein, J. Margit Holleboom, F. Schur, J. Victor Small, J. Schwarz, R. Gerhard, J. Faix, T.E. Stradal, C. Brakebusch, and K. Rottner. 2013. Rac Function Is Crucial for Cell Migration but Is Not Required for Spreading and Focal Adhesion Formation. *J Cell Sci*. 126:4572-4588.

341 Steffen, A., K. Rottner, J. Ehinger, M. Innocenti, G. Scita, J. Wehland, and T.E. Stradal. 2004. Sra-1 and Nap1 Link Rac to Actin Assembly Driving Lamellipodia Formation. *EMBO J*. 23:749-759.

342 Straight, A.F., C.M. Field, and T.J. Mitchison. 2005. Anillin Binds Nonmuscle Myosin Ii and Regulates the Contractile Ring. *Mol Biol Cell*. 16:193-201.

343 Strand, M., and C.A. Micchelli. 2011. Quiescent Gastric Stem Cells Maintain the Adult Drosophila Stomach. *Proc Natl Acad Sci U S A*. 108:17696-17701.

344 Strome, S., and W.B. Wood. 1982. Immunofluorescence Visualization of Germ-Line-Specific Cytoplasmic Granules in Embryos, Larvae, and Adults of Caenorhabditis Elegans. *Proc Natl Acad Sci U S A*. 79:1558-1562.

345 Su, K.C., T. Takaki, and M. Petronczki. 2011. Targeting of the Rhogef Ect2 to the Equatorial Membrane Controls Cleavage Furrow Formation During Cytokinesis. *Dev Cell*. 21:1104-1115.

346 Subramanian, R., E.M. Wilson-Kubalek, C.P. Arthur, M.J. Bick, E.A. Campbell, S.A. Darst, R.A. Milligan, and T.M. Kapoor. 2010. Insights into Antiparallel Microtubule Crosslinking by Prc1, a Conserved Nonmotor Microtubule Binding Protein. *Cell*. 142:433-443.

347 Sun, L., O. Liu, J. Desai, F. Karbassi, M.A. Sylvain, A. Shi, Z. Zhou, C.E. Rocheleau, and B.D. Grant. 2012. Ced-10/Rac1 Regulates Endocytic Recycling through the Rab-5 Gap Tbc-2. *PLoS Genet*. 8:e1002785.

348 Sunkel, C.E., and D.M. Glover. 1988. Polo, a Mitotic Mutant of Drosophila Displaying Abnormal Spindle Poles. *J Cell Sci*. 89 (Pt 1):25-38.

349 Suzuki, A., and S. Ohno. 2006. The Par-Apkc System: Lessons in Polarity. *J Cell Sci*. 119:979-987.

350 Swan, K.A., A.F. Severson, J.C. Carter, P.R. Martin, H. Schnabel, R. Schnabel, and B. Bowerman. 1998. Cyk-1: A C. Elegans Fh Gene Required for a Late Step in Embryonic Cytokinesis. *J Cell Sci*. 111 (Pt 14):2017-2027.

351 Swann, M.M., and J.M. Mitchison. 1953. Cleavage of Sea-Urchin Eggs in Colchicine. *Journal of Experimental Biology*. 30:506-&.

352 T.Q. Nguyen, H.S., H. Okano, J.G. White. 2000. The C. Elegans Septin Genes, Unc-59 and Unc-61, Are Required for Normal Postembryonic Cytokineses and Morphogenesis but Have No Essential Function in Embryogenesis. *Journal Cell Science*. 113:3825-3837.

353 Takaishi, K., T. Sasaki, T. Kameyama, S. Tsukita, S. Tsukita, and Y. Takai. 1995. Translocation of Activated Rho from the Cytoplasm to Membrane Ruffling Area, Cell-Cell Adhesion Sites and Cleavage Furrows. *Oncogene*. 11:39-48.

354 Tan, J.L., S. Ravid, and J.A. Spudich. 1992. Control of Nonmuscle Myosins by Phosphorylation. *Annu Rev Biochem*. 61:721-759.

355 Tatsumoto, T., X. Xie, R. Blumenthal, I. Okamoto, and T. Miki. 1999. Human Ect2 Is an Exchange Factor for Rho Gtpases, Phosphorylated in G2/M Phases, and Involved in Cytokinesis. *J Cell Biol*. 147:921-928.

356 Tenlen, J.R., J.N. Molk, N. London, B.D. Page, and J.R. Priess. 2008. Mex-5 Asymmetry in One-Cell C. Elegans Embryos Requires Par-4- and Par-1-Dependent Phosphorylation. *Development*. 135:3665-3675.

357 Terada, Y. 2001. Role of Chromosomal Passenger Complex in Chromosome Segregation and Cytokinesis. *Cell Struct Funct*. 26:653-657.

358 Thorpe, C.J., A. Schlesinger, J.C. Carter, and B. Bowerman. 1997. Wnt Signaling Polarizes an Early C. Elegans Blastomere to Distinguish Endoderm from Mesoderm. *Cell*. 90:695-705.

359 Timmons, L., D.L. Court, and A. Fire. 2001. Ingestion of Bacterially Expressed Dsrnas Can Produce Specific and Potent Genetic Interference in Caenorhabditis Elegans. *Gene*. 263:103-112.

360 Tobacman, L.S., and E.D. Korn. 1983. The Kinetics of Actin Nucleation and Polymerization. *J Biol Chem*. 258:3207-3214.

361 Tolliday, N., M. Pitcher, and R. Li. 2003. Direct Evidence for a Critical Role of Myosin Ii in Budding Yeast Cytokinesis and the Evolvability of New Cytokinetic Mechanisms in the Absence of Myosin Ii. *Mol Biol Cell*. 14:798-809.

362 Tominaga, T., E. Sahai, P. Chardin, F. McCormick, S.A. Courtneidge, and A.S. Alberts. 2000. Diaphanous-Related Formins Bridge Rho Gtpase and Src Tyrosine Kinase Signaling. *Mol Cell*. 5:13-25.

363 Tormos, A.M., R. Talens-Visconti, and J. Sastre. 2015. Regulation of Cytokinesis and Its Clinical Significance. *Crit Rev Clin Lab Sci*. 52:159-167.

364 Toure, A., O. Dorseuil, L. Morin, P. Timmons, B. Jegou, L. Reibel, and G. Gacon. 1998. Mgcracgap, a New Human Gtpase-Activating Protein for Rac and Cdc42 Similar to Drosophila Rotundracgap Gene Product, Is Expressed in Male Germ Cells. *J Biol Chem*. 273:6019-6023.

365 Toyoda, H., O. Bregerie, A. Vallet, B. Nalpas, G. Pivert, C. Brechot, and C. Desdouets. 2005. Changes to Hepatocyte Ploidy and Binuclearity Profiles During Human Chronic Viral Hepatitis. *Gut*. 54:297-302.

366 Tse, Y.C., M. Werner, K.M. Longhini, J.C. Labbe, B. Goldstein, and M. Glotzer. 2012. Rhoa Activation During Polarization and Cytokinesis of the Early Caenorhabditis Elegans Embryo Is Differentially Dependent on Nop-1 and Cyk-4. *Mol Biol Cell*. 23:4020-4031.

367 Uehara, R., and G. Goshima. 2010. Functional Central Spindle Assembly Requires De Novo Microtubule Generation in the Interchromosomal Region During Anaphase. *J Cell Biol*. 191:259-267.

368 Velarde, N., K.C. Gunsalus, and F. Piano. 2007. Diverse Roles of Actin in C. Elegans Early Embryogenesis. *BMC Dev Biol*. 7:142.

369 Verbrugghe, K.J., and J.G. White. 2004. Spd-1 Is Required for the Formation of the Spindle Midzone but Is Not Essential for the Completion of Cytokinesis in C. Elegans Embryos. *Curr Biol*. 14:1755-1760.

370 Verbrugghe, K.J., and J.G. White. 2007. Cortical Centralspindlin and G Alpha Have Parallel Roles in Furrow Initiation in Early C. Elegans Embryos. *J Cell Sci*. 120:1772-1778.

371 Verbrugghe, K.J.C., and White, J.G. 2007. Cortical Centralspindlin and Galpha Have Parallel Roles in Furrow Initiation in Early C. Elegans Embryos. *Journal Cell Science*.

372 Vinciguerra, P., S.A. Godinho, K. Parmar, D. Pellman, and A.D. D'Andrea. 2010. Cytokinesis Failure Occurs in Fanconi Anemia Pathway-Deficient Murine and Human Bone Marrow Hematopoietic Cells. *J Clin Invest*. 120:3834-3842.

373 Walston, T., C. Tuskey, L. Edgar, N. Hawkins, G. Ellis, B. Bowerman, W. Wood, and J. Hardin. 2004. Multiple Wnt Signaling Pathways Converge to Orient the Mitotic Spindle in Early C. Elegans Embryos. *Dev Cell*. 7:831-841.

374 Wang, M.J., F. Chen, J.T.Y. Lau, and Y.P. Hu. 2017. Hepatocyte Polyploidization and Its Association with Pathophysiological Processes. *Cell Death Dis*. 8:e2805.

375 Wang, Z.B., Z.Z. Jiang, Q.H. Zhang, M.W. Hu, L. Huang, X.H. Ou, L. Guo, Y.C. Ouyang, Y. Hou, C. Brakebusch, H. Schatten, and Q.Y. Sun. 2013. Specific Deletion of Cdc42 Does Not Affect Meiotic Spindle Organization/Migration and Homologous Chromosome Segregation but Disrupts Polarity Establishment and Cytokinesis in Mouse Oocytes. *Mol Biol Cell*. 24:3832-3841.

376 Watanabe, N., T. Kato, A. Fujita, T. Ishizaki, and S. Narumiya. 1999. Cooperation between Mdia1 and Rock in Rho-Induced Actin Reorganization. *Nature Cell Biology*. 1:136-143.

377 Watanabe, S., Y. Ando, S. Yasuda, H. Hosoya, N. Watanabe, T. Ishizaki, and S. Narumiya. 2008. Mdia2 Induces the Actin Scaffold for the Contractile Ring and Stabilizes Its Position During Cytokinesis in Nih 3t3 Cells. *Mol Biol Cell*. 19:2328-2338.

378 Watanabe, S., K. Okawa, T. Miki, S. Sakamoto, T. Morinaga, K. Segawa, T. Arakawa, M. Kinoshita, T. Ishizaki, and S. Narumiya. 2010. Rho and Anillin-Dependent Control of Mdia2 Localization and Function in Cytokinesis. *Mol Biol Cell*. 21:3193-3204.

379 Watts, J.L., D.G. Morton, J. Bestman, and K.J. Kemphues. 2000. The C. Elegans Par-4 Gene Encodes a Putative Serine-Threonine Kinase Required for Establishing Embryonic Asymmetry. *Development*. 127:1467-1475.

380 Wernike, D., C. van Oostende, and A. Piekny. 2014. Visualizing Neuroblast Cytokinesis During C. Elegans Embryogenesis. *J Vis Exp*.

381 Wheatley, S.P., E.H. Hinchcliffe, M. Glotzer, A.A. Hyman, G. Sluder, and Y. Wang. 1997. Cdk1 Inactivation Regulates Anaphase Spindle Dynamics and Cytokinesis in Vivo. *J Cell Biol*. 138:385-393.

382 White, E.A., and M. Glotzer. 2012. Centralspindlin: At the Heart of Cytokinesis. *Cytoskeleton (Hoboken)*. 69:882-892.

383 White, J.G., and G.G. Borisy. 1983. On the Mechanisms of Cytokinesis in Animal Cells. *J Theor Biol*. 101:289-316.

384 Wilker, E.W., M.A. van Vugt, S.A. Artim, P.H. Huang, C.P. Petersen, H.C. Reinhardt, Y. Feng, P.A. Sharp, N. Sonenberg, F.M. White, and M.B. Yaffe. 2007. 14-3-3sigma Controls Mitotic Translation to Facilitate Cytokinesis. *Nature*. 446:329-332.

385 Willert, K., J.D. Brown, E. Danenberg, A.W. Duncan, I.L. Weissman, T. Reya, J.R. Yates, 3rd, and R. Nusse. 2003. Wnt Proteins Are Lipid-Modified and Can Act as Stem Cell Growth Factors. *Nature*. 423:448-452.

386 Williams, S.E., and E. Fuchs. 2013. Oriented Divisions, Fate Decisions. *Curr Opin Cell Biol*. 25:749-758.

387 Wloka, C., R. Nishihama, M. Onishi, Y. Oh, J. Hanna, J.R. Pringle, M. Krauss, and E. Bi. 2011. Evidence That a Septin Diffusion Barrier Is Dispensable for Cytokinesis in Budding Yeast. *Biol Chem*. 392:813-829.

388 Wolfe, B.A., T. Takaki, M. Petronczki, and M. Glotzer. 2009. Polo-Like Kinase 1 Directs Assembly of the Hscyk-4 Rhogap/Ect2 Rhogef Complex to Initiate Cleavage Furrow Formation. *PLoS Biol*. 7:e1000110.

389 Wollman, R., E.N. Cytrynbaum, J.T. Jones, T. Meyer, J.M. Scholey, and A. Mogilner. 2005. Efficient Chromosome Capture Requires a Bias in the 'Search-and-Capture' Process During Mitotic-Spindle Assembly. *Curr Biol*. 15:828-832.

390 Wolpert, L. 1960. The Mechanics and Mechanism of Cleavage. *Int Rev Cytol*. 10:163-216.

391 Wu, J.Q., Y. Ye, N. Wang, T.D. Pollard, and J.R. Pringle. 2010. Cooperation between the Septins and the Actomyosin Ring and Role of a Cell-Integrity Pathway During Cell Division in Fission Yeast. *Genetics*. 186:897-915.

392 Xu, Y., J.B. Moseley, I. Sagot, F. Poy, D. Pellman, B.L. Goode, and M.J. Eck. 2004. Crystal Structures of a Formin Homology-2 Domain Reveal a Tethered Dimer Architecture. *Cell*. 116:711-723.

393 Xuefei Ma, M.K., Mary Anne Conti, Aibing Wang, Yingfan Zhang, James R. Sellers, and Robert S. Adelstein. 2012. Nonmuscle Myosin Ii Exerts Tension but Does Not Translocate Actin in Vertebrate Cytokinesis. *PNAS*. 109:4509-4514.

394 Yamashiro, S., K. Mohri, and S. Ono. 2005. The Two Caenorhabditis Elegans Actin-Depolymerizing Factor/Cofilin Proteins Differently Enhance Actin Filament Severing and Depolymerization. *Biochemistry*. 44:14238-14247.

395 Yonemura, S., K. Hirao-Minakuchi, and Y. Nishimura. 2004. Rho Localization in Cells and Tissues. *Exp Cell Res*. 295:300-314.

396 Yoshigaki, T. 1999. Simulation of Density Gradients of Astral Microtubules at Cell Surface in Cytokinesis of Sea Urchin Eggs. *J Theor Biol*. 196:211-224.

397 Yoshizaki, H., Y. Ohba, M.C. Parrini, N.G. Dulyaninova, A.R. Bresnick, N. Mochizuki, and M. Matsuda. 2004. Cell Type-Specific Regulation of Rhoa Activity During Cytokinesis. *J Biol Chem*. 279:44756-44762.

398 Yuce, O., A. Piekny, and M. Glotzer. 2005. An Ect2-Centralspindlin Complex Regulates the Localization and Function of Rhoa. *J Cell Biol*. 170:571-582.

399 Zang, J.H., G. Cavet, J.H. Sabry, P. Wagner, S.L. Moores, and J.A. Spudich. 1997. On the Role of Myosin-Ii in Cytokinesis: Division of Dictyostelium Cells under Adhesive and Nonadhesive Conditions. *Mol Biol Cell*. 8:2617-2629.

400 Zanin, E., A. Desai, I. Poser, Y. Toyoda, C. Andree, C. Moebius, M. Bickle, B. Conradt, A. Piekny, and K. Oegema. 2013. A Conserved Rhogap Limits M Phase Contractility and Coordinates with Microtubule Asters to Confine Rhoa During Cytokinesis. *Dev Cell*. 26:496-510.

401 Zhang, D., and M. Glotzer. 2015. The Rhogap Activity of Cyk-4/Mgcracgap Functions Non-Canonically by Promoting Rhoa Activation During Cytokinesis. *Elife*. 4.

402 Zhang, D., Nicklas RB. 1996. 'Anaphase' and Cytokinesis in the Absence of Chromosomes. *Nature*. 382:466-468.

403 Zhang, W., and D.N. Robinson. 2005. Balance of Actively Generated Contractile and Resistive Forces Controls Cytokinesis Dynamics. *Proc Natl Acad Sci U S A*. 102:7186-7191.

404 Zhang, X., C. Ma, A.L. Miller, H.A. Katbi, W.M. Bement, and X.J. Liu. 2008. Polar Body Emission Requires a Rhoa Contractile Ring and Cdc42-Mediated Membrane Protrusion. *Dev Cell*. 15:386-400.

405 Zhao, W.M., and G. Fang. 2005a. Anillin Is a Substrate of Anaphase-Promoting Complex/Cyclosome (Apc/C) That Controls Spatial Contractility of Myosin During Late Cytokinesis. *J Biol Chem*. 280:33516-33524.

406 Zhao, W.M., and G. Fang. 2005b. Mgcracgap Controls the Assembly of the Contractile Ring and the Initiation of Cytokinesis. *Proc Natl Acad Sci U S A*. 102:13158-13163.

407 Zhao, W.M., A. Seki, and G. Fang. 2006. Cep55, a Microtubule-Bundling Protein, Associates with Centralspindlin to Control the Midbody Integrity and Cell Abscission During Cytokinesis. *Mol Biol Cell*. 17:3881-3896.

408 Zhu C, J.W. 2005. Cell Cycle-Dependent Translocation of Prc1 on the Spindle by Kif4 Is Essential for Midzone Formation and Cytokinesis. *Proc Natl Acad Sci U S A*. 102:343-348.

409 Zhu, C., E. Lau, R. Schwarzenbacher, E. Bossy-Wetzel, and W. Jiang. 2006. Spatiotemporal Control of Spindle Midzone Formation by Prc1 in Human Cells. *Proc Natl Acad Sci U S A*. 103:6196-6201.

410 Zhu, C.J., E. Bossy-Wetzel, and W. Jiang. 2005. Recruitment of Mklp1 to the Spindle Midzone/Midbody by Incenp Is Essential for Midbody Formation and Completion of Cytokinesis in Human Cells. *Biochemical Journal*. 389:373-381.

411 Zhu, X., J. Wang, K. Moriguchi, L.T. Liow, S. Ahmed, I. Kaverina, and M. Murata-Hori. 2011a. Proper Regulation of Cdc42 Activity Is Required for Tight Actin Concentration at the Equator During Cytokinesis in Adherent Mammalian Cells. *Experimental Cell Research*. 317:2384-2389.

412 Zhu, X., J. Wang, K. Moriguchi, L.T. Liow, S. Ahmed, I. Kaverina, and M. Murata-Hori. 2011b. Proper Regulation of Cdc42 Activity Is Required for Tight Actin Concentration at the Equator During Cytokinesis in Adherent Mammalian Cells. *Exp Cell Res*. 317:2384-2389.

413 Zhuravlev, Y., S.M. Hirsch, S.N. Jordan, J. Dumont, M. Shirasu-Hiza, and J.C. Canman. 2017. Cyk-4 Regulates Rac, but Not Rho, During Cytokinesis. *Mol Biol Cell*. 28:1258-1270.

414 Zonies, S., F. Motegi, Y. Hao, and G. Seydoux. 2010. Symmetry Breaking and Polarization of the C. Elegans Zygote by the Polarity Protein Par-2. *Development*. 137:1669-1677.

415 Zou, Y., Z. Shao, J. Peng, F. Li, D. Gong, C. Wang, X. Zuo, Z. Zhang, J. Wu, Y. Shi, and Q. Gong. 2014. Crystal Structure of Triple-Brct-Domain of Ect2 and Insights into the Binding Characteristics to Cyk-4. *FEBS Lett*. 588:2911-2920.

416 Zumdieck, A., K. Kruse, H. Bringmann, A.A. Hyman, and F. Julicher. 2007. Stress Generation and Filament Turnover During Actin Ring Constriction. *PLoS One*. 2:e696.

417 Zuo, Y., W. Oh, and J.A. Frost. 2014. Controlling the Switches: Rho Gtpase Regulation During Animal Cell Mitosis. *Cell Signal*. 26:2998-3006.